JACC
Basic to Translational Science

A Journal of the American College of Cardiology

JACC
Basic to Translational Science

A Journal of the American College of Cardiology

CORRESPONDENCE FOR AMERICAN COLLEGE OF CARDIOLOGY

All correspondence for the College, other than that related to *JACC: Basic to Translational Science* should be sent to Resource Center, American College of Cardiology, 2400 N Street, NW, Washington, DC 20037

Instructions For Authors

JACC: Basic to Translational Science, an open access journal, serves a forum for advancing the field Translational Cardiovascular Medicine, and as a platform for accelerating the translation of novel scientific discoveries into new therapies that improve clinical outcomes for patients affected with or at risk for Cardiovascular Disease. Thematic areas of interest include pre-clinical research; clinical trials; personalized medicine; novel drugs, devices, and biologics; proteomics, genomics and metabolomics; and early phase clinical trial methodology.

We request that all manuscripts be submitted online at http://www.jaccsubmit-basicts.org

Manuscript submissions should conform to the guidelines set forth in the ''Uniform Requirements for Manuscripts Submitted to Biomedical Journals: Writing and Editing for Biomedical Publication,'' available from http://www.ICMJE.org and most recently updated in April 2010.

English language help service: Upon request, Elsevier will direct authors to an agent who can check and improve the English of their paper (before submission). Please contact authorsupport@elsevier.com for further information.

The *JACC* Journals use a single-blind peer-review process. Papers are assigned an Associate Editor, who can assign up to two peer-reviewers, although more can be assigned if necessary.

AUTHOR ENQUIRIES

For enquiries relating to the submission of articles or to articles currently under review, please contact the *JACC: Basic to Translational Science* editorial office at jaccbts@acc.org. For information on articles that have been accepted for publication, please visit Elsevier's Authors Home at www.elsevier.com/authors. Elsevier's Authors Home also provides the facility to track accepted articles and set up e-mail alerts to inform you of when an article's status has changed, as well as detailed artwork guidelines, copyright information, frequently asked questions, and more. Authors can order copies of the issue in which their article appears at a discounted rate; please contact Elsevier Health Sciences Division, Subscription Customer Service, 3251 Riverport Lane, Maryland Heights, MO 63043, Tel: 1-800-654- 2452, E-mail: journalscustomerservice-usa@elsevier.com.

EXCLUSIVE SUBMISSION/PUBLICATION POLICY

Manuscripts are eligible for review only under the conditions that they are not under consideration elsewhere and that the data presented have not appeared on the Internet or have not been previously published (including symposia, proceedings, transactions, books, articles published by invitation, or preliminary publications of any kind except abstracts not exceeding 400 words).

COPYRIGHT

Upon acceptance of an article, authors will be asked to complete an 'Exclusive License Agreement' (for more information see http://www.elsevier.com/OAauthoragreement). Permitted third party reuse of open access articles is determined by the author's choice of user license (see http://www.elsevier.com/openaccesslicenses). As an author you (or your employer or institution) have certain rights to reuse your work. For more information on author rights please see http://www.elsevier.com/copyright.

FUNDING BODY AGREEMENTS AND POLICIES

Elsevier has established a number of agreements with funding bodies which allow authors to comply with their funder's open access policies. Some authors may also be reimbursed for associated publication fees. To learn more about existing agreements please visit http://www.elsevier.com/fundingbodies. After acceptance, open access papers will be published under a noncommercial license. For authors requiring a commercial CC BY license, you can apply after your manuscript is accepted for publication.

OPEN ACCESS

This is an open access journal: all articles will be immediately and permanently available for everyone to read and download without cost. Permitted third party (re)use is defined by the following Creative Commons user licenses (see http://www.elsevier.com/openaccesslicenses):

Creative Commons Attribution-NonCommericial-NoDerivs (CC BY-NC-ND)—For non-commercial purposes, lets others distribute and copy the article, and to include in a collective work (such as an anthology), as long as they credit the author(s) and provided they do not alter or modify the article.

If you need to comply with your funding body policy you can apply for a CC-BY license after your manuscript is accepted for publication.

To provide open access, this journal has an open access fee (also known as an article publishing charge, aka APC) which needs to be paid by the authors or on their behalf, e.g., by their research funder or institution. The open access fee for full articles is $3,200 for members of the American College of Cardiology and $3,400 for non-members, excluding taxes. The open access fee for research letters is $1,600 for members of the American College of Cardiology and $1,700 for non-members, excluding taxes. Learn more about Elsevier's pricing policy: http://www.elsevier.com/openaccesspricing.

RELATIONSHIP WITH INDUSTRY POLICY

Authors are required to disclose any relationship with industry and other relevant entities—financial or otherwise—within the past 2 years that might pose a conflict of interest in connection with the submitted article in both the cover letter and on the title page. All sources of funding for the work should be acknowledged in a footnote on the title page, as should all institutional affiliations of the authors (including corporate appointments). Other kinds of associations, such as consultancies, stock ownership, or other equity interests or patent-licensing arrangements, should be disclosed to the Editors in the cover letter at the time of submission. If no conflict of interest exists, please state this in the cover letter and on the title page. Relationship with industry guidelines apply to authors of all the following: Original Research Papers, State-of-the-Art Papers, Editorials and Viewpoints, Images, Editorial Comments, and Letters to the Editor.

ALL FORMS ARE NOW SIGNED AND SUBMITTED ELECTRONICALLY. Once a manuscript is accepted, the authors will be sent links to complete electronic Copyright Transfer and Relationship with Industry forms. Only the corresponding author may electronically sign the copyright form; however, ALL AUTHORS ARE REQUIRED TO ELECTRONICALLY SIGN A RELATIONSHIP WITH INDUSTRY FORM. Once completed, a PDF version of the form is e-mailed to the author. Authors can access and confirm receipt of forms by logging into their account online. Each author will be alerted if his/her form has not been completed by the deadline. The *JACC* Journals program prefers the term Relationships with Industry and Other Entities as opposed to the term Conflict of Interest, because, by definition, it does NOT necessarily imply a conflict. When all relationships are disclosed with the appropriate detail regarding category and amount, and managed appropriately for building consensus and voting, the *JACC* Journals program believes that potential bias can be avoided and the final published document is strengthened since the necessary expertise is accessible.

Only authors appearing on the final title page will be sent a form. YOU CANNOT ADD AUTHORS AFTER ACCEPTANCE OR ON PROOFS. After a paper is sent to the publisher, the links to the electronic forms will no longer be active. In this case, authors will be sent links to download hard

copy forms that they may mail or fax to the *JACC: Basic to Translational Science* office.

ETHICS

Studies should be in compliance with human studies committees and animal welfare regulations of the authors' institutions and Food and Drug Administration guidelines.

Human studies must be performed with the subjects' written informed consent. Authors must provide the details of this procedure and indicate that the institutional committee on human research has approved the study protocol. If radiation is used in a research procedure, the radiation exposure must be specified in the Methods. Clinical trials should be registered.

Studies on patients or volunteers require ethics committee approval and informed consent which should be documented in your paper. Patients have a right to privacy. Therefore, identifying information, including patients' images, names, initials, or hospital numbers, should not be included in videos, recordings, written descriptions, photographs, and pedigrees unless the information is essential for scientific purposes and you have obtained written informed consent for publication in print and electronic form from the patient (or parent, guardian or next of kin where applicable). If such consent is made subject to any conditions, the editorial office must be made aware of all such conditions.

Written consents must be provided to the editorial office on request. Even where consent has been given, identifying details should be omitted if they are not essential. If identifying characteristics are altered to protect anonymity, such as in genetic pedigrees, authors should provide assurance that alterations do not distort scientific meaning and editors should so note. If such consent has not been obtained, personal details of patients included in any part of the paper and in any supplementary materials (including all illustrations and videos) must be removed before submission. Animal investigation must conform to the ''Position of the American Heart Association on Research Animal Use,'' adopted by the AHA on November 11, 1984. If equivalent guidelines are used, they should be indicated. The AHA position includes: 1) animal care and use by qualified individuals, supervised by veterinarians, and all facilities and transportation must comply with current legal requirements and guidelines; 2) research involving animals should be done only when alternative methods to yield needed information are not possible; 3) anesthesia must be used in all surgical interventions, all unnecessary suffering should be avoided and research must be terminated if unnecessary pain or fear results; and 4) animal facilities must meet the standards of the American Association for Accreditation of Laboratory Animal Care (AAALAC).

The *JACC* Journals has an ethics committee comprised of 7 members, which oversees quality control and will look into the issues of concern, if any.

AUTHORSHIP/COVER LETTER

Each author must have contributed significantly to the submitted work. If there are more than 4 authors, the contribution of each must be substantiated in the cover letter. If authorship is attributed to a group (either solely or in addition to 1 or more individual authors), all members of the group must meet the full criteria and requirements for authorship. To save space, if group members have been listed in *JACC: Basic to Translational Science*, the article should be referenced rather than reprinting the list. The Editors consider authorship to include all of the following: 1) conception and design or analysis and interpretation of data, or both; 2) drafting of the manuscript or revising it critically for important intellectual content; and 3) final approval of the manuscript submitted. Participation solely in the collection of data does not justify authorship but may be appropriately acknowledged in the Acknowledgment section.

Manuscripts must be submitted with a cover letter stating: 1) the paper is not under consideration elsewhere; 2) none of the paper's contents have been previously published; 3) all authors have read and approved the manuscript; and 4) the full disclosure of any potential conflict of interest (see ''Relationship With Industry Policy''). Exceptions must be explained. If there is no conflict of interest, this should also be stated in the cover letter.

The corresponding author should be specified in the cover letter. All editorial communications will be sent to this author. The corresponding author will be whom we contact for submission queries.

GENERAL GUIDELINES FOR SUBMISSION OF ORIGINAL RESEARCH PAPERS

JACC: Basic to Translational Science is not restricted to page length, however the Editors prefer that manuscripts not exceed 5,500 words (including references and figure legends). Note that if you are asked to revise your paper an alternate word limit may be specified by the Editors. Illustrations and tables should be limited to those necessary to highlight key data. Please provide gender-specific data, when appropriate, in describing outcomes of epidemiologic analyses or clinical trials; or specifically state that no gender-based differences were present.

The manuscript should be submitted in Microsoft Word format and be arranged as follows: 1) title page; 2) structured abstract and key words; 3) condensed abstract; 4) abbreviations list; 5) text; 6) Perspectives (Clinical Competencies/Translational Outlook); 7) acknowledgments (if applicable); 8) Funding Sources 9) references; 10) figure titles and legends; and 11) tables.

OTHER PAPER CATEGORIES

The following information should be noted for these paper types:

STATE-OF-THE-ART PAPERS. The Editors will consider both invited and volunteered review articles. Such manuscripts must adhere to preferred length guidelines of no more than 5,000 words and require an unstructured abstract, a central illustration and a list of 3-4 brief (15 words or fewer for each bullet, or 85 characters for each bullet) bullet points that highlight the main message of the review. The first bullet should provide the translational/clinical context or background that establishes the relevance or need for this review. The second bullet should speak to the main message and focus of the review, including any recommendations made by the authors. The final bullet should summarize where the field needs to move forward from this point. Authors should detail in their cover letters how their submission differs from existing reviews on the subject.

Example of bullet points:

- The acute inflammatory response is a critical mechanism for host defense, whereas the resolution of inflammation is equally important for tissue homeostasis by delimiting the destructive effects of chronic inflammation.
- This review will discuss the role of the activation of the G-protein coupled formyl peptide receptor 2 (ALX/FPR2) in terms of regulating the resolution of inflammation following tissue injury, and will specifically focus on the role of lipid mediators in activating the ALX/FPR2 receptor.
- Additional studies will be required to clarify whether activation of the ALX/FPR2 receptor can be used therapeutically to prevent chronic inflammation, scar tissue formation following acute tissue injury.

LEADING EDGE TRANSLATIONAL RESEARCH articles are discrete, highly significant, innovative or novel findings reported in a shorter format of 3,500 words or fewer in length. Editors will review for interest within seven (7) days of submission. These may be invited or volunteered manuscripts.

TRANSLATIONAL PERSPECTIVES. Although usually invited, succinct opinion pieces relevant to a specific aspect of translational medicine will also be considered for *JACC: Basic to Translational Science*. They should not exceed 2,500 words and should have no more than a total of 2 figures and tables than 5 references.

RESEARCH LETTERS. Both Research Letters and Letters to the Editor are published under the heading "Letters." *JACC: Basic to Translation Science* will publish a limited number of research letters that are tightly focused on a new or novel research observation. Research letters will generally be solicited by the Editors; however, authors can also submit original investigations of a focused nature as a research letter. Research Letters should be submitted online at www.jaccsubmit-basictr.org. They should not exceed 1000 words, including references and figure legend, with no more than 5 references, one Figure (in no more than 2 parts) or one simple Table. A title page is required. Online or Supplemental Material is not permitted.

LETTERS TO THE EDITOR AND REPLIES. *JACC: Basic to Translation Science* will publish a limited number of letters that focus on a specific manuscript that has appeared in the journal. Letters must be submitted within 3 weeks of the issue date of the article. *JACC: Basic to Translation Science* does not consider letters to the editor on review articles, editorials, or any correspondence, including research letters. Letters should be submitted online at www.jaccsubmit-basictr.org. They should not exceed 500 words, including references and figure legend, with no more than 5 references, one Figure (in no more than 2 parts) or one simple Table. A title page is required with a unique title of 15 words or less that does not include the title of the original research paper. Replies will generally be solicited by the Editors.

MANUSCRIPT CONTENT

TITLE PAGE

Include the full title, authors' names (including full first name and middle initial and degrees), total word count, and a brief title of no more than 15 words. List the departments and institutions with which the authors are affiliated, and indicate the specific affiliations if the work is generated from more than one institution (use superscript letters [a, b, c, d], and so on). Also provide information on grants, contracts, and other forms of financial support, and list the cities and states of all foundations, funds and institutions involved in the work. Include any relationship with industry (see "Relationship With Industry Policy"). If there are no relationships with industry, this should be stated. Under the heading, "Address for correspondence," give the full name and complete postal address of the author to whom communications, author proofs, and reprint requests should be sent. Also provide telephone and fax numbers and an email address for the corresponding author.

STRUCTURED ABSTRACT

Provide a structured abstract of no more than 250 words, presenting essential data in 5 paragraphs introduced by separate headings in the following order: Objectives, Background, Methods, Results, and Conclusions. Use complete sentences. All data in the abstract must also appear in the manuscript text or tables. For general information on preparing structured abstracts, see "Haynes RB, Mulrow CD, Huth EJ, Altman DG, Gardner MJ. More informative abstracts revisited. Ann Intern Med 1990;113:69-76." An unstructured abstract is appropriate for review articles.

For accepted papers, authors will be asked to provide a list of bulleted highlights and a summary to replace the abstract (see Visual Abstract instructions below).

CONDENSED ABSTRACT

Provide a condensed abstract of no more than 100 words, stressing clinical implications, for the expanded table of contents. Include no data that do not also appear in the manuscript text or tables.

TEXT

The text should be structured as Introduction, Methods, Results, and Discussion. Use headings and subheadings in the Methods, Results, and particularly, Discussion sections. Every reference, figure, and table should be cited in the text in numerical order according to order of mention.

The abbreviations of common terms (e.g., ECG, PTCA, CABG) or acronyms (GUSTO, SOLVD, TIMI) may be used in the manuscript. On a separate page following the condensed abstract, list the selected abbreviations and their definitions (e.g., TEE = transesophageal echocardiography). The Editors may determine which lesser known terms should not be abbreviated. Please consult "Uniform Requirements for Manuscripts Submitted to Biomedical Journals: Writing and Editing for Biomedical Publication," available from http://www.ICMJE.org and most recently updated in April 2010, for appropriate use of units of measure.

STATISTICS

All publishable manuscripts will be reviewed for appropriateness and accuracy of statistical methods and statistical interpretation of results. We subscribe to the statistics section of the "Uniform Requirements for Manuscripts Submitted to Biomedical Journals: Writing and Editing for Biomedical Publication," available from http://www.ICMJE.org and most recently updated in April 2010. In the Methods section, provide a subsection detailing the statistical methods, including specific methods used to summarize the data, methods used for hypothesis testing (if any), and the level of significance used for hypothesis testing. When using more sophisticated statistical methods (beyond *t* tests, chi-square, simple linear regression), specify the statistical package, version number, and nondefault options used. For more information on statistical review, see "Glantz SA. It is all in the numbers. J Am Coll Cardiol 1993;21:835-7."

PERSPECTIVES

The authors should delineate clinical implications and translational outlook recommendations for their manuscripts. These should be listed in the manuscript after the Text and before the Acknowledgments and References. Please review the examples provided below. The implications describe the consequences of the study for current practice. The translational outlook identifies the potential barriers to clinical translation, emphasizing directions for additional research.

Clinical Competencies. Competency-based learning in cardiovascular medicine addresses the 6 domains promulgated by the Accreditation Council on Graduate Medical Education (ACGME) and endorsed by the American Board of Internal Medicine (Medical Knowledge, Patient Care and Procedural Skills, Interpersonal and Communication Skills, Systems-Based Practice, Practice-Based Learning, and Professionalism) (www.acgme.org/acgmeweb). The ACCF has adopted this format for its competency and training statements, career milestones, lifelong learning, and educational programs. The ACCF also has developed tools to assist physicians in assessing, enhancing, and documenting these competencies (www.acc.org/Lifelong-Learning-and-MOC/Resources/Competencies).

Authors are asked to consider the clinical implications of their report and identify applications in one or more of these competency domains that could be used by clinician readers to enhance their competency as professional caregivers.

This applies not only to physicians in training, but to the sustained commitment to education and continuous improvement across the span of their professional careers.

Translational Outlook. Translating biomedical research from the laboratory bench, clinical trials or global observations to the care of individual patients can expedite discovery of new diagnostic tools and treatments through multidisciplinary collaboration. Effective translational medicine facilitates implementation of evolving strategies for prevention and treatment of

disease in the community. The Institute of Medicine identified two areas needing improvement: testing basic research findings in properly designed clinical trials and, once the safety and efficacy of an intervention has been confirmed, more efficiently promulgating its adoption into standard practice (Sung NS, Crowley WF, Genel M. The meaning of translational research and why it matters. JAMA 2008;299:3140-3148).

The National Institutes of Health (NIH) has recognized the importance of translational biomedical research, emphasizing multifunctional collaborations between researchers and clinicians to leverage new technology and accelerate the delivery of new therapies to patients (www.ncats.nih.gov/about/about.html).

Authors are asked to place their work in the context of the scientific continuum, by identifying impediments and challenges requiring further investigation and anticipating next steps and directions for future research.

VISUAL ABSTRACT

A visual abstract is a single, concise, pictorial summary of the main findings of the article. Our in-house medical illustrators will create the final printable versions of these figures in consultation with the Editor-in-Chief and the authors. The visual abstract is specially designed to be placed at the beginning of the article and is accompanied by 3-5 "bulleted highlights" and a short summary written by the author and ultimately replaces the written abstract. See examples of articles with visual abstracts:

Example #1: http://basictranslational.onlinejacc.org/content/1/1-2/3

Example #2: http://basictranslational.onlinejacc.org/content/1/1-2/32

ACKNOWLEDGMENTS

Acknowledgments or appendices should be concise. Signed letters of permission from all individuals listed in the acknowledgments must be submitted to *JACC: Basic to Translational Science*.

REFERENCES

Identify references in the text by Arabic numerals in parentheses on the line. The reference list should be typed double-spaced on pages separate from the text. The references should be numbered consecutively in the order in which they are mentioned in the text.

Do not cite personal communications, manuscripts in preparation, or other unpublished data in the references; however, these may be included in the text in parentheses. *Do not cite abstracts that are older than 2 years.* Identify abstracts by the abbreviation "abstr" in parentheses. If letters to the editor are cited, identify them with the word "letter" in parentheses.

Use *Index Medicus* (National Library of Medicine) abbreviations for journal titles. It is important to note that when citing an article from the *JACC: Basic to Translational Science*, the correct citation format is J Am Coll Cardiol Basic Trans Science.

Use the following style and punctuation for references:

Periodical

List all authors if 6 or fewer, otherwise list the first 3 and add et al.; do not use periods after the authors' initials. Please do provide inclusive page numbers as in example below.

5. Glantz SA. It is all in the numbers. J Am Coll Cardiol 1993; 21:835-7.

Doi-based citation for an article in press

If the ahead-of-print date is known, provide as in example below.

16. Winchester D, Wen X, Xie L, et al. Evidence for pre-procedural statin therapy: meta-analysis of randomized trials. J Am Coll Cardiol 2010 Sept 28 [E-pub ahead of print], http://dx.doi.org/10.1016/j.jacc.2010.09.028.

If the ahead-of-print date is unknown, omit as in example below.

16. Winchester D, Wen X, Xie L, et al. Evidence for pre-procedural statin therapy: meta-analysis of randomized trials. J Am Coll Cardiol 2010 [E-pub ahead of print], http://dx.doi.org/10.1016/j.jacc.2010.

Chapter in book

Provide authors, chapter title, editor(s), book title, publisher location, publisher name, year, and inclusive page numbers.

27. Meidell RS, Gerard RD, Sambrook JF. Molecular biology of thrombolytic agents. In: Roberts R, editor. Molecular Basis of Cardiology. Cambridge, MA: Blackwell Scientific Publications, 1993:295-324.

Online media

Provide specific URL address and date information was accessed.

10. Henkel J. Testicular Cancer: Survival High With Early Treatment. FDA Consumer magazine [serial online]. January-February 1996. Available at: http://www.fda.gov/fdac/features/196_test.html. Accessed August 31, 1998.

Material presented at a meeting but not published

Provide authors, presentation title, full meeting title, meeting dates, and meeting location.

20. Eisenberg J. Market forces and physician workforce reform: why they may not work. Paper presented at: Annual Meeting of the Association of Medical Colleges; October 28, 1995; Washington, DC.

FIGURE LEGENDS

Figure legends should be typed double-spaced on pages separate from the text; figure numbers must correspond with the order in which they are mentioned in the text.

ALL FIGURES MUST HAVE A TITLE AS WELL AS A CAPTION.

For example, Figure 1: Title - Caption, etc.

All abbreviations used in the figure should be identified either after their first mention in the legend or in alphabetical order at the end of each legend.

All symbols used (arrows, circles, etc.) must be explained.

If previously published figures are used, written permission from the original publisher is required. See STM Guidelines for details: http://www.stm-assoc.org/permissions-guidelines. Cite the source of the figure in the legend.

FIGURES

Figures and graphs submitted in electronic format should be provided in EPS or TIF format. Graphics software such as Photoshop and Illustrator, NOT presentation software such as Powerpoint, CorelDraw, or Harvard Graphics, should be used to create the art. Color images must be at least 300 DPI. Gray scale images should be at least 300 DPI. Line art (black and white or color) should be at least 1200 DPI and combinations of gray scale images and line art should be at least 1200 DPI. Lettering should be of sufficient size to be legible after reduction for publication. The optimal size is 12 points. Symbols should be of a similar size. Figures should be no smaller than 13 cm× 18 cm (5″ × 7″). Please do not reduce figures to fit publication layout. If the manuscript is accepted for publication, the publisher will re-size the figures accordingly.

ALL FIGURES MUST HAVE A TITLE AND A LEGEND.

Our editors encourage authors to submit figures in color, as we feel it improves the clarity and visual impact of the images. If your original submission contains any line art or black and white figures that you would like to change to color, please email the revised color figures to the *JACC: Basic to Translational Science* editorial office during the revision process. Be sure to include correspondence, with the manuscript number, explaining the change.

Decimals, lines, and other details must be strong enough for reproduction.

Designate special features with arrows. All symbols, arrows, and lettering on halftone illustrations must contrast with the background.

TABLES

Tables should be typed double-spaced on separate sheets, with the table number and title centered above the table and explanatory notes below the table. Use Arabic numbers. Table numbers must correspond with the order cited in the text.

ALL TABLES MUST HAVE A TITLE.

Abbreviations should be listed in a footnote under the table in alphabetical order. Footnote symbols should appear in the following order: *, †, ‡, §, ||, ¶, #, **, ††, etc.

Tables should be self-explanatory, and the data presented in them should not be duplicated in the text or figures. If previously published tables are used, written permission from the copyright holder (typically the original publisher) is required. Cite the source of the table in the legend.

VIDEO REQUIREMENTS

Inclusion of videos in the published paper is at the discretion of the Editors.

1. Video submissions for viewing online should be one of the following formats: Audio Video Interleave (.avi), MPEG (.mpg), or Quick Time (.qt, .mov).

   AVI files can be displayed via Windows Media Player

   MPEG files can be displayed via Windows Media Player

   http://www.microsoft.com/windows/windowsmedia

   http://www.microsoft.com/windows/windowsmedia/players.aspx

   Quick Time files require Quick Time software (free) from Apple, http://www.apple.com/quicktime/download/index.html
2. Videos should be brief (<2-5 min). Longer videos will require longer download times and may have difficulty playing online. Videos should be restricted to the most critical aspects of your research. A longer procedure can be restructured as several shorter videos and submitted in that form.
3. It is advisable to compress files to use as little bandwidth as possible and to avoid overly long download times. Video files should be no larger than 5 megabytes. This is a suggested maximum. If files are larger please contact the *JACC: Basic to Translational Science* office.
4. A video legends page giving a brief description of the content of each video should be included in the manuscript. Please note that ALL videos must be linked to figures or panels of a figure(s).
5. If your paper is accepted for publication you may wish to supply the editorial office with several different resolutions of your video files. This will allow viewers with slower connections to download a lower resolution version of your video.

It is important to note that when citing an article from *JACC: Basic to Translational Science*, the correct citation format is J Am Coll Cardiol Basic Trans Science

JACC: BASIC TO TRANSLATIONAL SCIENCE VOL. 4, NO. 7, 2019

CLINICAL RESEARCH

Pharmacodynamic Effects of Vorapaxar in Patients With and Without Diabetes Mellitus

Results of the OPTIMUS-5 Study

Francesco Franchi, MD,[a] Fabiana Rollini, MD,[a] Victor Kairouz, MD,[a] Jose Rivas Rios, MD,[a] Andrea Rivas, MD,[a] Malhar Agarwal, MD,[a] Maryuri Briceno, MD,[a] Mustafa Wali, MD,[a] Ahmed Nawaz, MD,[a] Gabriel Silva, MD,[a] Zubair Shaikh, MD,[a] Naji Maaliki, MD,[a] Latonya Been, AAS,[a] Jason Piraino, DPM,[b] Andres M. Pineda, MD,[a] Siva Suryadevara, MD,[a] Daniel Soffer, MD,[a] Martin M. Zenni, MD,[a] Lisa K. Jennings, PHD,[c] Theodore A. Bass, MD,[a] Dominick J. Angiolillo, MD, PHD[a]

JACC: BASIC TO TRANSLATIONAL SCIENCE CME/MOC/ECME

This article has been selected as this month's *JACC: Basic to Translational Science* CME/MOC/ECME activity, available online at http://www.acc.org/jacc-journals-cme by selecting the *JACC* Journals CME/MOC/ECME tab.

Accreditation and Designation Statement

The American College of Cardiology Foundation (ACCF) is accredited by the Accreditation Council for Continuing Medical Education (ACCME) and the European Board for Accreditation in Cardiology (EBAC) to provide continuing medical education for physicians.

The ACCF designates this Journal-based CME/MOC/ECME activity for a maximum of 1 AMAPRA Category 1 Credit or 1 EBAC Credit. Physicians should only claim credit commensurate with the extent of their participation in the activity.

Successful completion of this CME activity, which includes participation in the evaluation component, enables the participant to earn up to 1 Medical Knowledge MOC point in the American Board of Internal Medicine's (ABIM) Maintenance of Certification (MOC) program. Participants will earn MOC points equivalent to the amount of CME credits claimed for the activity. It is the CME activity provider's responsibility to submit participant completion information to ACCME for the purpose of granting ABIM MOC credit.

Pharmacodynamic Effects of Vorapaxar in Patients With and Without Diabetes Mellitus: Results of the OPTIMUS-5 Study will be accredited by the European Board for Accreditation in Cardiology (EBAC) for 1 hour of External CME credits. Each participant should claim only those hours of credit that have actually been spent in the educational activity. The Accreditation Council for Continuing Medical Education (ACCME) and the European Board for Accreditation in Cardiology (EBAC) have recognized each other's accreditation systems as substantially equivalent. Apply for credit through the post-course evaluation.

Method of Participation and Receipt of CME/MOC/ECME Certificate

To obtain credit for *JACC: Basic to Translational Science* CME/MOC/ECME, you must:

1. Be an ACC member or JACBTS subscriber.
2. Carefully read the CME/MOC/ECME-designated article available online and in this issue of the *journal*.
3. Answer the post-test questions. At least 2 questions provided must be answered correctly to obtain credit.
4. Complete a brief evaluation.
5. Claim your CME/MOC/ECME credit and receive your certificate electronically by following the instructions given at the conclusion of the activity.

CME/MOC/ECME Objective for This Article: Upon completion of this activity, the learner should be able to: 1) compare the mechanism of action of various antiplatelet agents used for the management of acute coronary syndromes; 2) identify the indications and contraindications for antiplatelet agents used in acute coronary syndromes; and 3) discuss the benefits and risks of preventative aspirin in diabetic patients.

CME/MOC/ECME Editor Disclosure: CME/MOC/ECME Editor L. Kristin Newby, MD, is supported by research grants from Amylin, Bristol-Myers Squibb Company, GlaxoSmithKline, Sanofi, Verily Life Sciences (formerly Google Life Sciences), the MURDOCK Study, NIH, and PCORI; receives consultant fees/honoraria from BioKier, DemeRx, MedScape/TheHeart.org, Metanomics, Philips Healthcare, Roche Diagnostics, CMAC Health Education & Research Institute; serves as an Officer, Director, Trustee, or other fiduciary role for the AstraZeneca HealthCare Foundation and the Society of Chest Pain Centers (now part of ACC); and serves in another role for the American Heart Association and is the Deputy Editor of *JACC: Basic to Translational Science*.

Author Disclosures: The study was originally funded by a grant from Merck until transfer of marketing rights of vorapaxar, including grant responsibilities, to Aralez. At the time of transfer, Merck had funded 60% of overall grant costs. Following such transfer, Aralez filed for bankruptcy and did not cover any of the residual grant costs, which was completed using research funds from the Division of Cardiology, University of Florida College of Medicine-Jacksonville. Upon completion of the study, Deerfield acquired marketing rights of vorapaxar and provided a nominal fee for the final phases of investigator-initiated research studies conducted with vorapaxar at our institution (NCT02548650 and NCT02545933). Dr. Franchi has received payment as an individual for consulting fees or honoraria from AstraZeneca and Sanofi. Dr. Rollini has received payment as an individual for consulting fees or honoraria from Chiesi. Dr. Angiolillo has received payment as an

ISSN 2452-302X https://doi.org/10.1016/j.jacbts.2019.07.011

individual for consulting fees or honoraria from Amgen, Aralez, AstraZeneca, Bayer, Biosensors, Boehringer Ingelheim, Bristol-Myers Squibb, Chiesi, Daiichi-Sankyo, Eli Lilly, Haemonetics, Janssen, Merck, PhaseBio, PLx Pharma, Pfizer, Sanofi, and The Medicines Company; participation in review activities from CeloNova and St. Jude Medical; and institutional payments for grants from Amgen, AstraZeneca, Bayer, Biosensors, CeloNova, CSL Behring, Daiichi-Sankyo, Eisai, Eli Lilly, Gilead, Idorsia, Janssen, Matsutani Chemical Industry Co., Merck, Novartis, Osprey Medical, and Renal Guard Solutions. Dr. Jennings has received payments as an individual for consulting fees or honoraria from Bayer, Janssen, PhaseBio, and Portola; and institutional payments for grants from Janssen and In Motion Musculoskeletal Institute. All other authors have reported that they have no relationships relevant to the contents of this paper to disclose.

Medium of Participation: Online (article and quiz).

CME/MOC/ECME Term of Approval

Issue Date: November 2019
Expiration Date: October 31, 2020

From the [a]Division of Cardiology, Department of Medicine, University of Florida College of Medicine-Jacksonville, Jacksonville, Florida; [b]Division of Foot and Ankle, Department of Orthopaedic Surgery and Rehabilitation, University of Florida College of Medicine-Jacksonville, Jacksonville, Florida; and [c]CirQuest Labs, Memphis, Tennessee. The present study was investigator-initiated. The study was originally funded by a grant from Merck until transfer of marketing rights of vorapaxar, including grant responsibilities, to Aralez. At the time of transfer, Merck had funded 60% of overall grant costs. Following such transfer, Aralez filed for bankruptcy and did not cover any of the residual grant costs, which was completed using research funds from the Division of Cardiology, University of Florida College of Medicine-Jacksonville. Upon completion of the study, Deerfield acquired marketing rights of vorapaxar and provided a nominal fee for the final phases of investigator-initiated research studies conducted with vorapaxar at our institution (NCT02548650 and NCT02545933). Dr. Franchi has received payment as an individual for consulting fees or honoraria from AstraZeneca and Sanofi. Dr. Rollini has received payment as an individual for consulting fees or honoraria from Chiesi. Dr. Angiolillo has received payment as an individual for consulting fees or honoraria from Amgen, Aralez, AstraZeneca, Bayer, Biosensors, Boehringer Ingelheim, Bristol-Myers Squibb, Chiesi, Daiichi-Sankyo, Eli Lilly, Haemonetics, Janssen, Merck, PhaseBio, PLx Pharma, Pfizer, Sanofi, and The Medicines Company; participation in review activities from CeloNova and St. Jude Medical; and institutional payments for grants from Amgen, AstraZeneca, Bayer, Biosensors, CeloNova, CSL Behring, Daiichi-Sankyo, Eisai, Eli Lilly, Gilead, Idorsia, Janssen, Matsutani Chemical Industry Co., Merck, Novartis, Osprey Medical, and Renal Guard Solutions. Dr. Jennings has received payments as an individual for consulting fees or honoraria from Bayer, Janssen, PhaseBio, and Portola; and institutional payments for grants from Janssen and In Motion Musculoskeletal Institute. All other authors have reported that they have no relationships relevant to the contents of this paper to disclose.
The authors attest they are in compliance with human studies committees and animal welfare regulations of the authors' institutions and Food and Drug Administration guidelines, including patient consent where appropriate. For more information, visit the *JACC: Basic to Translational Science* author instructions page.

Manuscript received July 20, 2019; revised manuscript received July 31, 2019, accepted July 31, 2019.

Pharmacodynamic Effects of Vorapaxar in Patients With and Without Diabetes Mellitus

Results of the OPTIMUS-5 Study

Francesco Franchi, MD,[a] Fabiana Rollini, MD,[a] Victor Kairouz, MD,[a] Jose Rivas Rios, MD,[a] Andrea Rivas, MD,[a] Malhar Agarwal, MD,[a] Maryuri Briceno, MD,[a] Mustafa Wali, MD,[a] Ahmed Nawaz, MD,[a] Gabriel Silva, MD,[a] Zubair Shaikh, MD,[a] Naji Maaliki, MD,[a] Latonya Been, AAS,[a] Jason Piraino, DPM,[b] Andres M. Pineda, MD,[a] Siva Suryadevara, MD,[a] Daniel Soffer, MD,[a] Martin M. Zenni, MD,[a] Lisa K. Jennings, PHD,[c] Theodore A. Bass, MD,[a] Dominick J. Angiolillo, MD, PHD[a]

VISUAL ABSTRACT

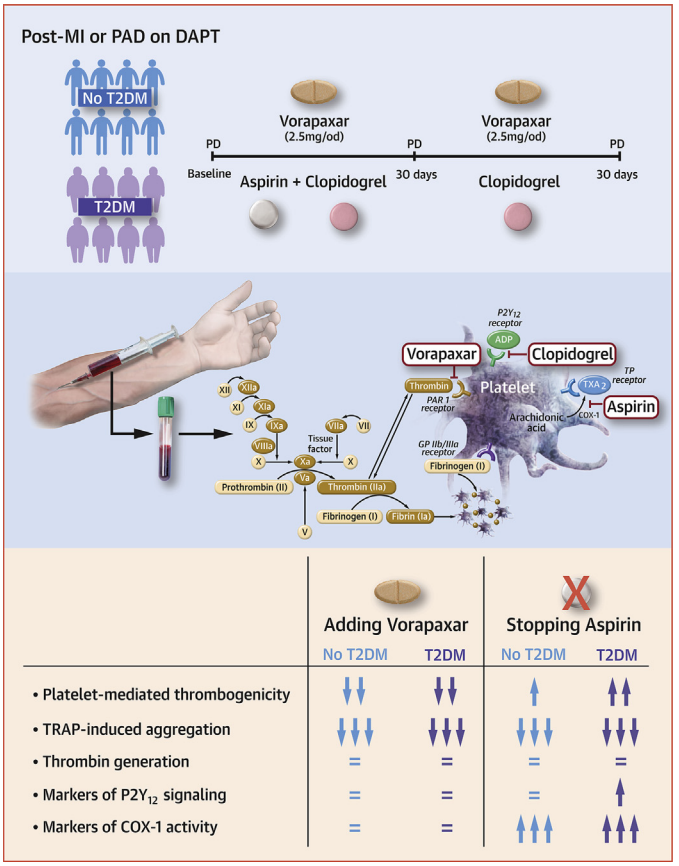

Franchi, F. et al. J Am Coll Cardiol Basic Trans Science. 2019;4(7):763–75.

HIGHLIGHTS

- **Vorapaxar reduces thrombotic cardiovascular events in patients with atherosclerotic disease, with enhanced effects in those with DM.**
- **Adjunctive vorapaxar therapy reduces platelet-mediated thrombogenicity without affecting clot kinetics in both patients with and those without DM having prior MI/PAD on dual antiplatelet therapy with aspirin and clopidogrel.**
- **The pharmacodynamic effects of vorapaxar occur via selective blockade of the PAR-1 on the platelet membrane without apparent interplay with other platelet signaling pathways.**
- **Aspirin withdrawal, which leaves patients on a background of clopidogrel and vorapaxar, increases markers specific to COX-1-mediated blockade, leading to an increase in platelet-mediated global thrombogenicity, particularly among patients with DM.**

JACC: BASIC TO TRANSLATIONAL SCIENCE VOL. 4, NO. 7, 2019
NOVEMBER 2019:763–75

ABBREVIATIONS AND ACRONYMS

ADP = adenosine diphosphate

CAT = collagen-related peptide + adenosine diphosphate + thrombin receptor activating peptide

CI = confidence interval

COX = cyclooxygenase

DAPT = dual antiplatelet therapy

DM = diabetes mellitus

LTA = light transmittance aggregometry

MI = myocardial infarction

MPA = maximum platelet aggregation

o.d. = once daily

PAD = peripheral arterial disease

PAR = protease-activated receptor

PD = pharmacodynamic

TRAP = thrombin receptor activating peptide

TXB_2 = thromboxane B_2

VASP = vasodilator-stimulated phosphoprotein

SUMMARY

Vorapaxar reduces thrombotic cardiovascular events at the expense of increased bleeding. However, the differential pharmacodynamic (PD) effects of vorapaxar according to diabetes mellitus (DM) status are unknown. Moreover, although withdrawal of aspirin has emerged as a bleeding reduction strategy, the PD effects of stopping aspirin in patients treated with vorapaxar also are unknown. In this prospective PD investigation, vorapaxar was associated with reduced platelet-mediated thrombogenicity without affecting clot kinetics irrespective of DM status. However, platelet-mediated thrombogenicity increased after aspirin withdrawal, particularly among patients with DM. (Optimizing anti-Platelet Therapy In diabetes MellitUS-5 Study [OPTIMUS-5]; NCT02548650) (J Am Coll Cardiol Basic Trans Science 2019;4:763–75)

Patients with diabetes mellitus (DM) remain at increased risk for recurrent atherothrombotic events despite standard-of-care oral antiplatelet therapy (1,2). This risk is in part due to their hyperreactive platelet phenotype, which can contribute to inadequate response to oral antiplatelet agents, including dual antiplatelet therapy (DAPT) with aspirin and clopidogrel, which is commonly used for secondary prevention of ischemic recurrences (2–4). Importantly, platelets of patients with DM are characterized by up-regulation of platelet signaling pathways that are not inhibited by DAPT, including thrombin-mediated signaling (2). Of note, thrombin is the most potent inducer of platelet activation and plays a key role in thrombus formation (5,6). Hence, modulating the effects of thrombin represents an attractive option to reduce the risk of thrombotic complications, particularly in high-risk patients such as those with DM (7).

SEE PAGE 776

Vorapaxar is a novel, orally active, highly selective, competitive, slowly reversible protease-activated receptor (PAR)-1 inhibitor, which exerts potent inhibition of thrombin-mediated platelet aggregation (7–9). In a large-scale clinical trial, vorapaxar (as adjunct to standard-of-care antiplatelet therapy, mostly aspirin and clopidogrel) significantly reduced recurrent thrombotic events in patients with previous atherothrombosis, particularly those with prior myocardial infarction (MI) or peripheral arterial disease (PAD), albeit at the cost of increased bleeding (10–12). Notably, the absolute risk reduction of thrombotic complications associated with the adjunctive use of vorapaxar was greater among DM compared with patients without DM (13). These clinical observations in conjunction with the distinctive platelet phenotype of patients with DM make these patients particularly attractive for treatment with vorapaxar. However, the differential pharmacodynamic (PD) effects of vorapaxar in DM compared with patients without DM are unknown. Moreover, despite the proven efficacy of vorapaxar in reducing thrombotic complications, the increased risk of bleeding complications remains of concern. Withdrawal of aspirin when potent adjunctive antithrombotic therapies are used has been suggested as a strategy to reduce the risk of bleeding (14). Reduction of bleeding complications with aspirin withdrawal has been consistently shown among patients undergoing coronary stenting treated with a $P2Y_{12}$ receptor inhibitor (mostly clopidogrel) and requiring oral anticoagulant therapy (i.e., blockade of circulating thrombin) (15–18). However, the PD effects associated with a combination of vorapaxar and clopidogrel, without aspirin, is unknown.

METHODS

STUDY DESIGN AND PARTICIPANTS. The OPTIMUS (Optimizing anti-Platelet Therapy In diabetes MellitUS)-5 study (NCT02548650) was a prospective, parallel-design, open-label investigation aimed at assessing the PD effects of adjunctive use of vorapaxar in patients with a history of MI or PAD, with and without type 2 DM, on treatment with DAPT (aspirin and clopidogrel) and assessing the PD impact associated with discontinuation of aspirin therapy. The study was conducted in patients with a history of MI or PAD in line with the approved indication for use of vorapaxar (19,20). In particular, vorapaxar is approved by the United States Food and Drug Administration and the European Medicines Agency for the reduction of thrombotic cardiovascular events in patients with a history of MI or PAD and is required to be used in addition to standard-of-care antiplatelet therapy with aspirin and/or clopidogrel (20,21). The study was performed at the University of Florida Health-Jacksonville (Jacksonville, Florida). Patients

FIGURE 1 Study Design

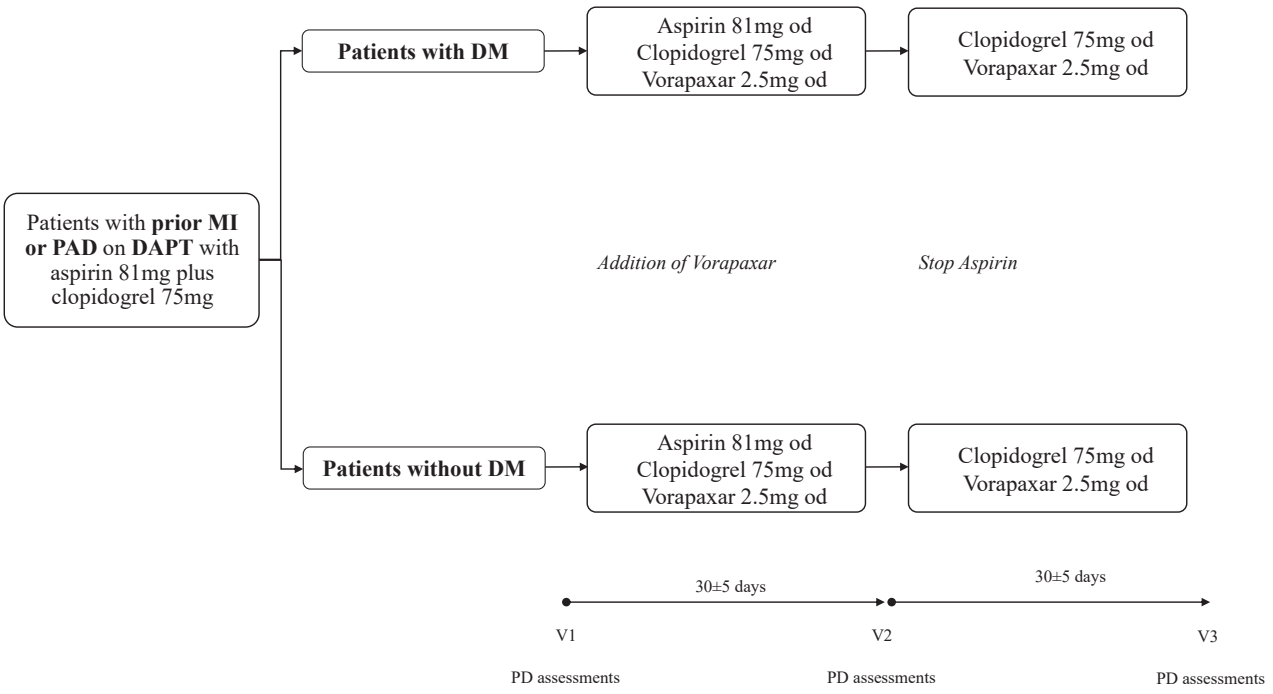

DAPT = dual antiplatelet therapy; DM = diabetes mellitus; MI = myocardial infarction; od = once daily; PAD = peripheral arterial disease; PD = pharmacodynamics.

with a history of MI or PAD older than 18 years on DAPT with aspirin and clopidogrel as part of their standard of care for at least 2 weeks were screened for study eligibility at the outpatient cardiology clinics of our institution (see Supplemental Material for details on study inclusion and exclusion criteria). The study complied with the Declaration of Helsinki and was approved by the Western Institutional Review Board. All patients gave written informed consent.

Patients on DAPT with aspirin and clopidogrel who met study entry criteria were divided into 2 cohorts according to the presence or absence of type 2 DM. Type 2 DM status was defined according to the World Heart Organization criteria, and patients needed to be on treatment with oral hypoglycemic agents and/or insulin for at least 2 months, without any changes in regimen (22). Vorapaxar (2.5 mg once daily [o.d.]) was added to the standard DAPT regimen of aspirin (81 mg o.d.) plus clopidogrel (75 mg o.d.), also known as triple therapy. Triple therapy was maintained for 30 ± 5 days. Patients then stopped taking aspirin and maintained dual therapy with vorapaxar (2.5 mg o.d.) plus clopidogrel (75 mg o.d.) for 30 ± 5 days. Blood sampling for PD testing was conducted at 3 time points: baseline (while patients were on standard DAPT); after 30 ± 5 days of triple therapy; and 30 ± 5 days after dual therapy. At each time point, blood was collected before the morning dose of clopidogrel and vorapaxar, in order to measure trough levels of platelet inhibition. Laboratory personnel were blinded to treatment assignments. Compliance to randomized treatment was assessed by pill count and patient interview. After completing the study, patients resumed their standard DAPT regimen. A flow diagram of the study design is illustrated in **Figure 1**.

BLOOD SAMPLING AND LABORATORY ASSESSMENTS. Peripheral venous blood samples were drawn through a short venous catheter inserted into a forearm vein and collected in citrate, EDTA, and serum tubes as appropriate for assessments. The first 2 to 4 ml of blood was discarded to avoid spontaneous platelet activation. Blood sampling for PD assessments was performed at 3 time points as indicated in the study design section. Multiple assays were used, including light transmittance aggregometry (LTA); whole blood vasodilator-stimulated phosphoprotein (VASP); TEG 6s (Haemonetics Corp., Braintree, Massachusetts) thrombelastograph coagulation analyzer, which also included the platelet mapping assay using adenosine diphosphate (ADP); and enzyme-linked immunosorbent assay-based assessment of serum thromboxane

TABLE 1 Baseline Characteristics of the PD Population

	DM (n = 30)	Non-DM (n = 34)	p Value
Age, yrs	61 ± 8	56 ± 9	0.015
Male	23 (77)	23 (67)	0.579
BMI, kg/m^2	31 ± 5	32 ± 8	0.757
Race			0.487
White	15 (50)	22 (65)	
Black	14 (47)	11 (32)	
Other	1 (3)	1 (3)	
Enrollment criteria*			0.002
Prior MI	13 (43)	28 (82)	
PAD	17 (57)	6 (18)	
CKD	2 (7)	2 (6)	1
Hypertension	29 (97)	25 (74)	0.015
Dyslipidemia	27 (90)	22 (65)	0.020
Active smoking	10 (33)	14 (41)	0.408
CAD	22 (73)	30 (88)	0.199
Prior PCI	20 (67)	25 (73)	0.593
Prior CABG	7 (23)	4 (12)	0.322
Creatinine, mg/dl	1.1 ± 0.3	0.9 ± 0.2	0.073
CrCl, ml/min	102 ± 40	117 ± 58	0.232
Platelet count, 10^3/μl	249 ± 62	227 ± 59	0.160
Hematocrit, %	39 ± 4	41 ± 4	0.182
Hemoglobin, g/dl	12.9 ± 1.3	13.5 ± 1.6	0.145
Medications			
Insulin therapy	16 (53)	0 (0)	<0.001
OAD	23 (77)	0 (0)	<0.001
Beta-blockers	27 (90)	30 (88)	1
ACE inhibitor/ARB	25 (83)	21 (62)	0.093
Statins	30 (100)	32 (94)	0.494

Values are mean ± SD or n (%). *2 patients categorized as MI also had PAD (see Supplemental Material for definition of study entry criteria).

ACE = angiotensin-converting enzyme; ARB = angiotensin receptor blocker; BMI = body mass index; CABG = coronary artery bypass graft; CAD = coronary artery disease; CKD = chronic kidney disease; CrCl = creatinine clearance; DM = diabetes mellitus; MI = myocardial infarction; OAD = oral antidiabetic drug; PAD = peripheral arterial disease; PCI = percutaneous coronary intervention; PD = pharmacodynamic.

B_2 (TXB_2) (23-26). A detailed description of the assays is provided in the Supplemental Material. Assessments were performed and described with the following objectives: 1) to define the PD effect of vorapaxar on thrombin-mediated effects on platelets and systemically; to this extent, LTA following thrombin receptor activating peptide (TRAP) (15 μM) stimuli and markers of clot kinetics using the TEG 6s system were utilized, respectively; 2) to define the PD effect of vorapaxar on platelet-mediated thrombogenicity; to this extent, LTA following stimuli with combination of 2 μg/ml collagen-related peptide + 5 μM ADP + 15 μM TRAP (CAT) was used; and 3) to define the PD effect of vorapaxar on $P2Y_{12}$ inhibition induced by clopidogrel and the impact of aspirin withdrawal; to this extent LTA following stimuli with ADP (20 μM) and VASP as well as markers sensitive to cyclooxygenase (COX)-1 blockade, including LTA following arachidonic acid (1 mM) and collagen (3 μg/ml) stimuli, and measurement of serum TXB_2 levels, respectively, were assessed. LTA results are reported as maximum platelet aggregation (MPA%), VASP results as platelet reactivity index, and serum TXB_2 levels in ng/ml.

STUDY ENDPOINTS AND SAMPLE SIZE CALCULATION. The primary endpoint of our study was the comparison of CAT-induced MPA measured by LTA between triple (vorapaxar plus DAPT) and dual (vorapaxar plus clopidogrel) therapy. The rationale for choosing CAT-induced MPA for the primary endpoint was that this combination of agonist is more reflective of global thrombogenicity as it stimulates multiple platelet signaling pathways. We hypothesized that dual therapy would be noninferior to triple therapy after 30 ± 5 days of treatment in both patients with and without DM. Under the null hypothesis that the mean CAT-induced MPA between dual and triple therapy is not equal to 0 and a common standard deviation of 13%, a sample size of 28 patients per group with a valid primary endpoint time point allowed for the 95% confidence interval (CI) to stay within ±10% with 80% power and 2-sided $\alpha = 0.05$. Considering the 2 groups (patients with and without DM), a total of 56 patients with valid primary endpoint data needed to be included. Assuming up to 40% rate of invalid results due to hemolysis or dropout, we estimated that up to 79 patients would need to be enrolled. Noninferiority was assessed using a 95% CI of the difference in mean MPA between the 2 arms. As there were no preliminary data in this setting, the 10% noninferiority margin was arbitrarily defined. Mean values of platelet aggregation and variability were estimated based on previous data of vorapaxar (26). Our approach for the statistical assumption is in agreement with recommendations for pilot investigations (27).

Other exploratory objectives included comparisons between patients with and without DM of all PD parameters measured by multiple assays, and comparisons between levels of platelet inhibition achieved by DAPT (baseline therapy) versus levels achieved by adding vorapaxar. The effects of additive inhibition of the thrombin-mediated platelet activation pathway, with or without aspirin therapy, on serum thromboxane levels also were evaluated.

STATISTICAL ANALYSIS. Categorical variables are expressed as frequencies and proportions. Continuous variables were analyzed for normal distribution with the Kolmogorov-Smirnov test and are expressed as mean ± SD. Comparisons between categorical variables were performed using the 2-tailed Fisher exact test or the Pearson chi-square test. The

FIGURE 2 Thrombin-Mediated Effects on Platelets and Systemically

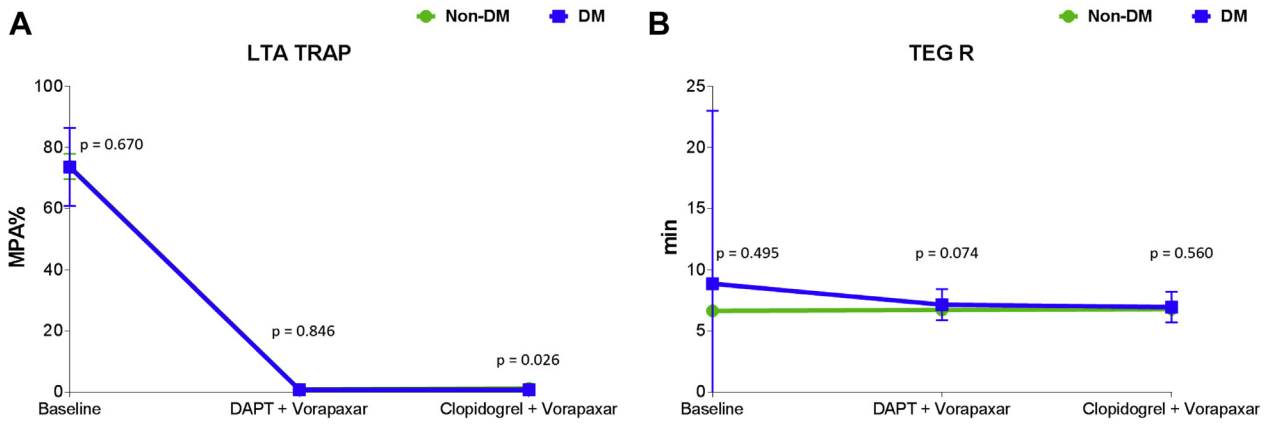

(A) Thrombin receptor activating peptide (TRAP)-induced maximal platelet aggregation (MPA%) measured by light transmittance aggregometry (LTA). The p values represent comparisons between the 2 groups at each time point. Error bars indicate SD. Intragroup comparisons for non-DM: Baseline versus DAPT + vorapaxar: mean difference = 72; 95% confidence interval (CI): 67 to 77; $p < 0.001$. Baseline versus clopidogrel + vorapaxar: mean difference = 72; 95% CI: 67 to 77; $p < 0.001$. DAPT + vorapaxar versus clopidogrel + vorapaxar: mean difference = 0.3; 95% CI: −1.6 to 0.72; $p = 0.20$. Intragroup comparisons for DM: Baseline versus DAPT + vorapaxar: mean difference = 73; 95% CI: 68 to 78; $p < 0.001$. Baseline versus clopidogrel + vorapaxar: mean difference = 73; 95% CI: 68 to 78; $p < 0.001$. DAPT + vorapaxar versus clopidogrel + vorapaxar: mean difference = 0; 95% CI: −0.35 to 0.35; $p = 1.00$. **(B)** Reaction time (R) measured by thromboelastography (TEG) using kaolin as agonist. The p values represent comparisons between the 2 groups at each time point. Error bars indicate SD. Intragroup comparisons for non-DM: Baseline versus DAPT + vorapaxar: $p = 0.736$. Baseline versus clopidogrel + vorapaxar: $p = 0.829$. DAPT + vorapaxar versus clopidogrel + vorapaxar: $p = 0.886$. Intragroup comparisons for DM: Baseline versus DAPT + vorapaxar: $p = 0.436$. Baseline versus clopidogrel + vorapaxar: $p = 0.416$. DAPT + vorapaxar versus clopidogrel + vorapaxar: $p = 0.412$. Abbreviations as in Figure 1.

Student's *t*-test was used to compare continuous variables. A full-factorial repeated measure analysis of variance method for dependent variables with a general linear model was used to evaluate intragroup comparisons between time points (3). Least square mean differences in MPA between groups and the corresponding 2-sided 95% CI for the difference were obtained to assess noninferiority based on the linear model. The Student's *t*-test was used to compare continuous variables between groups. Platelet reactivity results are reported as mean ± SD for the detailed analyses. p Values are used to report superiority testing, and CIs are used to determine noninferiority. A 2-tailed $p < 0.05$ is considered to indicate a statistically significant difference for all the analyses performed. Given the exploratory nature of superiority intragroup comparisons, adjustment for multiple comparisons was not performed. Statistical analysis was performed using SPSS version 25.0 software (SPSS Inc., Chicago, Illinois).

The safety population was composed of all patients exposed to at least 1 dose of study medication (any time from enrollment until completion of the study). Any adverse event during the study period was recorded. The PD population included all patients with PD data and without a major protocol deviation thought to affect the PD effects of vorapaxar, aspirin, and clopidogrel. The PD population was used for analysis of all primary and secondary PD variables.

RESULTS

PATIENT POPULATION. Between March 25, 2016 and October 22, 2018, 132 patients were screened. A total of 71 patients on maintenance therapy agreed to participate in the study; 5 patients were not eligible for randomization due to the presence of an exclusion criteria. A total of 66 patients (30 with DM, 36 without DM) were exposed to at least 1 dose of study medication, representing the safety population. Two patients were not compliant with medications and therefore were excluded from the PD analysis. Thus, a total of 64 patients (30 with DM, 34 without DM) represented the PD population of the study. Of these patients, 56 (28 with DM, 28 without DM) had valid primary endpoint data. Prior MI and PAD were the enrollment criteria for 41 (64%) and 23 (36%) patients, respectively. Baseline characteristics of the study population are summarized in Table 1. Patients with DM were older and had higher rates of PAD, hypertension, and hyperlipidemia. No ischemic or Bleeding Academic Research Consortium type 2 to 5 bleeding events were observed. One DM patient had a Bleeding Academic Research Consortium type 1 bleeding

FIGURE 3 Markers of Platelet-Mediated Thrombogenicity

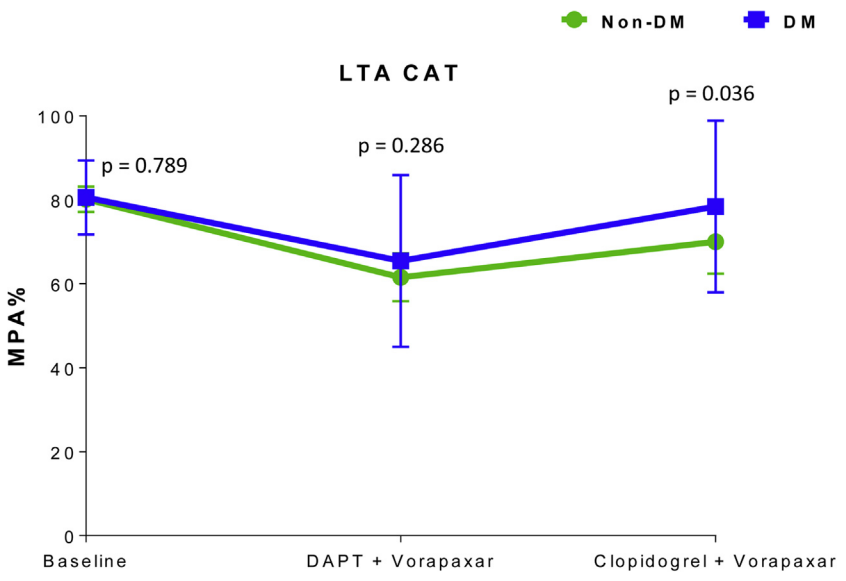

CAT-induced maximal platelet aggregation (MPA%) measured by light transmittance aggregometry (LTA). The p values represent comparisons between the 2 groups at each time point. Error bars indicate SD. The agonist CAT is a combination of collagen-related peptide, adenosine diphosphate, and thrombin receptor activating peptide. Intragroup comparisons for non-DM: Baseline versus DAPT + vorapaxar: mean difference = 20; 95% CI: 15 to 25; $p < 0.001$. Baseline versus clopidogrel + vorapaxar: mean difference = 10; 95% CI: 3 to 16; $p < 0.001$. DAPT + vorapaxar versus clopidogrel + vorapaxar: mean difference = 10; 95% CI: 4 to 16; $p = 0.003$. Intragroup comparisons for DM: Baseline versus DAPT + vorapaxar: mean difference = 15; 95% CI: 7 to 23; $p < 0.001$. Baseline versus clopidogrel + vorapaxar: mean difference = 3; 95% CI: −6 to 11; $p = 0.542$. DAPT + vorapaxar versus clopidogrel + vorapaxar: mean difference = 12; 95% CI: 3 to 21; $p = 0.010$. Abbreviations as in Figure 1.

(hematuria) while on triple therapy that led to study drug discontinuation, and 11 patients (7 with DM, 4 without DM) had nonbleeding adverse events (see Supplemental Material for details).

PD FINDINGS. Effects of vorapaxar on thrombin-mediated effects. Adjunctive treatment with vorapaxar was associated with complete blockade of TRAP-induced platelet aggregation ($p < 0.001$). Complete suppression of TRAP-induced platelet aggregation persisted after discontinuation of aspirin therapy ($p < 0.001$). Overall, such effects were consistent irrespective of DM status (Figure 2A). On the contrary, vorapaxar did not affect markers of clot kinetics, including speed of thrombin generation, which remained unvaried even after discontinuation of aspirin therapy (Figure 2B). Findings were consistent irrespective of DM status (Supplemental Figures 1 to 4). These observations are supportive of the platelet-specific, and not systemic, effects of vorapaxar on modulating thrombin-mediated effects.

Effects of vorapaxar on global thrombogenicity. Adding vorapaxar to DAPT significantly reduced CAT-induced aggregation in both patients with DM (mean difference = 15; 95% CI: 7 to 23; $p < 0.001$) and patients without DM (mean difference = 20; 95% CI: 15 to 25; $p < 0.001$). However, stopping aspirin was associated with an increase in CAT-induced aggregation in both patients with DM (mean difference = 12; 95% CI: 3 to 21; $p = 0.010$) and patients without DM (mean difference =10; 95% CI: 4 to 16; $p = 0.003$), thus not meeting the primary endpoint of non-inferiority (Figure 3). After aspirin withdrawal, CAT-induced aggregation was significantly lower compared with baseline in patients without DM (mean difference = 10; 95% CI: 3 to 16; $p < 0.001$) but not in DM (mean difference = 3; 95% CI; -6 to 11; $p = 0.542$) patients. Overall, the magnitude of increase in CAT-induced aggregation after aspirin withdrawal in the presence of vorapaxar and clopidogrel therapy was higher in DM patients compared with patients without DM ($p = 0.036$) (Figure 3).

Effects of vorapaxar on modulating $P2Y_{12}$ inhibition induced by clopidogrel in the presence and absence of aspirin. Adding vorapaxar to DAPT did not affect markers assessing $P2Y_{12}$ inhibition using all assays, including LTA and VASP. After aspirin withdrawal, there were no significant differences in levels of these

FIGURE 4 Markers of $P2Y_{12}$ Signaling

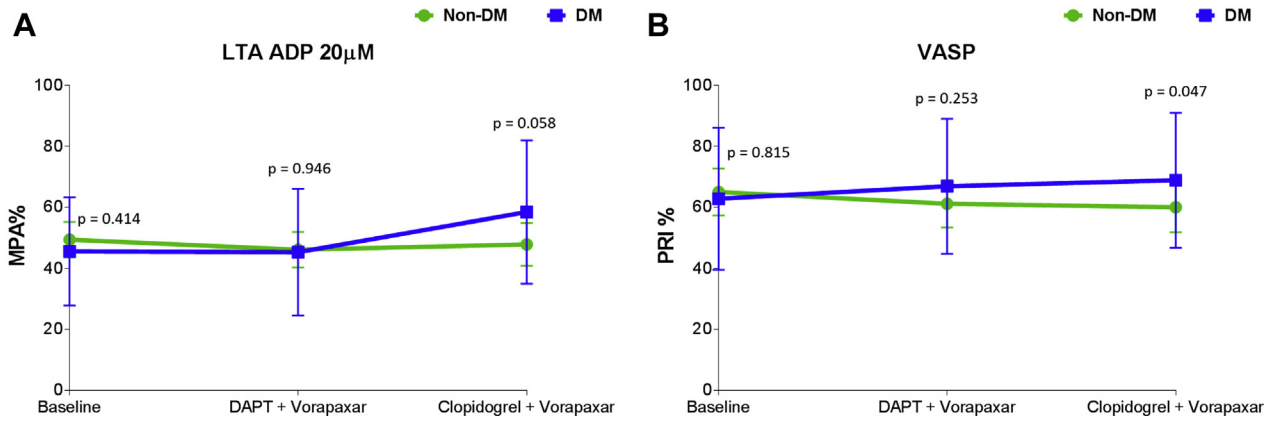

(A) Adenosine diphosphate (ADP)-induced maximal platelet aggregation (MPA%) measured by light transmittance aggregometry (LTA). The p values represent comparisons between the 2 groups at each time point. Error bars indicate SD. Intragroup comparisons for non-DM: Baseline versus DAPT + vorapaxar: p = 0.166. Baseline versus clopidogrel + vorapaxar: p = 0.811. DAPT + vorapaxar versus clopidogrel + vorapaxar: p = 0.269. Intragroup comparisons for DM: Baseline versus DAPT + vorapaxar: p = 0.837. Baseline versus clopidogrel + vorapaxar: mean difference = 12; 95% CI: 5 to 20; p = 0.002. DAPT + vorapaxar versus clopidogrel + vorapaxar: mean difference = 13; 95% CI: 5 to 20; p = 0.002. **(B)** Platelet reactivity index (PRI) measured by vasodilator-stimulated phosphoprotein (VASP). The p values represent comparisons between the 2 groups at each time point. Error bars indicate SD. Intragroup comparisons for non-DM: Baseline versus DAPT + vorapaxar: p = 0.063. Baseline versus clopidogrel + vorapaxar: p = 0.067. DAPT + vorapaxar versus clopidogrel + vorapaxar: p = 0.959. Intragroup comparisons for DM: Baseline versus DAPT + vorapaxar: p = 0.296. Baseline versus clopidogrel + vorapaxar: p = 0.142. DAPT + vorapaxar versus clopidogrel + vorapaxar: p = 0.398. Abbreviations as in Figure 1.

markers among patients without DM, but these levels modestly increased in patients with DM (Figure 4, Supplemental Figure 5). Aspirin withdrawal was associated with a marked increase in makers sensitive to COX-1 blockade, including arachidonic acid- and collagen-induced aggregation as well as serum TXB_2 levels, in both patients with and without DM (Figure 5, Supplemental Figure 6).

DISCUSSION

Vorapaxar is a PAR-1 inhibitor clinically approved for reduction of thrombotic cardiovascular events in patients with a history of MI or PAD treated with standard-of-care antiplatelet therapy with aspirin and/or clopidogrel (19–21). The OPTIMUS-5 study was conducted to provide insights on the PD effects of vorapaxar in this setting, particularly exploring profiles among patients with and without DM treated with DAPT (aspirin and clopidogrel), which to date have not been explored. Moreover, in light of the emerging interest in an aspirin-free approach as a strategy to reduce the risk of bleeding complications in patients treated with more potent antithrombotic therapies, this investigation also explored the PD effects associated with aspirin withdrawal in the presence of vorapaxar and clopidogrel therapy. The results of OPTIMUS-5 can be summarized as follows: 1) adjunctive treatment with vorapaxar reduces platelet-mediated thrombogenicity without affecting clot kinetics in both patients with and without DM treated with DAPT (aspirin and clopidogrel); 2) reduction of platelet-mediated thrombogenicity induced by vorapaxar occurs selectively via PAR-1 blockade without apparent interplay with other platelet signaling pathways (e.g., $P2Y_{12}$ or thromboxane); and 3) platelet-mediated thrombogenicity is increased after aspirin withdrawal, particularly among patients with DM.

The TRA 2°P-TIMI 50 (Thrombin Receptor Antagonist in Secondary Prevention of Atherothrombotic Ischemic Events-Thrombolysis In Myocardial Infarction 50) trial, conducted in patients with previous atherothrombosis, demonstrated that, when added to standard-of-care treatment, including antiplatelet therapy with aspirin and clopidogrel, vorapaxar significantly reduces recurrent thrombotic events (10). This benefit was limited to patients with a history of prior MI or PAD but not to patients with a prior cerebrovascular event, in whom vorapaxar was associated with increased harm (i.e., increased rates of intracranial hemorrhage) (10–12). Notably, in the cohort of patients with DM and prior MI included in the TRA 2°P trial, vorapaxar reduced the primary composite endpoint at 3 years by 27% (p = 0.002) and led to a greater absolute risk reduction (absolute risk difference: −3.50%) compared with those without DM (absolute risk difference: −1.36%), with a number needed to treat of 29 (13). The benefit of vorapaxar

FIGURE 5 Markers Sensitive to Cyclooxygenase-1 Blockade

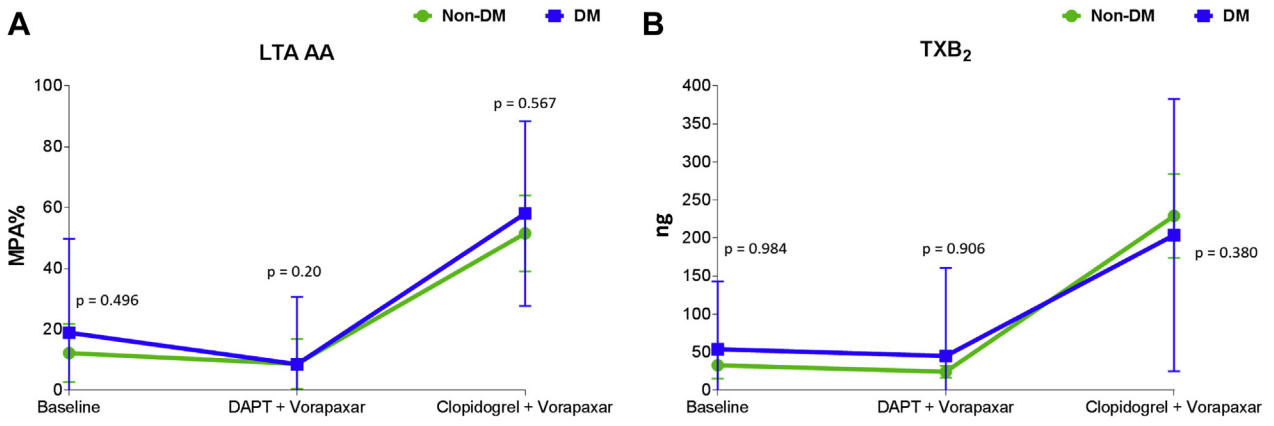

(A) Arachidonic acid (AA)-induced maximal platelet aggregation (MPA%) measured by light transmittance aggregometry (LTA). The p values represent comparisons between the 2 groups at each time point. Error bars indicate SD. Intragroup comparisons for non-DM: Baseline versus DAPT + vorapaxar: mean difference = 2; 95% CI: −10 to 15; p = 0.734. Baseline versus clopidogrel + vorapaxar: mean difference = 42; 95% CI: 26 to 58; p < 0.001. DAPT + vorapaxar versus clopidogrel + vorapaxar: mean difference = 44; 95% CI: 28 to 60; p < 0.001. Intragroup comparisons for DM: Baseline versus DAPT + vorapaxar: mean difference = 9; 95% CI: −2 to 21; p = 0.108. Baseline versus clopidogrel + vorapaxar: mean difference = 40; 95% CI: 25 to 54; p < 0.001. DAPT + vorapaxar versus clopidogrel + vorapaxar: mean difference = 49; 95% CI: 36 to 63; p < 0.001. **(B)** Serum thromboxane B_2 (TXB_2). The p values represent comparisons between the 2 groups at each time point. Error bars indicate SD. Intragroup comparisons for non-DM: Baseline versus DAPT + vorapaxar: p = 0.545. Baseline versus clopidogrel + vorapaxar: p < 0.001. DAPT + vorapaxar versus clopidogrel + vorapaxar: p < 0.001. Intragroup comparisons for DM: Baseline versus DAPT + vorapaxar: p = 0.671. Baseline versus clopidogrel + vorapaxar: p < 0.001. DAPT + vorapaxar versus clopidogrel + vorapaxar: p < 0.001. Abbreviations as in Figure 1.

also was consistent in patients with PAD, although no specific subgroup data according to DM status were available (12,13). These observations make patients with DM an attractive population for treatment with vorapaxar. The reason for the enhanced benefit of vorapaxar among patients with DM has been hypothesized to be attributed to an up-regulated status of thrombin-mediated platelet activation, which makes these patients more susceptible to the antithrombotic effects of the drug (13). However, in our investigation we found that vorapaxar completely abolished TRAP-induced aggregation irrespective of DM status. In addition, the effects on global thrombogenicity were similar in patients with and without DM. Thus, it is more likely that the clinical observations from TRA 2°P-TIMI 50 can be attributed to the greater baseline risk of patients with DM, which allows for a greater magnitude of treatment effects with vorapaxar. This observation is consistent with other secondary prevention studies in patients with DM using potent antiplatelet therapies (28).

The increased risk of bleeding complications with vorapaxar remains a clinical concern. PD investigations have suggested that in the presence of potent $P2Y_{12}$ blockade, aspirin provides limited adjunctive antithrombotic effects (14,29,30). Although the GLOBAL LEADERS trial, which tested a strategy of ticagrelor monotherapy after only 1 month of DAPT versus standard DAPT in a large all-comers population undergoing percutaneous coronary intervention, failed to meet its primary endpoint for superior efficacy of aspirin withdrawal, such an experimental strategy was not associated with any safety concerns (31). Several ongoing investigations are evaluating the safety and efficacy of dropping aspirin in the presence of potent $P2Y_{12}$ receptor blockade in patients undergoing percutaneous coronary intervention (14,32). However, a number of other studies, mostly conducted in patients with atrial fibrillation undergoing coronary stenting and requiring treatment with both oral anticoagulant (OAC) and antiplatelet therapy, have shown that stopping aspirin and maintaining treatment with OAC and a $P2Y_{12}$ inhibitor (mostly clopidogrel) significantly reduced bleeding complications without any apparent trade-off in ischemic events (15–18,33). Accordingly, current recommendations are to minimize the duration of DAPT in patients also taking OAC (34,35). OPTIMUS-5 also explored the effects of dropping aspirin in the setting of a platelet-specific, rather than systemic, modulation of thrombin-mediated effects. We showed that stopping aspirin was associated with an increase in markers specific to COX-1-mediated blockade leading to an increase in platelet-mediated global thrombogenicity. Importantly, the magnitude of increase was

higher in patients with DM compared with patients without DM, and patients with DM achieved levels of global thrombogenicity while on vorapaxar and clopidogrel that were similar to those while on aspirin and clopidogrel.

Our finding that markers specifically assessing COX-1 blockade increase with aspirin withdrawal provides support that alternative antithrombotic treatment regimens cannot replace the selective effects of aspirin on platelet COX-1 blockade. The increase in platelet-mediated global thrombogenicity could also be attributed to the loss of synergism that is known to occur when aspirin and clopidogrel are concomitantly used (36). Such synergism may be less relevant in the presence of more potent $P2Y_{12}$ blockade (29,30). It may be hypothesized that the enhanced increase in platelet-mediated thrombogenicity among patients with DM may be attributed to the fact that these patients are more susceptible to such loss of synergism as reflected by the increase in markers of $P2Y_{12}$ signaling. Overall, these findings should caution against strategies of aspirin withdrawal in the absence of effective alternative antithrombotic treatment (14). Indeed, our PD observations question any potential clinical advantage of dual therapy with vorapaxar and clopidogrel compared with standard-of-care DAPT with aspirin and clopidogrel, especially in patients with DM. The use of OAC, which provides a block of systemic levels of thrombin, may be more effective in this regard, as modulation of circulating thrombin can also indirectly affect platelet reactivity (37). Thus, this approach would result in more wide-ranging antithrombotic effects compared with vorapaxar, which only selectively inhibits the effects of thrombin on platelets via selective PAR-1 blockade (7). The benefits of the antithrombotic efficacy of an OAC in addition to a single antiplatelet agent (e.g., aspirin) was recently supported by a large-scale secondary prevention study conducted in patients with CAD and PAD, which showed a significant reduction in ischemic recurrences and reduced cardiovascular mortality associated with a very low dosing regimen of rivaroxaban in adjunct to aspirin (38).

Despite the known interplay between thrombin- and $P2Y_{12}$-mediated signaling, adjunctive treatment with vorapaxar does not interfere with markers of $P2Y_{12}$ receptor blockade (39). This is consistent with other studies modulating systemic levels of thrombin with oral anticoagulant therapies (40–42). These findings may be attributed to the fact that these patients already are on $P2Y_{12}$-inhibiting therapy, which may not allow unraveling such interplay as previously observed in in vitro investigations and in platelets from nonmedicated patients (43–45).

STUDY LIMITATIONS. Our study was not designed to assess clinical outcomes. Moreover, our study was conducted in patients treated with aspirin and clopidogrel, and it may be argued that many patients with a history of MI are currently treated with more potent $P2Y_{12}$ inhibitors (prasugrel or ticagrelor). However, in the TRA 2°P study, clopidogrel was the $P2Y_{12}$ inhibitor utilized in 99.3% of patients, and the approved indication for vorapaxar was based on this background antiplatelet therapy. Accordingly, our PD study was conducted to mimic how vorapaxar was approved for clinical use based on the TRA 2°P trial (10,20,21). Moreover, clopidogrel is still the most frequently used $P2Y_{12}$ inhibitor and is the only agent of this class approved for treatment of PAD (46). If similar findings would have been observed in patients on DAPT with aspirin and prasugrel or ticagrelor is unknown. The PD effects associated with the addition of vorapaxar to patients with a history of MI, treated with potent $P2Y_{12}$ inhibitors (prasugrel or ticagrelor) and the effects associated with aspirin withdrawal in these patients are currently under investigation (NCT02545933).

CONCLUSIONS

Adjunctive treatment with vorapaxar reduces platelet-mediated thrombogenicity without affecting clot kinetics in both patients with DM and patients without DM, while on DAPT. However, platelet-mediated thrombogenicity is increased after aspirin withdrawal, particularly among patients with DM. These PD observations do not support any potential clinical advantage of dual therapy with vorapaxar and clopidogrel compared with standard-of-care DAPT with aspirin and clopidogrel, especially in patients with DM. The PD findings of this study suggest that the enhanced clinical benefit among patients with DM associated with adjunctive treatment with vorapaxar in addition to standard-of-care oral antiplatelet therapy, including aspirin and clopidogrel, is more likely due to the greater baseline risk profile of these patients, which allows for a greater magnitude of treatment effects, rather than a differential effect on platelets from patients with DM compared to patients without DM.

ADDRESS FOR CORRESPONDENCE: Dr. Dominick J. Angiolillo, University of Florida College of Medicine-Jacksonville, 655 West 8th Street, Jacksonville, Florida 32209. E-mail: dominick.angiolillo@jax.ufl.edu.

PERSPECTIVES

COMPETENCY IN MEDICAL KNOWLEDGE: Vorapaxar is a PAR-1 inhibitor clinically approved for the reduction of thrombotic cardiovascular events in patients with a history of MI or PAD treated with standard-of-care antiplatelet therapy with aspirin and/or clopidogrel. This study provides evidence that adjunctive treatment with vorapaxar in addition to DAPT reduces platelet-mediated thrombogenicity without affecting clot kinetics in both patients and patients without DM. Notably, this reduction occurs selectively via PAR-1 blockade without apparent interplay with other platelet signaling pathways, and platelet-mediated thrombogenicity is increased after aspirin withdrawal, particularly among patients with DM. This has clinical implications as it demonstrates that the enhanced benefit of vorapaxar shown in clinical trials among patients with DM is likely just attributed to the greater baseline risk of patients with DM, thus underscoring the need for more aggressive treatment of these patients. In addition, the study shows that alternative antithrombotic treatment regimens cannot replace the selective effects of aspirin on platelet COX-1 blockade and cautions against strategies of aspirin withdrawal in the absence of effective alternative antithrombotic treatment.

TRANSLATIONAL OUTLOOK: Our study was conducted in patients treated with aspirin and clopidogrel, and it may be argued that many patients with a history of MI are currently treated with the more potent $P2Y_{12}$ inhibitors prasugrel and ticagrelor. The PD effects associated with the addition of vorapaxar to treatment with prasugrel or ticagrelor and the effects associated with aspirin withdrawal in these patients need to be investigated in specifically designed studies. Use of direct oral anticoagulants, which inhibit systemic thrombin, may be more effective in reducing platelet-mediated global thrombogenicity, as modulation of circulating thrombin (rather than just its selective effect on the platelet PAR-1 receptor) can also indirectly affect platelet reactivity and result in more wide-ranging antithrombotic effects. The association between PD findings and clinical outcomes in patients with vascular disease manifestations treated with strategies that modulate the effects of thrombin warrants further investigation.

REFERENCES

1. Donahoe SM, Stewart GC, McCabe CH, et al. Diabetes and mortality following acute coronary syndromes. JAMA 2007;298:765–75.

2. Ferreiro JL, Angiolillo DJ. Diabetes and antiplatelet therapy in acute coronary syndrome. Circulation 2011;123:798–813.

3. Angiolillo DJ, Jakubowski JA, Ferreiro JL, et al. Impaired responsiveness to the platelet P2Y12 receptor antagonist clopidogrel in patients with type 2 diabetes and coronary artery disease. J Am Coll Cardiol 2014;64:1005–14.

4. Angiolillo DJ, Fernandez-Ortiz A, Bernardo E, et al. Platelet function profiles in patients with type 2 diabetes and coronary artery disease on combined aspirin and clopidogrel treatment. Diabetes 2005;54:2430–5.

5. Davì G, Patrono C. Platelet activation and atherothrombosis. N Engl J Med 2007;357:2482–94.

6. Angiolillo DJ, Ueno M, Goto S. Basic principles of platelet biology and clinical implications. Circ J 2010;74:597–607.

7. Angiolillo DJ, Capodanno D, Goto S. Platelet thrombin receptor antagonism and atherothrombosis. Eur Heart J 2010;31:17–28.

8. Franchi F, Angiolillo DJ. Novel antiplatelet agents in acute coronary syndrome. Nat Rev Cardiol 2015;12:30–47.

9. Franchi F, Rollini F, Park Y, Angiolillo DJ. Platelet thrombin receptor antagonism with vorapaxar: pharmacology and clinical trial development. Future Cardiol 2015;11:547–64.

10. Morrow DA, Braunwald E, Bonaca MP, et al. Vorapaxar in the secondary prevention of atherothrombotic events. N Engl J Med 2012;366:1404–13.

11. Scirica BM, Bonaca MP, Braunwald E, et al. Vorapaxar for secondary prevention of thrombotic events for patients with previous myocardial infarction: a prespecified subgroup analysis of the TRA 2°P-TIMI 50 trial. Lancet 2012;380:1317–24.

12. Bonaca MP, Scirica BM, Creager MA, et al. Vorapaxar in patients with peripheral artery disease: results from TRA2°P-TIMI 50. Circulation 2013;127:1522–9.

13. Cavender MA, Scirica BM, Bonaca MP, et al. Vorapaxar in patients with diabetes mellitus and previous myocardial infarction: findings from the thrombin receptor antagonist in secondary prevention of atherothrombotic ischemic events-TIMI 50 trial. Circulation 2015;131:1047–53.

14. Capodanno D, Mehran R, Valgimigli M, et al. Aspirin-free strategies in cardiovascular disease and cardioembolic stroke prevention. Nat Rev Cardiol 2018;15:480–96.

15. Dewilde WJ, Oirbans T, Verheugt FW, et al. Use of clopidogrel with or without aspirin in patients taking oral anticoagulant therapy and undergoing percutaneous coronary intervention: an open-label, randomised, controlled trial. Lancet 2013;381:1107–15.

16. Gibson CM, Mehran R, Bode C, et al. Prevention of bleeding in patients with atrial fibrillation undergoing PCI. N Engl J Med 2016;375:2423–34.

17. Cannon CP, Bhatt DL, Oldgren J, et al. Dual antithrombotic therapy with dabigatran after PCI in atrial fibrillation. N Engl J Med 2017;377:1513–24.

18. Lopes RD, Heizer G, Aronson R, et al. Antithrombotic therapy after acute coronary syndrome or PCI in atrial fibrillation. N Engl J Med 2019;380:1509–24.

19. Magnani G, Bonaca MP, Braunwald E, et al. Efficacy and safety of vorapaxar as approved for clinical use in the United States. J Am Heart Assoc 2015;4:e001505.

20. U.S. Food and Drug Administration (FDA). Vorapaxar prescribing information. Available at: http://www.fda.gov/drugs/informationondrugs/ucm423935.htm. Accessed June 1, 2019.

21. European Medicines Agency (EMA). Vorapaxar prescribing information. Available at: http://www.ema.europa.eu/ema/index.jsp?curl=pages/medicines/human/medicines/002814/

human_med_001839.jsp&mid=WC0b01ac058001d124. Accessed June 1, 2019.

22. World Health Organization (WHO). Definition and diagnosis of diabetes mellitus and intermediate hyperglycaemia: report of a WHO/IDF consultation. Available at: http://www.who.int/diabetes/publications/diagnosis_diabetes2006/en/. Accessed June 1, 2019.

23. Capodanno D, Patel A, Dharmashankar K, et al. Pharmacodynamic effects of different aspirin dosing regimens in type 2 diabetes mellitus patients with coronary artery disease. Circ Cardiovasc Interv 2011;4:180–7.

24. Franchi F, Rollini F, Aggarwal N, et al. Pharmacodynamic comparison of prasugrel versus ticagrelor in patients with type 2 diabetes mellitus and coronary artery disease: the OPTIMUS (Optimizing Antiplatelet Therapy in Diabetes Mellitus)-4 Study. Circulation 2016;134:780–92.

25. Gurbel PA, Bliden KP, Tantry US, et al. First report of the point-of-care TEG: a technical validation study of the TEG-6S system. Platelets 2016;27:642–9.

26. Storey RF, Kotha J, Smyth SS, et al. Effects of vorapaxar on platelet reactivity and biomarker expression in non-ST-elevation acute coronary syndromes. The TRACER Pharmacodynamic Substudy. Thromb Haemost 2014;111:883–91.

27. Lancaster GA, Dodd S, Williamson PR. Design and analysis of pilot studies: recommendations for good practice. J Eval Clin Pract 2004;10:307–12.

28. Bhatt DL, Bonaca MP, Bansilal S, et al. Reduction in ischemic events with ticagrelor in diabetic patients with prior myocardial infarction in PEGASUS-TIMI 54. J Am Coll Cardiol 2016;67:2732–40.

29. Armstrong PC, Leadbeater PD, Chan MV, et al. In the presence of strong P2Y12 receptor blockade, aspirin provides little additional inhibition of platelet aggregation. J Thromb Haemost 2011;9:552–61.

30. Traby L, Kollars M, Kaider A, Eichinger S, Wolzt M, Kyrle PA. Effects of P2Y12 receptor inhibition with or without aspirin on hemostatic system activation: a randomized trial in healthy subjects. J Thromb Haemost 2016;14:273–81.

31. Vranckx P, Valgimigli M, Jüni P, et al. Ticagrelor plus aspirin for 1 month, followed by ticagrelor monotherapy for 23 months vs aspirin plus clopidogrel or ticagrelor for 12 months, followed by aspirin monotherapy for 12 months after implantation of a drug-eluting stent: a multicentre, open-label, randomised superiority trial. Lancet 2018;392:940–9.

32. Baber U, Dangas G, Cohen DJ, et al. Ticagrelor with aspirin or alone in high-risk patients after coronary intervention: rationale and design of the TWILIGHT study. Am Heart J 2016;182:125–34.

33. Lopes RD, Hong H, Harskamp RE, et al. Safety and efficacy of antithrombotic strategies in patients with atrial fibrillation undergoing percutaneous coronary intervention: a network meta-analysis of randomized controlled trials. JAMA Cardiol 2019 June 19 [E-pub ahead of print].

34. Angiolillo DJ, Goodman SG, Bhatt DL, et al. Antithrombotic therapy in patients with atrial fibrillation treated with oral anticoagulation undergoing percutaneous coronary intervention. Circulation 2018;138:527–36.

35. Capodanno D, Huber K, Mehran R, et al. Management of antithrombotic therapy in atrial fibrillation patients undergoing PCI: current status and future directions. J Am Coll Cardiol 2019;74:83–99.

36. Cadroy Y, Bossavy JP, Thalamas C, Sagnard L, Sakariassen K, Boneu B. Early potent antithrombotic effect with combined aspirin and a loading dose of clopidogrel on experimental arterial thrombogenesis in humans. Circulation 2000;101:2823–8.

37. Borissoff JI, Spronk HM, ten Cate H. The hemostatic system as a modulator of atherosclerosis. N Engl J Med 2011;364:1746–60.

38. Eikelboom JW, Connolly SJ, Bosch J, et al. Rivaroxaban with or without aspirin in stable cardiovascular disease. N Engl J Med 2017;377:1319–30.

39. Nylander S, Mattsson C, Ramström S, Lindahl TL. Synergistic action between inhibition of P2Y12/P2Y1 and P2Y12/thrombin in ADP- and thrombin-induced human platelet activation. Br J Pharmacol 2004;142:1325–31.

40. Franchi F, Rollini F, Cho JR, et al. Effects of dabigatran on the cellular and protein phase of coagulation in patients with coronary artery disease on dual antiplatelet therapy with aspirin and clopidogrel. Results from a prospective, randomised, double-blind, placebo-controlled study. Thromb Haemost 2016;115:622–31.

41. Borst O, Münzer P, Alnaggar N, et al. Inhibitory mechanisms of very low-dose rivaroxaban in non-ST-elevation myocardial infarction. Blood Adv 2018;2:715–30.

42. Franchi F, Rollini F, Garcia E, et al. Effects of edoxaban on the cellular and protein phase of coagulation in patients with coronary artery disease on dual antiplatelet therapy with aspirin and clopidogrel: results of the EDOX-APT study. Thromb Haemost 2019. Aug 30 [Epub ahead of print].

43. Furugohri T, Isobe K, Honda Y, et al. DU-176b, a potent and orally active factor Xa inhibitor: in vitro and in vivo pharmacological profiles. J Thromb Haemost 2008;6:1542–9.

44. Honda Y, Kamisato C, Morishima Y. Edoxaban, a direct factor Xa inhibitor, suppresses tissue-factor induced human platelet aggregation and clot-bound factor Xa in vitro: comparison with an antithrombin-dependent factor Xa inhibitor, fondaparinux. Thromb Res 2016;141:17–21.

45. Wong PC, Jiang X. Apixaban, a direct factor Xa inhibitor, inhibits tissue-factor induced human platelet aggregation in vitro: comparison with direct inhibitors of factor VIIa, XIa and thrombin. Thromb Haemost 2010;104:302–10.

46. Jones WS, Patel MR. Antithrombotic therapy in peripheral artery disease: generating and translating evidence into practice. J Am Coll Cardiol 2018;71:352–62.

KEY WORDS dual antiplatelet therapy, pharmacodynamics, platelets, thrombin, vorapaxar

APPENDIX For an expanded Methods section as well as supplemental figures and references, please see the online version of this paper.

Go to http://www.acc.org/jacc-journals-cme to take the CME/MOC/ECME quiz for this article.

JACC: BASIC TO TRANSLATIONAL SCIENCE VOL. 4, NO. 7, 2019

EDITORIAL COMMENT

Platelet Function Testing and Clinical Outcomes

Connecting the Dots*

David J. Schneider, MD

Although platelet function testing can demonstrate the pharmacodynamic effects of antiplatelet agents, it has not been shown to be an effective tool to guide individualized therapy. Increased platelet reactivity has been consistently associated with a greater risk of cardiovascular events (1). By contrast, randomized trials that used platelet function testing to guide individualized therapy failed to demonstrate improved outcomes (2,3).

SEE PAGE 763

In this issue of *JACC: Basic to Translational Science*, Franchi et al. (4) sought to elucidate pharmacodynamic mechanisms by which vorapaxar reduced recurrent thrombotic events when added to treatment with aspirin plus clopidogrel in high-risk patients including those with prior myocardial infarction, peripheral arterial disease, and diabetes. Because the reduction in thrombotic events was associated with an increase in bleeding events, the authors assessed the pharmacodynamic effects of aspirin withdrawal.

The investigators used a series of assays to assess pharmacodynamic effects that included measures of both platelet function and coagulation. Their findings demonstrated that vorapaxar inhibited the effects of thrombin receptor agonist peptide on platelet aggregation without an effect on clot kinetics. The withdrawal of aspirin was associated with increased platelet aggregation in response to agonists (collagen and arachidonic acid) that are sensitive to the effects of aspirin. Accordingly, their results are consistent with the primary mechanisms by which aspirin, clopidogrel, and vorapaxar inhibit platelets, and they did not demonstrate effects on measures of coagulation nor did they show interplay between platelet activation pathways.

This is a well-designed study performed by an experienced group of investigators. The results are clearly presented and elucidate the pharmacodynamic effect of the selected combinations. The authors deserve credit for bringing this study to completion. Despite the loss of committed financial support, the investigators completed the study with the use of institutional research funds.

These results underscore the challenges associated with the translation of pharmacodynamic effects to the clinical care of patients. The investigators appropriately chose to use agonists that would reflect the mechanisms by which aspirin, clopidogrel, and vorapaxar influence platelet activation. Studies assessing the prognostic implications of platelet reactivity have predominantly used adenosine diphosphate (1). Accordingly, the prognostic implications of other agonists, alone or in combination, are limited. Additional potentially confounding aspects of platelet function testing include the method of preparation (phlebotomy technique and anticoagulant used) as well as the concentration of agonist (5). Intraindividual variability in platelet reactivity appears to be a major contributor to the failure of platelet function tests to guide individualized therapy. Pharmacodynamic assessment has not been

*Editorials published in *JACC: Basic to Translational Science* reflect the views of the authors and do not necessarily represent the views of *JACC: Basic to Translational Science* or the American College of Cardiology.

From the Cardiology Unit, Department of Medicine, Cardiovascular Research Institute, University of Vermont, Burlington, Vermont. Dr. Schneider has reported that he has no relationships relevant to the contents of this paper to disclose.

The author attests they are in compliance with human studies committees and animal welfare regulations of the authors' institutions and Food and Drug Administration guidelines, including patient consent where appropriate. For more information, visit the *JACC: Basic to Translational Science* author instructions page.

ISSN 2452-302X https://doi.org/10.1016/j.jacbts.2019.09.007

effective in identifying patients at greater risk of bleeding complications. In aggregate, these issues limit our ability to project the clinical implications of the pharmacodynamic effects observed.

In summary, the authors found that the addition of vorapaxar to treatment with aspirin plus clopidogrel would be expected to attenuate thrombin-induced activation of platelets, and the withdrawal of aspirin was associated with an increase in arachidonic acid and collagen-induced aggregation. Although it is plausible that the recovery of collagen-induced aggregation might reduce the incidence of bleeding, this must be proven in clinical trials. Clinical trials with vorapaxar have demonstrated that attenuation of thrombin-induced platelet activation reduces the risk of thrombotic events; however, clinical trials are necessary to determine whether this benefit will be preserved in the absence of aspirin.

ADDRESS FOR CORRESPONDENCE: Dr. David J. Schneider, Cardiology Unit, Department of Medicine, Cardiovascular Research Institute, University of Vermont, 360 South Park Drive, Colchester, Vermont 05446. E-mail: david.schneider@med.uvm.edu.

REFERENCES

1. Wisman PP, Roest M, Asselbergs FW, et al. Platelet-reactivity tests identify patients at risk of secondary cardiovascular events: a systematic review and meta-analysis. J Thromb Haemost 2014;12:736–47.

2. Price MJ, Berger PB, Teirstein PS, et al., GRAVITAS Investigators. Standard- vs high-dose clopidogrel based on platelet function testing after percutaneous coronary intervention: the GRAVITAS randomized trial. JAMA 2011;305:1097–105.

3. Collet JP, Cuisset T, Rangé G, et al., ARCTIC Investigators. Bedside monitoring to adjust antiplatelet therapy for coronary stenting. N Engl J Med 2012;367:2100–9.

4. Franchi F, Rollini F, Kairouz V, et al. Pharmacodynamic effects of vorapaxar in patients with and without diabetes mellitus: results of the OPTIMUS-5 study. J Am Coll Cardiol Basic Trans Science 2019;4:763–75.

5. Madsen NJ, Holmes CE, Serrano FA, Sobel BE, Schneider DJ. Influence of preparative procedures on assay of platelet function and apparent effects of antiplatelet agents. Am J Cardiol 2007;100:722–7.

KEY WORDS diabetes, platelet, thrombin, vorapaxar

JACC: BASIC TO TRANSLATIONAL SCIENCE VOL. 4, NO. 7, 2019

PRECLINICAL RESEARCH

Gene Therapy Rescues Cardiac Dysfunction in Duchenne Muscular Dystrophy Mice by Elevating Cardiomyocyte Deoxy-Adenosine Triphosphate

Stephen C. Kolwicz, Jr, PhD,[a] John K. Hall, PhD,[b] Farid Moussavi-Harami, MD,[c] Xiolan Chen, PhD,[d,e] Stephen D. Hauschka, PhD,[d,e] Jeffrey S. Chamberlain, PhD,[b,d,e] Michael Regnier, PhD,[e,f,g,*] Guy L. Odom, PhD[b,e,g,*]

VISUAL ABSTRACT

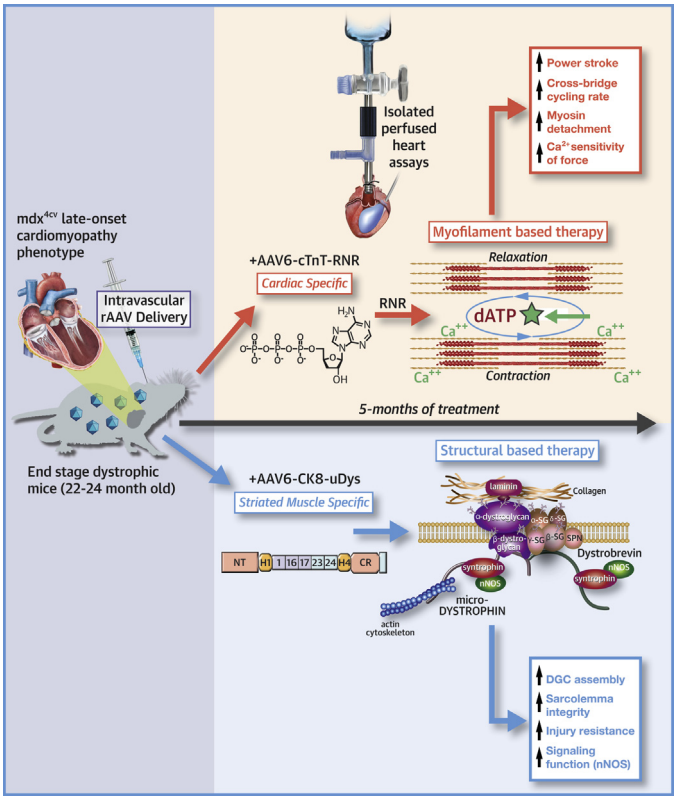

Kolwicz, S.C. Jr. et al. J Am Coll Cardiol Basic Trans Science. 2019;4(7):778-91.

HIGHLIGHTS

- **rAAV vectors increase cardiac-specific expression of RNR and elevate cardiomyocyte 2-dATP levels.**
- **Elevated myocardial RNR and subsequent increase in 2-dATP rescues the performance of failing myocardium, an effect that persists long term.**

ISSN 2452-302X https://doi.org/10.1016/j.jacbts.2019.06.006

- **We show the ability to increase both cardiac baseline function and high workload contractile performance in aged (22- to 24-month old) mdx4cv mice, by high-level muscle-specific expression of either microdystrophin or RNR.**
- **Five months post-treatment, mice systemically injected with rAAV6 vector carrying a striated muscle-specific regulatory cassette driving expression of microdystrophin in both skeletal and cardiac muscle, exhibited the greatest effect on systolic function. In comparison, mice treated with rAAV6 vector carrying RNR that expresses exclusively in cardiac muscle not only exhibited greatly improved baseline systolic function but also improved diastolic function.**
- **Importantly, vector-directed overexpression of RNR did not impair cardiac reserve during increased physiological demand in aged mdx4cv hearts.**

ABBREVIATIONS AND ACRONYMS

μDys = microdystrophin

CK8 = miniaturized murine creatine kinase regulatory cassette

CMV = cytomegalovirus

cTnT = cardiac troponin T

dADP = deoxy-adenosine diphosphate

dATP = deoxy-adenosine triphosphate

DMD = Duchenne muscular dystrophy

mdx = mouse muscular dystrophy model

rAAV = recombinant adeno-associated viral vector

RNR = ribonucleotide reductase

SUMMARY

Mutations in the gene encoding for dystrophin leads to structural and functional deterioration of cardiomyocytes and is a hallmark of cardiomyopathy in Duchenne muscular dystrophy (DMD) patients. Administration of recombinant adeno-associated viral vectors delivering microdystrophin or ribonucleotide reductase (RNR), under muscle-specific regulatory control, rescues both baseline and high workload-challenged hearts in an aged, DMD mouse model. However, only RNR treatments improved both systolic and diastolic function under those conditions. Cardiac-specific recombinant adeno-associated viral treatment of RNR holds therapeutic promise for improvement of cardiomyopathy in DMD patients. (J Am Coll Cardiol Basic Trans Science 2019;4:778–91)

Duchenne muscular dystrophy (DMD) and its milder and allelic form, Becker muscular dystrophy (BMD), are the most frequent muscular dystrophies, occurring once in ~5,000 male births, and are due to mutations in the dystrophin gene (1). DMD patients typically die due to cardiac and respiratory muscle failure; thus, maintenance of adequate function in both cardiac and skeletal muscle is critical for optimal DMD therapy. The primary function of dystrophin is to provide a structural role by mechanically linking the subsarcolemmal cytoskeleton to the extracellular matrix through the dystrophin-glycoprotein complex (DGC) (2). This linkage transmits the forces of contraction to the extracellular matrix and protects muscles from contraction-induced injury (3–7). In addition to a structural or mechanical role, the DGC also serves as a scaffold for cytoplasmic and membrane-associated signaling proteins and ion channels (8–11). The complete absence of dystrophin results in drastic reductions of all DGC components (12–14). Together, an absence of dystrophin and reduction in the DGC components causes membrane destabilization and permeability defects that lead to myofiber degeneration, repeated cycles of degeneration/regeneration, and the gradual replacement of muscle fibers with fibrotic, connective, and adipose tissue.

In contrast, some in-frame deletions, truncations, and missense mutations lead to reduced dystrophin expression associated with milder phenotypes. These

From the [a]Mitochondria and Metabolism Center, University of Washington, Seattle, Washington; [b]Department of Neurology, University of Washington, Seattle, Washington; [c]Division of Cardiology, Department of Medicine, University of Washington, Seattle, Washington; [d]Department of Biochemistry, University of Washington, Seattle, Washington; [e]Wellstone Muscular Dystrophy Specialized Research Center, University of Washington, Seattle, Washington; [f]Department of Bioengineering, University of Washington, Seattle, Washington; and the [g]Center for Cardiovascular Biology, University of Washington, Seattle, Washington. *Drs. Regnier and Odom contributed equally to this work and are joint senior authors.
This work was supported by grants from the National Institutes of Health (NIH): R01 HL111197 (to Dr. Regnier and Hauschka), R01 HD048895, K08 HL128826 (to Dr. Moussavi-Harami) and R01 HL128368 (to Dr. Regnier) and 1U54AR065139-01A1 (to Drs. Hauschka, Chamberlain, Regnier, and Odom). Dr. Kolwicz was funded by the American Heart Association 14SDG18590020. Dr. Chamberlain has received personal fees from Solid Biosciences, SAB. All other authors have reported that they have no relationships relevant to the contents of this paper to disclose.
The authors attest they are in compliance with human studies committees and animal welfare regulations of the authors' institutions and US Food and Drug Administration guidelines, including patient consent where appropriate. For more information, visit the *JACC: Basic to Translational Science* author instructions page.

Manuscript received February 27, 2019; revised manuscript received June 20, 2019, accepted June 20, 2019.

pathologies are largely curtailed in mouse (*mdx*) and canine (*cxmd*) models of DMD following the vector-mediated delivery of muscle-specific expression of highly functional miniaturized versions of dystrophin, microdystrophin (μDys) (15-24). In *mdx* mice, muscle pathology is milder than in humans, with the exception of the diaphragm; however, the dystrophic phenotype worsens with increasing age including the development of cardiac dysfunction (25-32). Administration of recombinant adeno-associated viral (rAAV)-mediated μDys therapy in *mdx* mice preceding the onset of cardiomyopathy is highly cardioprotective (33-35). However, when *mdx* mice are treated with μDys at a late stage of cardiomyopathy, such as would be the case for a number of DMD patients, a full rescue of the dysfunctional cardiac phenotype is not achieved (30,35-37).

SEE PAGE 792

We have developed a cardiac function-enhancing gene therapy approach that targets myosin in contractile filaments by overexpressing the enzyme ribonucleotide reductase (RNR). RNR converts adenosine diphosphate (ADP) to deoxy-ADP (dADP), which is rapidly converted to deoxy-adenosine triphosphate (dATP) in cells. In numerous in vitro studies, we have shown that dATP increases cross-bridge binding and cycling, resulting in stronger, faster contraction and faster relaxation (38-45). We have also reported that dATP improves contractile properties of myocardium from end-stage human heart failure (HF) in vitro (42) and dogs with end-stage idiopathic dilated cardiomyopathy (46). In normal rodent muscle, we reported that increases in cardiomyocytes and cardiac function occur with as little as ~1% of the ATP pool in the dATP form (40,47). Similarly, rAAV-mediated delivery of RNR under cardiac-specific regulatory control resulted in enzyme overexpression exclusively in cardiomyocytes and significantly improved left ventricular function without adverse cardiac remodeling in normal and infarcted rodent hearts (48). Our data indicated that dATP could rescue the preload responsiveness of failing hearts, suggesting restoration of the abnormal Frank-Starling Law of the Heart that often occurs in HF.

In the current study, we compare the relative therapeutic capacity of CK8-driven μDys or cardiac troponin T (cTnT)-driven RNR, via intravenously administered rAAV vectors in an advanced-age, DMD cardiomyopathy mouse model. We show a restoration of myocardial workload as indicated by rate pressure product (RPP) for baseline function in mdx^{4cv} mice treated with RNR. This outcome was primarily attributed to the normalization of left ventricular developed pressure (LVDevP). Although mdx^{4cv} mice treated with μDys appeared to normalize LVDevP, this did not result in a significant increase in RPP. Upon further evaluation of cardiac function, the pressure-volume relationship revealed that systolic pressure response with increased preload was significantly improved with the treatment of either RNR or μDys. However, only RNR treatment resulted in significant improvements in diastolic functional parameters, returning them to values that were similar to wild-type (WT) control hearts. As a further assessment of cardiac function, we tested hearts using a high workload challenge protocol. Both RNR and μDys treatments improved systolic function in mdx^{4cv} hearts without compromising cardiac reserve. These positive results suggest that targeted expression of RNR within the myocardium can significantly improve contractile performance in an advanced-age model of DMD cardiomyopathy and may have therapeutic implications for DMD patients.

METHODS

ANIMAL EXPERIMENTS. Male WT C57Bl/6J (The Jackson Laboratory, Bar Harbor, Maine) and mdx^{4cv} (generated in-house) mice were used for these studies (17). All animals were experimentally manipulated in accordance with the Institutional Animal Care and Use Committee of the University of Washington. Experimental mice were administered vector at 22 to 24 months of age via the retro-orbital sinus with a 200-μl bolus injection in Hanks balanced saline solution at a dose of 2×10^{14} vg/kg. All mice were housed in a specific-pathogen free animal care facility using a 12-h light/12-h dark cycle with access to food and water ad libitum.

VECTOR PRODUCTION. rAAV genomes containing the CK8 regulatory cassette (expressed exclusively in skeletal and cardiac muscle) and the human codon optimized (GenScript) μDys (ΔR2-15/ΔR18-22/ΔCT) (24), followed by the rabbit beta-globin poly-adenylation (pA) signal, were generated using standard cloning techniques. The rAAV genomes containing the cardiac muscle-specific cTnT455 regulatory cassette, the codon optimized human RNR transgene flanked by 100-bp untranslated regions, and the rabbit beta-globin pA were generated as previously described (48). The "dead" rAAV genomes or promoter-less firefly luciferase followed by the human growth hormone (hGH) pA (kindly provided by J.S.C., University of Washington, Seattle, Washington) were used to generate the control rAAV genomes. The resulting constructs were cotransfected with the pDG6 packaging plasmid into HEK293 cells to

generate rAAV vectors carrying serotype 6 capsids, which were harvested, enriched, and quantitated as previously described (49).

VECTOR GENOME QUANTIFICATION. Total DNA was extracted from flash-frozen tissue samples with Tri-Reagent (MRC Inc., Cincinnati, Ohio), according to manufacturer's instructions. All real-time polymerase chain reaction (PCR) reactions were performed on a QuantStudio 3 Real Time PCR System (Applied Biosystems, Foster City, California) in a total volume of 15 μl, consisting of 5 μl sample DNA, 10.0 μl TaqMan Universal PCR Master Mix (Applied Biosystems), 0.2 μM of each primer, and 0.1 μM TaqMan custom probe (Applied Biosystems). Reaction conditions were 50° C for 2 min, 95° C for 10 min, and 40 cycles of [95° C for 15 s followed by 60° C for 1 min]. Each sample was analyzed in triplicate for concentration of total murine genomes and of total vector genomes. For vector genome detection by quantitative PCR, the primers used to amplify either the rAAV6-cTnT455-RNR or rAAV6-CK8-μDys, or rAAV6-Δcytomegalovirus(CMV)-Luc (control vector) were unique to each vector. For the RNR vector, the amplicon spanned from the distal region of the cTnT promoter, continuing into the proximal RNR1 subunit. For the μDys vector, the amplicon was contained within the CK8 regulatory cassette, whereas the amplicon for the control vector resided within the hGH pA. hGH primers included: 5′-CACAATCTTGGCTCACTGCAA-3′, 5′-GGAGGCTGAG GCAGGAGAA-3′; TaqMan probe: 5′-6FAM- CTCCGCC TCCTGGGTTCAAGCG-MBGNQ-3′; CK8 RC primers: 5′-CCCGAGATGCCTGGTTATAATT-3′, 5′- CGGGAACAT GGCATGCA-3′; TaqMan probe: 5′-6FAM-CCCCCCAAC ACCTGCTGCCTCT-MBGNQ-3′; cTnT455-RNR1 primers: 5′-CCCAGTCCCCGCTGAGA-3′, 5′-AGGTTCCAGGCGCT GCT-3′; and TaqMan probe: 5′-6FAM-ACTCATCAATG TATCTTATCATG-MBGNQ-3′. Results were presented relative to DNA content in each 5-μl DNA tissue sample to determine vector genomes per ng DNA.

TISSUE PROCESSING AND IMAGING ANALYSIS. Tissues were collected and analyzed 5 months post-administration of vectors and compared with age-matched male control vector (rAAV6-ΔCMV-Luc) injected *mdx*^{4cv} and WT mice. Hearts were either snap frozen in liquid nitrogen or were embedded in optimal cutting temperature compound (VWR International, Bridgeport, New Jersey) and flash frozen in liquid nitrogen cooled isopentane for histochemical or immunofluorescence analysis. The snap frozen samples were further processed by grinding to a powder under liquid nitrogen in a mortar kept on dry ice for subsequent extraction of nucleic acid and protein.

Heart cross-sections (10 μm) were co-stained with antibodies raised against alpha 2-laminin (Sigma, St. Louis, Missouri; rat monoclonal, 1:200), the hinge-1 domain of dystrophin (alexa488 conjugated MANEX1011b, Developmental Studies Hybridoma Bank, University of Iowa, mouse monoclonal, 1:200), the human RRM1 (Abcam, Cambridge, United Kingdom; rabbit monoclonal, 1:200), and the human RRM2 (Abcam, rabbit monoclonal, 1:200). Conjugated secondary antibodies (Jackson Immuno, Goat anti-Rabbit) were used at a 1:500 dilution. Slides were mounted using ProLong Gold with DAPI (Thermo Fisher Scientific) and imaged via a Leica SPV confocal microscope. Confocal micrographs covering a majority of the heart left ventricular muscle sections were acquired and montaged via the Fiji toolset (ImageJ) and InDesign (Adobe, San Jose, California). For histology, Masson's trichrome staining was used to examine heart cross-sections. Briefly, 10-μm muscle cryosections were sequentially stained in Wiegerts' iron hematoxylin (10 min), 1% Ponceau-acetic acid (5 min), and 1% aniline blue (5 s).

WESTERN BLOTTING. Radioimmunoprecipitation analysis buffer supplemented with 5 mM ethylenediaminetetraacetic acid and 3% protease inhibitor cocktail (Sigma, Cat# P8340), was used to extract muscle proteins for 0.5 h on ice with gentle agitation every 10 min. Total protein concentration was determined using Pierce BCA assay kit (Fisher Scientific, Kent, Washington). Muscle lysates from WT, control *mdx*^{4cv}, and treated *mdx*^{4cv} (30 μg) mice were denatured at 99°C for 10 min, quenched on ice, and separated via gel electrophoresis after loading onto Criterion 4-12% Bis-Tris polyacrylamide gels (BioRad). Overnight protein transfer to 0.45 mm polyvinylidene difluoride membranes was performed at constant 43 volts at 4°C in Towbin's buffer containing 20% methanol. Blots were blocked for 1 h at room temperature in 5% non-fat dry milk for 1 h before overnight incubation with antibodies raised against the hinge-1 region of dystrophin (Developmental Studies Hybridoma Bank, University of Iowa, 1:300), anti-RRM1 (Abcam, rabbit monoclonal, 1:1,000), anti-RRM2 (Abcam, rabbit monoclonal 1:1,000), and anti-GAPDH (Sigma, Rabbit polyclonal, 1:50,000). Horseradish-peroxidase conjugated secondary antibody staining (1:50,000) was performed for 1 h at room temperature before signal development using Clarity Western ECL substrate (BioRad) and visualization using a Chemidoc MP imaging system (BioRad).

QUANTIFICATION OF CARDIAC dATP. Approximately 25 μg of flash frozen, freshly ground ventricle

cardiac tissue was used for direct quantification of intracellular dATP using the high-performance liquid chromatography (HPLC)-with tandem mass spectrometry (MS/MS) method previously described (50). Briefly, samples were extracted 1 to 3 days before measurement using a 50% methanol solution. The supernatant was stored at -20°C until ready for injection into the HPLC-MS/MS system. A Water's Xevo-TQ-S mass spectrometer coupled with a Water's Acquity I-Class HPLC was used for the analysis (Milford, Massachusetts). Monitoring in negative mode via electrospray ionization was used to acquire MS/MS ions. dATP concentrations were quantified with standards and normalized to tissue weight.

LANGENDORFF ISOLATED PERFUSED HEART EXPERIMENTS. Ex vivo cardiac function was assessed in Langendorff isolated heart preparations as previously described (47,48,51). Hearts were perfused at a constant pressure of 80 mm Hg with a modified Krebs-Henseleit buffer supplemented with glucose and pyruvate. The perfusate contained (mmol/l): 118 NaCl, 25 $NaHCO_3$, 5.3 KCl, 2.0 $CaCl_2$, 1.2 $MgSO_4$, 0.5 ethylenediaminetetraacetic acid, 10.0 glucose, and 0.5 pyruvate, equilibrated with 95% O_2 and 5% CO_2 (pH 7.4). Temperature was maintained at 37.5°C throughout the protocol. Left ventricular (LV) function was monitored via a water-filled balloon inserted into the LV and connected to a pressure transducer. LV systolic pressure (LVSP), end diastolic pressure, heart rate (HR), and minimum and maximum rate of pressure change in the ventricle (±dP/dt) were obtained from the attached data acquisition system (PowerLab, ADInstruments, Colorado Springs, Colorado). After 5 min of stabilization, hearts were equilibrated for 10 min at spontaneous HRs and then fixed at a HR of ~450 beats/min with an electrical stimulator (Grass Technologies, Warwick, Rhode Island). Pressure-volume relationships (i.e., Frank-Starling curves) were assessed by gradually increasing the volume of the LV balloon. After a 5-min recovery period, the perfusate was changed to an identical buffer as above except for the addition of 4.0 mmol/l $CaCl_2$ to simulate a high workload challenge for 20 min.

STATISTICAL ANALYSIS. All values are reported as means\ ± SEM. Starling curves and high workload function were analyzed by 2-way repeated measures analysis of variance followed by pairwise comparisons using Tukey's alpha adjustment method. Other endpoint data were analyzed via 1-way analysis of variance or Student's *t*-tests as appropriate. Kaplan-Meier methods were used to analyze survival curves and compared using the log-rank test. Statistical significance was tested at the $p < 0.05$ level. Statistical analyses were completed using Prism 7.0 (GraphPad Software, San Diego, California).

RESULTS

IMPROVEMENTS IN BASELINE CARDIAC FUNCTION IN VECTOR-TREATED MDX^{4CV} HEARTS. As depicted in **Figure 1**, 22- to 24-month-old *mdx*^{4cv} mice were administered 1 of 3 treatments: rAAV6-cTnT455- RNR (referred to as *mdx*^{4cv}+RNR); rAAV6-CK8- μDys (referred to as *mdx*^{4cv}+ μDys), or rAAV6-ΔCMV-Firefly Luciferase control vector (referred to as*mdx*^{4cv}) at a dose of 2×10^{14} vg/kg. By the end of the 20-week treatment period, both *mdx*^{4cv}+RNR and *mdx*^{4cv}+ μDys mice showed improvements in survival rates compared to *mdx*^{4cv} mice, although this did not reach statistical significance (Supplemental Figure 1). At the end of 5 months, an extensive evaluation of ex vivo cardiac function using the Langendorff isolated heart preparation was performed. The isolated heart technique allows for the direct assessment of inherent myocardial function without the confounding effects of neuro-humoral or other systemic variables. An additional cohort of age-matched, untreated C57BL6 mice (WT) was used as comparison control. At baseline, RPP was significantly decreased in *mdx*^{4cv} hearts due to an approximate 20% decrease in LVDevP (Supplemental Figures 1A and 1B). RNR-treated *mdx*^{4cv} mice exhibited a restoration of RPP ($p = 0.056$) primarily due to a normalization of LVDevP (Supplemental Figures 2A and 2B). Although μDys-treated *mdx*^{4cv} hearts appeared to normalize LVDevP, this did not lead to a significant improvement in RPP (Supplemental Figures 2A and 2B). Both +dP/dt and -dP/dt, an index of ventricular contractility and relaxation, respectively, were decreased 30% in *mdx*^{4cv} hearts ($p = 0.061$). The +dP/dt was similar to control in both RNR-treated *mdx*^{4cv} and μDys-treated *mdx*^{4cv} hearts. However, only RNR-treated *mdx*^{4cv} hearts showed -dP/dt values similar to control levels (Supplemental Figures 2C and 2D).

POSITIVE CHANGES IN FRANK-STARLING MECHANICS IN VECTOR-TREATED MDX^{4CV} HEARTS. To evaluate further systolic and diastolic function in vector-treated *mdx*^{4cv} hearts, we examined the pressure-volume relationship (i.e., Frank-Starling mechanism) in the isolated perfused heart preparation. The LVSP response to increased preload was significantly improved in both in *mdx*^{4cv}+RNR and *mdx*^{4cv}+μDys hearts compared to *mdx*^{4cv} (**Figure 2A**). However, only RNR treatment improved the diastolic response in *mdx*^{4cv} hearts, to levels similar to WT (**Figure 2B**). Both contractility and relaxation (i.e., +dP/dt and

FIGURE 1 Overview of Experimental Design for the Treatment of Aged (22-24 Month) *mdx*^{4cv} Mice

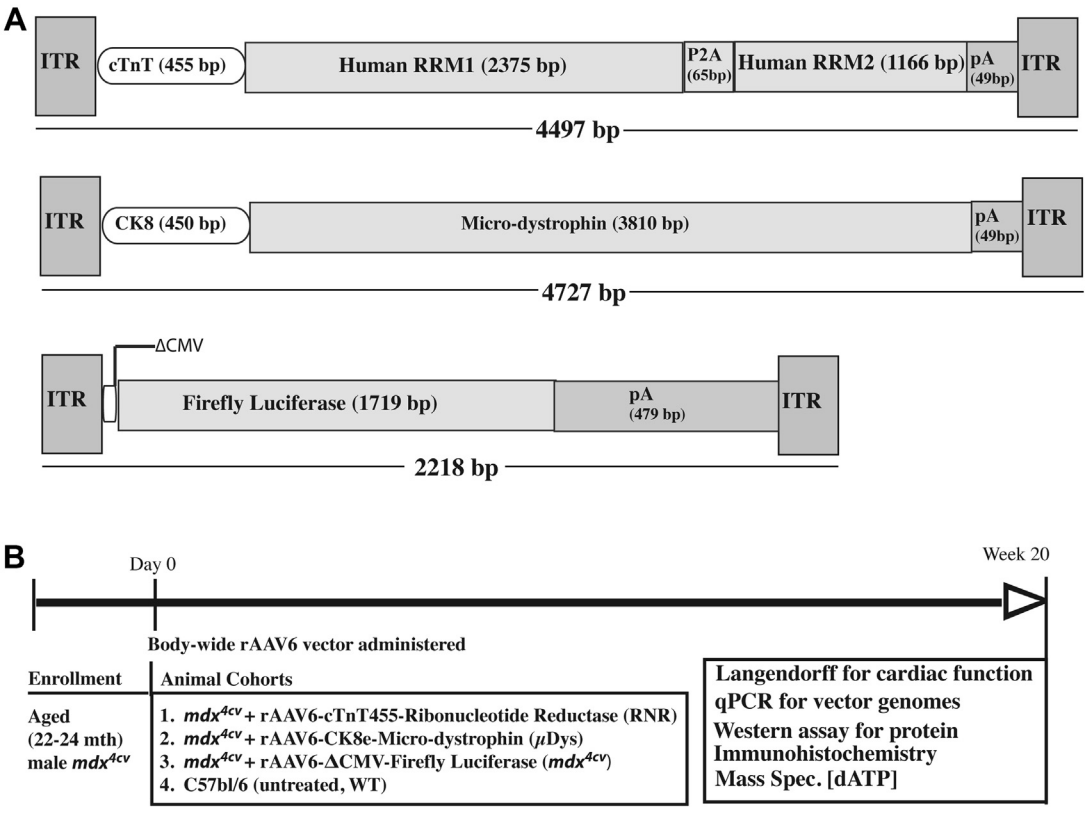

(A) Graphic representation of rAAV6 vectors used in the present study. The ribonucleotide reductase vector contains the human cDNA for the RRM1 and RRM2 subunits whose expression is driven by the cardiac specific (cTnT455) regulatory cassette (RC). The human microdystrophin (ΔR2-R15/ΔR18-R22/ΔCT) vector has expression driven by the CK8 muscle-specific RC. The control vector used in the present study carries the firefly luciferase transgene whose CMV early promoter/enhancer RC has been deleted. **(B)** Outline of animal enrollment, vector administration, and experimental protocols implemented following a treatment period of 5 months. cDNA = complementary DNA; CMV = cytomegalovirus; ITR = inverted terminal repeat; dATP = deoxy-adenosine triphosphate; p2A = porcine teschovirus-1 2A; pA = poly-adenylation; qPCR = quantitative polymerase chain reaction; rAAV6 = recombinant adeno-associated viral vector 6; RC = regulatory cassette; WT = wild-type.

-dP/dt, respectively) were impaired in *mdx*^{4cv} compared to age-matched control subjects (Figures 2D and 2E). Both *mdx*^{4cv}+ RNR and *mdx*^{4cv}+ μDys hearts had significantly elevated +dP/dt values above *mdx*^{4cv} (Figure 2D). Interestingly, treatment of *mdx*^{4cv} hearts with RNR also significantly improved -dP/dt values (Figure 2E). All told, these data suggest that both RNR and μDys treatment can improve systolic function in *mdx*^{4cv} hearts. However, only the RNR treatment corrected diastolic dysfunction in *mdx*^{4cv} hearts.

AUGMENTED RESPONSE TO INCREASED CARDIAC WORKLOAD IN TREATED MDX^{4CV} HEARTS. We previously reported that RNR overexpression in transgenic or vector-treated mouse hearts elevated baseline function but did not impair the response to a short-term physiologic increase in cardiac work (47,48). To verify that the improved systolic and diastolic function in RNR-treated *mdx*^{4cv} hearts at baseline was not associated with an inability to respond to an increased energetic demand, we stressed hearts with a combination of high calcium and elevated heart rates, via pacing stimulation. As shown in Figures 3A and 3B, *mdx*^{4cv} hearts had a blunted response to the increased workload as both LVDevP and RPP were ~25% to 30% lower than WT hearts. In addition, both +dP/dt and -dP/dt were impaired in *mdx*^{4cv} relative to WT hearts (Figures 3C and 3D). Systolic parameters in *mdx*^{4cv}+μDys hearts were effectively improved and similar to age-matched WT hearts for the entire duration of the workload challenge

FIGURE 2 Pressure-Volume Relationships in Isolated Perfused Hearts From Vector-Treated *mdx*^{4cv} Mice

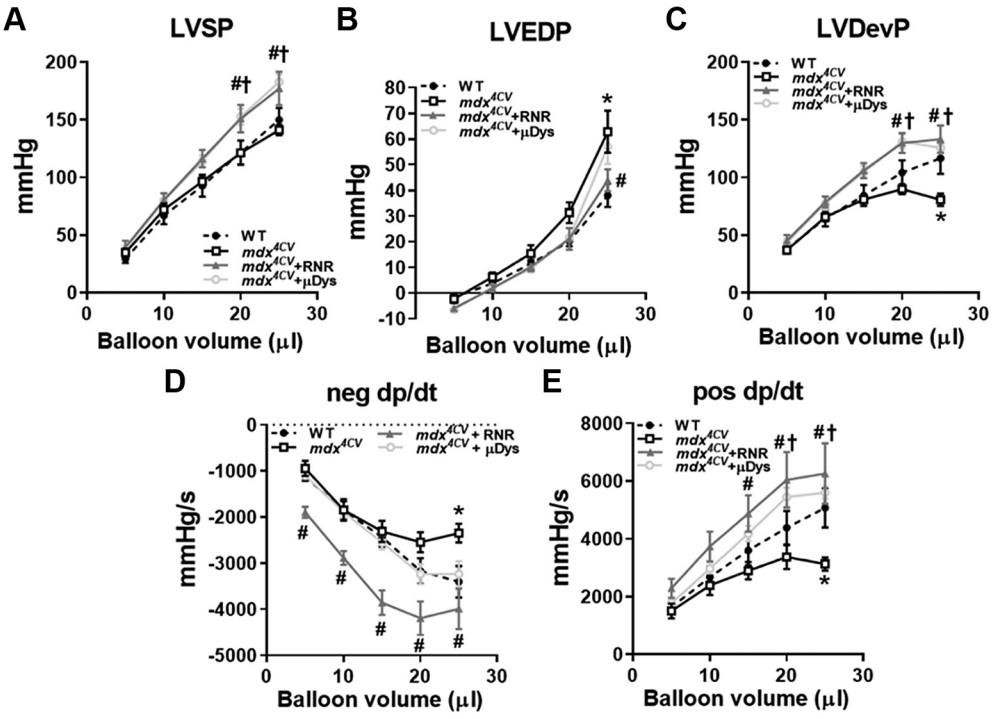

Hearts were isolated from *mdx*^{4cv} mice treated with control vector (*mdx*^{4cv}, n = 6), ribonucleotide reductase (*mdx*^{4cv}+ RNR, n = 6), or microdystrophin (*mdx*^{4cv}+ μDys, n = 5). Age-matched, nondiseased, nontreated wild-type (WT) mice were used as control subjects (n = 8). The pressure-volume relationship (i.e., Frank-Starling mechanism) was evaluated by gradually increasing the volume of the left ventricular (LV) balloon. Hearts were paced at 450 beats/min throughout the protocol. **(A)** Left ventricular systolic pressure (LVSP). **(B)** LV end-diastolic pressure (LVEDP). **(C)** LV developed pressure (LVDevP, the difference between systolic and diastolic pressures). **(D)** Positive (pos) rate of pressure change was calculated by the first derivative of the ascending LV pressure wave (+dP/dt), and is used as an index of ventricular contractility. **(E)** Negative (neg) rate of pressure change calculated by the first derivative of the descending LV pressure wave (–dP/dt), and is used as an index of ventricular relaxation. * $p < 0.05$ *mdx*^{4cv} versus WT; # $p < 0.05$ *mdx*^{4cv}+ RNR versus *mdx*^{4cv}; † $p < 0.05$ *mdx*^{4cv}+ μDys versus *mdx*^{4cv}.

(Figures 3A to 3C). Measures of systolic function significantly increased in *mdx*^{4cv}+ RNR hearts during the initial half of the high workload protocol and remained ~15% higher than *mdx*^{4cv} (Figures 3A to 3C). Interestingly, -dP/dt values tended to be elevated only in *mdx*^{4cv}+ RNR hearts during the physiologic challenge (Figure 3D). These data show that both RNR and μDys treatments improve systolic function in *mdx*^{4cv} hearts without compromising cardiac reserve. Combined with the baseline and pressure-volume relationship assessments, our data show that, in addition to the systolic enhancements, RNR has an added benefit of improving diastolic function.

RNR AND μDys TRANSDUCTION, EXPRESSION, AND CARDIOMYOCYTE LOCALIZATION. To evaluate the localization of RNR and μDys protein within the hearts of mice, we performed immunofluorescence imaging. As shown in Figure 4, the RNR subunit (Rrm1) was robustly expressed in ventricles of RNR-treated mice. The expression of μDys appeared to be saturated relative to full-length dystrophin levels, with both being properly localized to the sarcolemma of cardiomyocytes. We also evaluated general muscle histopathology and potential differences in myocardial fibrosis by Masson trichrome staining, and observed no discernable difference between treated or untreated *mdx*^{4cv} mice (Figure 5). In addition, neither RNR nor μDys treatment significantly altered body weight, heart weight, or the heart weight-to-body weight ratio (Supplemental Figure 3). Western blotting was performed to determine the extent of rAAV vector 6-mediated RNR and μDys protein expression profiles in ventricular tissue (Figure 6). We observed μDys protein expression in ventricular tissue that approached levels similar to WT mice, whereas both human RNR subunits were found to be elevated to comparable levels within ventricular tissue (Figure 6A). To evaluate the relative proportions of

FIGURE 3 The Response of Vector-Treated mdx^{4cv} Mice to High Workload Challenge in Langendorff Isolated Heart Preparations

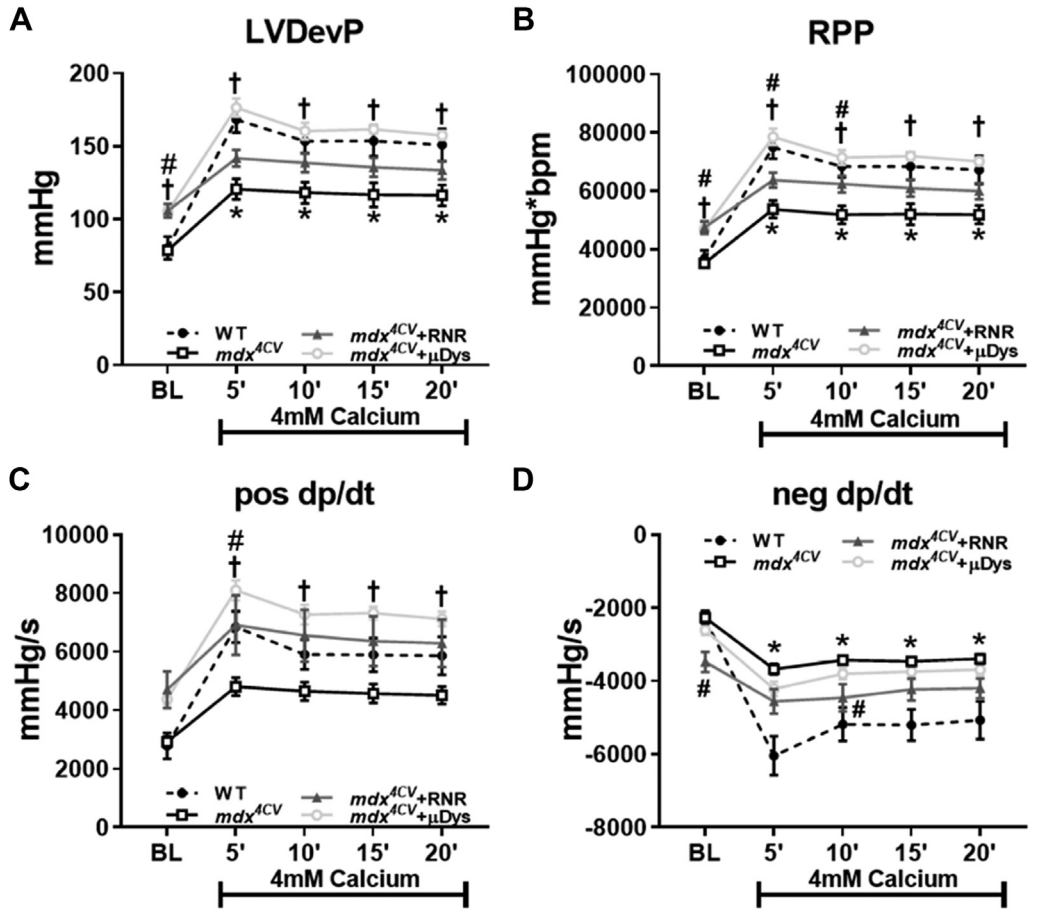

Hearts were isolated from mdx^{4cv} mice treated with control vector (mdx^{4cv}, n = 6), ribonucleotide reductase (mdx^{4cv}+ RNR, n = 6), or microdystrophin (mdx^{4cv}+ µDys, n = 5). Age-matched, nondiseased, nontreated wild-type (WT) mice were used as control subjects (n = 4). All hearts were perfused with a glucose-pyruvate buffer containing high calcium (4.0 mmol/l) to simulate a high workload challenge for 20 min. Hearts were paced at 450 beats per minute throughout the protocol. **(A)** LVDevP (the difference between systolic and diastolic pressures). **(B)** Rate pressure product (RPP, the product of LVDevP and HR). **(C)** Positive rate of pressure change calculated by the first derivative of the ascending LV pressure wave (+dP/dt), is used as an index of ventricular contractility. **(D)** Negative rate of pressure change calculated by the first derivative of the descending LV pressure wave (-dP/dt), is used as an index of ventricular relaxation. * $p < 0.05$ mdx^{4cv} versus WT; # $p < 0.05$ mdx^{4cv}+ RNR versus mdx^{4cv}; † $p < 0.05$ mdx^{4cv}+ µDys versus mdx^{4cv}. Abbreviations as in Figures 1 and 2.

dATP concentrations within ventricular tissue, we performed HPLC-MS/MS analysis on ground ventricular tissue from mdx^{4cv} and mdx^{4cv}+ RNR mice. The concentration of dATP within the ventricular tissue obtained from mdx^{4cv} mice treated with RNR (0.57 ± 0.22 pmol dATP/mg) was approximately 10-fold higher relative to mdx^{4cv} control subjects (0.05 ± 0.02 pmol dATP/mg) (Figure 6B). For adult WT, we previously reported an average dATP value of 0.02 pmol/mg tissue with a SD of 0.01 (50). Additionally, cardiac vector genome data was comparable relative to the vector dose administered (Figure 6C).

DISCUSSION

In the present study, we used a novel gene therapy approach that targets myosin in the contractile filaments of cardiomyocytes via overexpression of the RNR enzyme to rescue cardiomyopathy in a DMD mouse model. RNR overexpression results in elevated dATP, which can be used by cardiac myosin (in place of ATP), and increases cross-bridge binding and cycling, resulting in stronger, faster contraction and faster relaxation (38–45,52). We developed an rAAV vector that over-expresses RNR selectively in heart

FIGURE 4 Cardiac Transduction Following Intravenous Delivery of Ribonucleotide Reductase or Microdystrophin

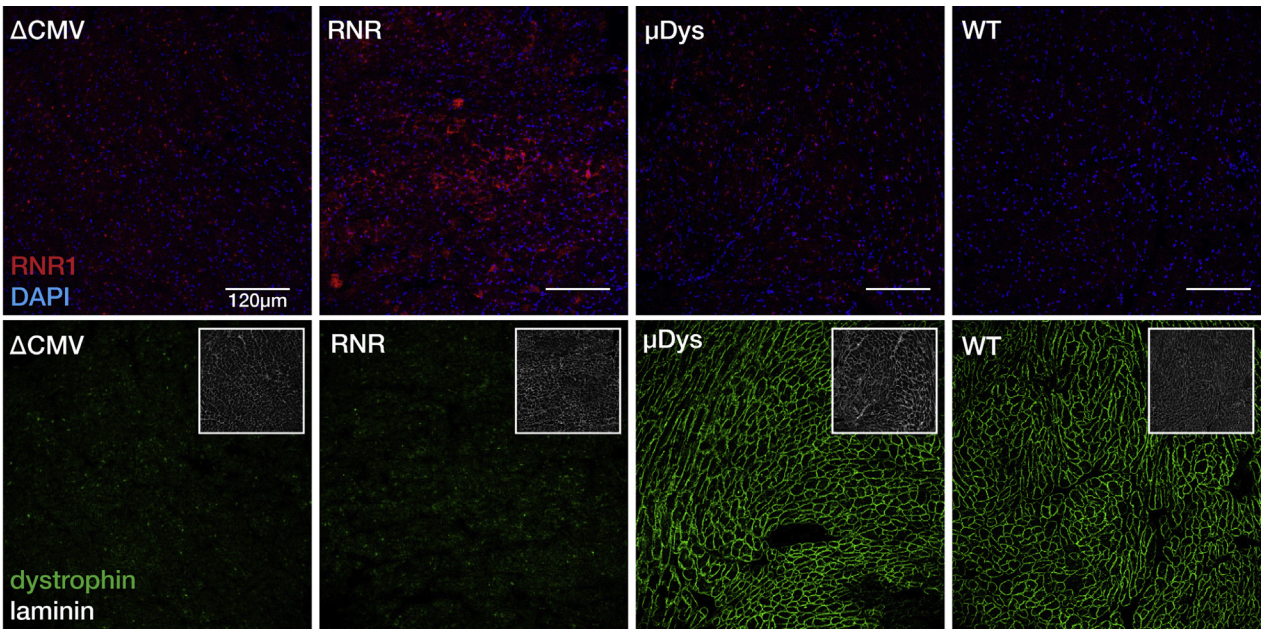

At 5 months after vector administration, cryosections were prepared and immunostained with antisera against dystrophin or ribonucleotide reductase. A considerable level of protein is detected for each ribonucleotide reductase subunit-1 (human specific) as indicated by immunofluorescent staining **(red)** localized primarily within the cytoplasm of cardiomyocytes with occasional perinuclear accumulation **(upper panel)**. On the lower panel, the robust level of expression for dystrophin in WT and in aged *mdx*^{4cv} mice treated with AAV6-CK8-μDys (laminin staining, **inset image**). Abbreviations as in Figures 1 and 2.

muscle via inclusion of a modified cardiac-specific enhancer/promoter derived from the human cTnT gene, which facilitates increases in myocyte contraction and cardiac performance in normal rodent hearts as well as in infarcted rodents and pig hearts (48,53). Importantly, we previously showed that dATP-producing cells deliver it to surrounding myocardium by diffusion through gap junctions (54), such that only a minority of cardiomyocytes needs to be transduced to have global benefits within the heart. We now show that using this vector technology leads to a clear benefit of improving cardiac function in an advanced-age model of DMD cardiomyopathy.

Early manifestations of impaired cardiac dysfunction in *mdx* mice are generally not reported. Khairallah et al.(55) observed a decline in LV function in isolated perfused hearts that coincided with decreased fatty acid oxidation and increased glucose oxidation. However, perfused heart function in *mdx* mice was maintained at 8 months, despite significant reductions in phosphocreatine levels and free energy availability from ATP hydrolysis (56). The authors surmised that young adult *mdx* hearts, akin to DMD patient hearts, experience right ventricular dilation, LV diastolic deficits, and abnormal energy metabolism. More recently, a declination in cardiac function was not observed until 12 months of age (57) and abnormal in vivo pressure-volume dynamics were observed in 22-month-old *mdx* mice (58). Treatment of young male *mdx* mice with rAAV6 vector delivering cytomegalovirus (CMV) promoter/enhancer driven microdystrophin did not correct the impairments in +dP/dt, -dP/dt, or LV systolic pressure when assessed at 5 months of age via hemodynamic analysis (35). However, an improvement was noted for the preload recruited stroke work in *mdx* mice treated with μDys compared to untreated *mdx* or WT control subjects (35).

In our current study, 27-month to 29-month-old mice were subjected to ex vivo assessment of cardiac function using the Langendorff isolated heart preparation, which is a century-old methodology with several advantages and limitations (59). The perfusate used is similar to, but not the same as blood, and situations of physiologic challenge (e.g., Frank-Starling and high calcium) may exaggerate the in vivo situation. However, the procedure remains a simple and reproducible experiment that allows for interrogation of cardiac physiology in the absence of confounding systemic variables and serves as a viable

FIGURE 5 Heart Histologic Staining of mdx^{4cv} Mice Suggests No Morphologic Alterations From RNR Therapy

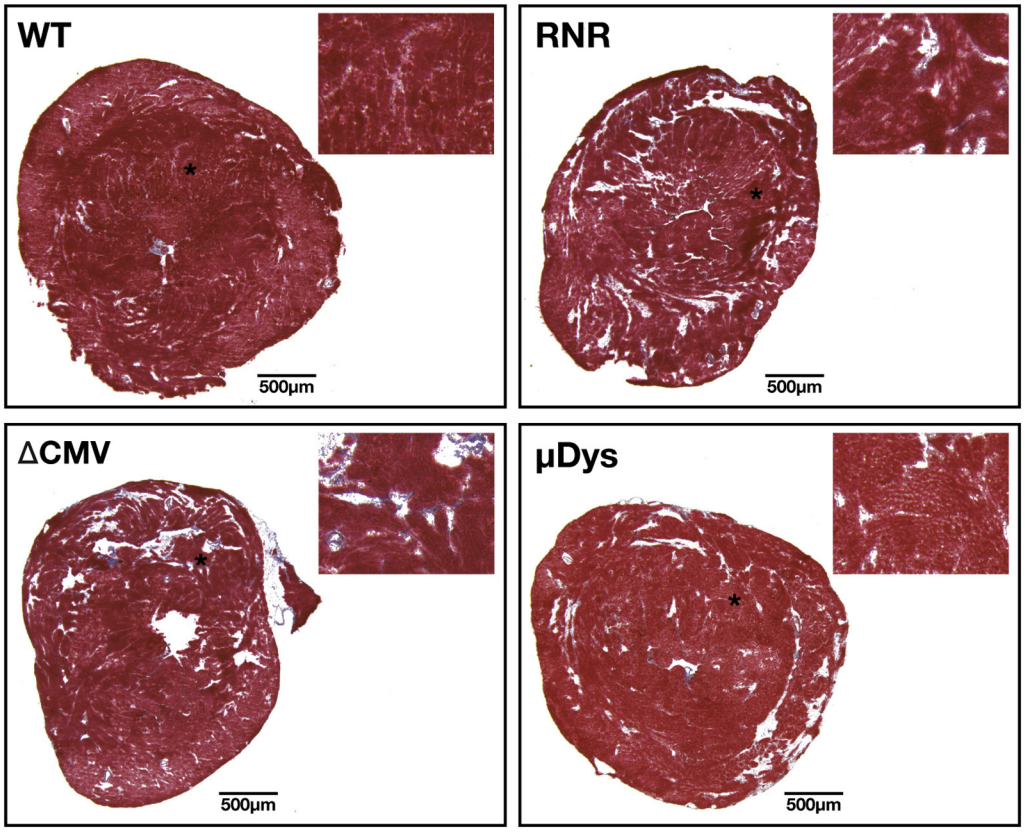

Representative full-view photomicrographs of Masson trichrome staining of the hearts from mdx^{4cv} mice displaying control vector (ΔCMV), and rAAV6-treated with either RNR or μDys from mdx4cv mice. Similarly, a 20× enlarged view of the corresponding images **(*)** is shown. Abbreviations as in **Figures 1 and 2**.

tool to perform cardiac phenotyping in preclinical studies (60). Under baseline conditions and at spontaneous heart rates, we observed a significant reduction in RPP in mdx^{4cv} hearts. Decreased systolic and diastolic performance in mdx^{4cv} hearts also existed while examining the length-tension relationship (i.e., Frank-Starling mechanism). Treatment of mdx^{4cv} mice with either the RNR or the μDys vector restored systolic pressure development without affecting spontaneous HRs at baseline. Both of the treatments restored the disrupted Frank-Starling response, particularly for systolic function. The RNR treatment also had beneficial effects on the diastolic properties of the mdx^{4cv} myocardium. This strongly supports our previous studies where we observed a tendency for overexpression of RNR to improve myocardial diastolic response in young, healthy, transgenic mice (47), mice treated with AAV (48), and in a porcine HF model (53).

In addition to the evaluation of basal cardiac performance, we tested cardiac reserve with a combination of high calcium plus elevated HRs and confirmed a significantly blunted response in 27-month to 29-month-old mdx^{4cv} hearts. Consistent with a previous report in young *mdx* mice (35), expressing μDys in aged mdx^{4cv} hearts significantly improved systolic performance during increased physiologic demand to a level similar to age-matched healthy control subjects. We previously reported that transgenic or vector-directed overexpression of RNR did not impair cardiac reserve during increased physiologic demand in young healthy hearts (47,48). Herein, we report that RNR over-expression in mdx^{4cv} hearts normalizes both the systolic and diastolic response to an increased cardiac challenge.

Approximately two-thirds of DMD mutations are deletions that span 1 or more exons, often leading to large deletions clustering around 2 mutational

FIGURE 6 Protein Expression Levels for μDys, RNR, and Resultant Vector Genomes Due to rAAV6-Mediated Gene Transfer

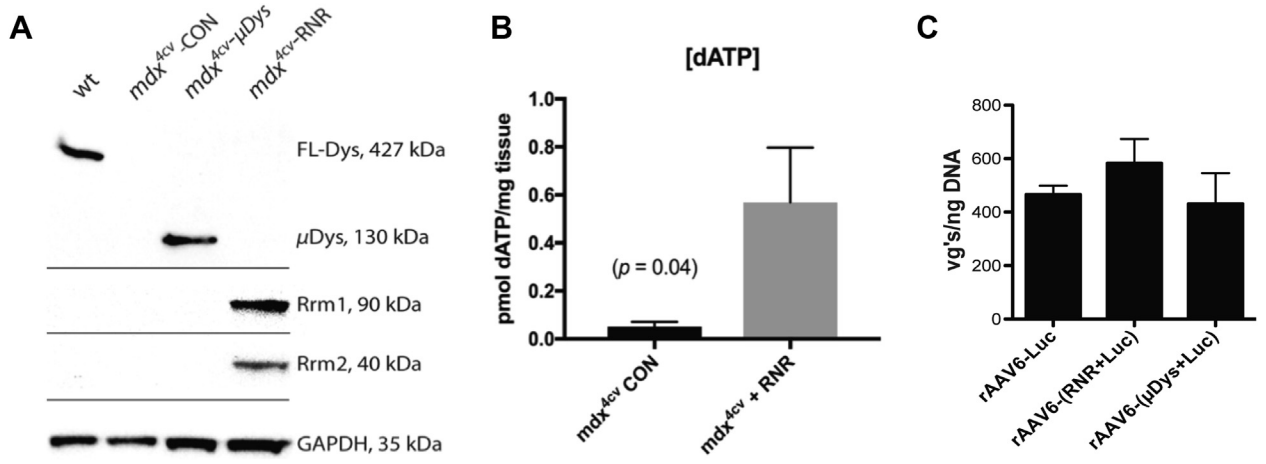

(A) RNR and μDys protein expression detection as revealed by immunoblotting of cardiac whole tissue lysates using either RRM1, RRM2, or antidystrophin antibody. **(B)** HPLC-MS/MS intracellular [dNTP] quantification from methanol extracted cardiac tissue. **(C)** qPCR analysis of vector genomes from cardiac tissue revealed similar vector genomes being represented for all treated cohorts. dNTP = deoxynucleotide triphosphate; HPLC-MS/MS = high-performance liquid chromatography–tandem mass spectrometry; qPCR = quantitative polymerase chain reaction; other abbreviations as in Figures 1 and 2.

hotspots; the most common spanning from exons 45-55 resulting in removal of a central portion of the rod domain inclusive of disrupting the neuronal nitric oxide synthase (nNOS) localization domain. The second most common hotspot spans from exons 3-19, and removes the majority of the amino-terminal actin-binding domain 1 which is essential for dystrophin function. When such deletions interrupt the reading frame, the resultant mutated protein usually expresses at extremely low levels and associates with the loss of ambulation at or before 12 years of age. Even when such deletions produce an in-frame partially functional truncated protein, such as occurs in BMD, dramatic phenotype diversity can occur. For example, in a previous study, BMD subjects whose out-of-phase deletions, toward the alignment of adjoining spectrin-like repeats, developed dilated cardiomyopathy at nearly a decade earlier than in patients with in-phase deletions (61). In contrast to large deletion mutations, there are reported cases where individual missense mutations lead to X-linked dilated cardiomyopathy (62-64). In one case, a novel missense mutation within exon 9 at nucleotide 1043 resulted in a T279A amino acid change in a highly conserved position of mutation. This mutation resulted in a substitution of a beta-sheet for alpha-helical structure, destabilizing the protein, and leading to the cardiac specific phenotype described by the authors (63).

DMD-related cardiomyopathy usually occurs during middle to late adolescence, but the clinical presentation is deceptive, as patients are wheelchair-bound and are not required to perform increased cardiac workload. The diversity of cardiac phenotype in DMD suggests many levels of pathogenic mechanisms. The pathologic heterogeneity of the DMD ventricular myocardium is a consequential result of myocardial atrophy (65,66), compensatory mechanisms leading to cardiac remodeling with ensuing ventricular dilation and fibrosis (67,68). Absence of clear genotype-phenotype correlation in DMD probably results from at least 4 secondary cellular processes including aberrant intracellular Ca^{2+} homeostasis, decreased nitric oxide–cyclic guanosine monophosphate pathways, mitochondrial dysfunction, and increased reactive oxygen species, which individually or collectively influence the clinical phenotype (69). As an indication of the progressive nature of DMD cardiomyopathy, the estimated overall incidence of latent DCM is 25% by 6 years of age and 59% by 10 years of age in DMD patients (70). As such, further evidence suggests latency in cardiac dysfunction at basal levels that becomes more pronounced with an induction of increased physiological demand. Consistent with these observations, an impaired response to beta-adrenergic stimulation by either dobutamine or isoproterenol can be detected in *mdx* mice at 3 to 4 months of age (35,71). Exercise can

potentially be a double-edged sword for DMD, where the enthusiasm for potential skeletal muscle benefits can be dampened by the insidious cardiotoxicity from training (72–74). With gene replacement therapy via rAAV-mediated μDys in current ongoing clinical trials, it will be of interest to assess cardiac function to determine whether additional therapeutic support in the form of increased contractility will be beneficial.

Relative expression assays by immunofluorescence and Western blotting indicate robust expression levels for the RNR subunits (RRM1 and RRM2) and μDys in the vast majority of cardiomyocytes. However, intracellular variability in RNR protein detection (via immunostaining) was observed for both RRM1 and RRM2, indicating that not all cardiomyocytes were effectively transduced. Nevertheless, we previously have shown that gap junction transport of dATP from transduced cardiomyocytes to adjacent cardiomyocytes occurs (54), which likely accounted for the consistently elevated LV function of mice treated with the rAAV vector that over-expresses RNR. This is in contrast to the anchored sarcolemma localization of μDys, which would occur only in transduced muscle cells. Additionally, because muscle-specific regulatory cassettes were used for expression of therapeutic proteins, we can surmise that <1% of protein expression would be generated from non-muscle cell types present in the heart, suggesting that the functional benefit was truly caused by cardiomyocyte transduction. As previously stated, the cTnT regulatory cassette drives RNR expression only in heart muscle, whereas the CK8 regulatory cassette drives μDys expression no selectively in both cardiac and skeletal muscle cells, but at only very low background levels in other tissues. This raises the possibility that the functional benefit of expressing μDys in skeletal muscles might increase energetic demands on the heart, thereby partially masking some of the μDys-derived cardiac functional benefits (37). Because RNR delivery to DMD mice of advanced age increased cardiac function in the absence of RNR expression in skeletal muscle, and because over-expression of endogenous RNR should be nonimmunogenic, supplemental RNR therapy in conjunction with μDys therapy might be beneficial for DMD patients. Future studies are aimed at determining the extent of functional restoration by combining both RNR- and μDys-based therapies.

ACKNOWLEDGMENTS The authors thank James Allen and Christine Halbert (Wellstone Muscular Dystrophy Specialized Research Center, University of Washington, Seattle, Washington) for assistance with vector production, purification, and quality assessment.

ADDRESS FOR CORRESPONDENCE: Dr. Guy L. Odom, Department of Neurology, University of Washington, 850 Republican Street, S248, Box 358055, Seattle, Washington 98109. E-mail: godom@uw.edu. OR Dr. Michael Regnier, Department of Bioengineering, University of Washington, 850 Republican Street, S180, Seattle, Washington 98109. E-mail: mregnier@uw.edu.

PERSPECTIVES

COMPETENCY IN MEDICAL KNOWLEDGE: RNR over-expression represents an emerging therapy for improving cardiac dysfunction via cardiac myosin activation in a variety of clinical situations. Currently, there are 3 ongoing clinical trials using rAAV-mediated variants of μDys that have shown broad promise in terms of safety, and in biomarker indicators suggesting pathologic improvements. If cardiac dysfunction is detected in the patients from these clinical studies, our studies in aged, *mdx* mice suggest that combinatorial RNR therapy may be beneficial.

TRANSLATIONAL OUTLOOK: Our novel strategy of vector-mediated, cardiac-specific over-expression of RNR shows promising potential for rescuing both systolic and diastolic function in aged, DMD mice even in the absence of addressing the underlying dystrophin deficiency. Future studies investigating the combined effects of μDys and RNR may disclose an improved therapeutic strategy to provide structural and functional improvement of DMD patient hearts.

REFERENCES

1. Emery AE, Muntoni F. Duchenne Muscular Dystrophy. 3rd ed. Oxford, United Kingdom: Oxford University Press, 2003:270.

2. Ervasti JM. Structure and function of the dystrophin-glycoprotein complex. In: Winder SJ, editor. Molecular Mechanisms of Muscular Dystrophies. Georgetown, Texas: Landes Biosciences, 2006:1–13.

3. Cox GA, Phelps SF, Chapman VM, Chamberlain JS. New *mdx* mutation disrupts expression of muscle and nonmuscle isoforms of dystrophin. Nature Genet 1993;4:87–93.

4. Brooks SV, Faulkner JA. Contractile properties of skeletal muscles from young, adult and aged mice. J Physiol (London) 1988;404:71–82.

5. Campbell KP. Three muscular dystrophies: loss of cytoskeleton-extracellular matrix linkage. Cell 1995;80:675–9.

6. Petrof BJ, Shrager JB, Stedman HH, Kelly AM, Sweeney HL. Dystrophin protects the sarcolemma from stresses developed during muscle contraction. Proc Natl Acad Sci U S A 1993;90:3710–4.

7. Ramaswamy KS, Palmer ML, van der Meulen JH, et al. Lateral transmission of force is impaired in skeletal muscles of dystrophic mice and very old rats. J Physiol 2011;589 Pt 5:1195–208.

8. Chao DS, Gorospe JR, Brenman JE, et al. Selective loss of sarcolemmal nitric oxide synthase in Becker muscular dystrophy. J Exp Med 1996;184:609–18.

9. Froehner SC. Just say NO to muscle degeneration? Trends Mol Med 2002;8:51–3.

10. Grady RM, Grange RW, Lau KS, et al. Role for alpha-dystrobrevin in the pathogenesis of dystrophin-dependent muscular dystrophies. Nat Cell Biol 1999;1:215–20.

11. Lapidos KA, Kakkar R, McNally EM. The dystrophin glycoprotein complex: signaling strength and integrity for the sarcolemma. Circ Res 2004;94:1023–31.

12. Ervasti JM, Campbell KP. A role for the dystrophin-glycoprotein complex as a transmembrane linker between laminin and actin. J Cell Biol 1993;122:809–23.

13. Ibraghimov-Beskrovnaya O, Ervasti JM, Leveille CJ, et al. Primary structure of dystrophin-associated glycoproteins linking dystrophin to the extracellular matrix. Nature 1992;355:696–702.

14. Yoshida M, Ozawa E. Glycoprotein complex anchoring dystrophin to sarcolemma. J Biochem (Tokyo) 1990;108:748–52.

15. England SB, Nicholson LV, Johnson MA, et al. Very mild muscular dystrophy associated with the deletion of 46% of dystrophin. Nature 1990;343:180–2.

16. Valentine BA, Winand NJ, Pradhan D, et al. Canine X-linked muscular dystrophy as an animal model of Duchenne muscular dystrophy: a review. Am J Med Genet 1992;42:352–6.

17. Im WB, Phelps SF, Copen EH, et al. Differential expression of dystrophin isoforms in strains of mdx mice with different mutations. Hum Mol Genet 1996;5:1149–53.

18. Phelps SF, Hauser MA, Cole NM, et al. Expression of full-length and truncated dystrophin mini-genes in transgenic *mdx* mice. Hum Mol Genet 1995;4:1251–8.

19. Crawford GE, Faulkner JA, Crosbie RH, et al. Assembly of the dystrophin-associated protein complex does not require the dystrophin COOH-terminal domain. J Cell Biol 2000;150:1399–410.

20. Harper SQ, Hauser MA, DelloRusso C, et al. Modular flexibility of dystrophin: implications for gene therapy of Duchenne muscular dystrophy. Nat Med 2002;8:253–61.

21. Wang B, Li J, Xiao X. Adeno-associated virus vector carrying human minidystrophin genes effectively ameliorates muscular dystrophy in mdx mouse model. Proc Natl Acad Sci U S A 2000;97:13714–9.

22. Sakamoto M, Yuasa K, Yoshimura M, et al. Micro-dystrophin cDNA ameliorates dystrophic phenotypes when introduced into mdx mice as a transgene. Biochem Biophys Res Commun 2002;293:1265–72.

23. Chamberlain JS. Gene therapy of muscular dystrophy. Hum Mol Genet 2002;11:2355–62.

24. Hakim CH, Wasala NB, Pan X, et al. A five-repeat micro-dystrophin gene ameliorated dystrophic phenotype in the severe DBA/2J-mdx model of Duchenne muscular dystrophy. Mol Ther Methods Clin Dev 2017;6:216–30.

25. Cox GA, Cole NM, Matsumura K, et al. Overexpression of dystrophin in transgenic mdx mice eliminates dystrophic symptoms without toxicity [see comments]. Nature 1993;364:725–9.

26. Stedman HH, Sweeney HL, Shrager JB, et al. The mdx mouse diaphragm reproduces the degenerative changes of Duchenne muscular dystrophy. Nature 1991;352:536–9.

27. Brooks SV, Faulkner JA. Skeletal muscle weakness in old age: underlying mechanisms. Med Sci Sports Exerc 1994;26:432–9.

28. DelloRusso C, Crawford R, Chamberlain J, Brooks S. Tibialis anterior muscles of *mdx* mice are highly susceptible to contraction-induced injury. J Muscle Res Cell Motility 2001;22:467–75.

29. Lynch GS, Hinkle RT, Chamberlain JS, Brooks SV, Faulkner JA. Force and power output of fast and slow skeletal muscles from mdx mice 6-28 months old. J Physiol 2001;535 Pt 2:591–600.

30. Bostick B, Shin JH, Yue Y, et al. AAV microdystrophin gene therapy alleviates stress-induced cardiac death but not myocardial fibrosis in >21-m-old mdx mice, an end-stage model of Duchenne muscular dystrophy cardiomyopathy. J Mol Cell Cardiol 2012;53:217–22.

31. Gregorevic P, Blankinship MJ, Allen JM, Chamberlain JS. Systemic microdystrophin gene delivery improves skeletal muscle structure and function in old dystrophic mdx mice. Mol Ther 2008;16:657–64.

32. Quinlan JG, Hahn HS, Wong BL, et al. Evolution of the mdx mouse cardiomyopathy: physiological and morphological findings. Neuromuscul Disord 2004;14:491–6.

33. Gregorevic P, Allen JM, Minami E, et al. rAAV6-microdystrophin preserves muscle function and extends lifespan in severely dystrophic mice. Nat Med 2006;12:787–9.

34. Shin JH, Nitahara-Kasahara Y, Hayashita-Kinoh H, et al. Improvement of cardiac fibrosis in dystrophic mice by rAAV9-mediated microdystrophin transduction. Gene Ther 2011;18:910–9.

35. Townsend D, Blankinship MJ, Allen JM, et al. Systemic administration of micro-dystrophin restores cardiac geometry and prevents dobutamine-induced cardiac pump failure. Mol Ther 2007;15:1086–92.

36. Bostick B, Shin JH, Yue Y, Duan D. AAV-microdystrophin therapy improves cardiac performance in aged female mdx mice. Mol Ther 2011;19:1826–32.

37. Townsend D, Yasuda S, Chamberlain J, Metzger JM. Cardiac consequences to skeletal muscle-centric therapeutics for Duchenne muscular dystrophy. Trends Cardiovasc Med 2009;19:50–5.

38. Adhikari BB, Regnier M, Rivera AJ, Kreutziger KL, Martyn DA. Cardiac length dependence of force and force development kinetics with altered cross-bridge cycling. Biophysical J 2004;87:1784–94.

39. Clemmens EW, Entezari M, Martyn DA, Regnier M. Different effects of cardiac versus skeletal muscle regulatory proteins on in vitro measures of actin filament speed and force. J Physiol 2005;566 Pt 3:737–46.

40. Korte FS, Dai J, Buckley K, et al. Upregulation of cardiomyocyte ribonucleotide reductase increases intracellular 2 deoxy-ATP, contractility, and relaxation. J Mol Cell Cardiol 2011;51:894–901.

41. Kreutziger KL, Piroddi N, McMichael JT, Poggesi C, Tesi C, Regnier M. Cooperative activation and tension kinetics in cardiac muscle are strongly modulated by calcium binding kinetics of troponin C. J Mol Cell Cardiol 2011;50:165–74.

42. Moussavi-Harami F, Razumova MV, Racca AW, et al. 2-deoxy adenosine triphosphate improves contraction in human end-stage heart failure. J Mol Cell Cardiol 2015;79:256–63.

43. Regnier M, Lee DM, Homsher E. ATP analogs and muscle contraction: mechanics and kinetics of nucleoside triphosphate binding and hydrolysis. Biophys J 1998;74:3044–58.

44. Regnier M, Martin H, Barsotti RJ, et al. Cross-bridge versus thin filament contributions to the level and rate of force development in cardiac muscle. Biophys J 2004;87:1815–24.

45. Regnier M, Rivera AJ, Chen Y, Chase PB. 2-deoxy-ATP enhances contractility of rat cardiac muscle. Circ Res 2000;86:1211–7.

46. Cheng Y, Hogarth KA, O'Sullivan ML, Regnier M, Pyle WG. 2-deoxyadenosine triphosphate restores the contractile function of cardiac myofibril from adult dogs with naturally occurring dilated cardiomyopathy. Am J Physiol Heart Circ Physiol 2016;310:H80–91.

47. Nowakowski SG, Kolwicz SC, Korte FS, et al. Transgenic overexpression of ribonucleotide reductase improves cardiac performance. Proc Natl Acad Sci U S A 2013;110:6187–92.

48. Kolwicz SC Jr., Odom GL, Nowakowski SG, et al. AAV6-mediated cardiac-specific overexpression of ribonucleotide reductase enhances myocardial contractility. Mol Ther 2016;24:240–50.

49. Halbert CL, Allen JM, Chamberlain JS. AAV6 vector production and purification for muscle gene therapy. Methods Mol Biol 2018;1687:257–66.

50. Olafsson S, Whittington D, Murray J, Regnier M, Moussavi-Harami F. Fast and sensitive HPLC-MS/MS method for direct quantification of intracellular deoxyribonucleoside triphosphates from tissue and cells. J Chromatogr B Analyt Technol Biomed Life Sci 2017;1068-1069:90–7.

51. Kolwicz SC Jr., Tian R. Assessment of cardiac function and energetics in isolated mouse hearts using 31P NMR spectroscopy. J Vis Exp 2010;42:e2069.

52. Kreutziger KL, Piroddi N, Belus A, Poggesi C, Regnier M. Ca^{2+}-binding kinetics of troponin C influence force generation kinetics in cardiac muscle. Biophysical J 2007;92:477a.

53. Kadota S, Carey J, Reinecke H, et al. Ribonucleotide reductase-mediated increase in dATP

improves cardiac performance via myosin activation in a large animal model of heart failure. Eur J Heart Fail 2015;17:772–81.

54. Lundy SD, Murphy SA, Dupras SK, et al. Cell-based delivery of dATP via gap junctions enhances cardiac contractility. J Mol Cell Cardiol 2014;72:350–9.

55. Khairallah M, Khairallah R, Young ME, et al. Metabolic and signaling alterations in dystrophin-deficient hearts precede overt cardiomyopathy. J Mol Cell Cardiol 2007;43:119–29.

56. Zhang W, ten Hove M, Schneider JE, et al. Abnormal cardiac morphology, function and energy metabolism in the dystrophic mdx mouse: an MRI and MRS study. J Mol Cell Cardiol 2008;45:754–60.

57. Stuckey DJ, Carr CA, Camelliti P, et al. In vivo MRI characterization of progressive cardiac dysfunction in the mdx mouse model of muscular dystrophy. PLoS One 2012;7:e28569.

58. Bostick B, Yue Y, Duan D. Gender influences cardiac function in the mdx model of Duchenne cardiomyopathy. Muscle Nerve 2010;42:600–3.

59. Bell RM, Mocanu MM, Yellon DM. Retrograde heart perfusion: the Langendorff technique of isolated heart perfusion. J Mol Cell Cardiol 2011;50:940–50.

60. Liao R, Podesser BK, Lim CC. The continuing evolution of the Langendorff and ejecting murine heart: new advances in cardiac phenotyping. Am J Physiol Heart Circ Physiol 2012;303:H156–67.

61. Kaspar RW, Allen HD, Ray WC, et al. Analysis of dystrophin deletion mutations predicts age of cardiomyopathy onset in becker muscular dystrophy. Circ Cardiovasc Genet 2009;2:544–51.

62. Feng J, Yan J, Buzin CH, Towbin JA, Sommer SS. Mutations in the dystrophin gene are associated with sporadic dilated cardiomyopathy. Mol Genet Metab 2002;77:119–26.

63. Ortiz-Lopez R, Li H, Su J, Goytia V, Towbin JA. Evidence for a dystrophin missense mutation as a cause of X-linked dilated cardiomyopathy. Circulation 1997;95:2434–40.

64. Singh SM, Bandi S, Shah DD, Armstrong G, Mallela KM. Missense mutation Lys18Asn in dystrophin that triggers X-linked dilated cardiomyopathy decreases protein stability, increases protein unfolding, and perturbs protein structure, but does not affect protein function. PLoS One 2014;9:e110439.

65. Lee TH, Eun LY, Choi JY, et al. Myocardial atrophy in children with mitochondrial disease and Duchenne muscular dystrophy. Korean J Pediatr 2014;57:232–9.

66. Matsuoka S, Ii K, Akita H, et al. Clinical features and cardiopulmonary function of patients with atrophic heart in Duchenne muscular dystrophy. Jpn Heart J 1987;28:687–94.

67. Konstam MA, Kramer DG, Patel AR, Maron MS, Udelson JE. Left ventricular remodeling in heart failure: current concepts in clinical significance and assessment. J Am Coll Cardiol Img 2011;4:98–108.

68. Silva MC, Meira ZM, Gurgel Giannetti J, et al. Myocardial delayed enhancement by magnetic resonance imaging in patients with muscular dystrophy. J Am Coll Cardiol 2007;49:1874–9.

69. Shirokova N, Niggli E. Cardiac phenotype of Duchenne muscular dystrophy: insights from cellular studies. J Mol Cell Cardiol 2013;58:217–24.

70. Nigro G, LComi LI, Politano L, Bain RJ. The incidence and evolution of cardiomyopathy in Duchenne muscular dystrophy. Int J Cardiol 1990;26:271–7.

71. Li Y, Zhang S, Zhang X, et al. Blunted cardiac beta-adrenergic response as an early indication of cardiac dysfunction in Duchenne muscular dystrophy. Cardiovasc Res 2014;103:60–71.

72. Barbin IC, Pereira JA, Bersan Rovere M, et al. Diaphragm degeneration and cardiac structure in mdx mouse: potential clinical implications for Duchenne muscular dystrophy. J Anat 2016;228:784–91.

73. Costas JM, Nye DJ, Henley JB, Plochocki JH. Voluntary exercise induces structural remodeling in the hearts of dystrophin-deficient mice. Muscle Nerve 2010;42:881–5.

74. Nakamura A, Yoshida K, Takeda S, Dohi N, Ikeda S. Progression of dystrophic features and activation of mitogen-activated protein kinases and calcineurin by physical exercise, in hearts of mdx mice. FEBS Lett 2002;520:18–24.

KEY WORDS cardiomyopathy, diastolic dysfunction, dystrophin, ribonucleotide reductase, recombinant adeno-associated virus vectors

APPENDIX For supplemental figures, please see the online version of this paper.

JACC: BASIC TO TRANSLATIONAL SCIENCE VOL. 4, NO. 7, 2019

EDITORIAL COMMENT

Emerging Therapies for Dystrophic Cardiomyopathy*

Daniel J. Garry, MD, PhD, Tamas Alexy, MD, PhD

Duchenne muscular dystrophy (DMD) is the most common form of muscular dystrophy that affects approximately 1 of every 5,000 boys born in the United States (1,2). This recessive X-linked genetic disease is a result of mutations in the dystrophin gene. The dystrophin gene is the largest known gene in the human genome as it spans 2.5 Mb, harbors 79 exons, and encodes a 14-kb transcript (2–4). Dystrophin is expressed in the heart (i.e., cardiomyocytes), skeletal muscle, and the brain (2,4). It is a rod-shaped cytoplasmic protein that provides structural stability to the multiprotein dystrophin glycoprotein complex in the plasma membrane and links the cytoskeleton to the extracellular matrix (5). Skeletal muscle lacking functional dystrophin is mechanically weak, and cellular (or sarcomeric) contraction results in membrane damage (6,7). Consequently, the loss of membrane integrity leads to a cascade of increased calcium influx into the cell and eventual cell death.

A majority of the dystrophin mutations are deletions that span 1 or more exons. Clinically, the loss of dystrophin manifests as progressive muscle weakness (5,8). Symptoms are first noted in early childhood, and patients progress to muscle atrophy, contractures, and subsequent loss of ambulation in their early teens. Ultimately, DMD is a lethal and devastating disease. However, with the advent of nocturnal ventilation and spinal stabilization, the life expectancy of young men with DMD has increased to late 20s to early 30s (2,9). Historically, respiratory or pulmonary complications were the leading cause of death in DMD patients, and now dilated cardiomyopathy and sudden cardiac death have emerged as the predominant cause of death in these patients (2,10). Dilated cardiomyopathy is nearly ubiquitous in DMD patients, with approximately 90% of young men over the age of 18 years demonstrating evidence of cardiomyopathy (10). Given the prevalence of cardiomyopathy in this patient population, an enhanced understanding of the pathophysiology of DMD cardiomyopathy is urgently needed.

The most commonly used animal model of DMD is the mdx mouse model (2). This genetic mouse model arose spontaneously and was found to have a point mutation in the dystrophin gene changing glutamine to an early termination codon producing a small, nonfunctional protein (11–13). This mouse model has a robust dystrophic skeletal muscle phenotype involving the diaphragm but otherwise has a relatively mild phenotype that may be due, in part, to the inactivity associated with the animal vivarium. However, the dystrophic skeletal muscle and cardiac phenotypes in the mdx mouse worsen with age (11–13). Although scores of studies using the mdx mouse model have examined the skeletal muscle phenotype, a limited number of studies have examined the cardiac phenotype or examined therapeutic interventions for dystrophic cardiac dysfunction. The high incidence of DMD and dystrophic cardiomyopathy in the general population and the terminal nature of the disease in early adulthood warrant the urgent development of new therapeutic approaches for this disease.

In the paper by Kolwicz et al. (14) in this issue of *JACC: Basic to Translational Science*, the authors used a recombinant adeno-associated viral vector strategy to examine the impact of deoxy-adenosine

*Editorials published in *JACC: Basic to Translational Science* reflect the views of the authors and do not necessarily represent the views of *JACC: Basic to Translational Science* or the American College of Cardiology.

From the Department of Medicine, Paul and Sheila Wellstone Muscular Dystrophy Center, University of Minnesota, Minneapolis, Minnesota. Dr. Garry has received grants from Regenerative Medicine Minnesota (RMM), the American Heart Association, the National Institutes of Health, and the Department of Defense. Both authors have reported that they have no relationships relevant to the contents of this paper to disclose.

The authors attest they are in compliance with human studies committees and animal welfare regulations of the authors' institutions and Food and Drug Administration guidelines, including patient consent where appropriate. For more information, visit the *JACC: Basic to Translational Science* author instructions page.

ISSN 2452-302X https://doi.org/10.1016/j.jacbts.2019.10.003

diphosphate elevation or microdystrophin (3.8 kb) in the aged dystrophic heart of the mdx mouse model.

SEE PAGE 778

These studies demonstrated that adeno-associated virus 6 (aAAV6)-mediated delivery of ribonucleotide reductase (RNR, which increases deoxy-adenosine diphosphate and has previously been shown to increase myosin cross bridge binding and cycling resulting in faster contraction and relaxation) or microdystrophin increased cardiac function at baseline and after an increased workload (i.e., pacing stimulation) in aged mdx mice. Furthermore, 5 months post-treatment, mdx mice that received microdystrophin had a marked improvement in cardiac systolic function, whereas mdx mice treated with aAAV6 to specifically overexpress RNR demonstrated improved systolic and diastolic function (14). Importantly, morphological studies verified that aAAV6 delivery of RNR or microdystrophin was localized to the cytoplasmic compartment and the sarcolemma of cardiomyocytes, respectively. In addition, RNR and microdystrophin delivery did not result in worsening cardiac fibrosis or perturbed cytoarchitecture compared with the age-matched mdx control heart (14).

These studies are important for a number of reasons. First, they used a gene therapy strategy that is feasible in the clinical setting. Second, they targeted and compared therapeutic strategies aimed at both the structural and metabolic defects associated with the dystrophic heart. Third, they utilized both the whole animal (mdx mouse) and an in vitro working heart model (i.e., the Langendorff heart preparation) to examine the impact of RNR or microdystrophin on the dystrophic heart function of the mdx mouse. Fourth, the authors examined the impact of RNR or microdystrophin under baseline conditions and after stimulation (i.e., a pacing protocol). Collectively, these studies provide new insights regarding systolic (heart failure with reduced ejection fraction) and diastolic (heart failure with preserved ejection fraction) dysfunction in the dystrophic heart, and they provide a platform for future studies.

Additional studies will be necessary to examine the impact of combined therapies such as the combination of both RNR and microdystrophin (together) on the dystrophic heart. It will also be important to explore the effect of the dystrophic mdx heart (treated with RNR and/or microdystrophin) with other stimuli such as beta-adrenergic stimulation (i.e., chronic isoproterenol stimulation), exercise stimulation (chronic wheel running or a swimming protocol), or other stress-mediated stimuli. Moreover, although the mdx mouse has a relatively mild phenotype, other DMD animal models (i.e., the mdx/utrophin heterozygous mouse model or the dystrophic golden retriever canine model) that reflect the human disease should be used and examined for their response to RNR and/or microdystrophin and their long-term impact on dystrophic cardiomyopathy. Moreover, although the current studies examined the physiological and morphological response to RNR and microdystrophin, future studies should also examine the whole genome response (using bulk RNA sequencing) to treatments directed to structural and metabolic improvements. Finally, studies will need to examine the ability of these therapies to prevent the onset of dystrophic cardiomyopathy as well as the long-term impact of these therapies in the dystrophic background.

In summary, dystrophic cardiomyopathy affects essentially all DMD patients and contributes to their demise. New studies are warranted aimed at increasing our understanding of DMD cardiomyopathy and the development of emerging therapies. The study by Kolwicz et al. (14) is an important step forward in the development of emerging therapies aimed at the structural and metabolic perturbations in the DMD heart.

ADDRESS FOR CORRESPONDENCE: Dr. Daniel J. Garry, Paul and Sheila Wellstone Muscular Dystrophy Center, 2231 6th Street Southeast (CCRB 4-146), University of Minnesota, Minneapolis, Minnesota 55455. E-mail: garry@umn.edu.

REFERENCES

1. Mendell JR, Lloyd-Puryear M. Report of MDA muscle disease symposium on newborn screening for Duchenne muscular dystrophy. Muscle Nerve 2013;48:21–6.

2. Kamdar F, Garry DJ. Dystrophin-deficient cardiomyopathy. J Am Coll Cardiol 2016;67:2533–46.

3. Emery AE. The muscular dystrophies. Lancet 2002;359:687–95.

4. Cox GF, Kunkel LM. Dystrophies and heart disease. Curr Opin Cardiol 1997;12:329–43.

5. Rybakova IN, Patel JR, Ervasti JM. The dystrophin complex forms a mechanically strong link between the sarcolemma and costameric actin. J Cell Biol 2000;150:1209–14.

6. Cox GA, Cole NM, Matsumura K, et al. Overexpression of dystrophin in transgenic mdx mice eliminates dystrophic symptoms without toxicity. Nature 1993;364:725–9.

7. Petrof BJ, Shrager JB, Stedman HH, Kelly AM, Sweeney HL. Dystrophin protects the sarcolemma from stresses developed during muscle contraction. Proc Natl Acad Sci U S A 1993;90:3710–4.

8. Petrof BJ. The molecular basis of activity-induced muscle injury in Duchenne muscular dystrophy. Mol Cell Biochem 1998;179:111–23.

JACC: BASIC TO TRANSLATIONAL SCIENCE VOL. 4, NO. 7, 2019
NOVEMBER 2019:792–4

9. Eagle M, Baudouin SV, Chandler C, Giddings DR, Bullock R, Bushby K. Survival in Duchenne muscular dystrophy: improvements in life expectancy since 1967 and the impact of home nocturnal ventilation. Neuromuscul Disord 2002;12:926–9.

10. Nigro G, Comi LI, Politano L, Bain RJ. The incidence and evolution of cardiomyopathy in Duchenne muscular dystrophy. Int J Cardiol 1990;26:271–7.

11. Coulton GR, Curtin NA, Morgan JE, Partridge TA. The mdx mouse skeletal muscle myopathy: II. Contractile properties. Neuropathol Appl Neurobiol 1988;14:299–314.

12. Kamogawa Y, Biro S, Maeda M, et al. Dystrophin-deficient myocardium is vulnerable to pressure overload in vivo. Cardiovasc Res 2001;50:509–15.

13. Quinlan JG, Hahn HS, Wong BL, Levin LS. Evolution of the mdx mouse cardiomyopathy: physiological and morphological findings. Neuromuscul Disord 2004;14:491–6.

14. Kolwicz SC Jr., Hall JK, Moussavi-Harami F, et al. Gene therapy rescues cardiac dysfunction in Duchenne muscular dystrophy mice by elevating cardiomyocyte deoxy-adenosine triphosphate. J Am Coll Cardiol Basic Trans Science 2019;4:778–91.

KEY WORDS cardiomyopathy, diastolic dysfunction, dystrophin, ribonucleotide reductase, recombinant adeno-associated virus vectors

JACC: BASIC TO TRANSLATIONAL SCIENCE VOL. 4, NO. 7, 2019

PRECLINICAL RESEARCH

Electrophysiological and Contractile Effects of Disopyramide in Patients With Obstructive Hypertrophic Cardiomyopathy

A Translational Study

Raffaele Coppini, MD, PhD,[a] Cecilia Ferrantini, MD, PhD,[b,c] Josè Manuel Pioner, PhD,[b] Lorenzo Santini, MS,[a] Zhinuo J. Wang, PhD,[d] Chiara Palandri, MS,[a] Marina Scardigli, PhD,[e] Giulia Vitale, MS,[b] Leonardo Sacconi, PhD,[e] Pierluigi Stefàno, MD,[b,c] Laura Flink, MD,[f] Katherine Riedy, MD,[g] Francesco Saverio Pavone, PhD,[e] Elisabetta Cerbai, PhD,[a] Corrado Poggesi, MD,[b] Alessandro Mugelli, MD,[a] Alfonso Bueno-Orovio, PhD,[d] Iacopo Olivotto, MD,[b,c] Mark V. Sherrid, MD[g]

VISUAL ABSTRACT

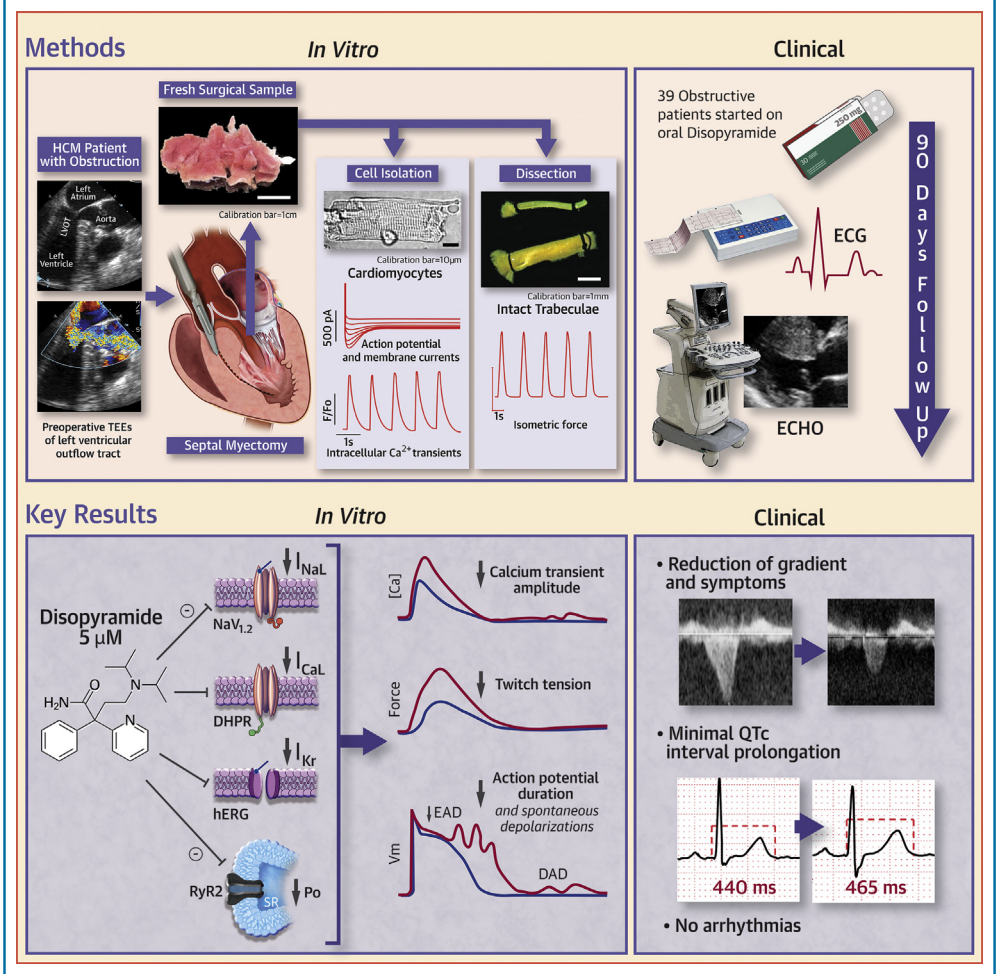

Coppini, R. et al. J Am Coll Cardiol Basic Trans Science. 2019;4(7):795–813.

ISSN 2452-302X https://doi.org/10.1016/j.jacbts.2019.06.004

ABBREVIATIONS AND ACRONYMS

AP = action potential

DAD = delayed afterdepolarization

EAD = early afterdepolarization

ECG = electrocardiography

hERG = human ether-à-go-go-related gene

HCM = hypertrophic cardiomyopathy

$I_{Ca\text{-}L}$ = L-type Ca current

I_K = delayed-rectifier K current

I_{NaL} = late Na current

LVOT = left ventricular outflow tract

NCX = Na^+/Ca^{2+} exchanger

pCa = Ca activation level

RyR = ryanodine receptor

SR = sarcoplasmic reticulum

HIGHLIGHTS

- **In patients with HCM and symptomatic LVOT-obstruction, first treatment with disopyramide leads to a marked reduction of LVOT gradients, with a slight decrease of resting ejection fraction and a modest increase of corrected QT interval, highlighting high efficacy and safety.**
- **In single cardiomyocytes and intact trabeculae from surgical samples of patients with obstructive HCM, in vitro treatment with 5 μmol/l disopyramide lowered force and $Ca2^+$ transients while reducing action potential duration and the rate of arrhythmic afterdepolarizations.**
- **These effects are mediated by the combined inhibition of peak and late Na^+ currents, L-type Ca^{2+} current, delayed-rectifier K^+ current, and ryanodine receptors.**
- **In addition to the negative inotropic effect of disopyramide, in vitro results suggest additional antiarrhythmic actions.**

SUMMARY

Disopyramide is effective and safe in patients with obstructive hypertrophic cardiomyopathy. However, its cellular and molecular mechanisms of action are unknown. We tested disopyramide in cardiomyocytes from the septum of surgical myectomy patients: disopyramide inhibits multiple ion channels, leading to lower Ca transients and force, and shortens action potentials, thus reducing cellular arrhythmias. The electrophysiological profile of disopyramide explains the efficient reduction of outflow gradients but also the limited prolongation of the QT interval and the absence of arrhythmic side effects observed in 39 disopyramide-treated patients. In conclusion, our results support the idea that disopyramide is safe for outpatient use in obstructive patients. (J Am Coll Cardiol Basic Trans Science 2019;4:795–813)

Disopyramide is a potent negative inotrope (1). It has been used to decrease left ventricular outflow tract (LVOT) obstruction in obstructive hypertrophic cardiomyopathy (HCM) since the first reports in the early 1980s and after confirmatory studies of its efficacy and safety (2–6). In patients with obstructive HCM and limiting symptoms, disopyramide in addition to a beta blocker has a Class I recommendation by the 2014 European Society of Cardiology guidelines and a Class IIa recommendation by the 2011 American Heart Association/American College of Cardiology Foundation guidelines (7,8). Most recently, safe initiation in outpatients has been retrospectively demonstrated (9). Its practical use and current place in the armamentarium for obstructive HCM has been described and reviewed elsewhere (10,11).

Despite its active use since the 1980s, there has been little work on the intracellular mechanism of therapeutic effects of disopyramide beyond its

From the [a]Department NeuroFarBa, University of Florence, Florence, Italy; [b]Department of Experimental and Clinical Medicine, University of Florence, Florence, Italy; [c]Cardiomyopathy Unit, Careggi University Hospital, Florence, Italy; [d]Department of Computer Sciences, University of Oxford, Oxford, United Kingdom; [e]European Laboratory for Nonlinear Spectroscopy (LENS), University of Florence, Sesto Fiorentino, Italy and National Institute of Optics, National Research Council, Florence, Italy; [f]Division of Cardiology, San Francisco Veterans Affairs Medical Center and University of California-San Francisco, San Francisco, California; and the [g]Hypertrophic Cardiomyopathy Program, New York University Langone Health, New York, New York. Supported by the European Union's Horizon 2020 Research and Innovation Programme (grant 777204, SILICO-FCM, to Drs. Ferrantini, Pioner, Poggesi, and Olivotto), the Italian Ministry of Health (grants RF-2013-02356787, NET-2011-02347173, and GR-2011-02350583 to Drs. Ferrantini and Olivotto), Regione Toscana (FAS-Salute 2014, project ToRSADE to Drs. Coppini, Santini, and Cerbai), a British Heart Foundation Intermediate Basic Science Research Fellowship (FS/17/22/32644 to Drs. Wang and Bueno-Orovio) and an ARCHER RAP Award. All authors have reported that they have no relationships relevant to the contents of this paper to disclose.

The authors attest they are in compliance with human studies committees and animal welfare regulations of the authors' institutions and Food and Drug Administration guidelines, including patient consent where appropriate. For more information, visit the *JACC: Basic to Translational Science* author instructions page.

Manuscript received April 15, 2019; revised manuscript received June 7, 2019, accepted June 7, 2019.

categorization as a type Ia antiarrhythmic, that is, as Na channel blocker with action potential (AP)-prolonging effects (12,13). A paper in the late 1980s suggested an effect on sarcolemmal Ca influx and efflux mediated by the Na^+/Ca^{2+} exchanger (NCX) (14). In light of its potent negative inotropic effects, it is not known whether the drug has additional direct effects on Ca^{2+} current, Ca^{2+} release from the sarcoplasmic reticulum (SR) or on the actin-myosin interaction and the effects of disopyramide in human HCM cardiomyocytes have not been characterized.

SEE PAGE 814

We previously analyzed the electromechanical profile of cardiomyocytes isolated from myectomy samples of patients with obstructive HCM (15,16). When compared with control cells, HCM cardiomyocytes showed prolonged AP, frequent afterdepolarizations, slower Ca^{2+} transients, and elevated diastolic Ca^{2+} concentration, largely determined by overexpression of the late Na^+ current (I_{NaL}). Indeed, these electromechanical abnormalities were reversed by the I_{NaL} inhibitor ranolazine, with beneficial effects on diastolic function and cellular arrhythmias (15,16).

In the present study, we sought to uncover mechanistic insights by applying electrophysiological and biophysical techniques to evaluate the effects of disopyramide on ion fluxes, afterdepolarizations, and twitch tension in isolated HCM cardiomyocytes and intact trabeculae harvested from patients undergoing surgical septal myectomy. In a translational approach, the in vitro study was combined with the first prospective characterization of the electrocardiographic and echocardiographic changes in patients with obstructive HCM started on disopyramide treatment.

METHODS

Detailed methods are available in the Supplemental Appendix data supplement.

PROSPECTIVE STUDY OF PATIENTS WITH OBSTRUCTIVE HCM TREATED WITH DISOPYRAMIDE. From October 1, 2015, to January 31, 2018, 39 patients with limiting heart failure symptoms and elevated LVOT gradients were initiated on sustained release disopyramide at New York University Langone Medical Center as previously described (4-6,9). Initial disopyramide dosage was 250 mg twice a day, followed by drug titration up to a maximum dosage of 300 mg every 12 h. Electrocardiography (ECG) was performed at each visit by recording 3 12-lead 15-s strips (collected at least 5 min apart), and QTc interval was calculated from each strip by averaging the QT intervals measured by a blinded operator from the 12 leads and correcting them for heart rate using the Bazett and the Fredericia methods. QTc values from the 3 repeated ECG strips were then averaged to obtain the final value. Echocardiography was performed to measure transmitral flow velocities and mitral annular diastolic velocities and to calculate resting LVOT gradients and LV ejection fraction before and after disopyramide.

PATIENTS FOR STUDIES IN CELLS AND TRABECULAE. In vitro studies were performed at the University of Florence. Protocols were approved by the ethical committee of Careggi University Hospital (2006/0024713, renewed May 2009). We enrolled 20 patients with HCM regularly followed by our Cardiomyopathy Unit and consecutively referred to surgical myectomy for relief of drug-refractory symptoms related to LVOT obstruction. Among the 20 patients, 12 agreed to undergo mutational screening in sarcomeric genes. Clinical and genetic data are found in Supplemental Table 1.

STATISTICS (CLINICAL STUDIES). Clinical data from patients are expressed as mean ± SD. Comparisons of clinical variables before and after disopyramide were performed using Student's paired *t*-tests. To assess the relationship between the initial QTc and the increase in QTc with disopyramide, we calculated the Pearson correlation coefficient (*r*) and its significance level using MedCalc version 19.0 (MedCalc Software, Ostend, Belgium).

TISSUE PROCESSING AND CELL ISOLATION. Septal specimens from 20 consecutive surgical patients were collected from the surgeon and immediately washed with cardioplegic solution and processed within 30 min from excision. Each sample was given a unique anonymous identification number (ID 1 to ID 20). Endocardial trabeculae suitable for mechanical measurements were dissected and the remaining tissue was minced and subjected to enzymatic dissociation to obtain viable single myocytes, as previously described (17).

SINGLE CELL STUDIES. A perforated patch whole-cell current clamp was used to measure membrane potential, as previously described (15). [Ca^{2+}] variations were simultaneously monitored using the Ca^{2+}-sensitive fluorescent dye FluoForte (Enzo Life Sciences, Farmingdale, New York). A whole-cell ruptured patch voltage clamp was used to record peak and late Na^+ current, L-type Ca^{2+} current ($I_{Ca\text{-}L}$), and delayed rectifier K^+ current (I_K), using appropriate protocols and solutions (15).

INTACT TRABECULAE STUDIES. Ventricular trabeculae were mounted between a force transducer and a motor for muscle length control (15), and isometric force was recorded under different stimulation

protocols. In brief, we evaluated the inotropic responses to increased pacing frequencies and the kinetics of isometric twitches. Resting sarcomere length was 1.9 ± 0.1 μm.

DEMEMBRANATED TRABECULAE. Ventricular trabeculae were skinned by exposure to 0.5% Triton X100 solution. Demembranated trabeculae were employed to obtain calcium concentration (pCa)-tension curves as previously described (15,18,19). Sarcomere energetics was assessed in demembranated trabeculae by simultaneous measurement of isometric force and adenosine triphosphatase activity with an enzyme-coupled assay (15,18,19); measurements were repeated in the presence of disopyramide.

DRUG STUDIES. For experiments on isolated cardiomyocytes and trabeculae, disopyramide was used at the concentration of 5 μmol/l, unless otherwise specified. Test recordings in presence of the drug were performed after >3 min from the beginning of drug exposure. Afterward, the drug was washed out for >5 min and measurements were repeated. Of note, all the effects of disopyramide in isolated cardiomyocytes and trabeculae disappeared after 5 min of drug washout.

CA^{2+} SPARKS IN PERMEABILIZED MYOCYTES. Ventricular myocytes were isolated from the hearts of 4 transgenic HCM mice carrying the R92Q troponin-T mutation, as previously described (18,19). Myocytes were permeabilized with saponin (20) and resuspended in an intracellular buffer containing 150 nmol/l free [Ca^{2+}] and 5 μmol/l of the Ca^{2+}-sensitive dye Asante Na^+-green K^+-salt (Teflabs, Austin, Texas). The frequency of spontaneous Ca^{2+} sparks was evaluated with a confocal microscope through line scan along the longitudinal cell axis (20). Myocytes incubated with vehicle were compared with cells exposed to 5 μmol/l of disopyramide. The rate of sparks was calculated from confocal line-scan recordings using the SparkMaster ImageJ plugin (National Institutes of Health, Bethesda, Maryland) for automated analysis (21).

STATISTICS (STUDIES ON CELLS AND TRABECULAE). None of the 20 consecutively collected patient samples was excluded from the final analysis. However, we were unable to perform all the different experimental procedures described herein in all 20 samples. Therefore, each dataset comprises results from cells or trabeculae isolated from 3 to 11 patient samples. For each dataset, we indicated in the respective figure legends, the total number of cells/trabeculae included, as well as the number (and ID) of patients' samples from which they were isolated. Results from each dataset are expressed as mean ± SEM. Statistical analysis, taking into account non-Gaussian distribution, inequality of variances and within-subject correlation, was performed as previously described (15,18). In brief, to reduce the risk of type I errors resulting from the stronger interrelationship among cells/trabeculae isolated from the same patient sample, we used hierarchical statistics including 2 nested levels (patients and cells/trabeculae) (22), plus a third hierarchical level (presence or absence of disopyramide in the same cell/trabecula) to assess the effects of drug treatment in a pairwise fashion. This approach was implemented using linear mixed models in Stata 12.0 (StataCorp LLC, College Station, Texas). The p values were calculated using linear-mixed models. For categorical data (e.g., occurrence of cellular arrhythmias), we used the Fisher exact test. We considered $p < 0.05$ statistically significant.

MODELING STUDIES. Cellular mechanisms of disopyramide action on dispersion of repolarization were investigated in a population of human ventricular cardiomyocyte models (n = 250) in control versus HCM remodeling, calibrated against human AP and Ca^{2+}-transient data, as previously described (23). Unpaired or paired *t* tests, as well as linear fitting with r-squared calculation, were employed to analyze data from populations of models. Mechanisms of dispersion at the whole ventricular level were investigated in a cardiac magnetic resonance-based anatomical model of a patient with obstructive HCM, under realistic human activation sequence and heterogeneity in repolarizing currents (24).

RESULTS

PROSPECTIVE STUDY OF PATIENTS WITH OBSTRUCTIVE HCM STARTED ON DISOPYRAMIDE. Thirty-nine patients were begun on disopyramide (age 66 ± 10 years; 59% were female). The mean daily dosage of disopyramide after 3 months was 497 ± 87 mg/day. No patient had clinically significant arrhythmia or organ toxicity during the study period. In 9 patients (23%), disopyramide was ineffective or there were limiting vagolytic side effects that led to termination of drug before 3 months.

Electrocardiograms After Disopyramide. ECG parameters before and at a median of 96 days after disopyramide initiation are shown in Table 1. There were prolongations in the QTc, QRS, JT, and PR intervals, but no significant change in heart rate at 3 months. The mean QTc interval increased from 458 ± 22 ms to 486 ± 27 ms ($p < 0.001$). Mean QTc prolongation was 27 ms, which corresponds to a 5.8% increase from baseline. Patients with an initially longer QTc

TABLE 1 Clinical Study: ECG (N = 39)

Interval (ms)	JT	QTc Interval (Bazett)	QTc Interval (Fredericia)	QRS Complex	PR	HR
Pre-disopyramide	354 ± 24	458 ± 22	453 ± 20	103 ± 19	179 ± 39	64 ± 12
4 days	368 ± 30	484 ± 34	485 ± 31	113 ± 23	200 ± 36	59 ± 11
% change	+4 ± 2	+5 ± 2	+6 ± 2	+9 ± 5	+10 ± 7	−8 ± 3
p value vs. pre-disopyramide	<0.002	<0.001	<0.001	<0.001	<0.001	0.022
23 days	366 ± 30	476 ± 37	479 ± 34	109 ± 26	191 ± 32	58 ± 10
% change	+3 ± 1	+4 ± 2	+5 ± 2	+6 ± 3	+6 ± 4	−10 ± 3
p value vs. pre-disopyramide	0.002	<0.001	<0.001	0.015	<0.001	0.002
96 days	375 ± 35	486 ± 27	485 ± 24	112 ± 23	190 ± 33	61 ± 11
% change	+6 ± 2	+6 ± 3	+7 ± 3	+8 ± 3	+6 ± 4	−5 ± 2
p value vs. pre- disopyramide	<0.001	<0.001	<0.001	<0.001	0.015	0.136

Values are mean ± SD. The p values were calculated using paired Student's *t*-test. Electrocardiographic (ECG) intervals were measured before disopyramide and after different periods from drug initiation (4, 23, 96 days), in 39 obstructive hypertrophic cardiomyopathy patients. QTc was determined using Bazett formula or Fredericia formula.

HR = heart rate; JT = time from the end of the QRS complex to the end of the T wave; PR = time from the beginning the P wave to the beginning of the QRS complex.

interval (greater than the median 457 ms) had a smaller increase in QTc interval than did patients with shorter initial QTc interval (ΔQTc: 18 ± 4 ms vs. 34 ± 8 ms, p = 0.007). There was an inverse correlation between the initial QTc interval and the increase in QTc interval with disopyramide (Pearson r = −0.44, p = 0.008).

Echocardiography. Initial resting LVOT gradients were 58 ± 49 mm Hg. After 96 days of disopyramide, gradients were reduced to 25 ± 26 mm Hg (p < 0.001). There were no differences in tissue Doppler variables, transmitral flow velocities, and in the calculations from tissue Doppler and transmitral flow velocities used to estimate left atrial pressure (Table 2). Ejection fraction was minimally reduced by disopyramide from 72.2% to 68%, an average decrease by 5.8 ± 3.1% (Table 2).

IN VITRO STUDY ON HUMAN MYOCARDIUM. Samples from 20 patients with HCM undergoing surgical myectomy for drug-refractory symptoms were assessed. Clinical data at pre-operative assessment are shown in Supplemental Table 1.

Disopyramide Reduces Force and Accelerates the Kinetics of Isometric Twitches. Disopyramide was added to standard perfusion solution while recording isometric tension from intact contracting trabeculae dissected from the endocardial surface.

TABLE 2 Clinical Study: Echocardiography (N = 39)

	Doppler Velocities (cm/s)			
	Septal TDI e′ (e'_S)	Lateral TDI e′ (e'_L)	Transmitral E	Transmitral A
Pre-disopyramide	4.3 ± 0.8	6.5 ± 2.0	85 ± 28	85 ± 20
Post-disopyramide	4.1 ± 1.0	6.0 ± 1.9	82 ± 23	90 ± 30
% change	−5 ± 15	−8 ± 25	−3 ± 16	+5 ± 21
p value	0.184	0.125	0.693	0.442
	Diastolic Function: Calculations			
	Septal E/e′	Lateral E/e′	$E/(e'_S+e'_L/2)$	
Pre-disopyramide	21.2 ± 8.7	13.8 ± 7.9	11.7 ± 5.4	
Post-disopyramide	20.7 ± 7.6	13.9 ± 9.1	11.5 ± 5.3	
% change	−3 ± 22	0 ± 17	−1 ± 14	
p value	0.915	0.643	0.894	
	Systolic Function			
	LVEDV (ml)	LVESV (ml)	LVEF (%)	
Pre-disopyramide	60.5 ± 18.2	17.0 ± 6.2	72.2 ± 5.0	
Post-disopyramide	63.2 ± 21.5	20.2 ± 7.3	68.0 ± 3.5	
% change	+5 ± 26	+15 ± 27	−6 ± 3	
p value	0.182	0.001	<0.001	

Values are mean ± SD. The p values were calculated using paired Student's *t*-test. Comparison between echocardiographic parameters obtained before disopyramide initiation (pre-disopyramide) and at the end of study (post-disopyramide).

LVEDV = left ventricular end-diastolic volume; LVEF= ejection fraction; LVESV = end-systolic volume; Lateral TDI e′(e'_L) = early diastolic downward velocity of the lateral (free wall) mitral annulus measured at tissue Doppler; Septal TDI e′ (e'_S) = early diastolic downward velocity of the medial (septal) mitral annulus measured at tissue Doppler; Transmitral A = late diastolic transmitral flow velocity (during atrial systole); Transmitral E = early diastolic flow velocity through the mitral valve.

FIGURE 1 Effects of Disopyramide in Myocardial Mechanics in Intact and Skinned Trabecuale

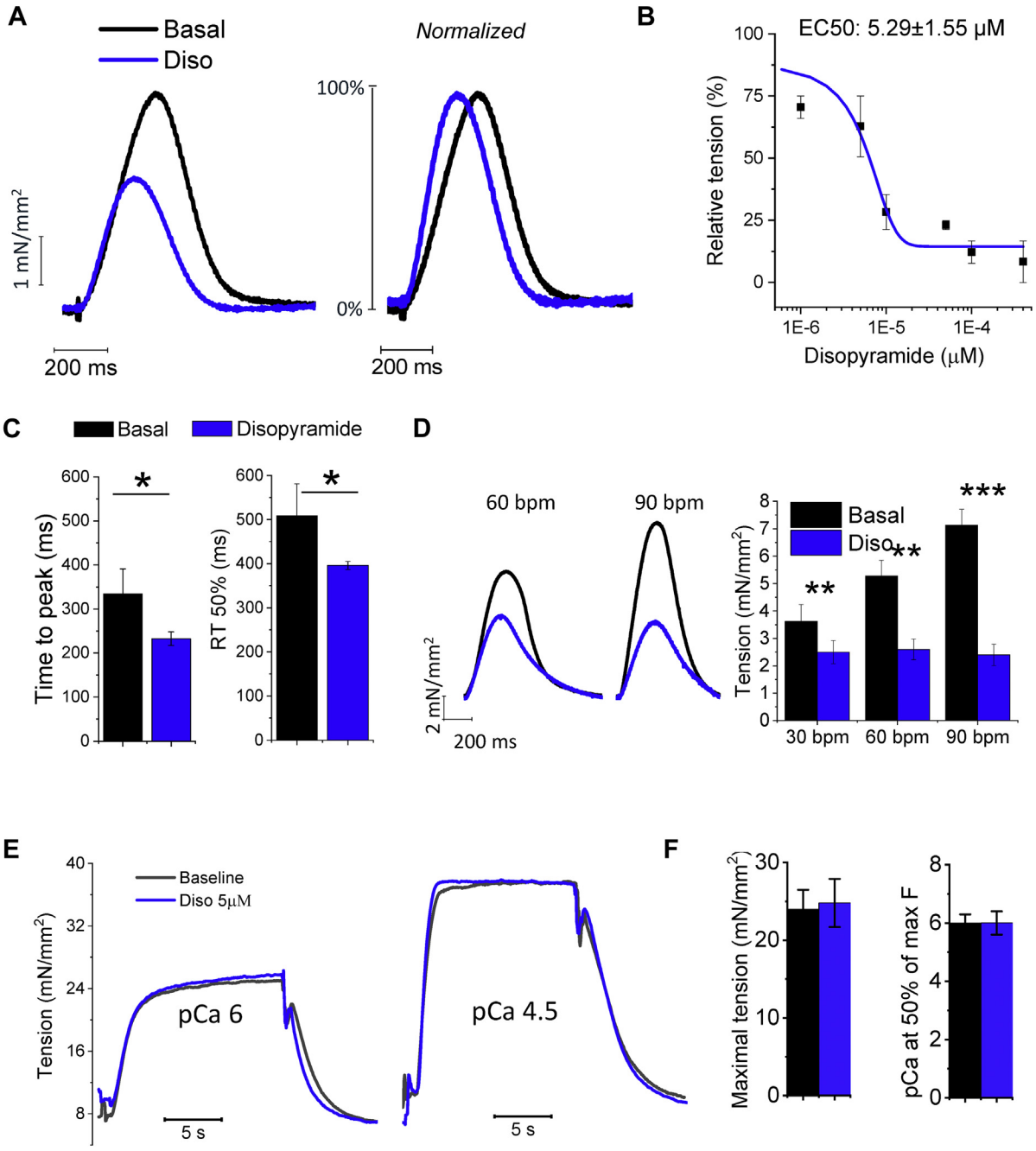

(A) Representative superimposed force twitches elicited at 0.5 Hz in hypertrophic cardiomyopathy (HCM) trabeculae in the absence **(black trace)** and presence **(blue trace)** of disopyramide 5 μmol/l (Diso). **(B)** Relationship between the negative inotropic effect of disopyramide and its concentration in the extracellular fluid; calculated concentration at which 50% of the maximal effect is obtained (EC50) is shown. Mean ± SEM from 5 trabeculae, 5 patients. **(C)** Time from stimulus to peak and time from peak to 50% relaxation (RT50%) of force twitches elicited at 1 Hz at baseline **(black)** and in the presence of disopyramide **(blue). (D)** Effects of disopyramide at different stimulation frequencies. Disopyramide slightly reduces the slope of force-frequency relationship at higher pacing rates. **(C,D)** Mean ± SEM from 13 trabeculae, 10 patients (ID# 1, 2, and 5 to 12). **(E)** Disopyramide in skinned trabeculae from patients with HCM. As shown in these superimposed traces from an HCM trabecula, disopyramide does not reduce isometric force at intermediate Ca activation level (pCa 6) or at maximal myofilament activation (pCa 4.5). **(F)** Maximal tension and pCa at one-half of maximal tension (Ca sensitivity) in HCM trabeculae, in the absence and presence of disopyramide. Means ± SEM from 6 trabeculae, 3 patients (ID# 12, 15, and 16). **(C,D,F)** *0.05 > p > 0.01; **0.01 > p > 0.001; ***p < 0.001; linear-mixed models. bpm = beats/min.

FIGURE 2 Effects of Disopyramide on Intracellular Ca^{2+}

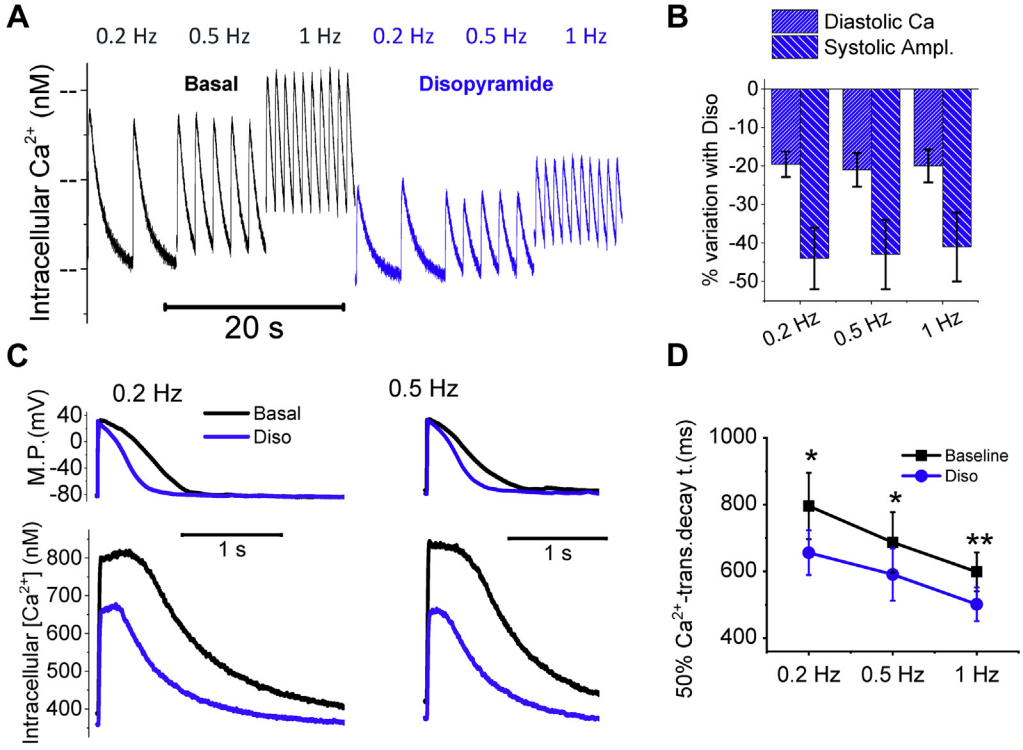

(A) Representative intracellular Ca^{2+} traces recorded during regular stimulation at 0.2, 0.5, and 1 Hz, in the absence **(left, black)** and presence of disopyramide 5 μmol/l (Diso) **(blue traces on the right). (B)** Percentage of variation of diastolic $[Ca^{2+}]_i$, and Ca-transient amplitude (Systolic Ampl) with the application of disopyramide 5 μmol/l with respect to baseline in hypertrophic cardiomyopathy cardiomyocytes, during regular stimulation at 0.2, 0.5, and 1 Hz at steady state. **(C)** Representative superimposed action potentials **(top)** and simultaneously recorded Ca transients **(bottom)** at baseline **(black traces)** and in the presence of disopyramide **(blue traces),** elicited at 0.2 Hz **(left)** and 0.5 Hz **(right). (D)** Time from peak to 50% decay of Ca transients at baseline **(black)** and in the presence of disopyramide 5 μmol/l **(blue),** elicited at 0.2, 0.5, and 1 Hz. **(B to D)** Mean ± SEM from 26 cardiomyocytes from 7 patients with hypertrophic cardiomyopathy (ID# 5 to 9 and 11 to 13). *0.05 > p > 0.01; **0.01 > p > 0.001; linear-mixed models. MP = membrane potential.

As expected, the drug displayed a consistent negative inotropic effect (Figure 1A). To assess the concentration dependency of this effect, we exposed the muscles to different concentrations of disopyramide (Figure 1B). Calculated disopyramide concentration at 50% of maximal effect on isometric twitch amplitude was 5.29 ± 1.55 μmol/l. We therefore decided to employ the drug at 5 μmol/l for all the following experiments; notably, 5 μmol/l corresponds to the average plasma concentration of disopyramide measured in patients under a standard treatment regimen (25). Importantly, 5 μmol/l disopyramide hastened isometric twitch kinetics in HCM trabeculae: both time to peak and relaxation time were reversibly shortened by the application of the drug (Figures 1A and 1C). We tested the effects of disopyramide at different stimulation frequencies (Figure 1D): the reduction of steady-state isometric twitch force was more pronounced at higher pacing rates as compared with lower rates. Isometric twitch force was reduced by 33 ± 5% at 0.5 Hz (30 beats/min) and by 62 ± 10% at 1.5 Hz (90 beats/min; p = 0.015 vs. 0.5 Hz; data from 13 trabeculae in 10 patients, calculated using linear-mixed models).

Disopyramide Has No Direct Effects on Myofilament Contraction. We tested the effects of disopyramide on demembranated trabeculae from 3 patients with HCM (Figure 1E). Disopyramide (5 μmol/l) did not affect maximal force obtained when exposing trabeculae to an activating solution with pCa 4.5 (Figure 1F). Force generation at lower $[Ca^{2+}]$, determining submaximal tension development, was also unaffected by disopyramide; we concluded that disopyramide does not modify myofilament Ca sensitivity (Figure 1F). Moreover, disopyramide did not alter the energy cost of tension generation (Supplemental Figure 1). The

TABLE 3 Effects of Disopyramide on AP and $[Ca^{2+}]_i$

0.2 Hz	Baseline	Disopyramide	% Change	p Value
$[Ca^{2+}]_i$, nmol/l				
Diastolic Ca	235 ± 44	189 ± 31	−22 ± 8	0.015
Ca^{2+}-transient amplitude	336 ± 53	188 ± 34	−44 ± 15	0.006
Ca^{2+}-transient kinetics, ms				
Time to peak	151 ± 15	128 ± 12	−15 ± 8	0.024
90% decay	1,260 ± 99	905 ± 88	−28 ± 8	0.008
Action potentials				
MDP, mV	−80 ± 3	−80 ± 3.	0 ± 3	>0.05
Amplitude, mV	129.1 ± 3.2	122.2 ± 2.8	−5 ± 1	0.012
Upstroke, V/s	139 ± 18	97 ± 12	−30 ± 9	0.002
APD20, ms	381 ± 44	284 ± 40	−25 ± 9	0.017
APD50, ms	653 ± 63	469 ± 61	−28 ± 7	<0.001

Values are mean ± SEM. The p values were calculated using linear mixed models. Additional data from action potentials and Ca transients were recorded in hypertrophic cardiomyopathy cardiomyocytes stimulated at 0.2 Hz before and during exposure to disopyramide. Data from 28 HCM cardiomyocytes isolated from 8 hypertrophic cardiomyopathy patient samples (ID# 3 to 6, 9, and 11 to 13). Diastolic Ca is the diastolic concentration of Ca during regular stimulation. Ca^{2+}-transient amplitude is the difference between peak systolic Ca and diastolic Ca. Time to peak is the measurement from stimulus to peak. The 90% decay is the time from peak to 90% decay of Ca transients. Upstroke is the upstroke speed of the action potentials.

APD20 (APD50) = action potential duration at 20% (50%) of repolarization; MDP = mean diastolic potential.

same results were obtained in demembranated trabeculae from healthy donors.

Disopyramide Reduces Diastolic Ca^{2+} and Hastens the Kinetics of Ca^{2+} Transients. Disopyramide was tested at 5 μmol/l in patch-clamped ventricular cardiomyocytes while simultaneously recording Ca^{2+} transients and AP during stimulation at different frequencies (Figures 2A and 2C). The drug reduced the amplitude of Ca^{2+} transients at all frequencies (Figure 2B), hastened the kinetics of Ca^{2+} transient rise and decay (Figures 2C and 2D, Table 3) and reduced diastolic Ca^{2+} concentration (Figures 2A and 2B, Table 3).

Disopyramide Reduces AP Duration and the Frequency of Afterdepolarizations. Disopyramide (5 μmol/l) shortened the duration of AP in HCM cardiomyocytes (Figures 2C and 3A, Table 3) at all frequencies (Figure 3B) and the effect was more pronounced at lower rates. For instance, average AP shortening at 0.1 Hz was 27 ± 5% and is comparable to that observed in human HCM cardiomyocytes with 10 μmol/l of ranolazine (17). In addition, disopyramide reduced AP amplitude and upstroke speed (Table 3). Finally, disopyramide reduced the incidence of spontaneous afterdepolarizations in HCM cardiomyocytes, both early afterdepolarizations (EAD) (occurring during the AP plateau) and delayed afterdepolarizations (DAD) (occurring during the diastolic phase), occurring during 3 min of regular stimulation (Figures 3C and 3D).

Disopyramide Inhibits Peak and Late Na^+, Ca^{2+}, and K^+ Currents. We previously have shown that in HCM cardiomyocytes there is markedly enhanced I_{NaL}, slightly increased $I_{Ca\text{-}L}$, and lower I_K, leading to prolonged AP duration (15). We assessed Na^+ currents in HCM cardiomyocytes during voltage clamp on depolarization to −10 mV. Peak current was measured in the first 10 ms of depolarization (Figure 4A), whereas I_{NaL} was estimated by integrating the residual inward current (50 to 800 ms after onset) (Figure 4B). In HCM myocytes, disopyramide (5 μmol/l) reduced peak Na^+ current by 22 ± 4% and greatly decreased I_{NaL} integral by 45 ± 6% (21 myocytes, n = 5).

We then assessed the effects of disopyramide on I_K, measured at steady state during depolarization at different potentials (Figure 4C). Disopyramide (5 μmol/l) exerted a small but significant inhibitory effect on I_K currents in HCM cardiomyocytes (Figure 4D). Notably, the density of steady-state I_K at baseline is reduced in our HCM myocytes as compared with control myocardium (Supplemental Figure 2). Moreover, disopyramide reduced the amplitude of $I_{Ca\text{-}L}$ in HCM cardiomyocytes (Figures 4E and 4F); the average $I_{Ca\text{-}L}$ reduction was 16 ± 4% (mean of 16 myocytes from 4 patients).

Taken together, the observed effects of disopyramide on Na^+, K^+, and Ca^{2+} currents explain the net reduction of AP duration by disopyramide (Figure 3). In HCM septal cells, in the presence of lower I_K (15), slightly increased $I_{Ca\text{-}L}$, and markedly enhanced I_{NaL}, the effect of disopyramide is a net decrease of depolarizing currents, ultimately leading to AP shortening. On the contrary, in control human ventricular myocytes, where the expression of I_K is preserved and I_{NaL} is small (15), inhibition of human ether-à-go-go-related gene (hERG) K^+ current by disopyramide (26) prevails over the reduction of $I_{Ca\text{-}L}$ and I_{NaL}, ultimately leading to a slight AP prolongation (Supplemental Figure 3), in agreement with previous reports (27).

Disopyramide Inhibits RyR. Similar to other class I antiarrhythmics (28), disopyramide exerts an inhibitory effects on the ryanodine receptor (RyR). We tested the effects on RyR channels by evaluating the rate of Ca sparks in permeabilized ventricular myocytes isolated from a transgenic HCM mouse model carrying the R92Q-TnT mutation (Figure 5A). The frequency of Ca^{2+} sparks in myocytes incubated with 5 μmol/l of disopyramide was lower than that observed in vehicle-treated cells (Figure 5B).

DISOPYRAMIDE DECREASES VENTRICULAR DISPERSION OF REPOLARIZATION IN SILICO. The effects of 5 μmol/l of disopyramide were modeled in silico based on the above-mentioned characterization of drug action. In agreement with the experimental findings, 5 μmol/l of disopyramide yielded AP

FIGURE 3 Effects of Disopyramide on AP and Cellular Arrhythmias

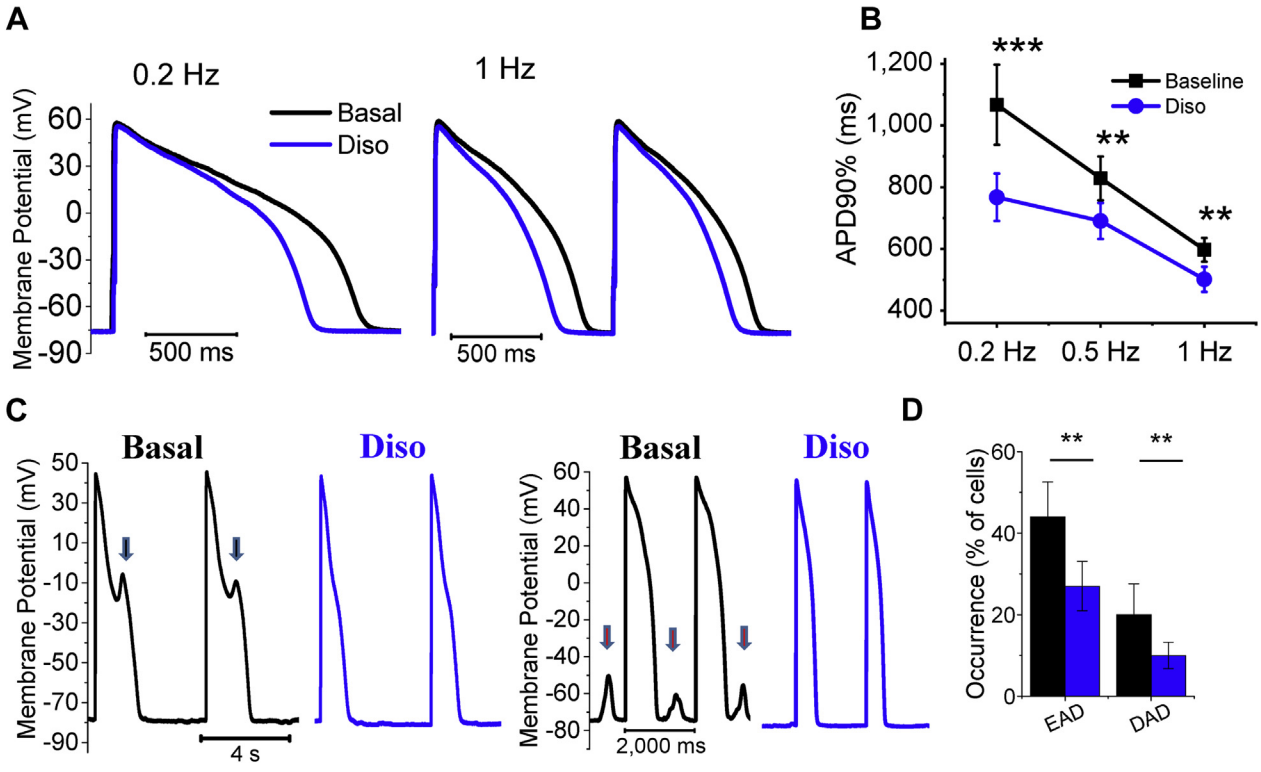

(A) Representative superimposed action potentials (AP) at baseline **(black traces)** and in the presence of disopyramide 5 μmol/l (Diso) **(blue traces),** elicited at 0.2 Hz **(left)** and at 1 Hz **(right). (B)** Action potential duration at 90% of repolarization (APD90%) at baseline **(black)** and in the presence of disopyramide **(blue). (C)** Representative action traces at baseline **(black traces)** and in the presence of disopyramide 5 μmol/l **(blue traces),** elicited at 0.2 Hz pacing rate. Disopyramide suppresses early afterdepolarizations (EAD) **(arrows). (D)** Percentage of HCM cardiomyocytes showing at least 2 EAD or delayed afterdepolarizations (DAD) during 3 min of continuous stimulation, at baseline **(black)** and in the presence of disopyramide **(blue). (B,D)** Mean ± SE from 28 hypertrophic cardiomyopathy cardiomyocytes from 8 patients with hypertrophic cardiomyopathy (ID# 3 to 6, 9, and 11 to 13). **$0.01 > p > 0.001$; ***$p < 0.001$; linear-mixed models.

shortening in HCM endocardial cardiomyocytes and left AP duration unaltered in control endocardium (Figures 6A and 6B). Due to transmural differences in ion channel expression, this trend was reversed in epicardial cardiomyocytes, where disopyramide slightly prolonged AP duration in control cells (Figures 6A and 6B). The magnitude of AP duration at 90% of repolarization shortening in HCM endocardial cells was inversely correlated with basal AP duration at 90% of repolarization (Figure 6C). Further analysis of responders to drug action indicates that I_{NaL} density is the primary determinant of the extent of AP shortening due to disopyramide (Figure 6D).

In the reconstructed ventricles of a patient with obstructive HCM, 5 μmol/l disopyramide reduced conduction velocity, increasing total activation time by 11 ms (Supplemental Figure 4), comparable to clinical data (QRS prolongation at ECG, see Table 1). In the region of septal hypertrophy, 5 μmol/l of disopyramide markedly decreased dispersion of repolarization times (baseline: 529 ± 62 ms, 625 ms maximum; 5 μmol/l of disopyramide: 504 ± 50 ms, 585 ms maximum) and slightly prolonged repolarization in the nonhypertrophic epicardium (Figure 6E). This heterogeneous ventricular action resulted in QT shortening in septal precordial ECG leads along with modest QT prolongation in the lateral ones (Figure 6E), hence explaining the apparent discrepancy between AP shortening and the clinical QTc prolongation observed in patients with HCM following disopyramide intake.

DISCUSSION

In the present work, we have investigated the effects of disopyramide in patients with obstructive HCM and on isolated HCM cardiomyocytes harvested from patients undergoing surgical septal myectomy. The

FIGURE 4 Effects of 5 μmol/l Disopyramide on Ion Channels

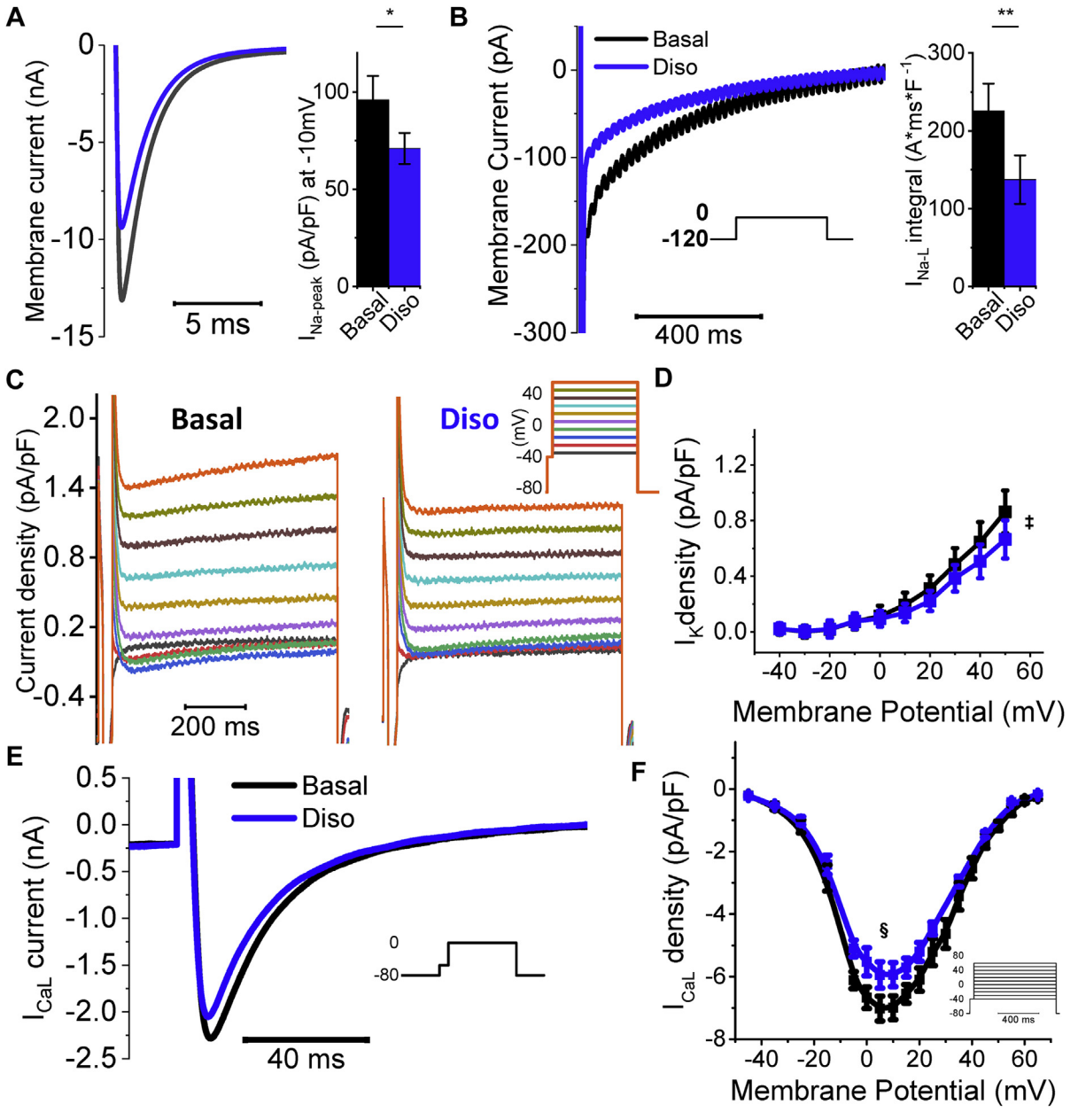

(A, left) Representative peak Na current traces elicited at −10 mV from −120 mV resting potential, in a hypertrophic cardiomyopathy cardiomyocyte in the absence **(black)** and presence of disopyramide (Diso) **(blue trace). (Right)** Average peak Na^+ current ($I_{Na\text{-}peak}$) density at −10 mV; effect of disopyramide. **(B, left)** Representative late Na^+ current (I_{NaL}) traces elicited at -10 mV from −120 mV resting potential, in the absence and presence of disopyramide. **(Right)** Average integral of the area of the current between 50 and 750 ms after onset of the −10 mV clamp pulse, normalized by cell capacitance, calculated in the absence and presence of disopyramide in hypertrophic cardiomyopathy cardiomyocytes. **(A,B)** Mean ± SEM from 22 cardiomyocytes, 5 patients (ID# 14 to 18). *$0.05 > p > 0.01$; **$0.01 > p > 0.001$; linear-mixed models. **(C)** Delayed-rectifier K currents (I_K) elicited at different voltages in hypertrophic cardiomyopathy cardiomyocytes (see inset for color codes), in the absence of disopyramide **(left)** and in its presence **(right). (D)** Average I_K current density in the absence and presence of disopyramide at different voltages. Mean ± SEM from 10 cardiomyocytes, 4 patients (ID# 14, 16, 19, and 20). ‡$p < 0.05$ for voltages ≥+20 mV, linear-mixed models used to compare each coupled pair of values. **(E)** Representative L-type Ca^{2+} current ($I_{Ca\text{-}L}$) traces elicited at 0 mV from −80 mV resting voltage. **(F)** Average $I_{Ca\text{-}L}$ current density in the absence and presence of disopyramide at different voltages. Mean ± SEM from 12 cardiomyocytes, 3 patients (ID# 15, 17, and 18). §$p < 0.05$ for voltages between −10 mV and +30 mV, linear-mixed models.

FIGURE 5 Effects of 5 μmol/l of Disopyramide on Ca Sparks in Permeabilized Myocytes

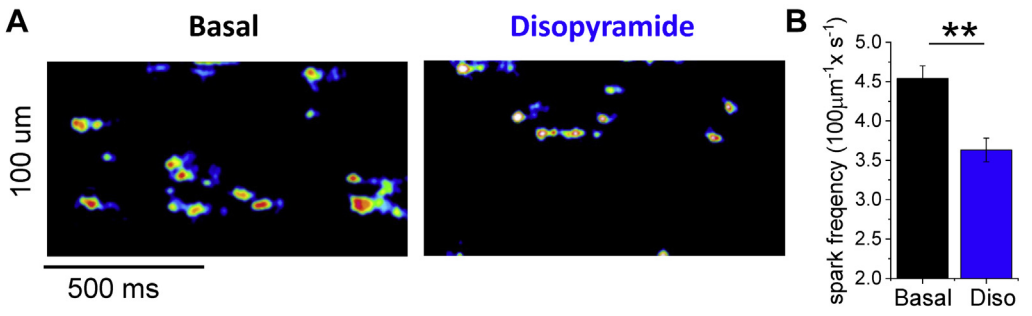

(A) Calcium sparks in permeabilized cardiomyocytes from the left ventricle of transgenic hypertrophic cardiomyopathy mice (R92Q-TnT mutation): the representative kymographic images show confocal line scans traced along the longitudinal cell axis, displaying fluorescence signals from the Ca-selective dye, recorded at a speed of 512 lines/s while bathing the permeabilized myocytes in an intracellular solution containing 150 nmol/l [Ca^{2+}] at room temperature. Spontaneous Ca sparks are visible as spontaneous elevations of local [Ca^{2+}] signal lasting 20 to 40 ms. Representative traces from cells in the absence **(left)** and presence of disopyramide (Diso) **(right)** in the bathing solution. Kymographic images are reported in false color (16-colors lookup table) after thresholding and filtering (Gaussian smoothing with 2*px* sigma). **(B)** Frequency of spontaneous Ca sparks per 100 μmol/l of scanned line length, in the absence and presence of 5 μmol/l disopyramide. Mean ± SEM from 74 cardiomyocytes (basal) and 63 cardiomyocytes (disopyramide) isolated from 4 mouse hearts. **0.01 > p > 0.001, unpaired Student's *t*-test.

results shed light on the agent's biophysical mechanisms of benefit, and its demonstrated clinical safety in patients with HCM. In addition, the suppressive effect of disopyramide on afterdepolarizations in vitro raises the possibility that disopyramide may reduce ventricular arrhythmia propensity in vulnerable patients with HCM.

NEGATIVE INOTROPIC EFFECT IN OBSTRUCTIVE PATIENTS. In patients with obstructive HCM, the beneficial effect of disopyramide is that it decreases LV contractility, specifically by decreasing early LV ejection flow acceleration (29). In patients with obstructive HCM, the mitral valve apposes with the septum very early in systole, and the duration of mitral-septal contact correlates with gradient magnitude, because of the amplifying feedback loop in which the presence of a gradient pushes the valve further into the septum. Thus, to reduce obstruction-related gradients, the impact of any negative inotropic medication must be very early in systole, before the onset mitral-septal contact. By decreasing early systolic ejection acceleration, disopyramide decreases early drag forces on the mitral valve, delaying or abolishing mitral-septal contact. Systolic anterior motion results from an equilibrium between the displacing anteriorly directed force of ejection flow striking the mitral valve, versus restraining forces, from the papillary muscles and chordae (30). Disopyramide displaces this equilibrium toward restraint by dint of its effects on early flow acceleration. Interestingly, despite the decreased velocity of pressure generation (dP/dt) during early systole and the lower peak LV pressure, disopyramide results in a modest reduction of global systolic function (5% to 6% decrease of ejection fraction in our study, in line with previous observations). In normal subjects, disopyramide causes a prolongation of total ejection time (1); in subjects with HCM, however, where ejection time is prolonged due to obstruction, the relief of obstruction by disopyramide leads to a 12% shorter ejection time (31). Moreover, disopyramide has a more potent gradient-lowering effect than other negative inotropic agents given for obstructive HCM (beta blockers and verapamil). In a head-to-head comparison in individual patients with HCM by intravenous administration of the 3 agents on sequential days, investigators found a 59% reduction of gradient with disopyramide, a 19% reduction with propranolol, and only 8% reduction with verapamil (11,32). On average, 60% to 70% of patients started on disopyramide will experience a significant drop in LVOT gradient and improvement in symptoms (5,6). Whereas the gradient-lowering effect of disopyramide shows a clear dependency on dose and plasma levels (1,3,33), the negative inotropic effect is always very modest and does not vary within the clinically relevant range of doses (up to 300 mg twice daily). These observations suggest that symptomatic gradients can be effectively lowered by negative inotropic agents without largely reducing ejection fraction. This may be related to the fact that most patients with obstructive HCM are pathologically hyperkinetic. In HCM hearts, negative inotropic drugs may counteract LV hypercontractility and reduce early ejection acceleration while at the same time allowing a more efficient

FIGURE 6 Modeling Results on the Action of Disopyramide on the Dispersion of Repolarization

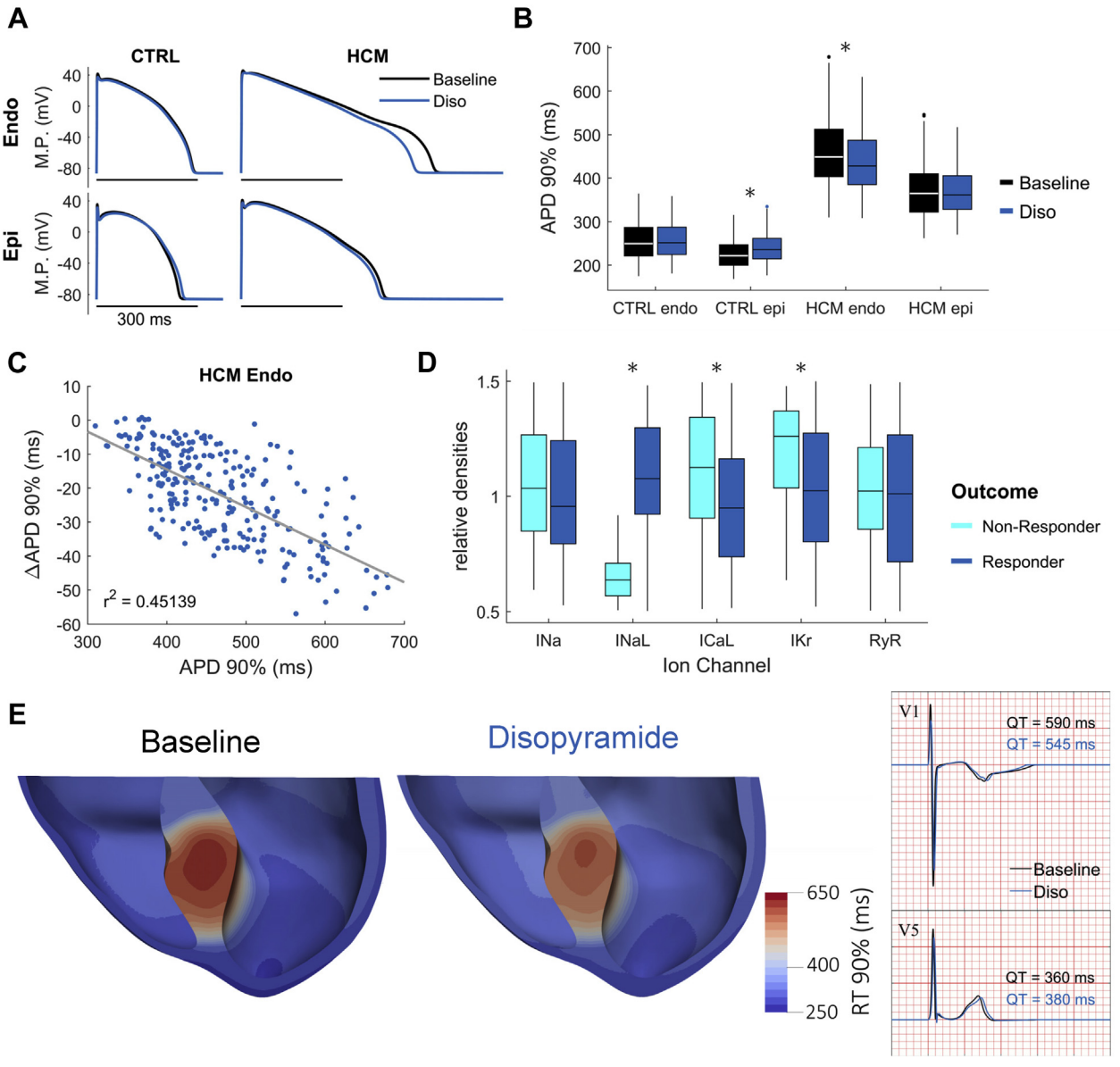

(A) Representative superimposed action potentials at baseline **(black traces)** and in the presence of disopyramide 5 μmol/l **(blue traces)** in endocardial (Endo) and epicardial (Epi) models of human ventricular cardiomyocytes at 1 Hz pacing. **(B)** APD90% at baseline **(black)** and in the presence of disopyramide 5 μmol/l **(blue),** for the different cell types. *$p < 0.05$, paired Student's *t*-test. **(C)** Endocardial APD shortening in HCM endocardial cardiomyocytes under disopyramide 5 μmol/l action as a function of baseline APD90%. **(D)** Cellular mechanisms underlying endocardial APD shortening in responders **(dark blue)** versus nonresponders **(light blue)** to disopyramide. *$p < 0.05$, unpaired Student's *t*-test. **(E)** RT90% in a ventricular model of obstructive HCM. Disopyramide reduces maximum dispersion of repolarization in the septal hypertrophic region while only slightly prolonging repolarization in nonhypertrophic epicardium, leading to QT shortening in septal compared with modest QT prolongation in lateral precordial electrocardiogram leads (V_1 and V_5 shown). CTRL = control model; I_{Kr} = rapid delayed-rectifier K^+ current; RyR = ryanodine receptor; other abbreviations as in Figures 1 to 4.

LV emptying due to loss of obstruction. Thus, the impact of negative inotropic drugs on end-systolic volume will be very limited, explaining the modest reduction of ejection fraction.

In the current study, disopyramide lowered resting LVOT gradients from mean 58 to 25 mm Hg after 3 months. This was similar to a prior report in 221 patients using disopyramide with an average dose of

500 mg/day, where resting LVOT gradients decreased from 63 to 25 mm Hg after 4.5 years (6). Symptoms and gradient in 64% of patients of this cohort could be managed pharmacologically, while 36% ultimately underwent septal reduction.

CELLULAR MECHANISMS UNDERLYING THE NEGATIVE INOTROPIC ACTION OF DISOPYRAMIDE. Our in vitro force assessments using human HCM samples confirm the negative inotropic action of disopyramide observed in patients. The results of our studies show that this effect is the result of the inhibitory action of disopyramide on multiple ion channels within the cardiomyocyte.

Disopyramide Has No Direct Effects on Myofilaments. Disopyramide does not modify the maximal force generated by the contractile apparatus in HCM and control trabeculae, and it does not change myofilament sensitivity to Ca^{2+}, suggesting that the drug does not directly target contractile proteins (**Figure 6**). Therefore, disopyramide must reduce force through modifications of the cardiomyocyte excitation-contraction coupling, that is, intracellular Ca^{2+} handling. By contrast, mavacamten (MYK-461) produces a negative inotropic effect by virtue of direct inhibitor of cardiac myosin (34) with no apparent off-target side effects. Mavacamten was recently tested in a small number of patients with obstructive HCM in a phase II study, showing that a clinically meaningful reduction of post-exercise LVOT gradients can be achieved with relatively small doses of the drug, while leading to a modest reduction of LV ejection fraction, on the order of 6% to 10% on average. This is in line with the idea that a large reduction of LVOT gradients in patients with obstructive HCM can be achieved using negative inotropic drugs with a minimal loss of global LV function.

Disopyramide Reduces the Amplitude of Calcium Transients. The negative inotropic effect of disopyramide is a consequence of the reduction of systolic intracellular Ca^{2+} levels in the cardiomyocyte, thus determining lower Ca-mediated activation of myofilaments and, ultimately, lower force. We found a number of concurrent mechanisms contributing to the reduction of Ca^{2+}-transient amplitude.

Disopyramide Reduces Peak Na^+ Current and I_{NaL}. Early studies demonstrated that Na^+ channel block (e.g., by tetrodotoxin) has a slight negative inotropic action per se in the myocardium. Interestingly, these studies compared the negative inotropic potency of different drugs with their efficacy in slowing down AP upstroke (a direct consequence of peak Na^+-current inhibition) (35,36). The ratio of negative inotropic efficacy versus Na^+-channel blocking potency was the lowest for tetrodotoxin (0.23) and the highest for disopyramide (2.2). Disopyramide has the most negative inotropic effect of all Class I antiarrhythmics, higher than mexiletine, procainamide, and quinidine (35). As tetrodotoxin is a pure Na^+-channel blocker, these results suggest that Na^+-channel inhibition only slightly contributes to the negative inotropic action of disopyramide, and that disopyramide has additional Na^+-channel-independent mechanisms that make it the most potent negative inotropic agent among class I antiarrhythmics (35).

Nonetheless, Na^+-channel inhibition may independently contribute to the reduction of Ca^{2+}-transient amplitude by disopyramide through modification of the activity of the NCX (37). When membrane potential is positive (peak and plateau of the AP) and subsarcolemmal $[Na^+]$ is high (due to large Na^+ influx by peak I_{Na}), NCX works in reverse mode, in other words, letting Ca^{2+} enter the cell in exchange for Na^+ (38). The contribution of reverse-mode NCX to Ca^{2+} transients is particularly high in HCM cardiomyocytes (16). In the presence of peak and late I_{Na} inhibition by disopyramide, maximal AP voltage is reduced (**Table 2**) and intracellular $[Na^+]$ is diminished (16): these changes lead to a decrease of reverse-mode NCX activity, thus reducing Ca^{2+} entry (39). Moreover, reduction of diastolic $[Na^+]$ may enhance the diastolic extrusion of Ca^{2+} via the NCX (forward mode) (15,18). The 2 mechanisms (reduced reverse- and enhanced forward-mode NCX) may contribute to reduce total Ca^{2+} load of the SR (15) and thus Ca^{2+}-transient amplitude. Selective inhibition of I_{NaL} without block of peak I_{Na} (e.g., with ranolazine or eleclazine) is not sufficient to induce a negative inotropic effect under basal conditions (15,16). Therefore, we can conclude that simultaneous inhibition of peak and late I_{Na} is required for the negative inotropic action of disopyramide.

Disopyramide Reduces $I_{Ca\text{-}L}$. Disopyramide exerts a slight but relevant inhibitory effect on $I_{Ca\text{-}L}$, which is substantially lower than that of verapamil. Nonetheless, the observed 15% inhibition of peak $I_{Ca\text{-}L}$ by disopyramide contributed to reduce Ca^{2+}-transient amplitude in ventricular myocytes, the effect being larger at higher stimulation rates. A similar rate-dependency of the negative inotropic effect is typical of pure Ca^{2+}-channel blockers such as verapamil (40). At variance with verapamil (41), however, disopyramide has minimal effects on heart rate and atrioventricular conduction (**Table 3**), and thus can be safely combined with -beta blockers.

Disopyramide Inhibits RyR. Na^+ channel blockers flecainide and propafenone stabilize the closed state of cardiac RyR channels (42). We observed that disopyramide reduced the rate of spontaneous Ca^{2+}

sparks in permeabilized myocytes, in the presence of fixed intracellular [Ca^{2+}]: the reduction in the spontaneous RyR opening rate is likely due to a direct effect of disopyramide on RyR channels. Notably, selective inhibition of RyR channels using JTV-519 in human ventricular trabeculae led a slight negative inotropic effect (43). Similarly, inhibition of RyR-mediated systolic Ca^{2+} release by disopyramide may contribute to the reduction of Ca^{2+}-transient amplitude.

DISOPYRAMIDE SHORTENS REPOLARIZATION IN HCM CARDIOMYOCYTES: MOLECULAR MECHANISMS. Early studies in healthy myocardium showed that disopyramide prolongs ventricular AP (13) due to decreased I_{Kr} current by direct inhibition of hERG channels (44). Similarly, we observed a slight AP prolongation in cardiomyocytes from patients without HCM (Supplemental Figure 3), also confirmed by modeling studies (**Figure 6A**). Interestingly, the AP prolonging effect in control cardiomyocytes was shown to be prevalent at concentrations below 8 μmol/l, whereas at higher concentrations, disopyramide tended to shorten AP (13,45). At low concentrations, hERG inhibition prevails over I_{NaL} and $I_{Ca\text{-}L}$ block, leading to a net decrease of repolarizing currents and AP prolongation; at higher concentrations, however, after maximal hERG inhibition is reached, the inhibition of depolarizing Ca^{2+} and Na^{+} currents becomes prevalent, leading to AP shortening in healthy myocardium. Based on our observations, we can speculate that the latter behavior occurs in HCM cardiomyocytes even at low, clinically relevant concentrations (such as 5 μmol/l, which we used in this work), due to the decreased expression of hERG channels in HCM myocardium (15). Moreover, I_{NaL} and $I_{Ca\text{-}L}$ are both increased in HCM versus control myocardia (15); therefore, their inhibition by disopyramide leads to greater AP shortening, especially at low pacing rates. Simulation studies suggested that AP shortening by disopyramide is more pronounced in cells that have larger I_{NaL} and smaller I_{Kr} (**Figures 6C and 6D**). Taken together, the altered balance of depolarizing and repolarizing currents in cardiomyocytes from the hypertrophic septum of patients with HCM causes disopyramide to decrease net depolarizing currents (Na^{+} and Ca^{2+}) without substantial reduction in repolarizing K^{+} currents, ultimately shortening AP plateau duration (**Figure 2, Table 1**).

SHORTENING OF AP DURATION AND QTc PROLONGATION: AN APPARENT CONTRAST. In the 39 patients begun on disopyramide, QTc interval increased from 458 ± 22 to 486 ± 27, an average 5.8% rise after 3 months. The shortening of AP observed in HCM cardiomyocytes in vitro is in apparent contrast with the slight QTc prolongation in patients. However, prolongation of QTc interval with disopyramide depends, at least in part, on the prolongation of QRS interval, reflecting delayed intraventricular electrical conduction velocity due to peak Na^{+}-current inhibition (**Table 1**) (46). However, even if we consider only the repolarization phase (JT interval), disopyramide still has a significant prolonging effect. All the cardiomyocytes analyzed in this work were isolated from the subendocardial region of the basal septum, the most hypertrophied region in patients with obstructive HCM. If the degree of cardiomyocyte electrical changes is heterogeneous across the LV and mirrors the asymmetrical distribution of hypertrophy, cardiomyocytes from other regions of the LV are likely to be similar to control cardiomyocytes. Therefore, we constructed a 3-dimensional model of the whole LV from an obstructive patient (**Figure 6E**) where we assumed that the HCM-specific ion current abnormalities we observed in isolated cardiomyocytes from septal myectomy samples (15,23) were limited to the hypertrophied septal region. In agreement with this assumption, the spatial dispersion of QTc interval is greatly increased in patients with HCM with asymmetrical hypertrophy (47). In this model, we found that disopyramide shortens the duration of septal AP while slightly prolonging the AP of the remaining LV myocardium, ultimately resulting in a slight prolongation of the global QT interval in the reconstructed ECG trace. In line with that prediction, the average prolongation of QTc interval in patients with HCM with disopyramide (5% to 6%) is lower than the average QT prolongation in healthy patients taking a similar dose of disopyramide (10% to 15%) (1,48). The model predicts that disopyramide determines marked reduction of QT dispersion across the different LV regions, as well as transmurally. Because the magnitude of the AP-shortening effect of disopyramide is linearly related with the AP duration at baseline (**Figure 6C**), the effect would be greater in cells with longer AP, globally reducing the heterogeneity of AP duration among different LV regions. In line with that, we observed in patients that the QTc prolonging effect of disopyramide is inversely related to the baseline QTc interval: patients with an initially longer QTc interval (>457 ms) had a smaller increase in QTc interval after disopyramide than did patients with shorter initial QTc interval. Interestingly, spatial QT dispersion is a substrate for sustained re-entrant arrhythmias and is related with the occurrence of nonsustained ventricular tachycardia in patients with HCM (47);

therefore, its reduction by disopyramide could be antiarrhythmic.

EFFECT ON EARLY AND LATE AFTERDEPOLARIZATIONS: ANTIARRHYTHMIC POTENTIAL. We observed a reduction of the cellular triggers of arrhythmias in HCM cardiomyocytes treated with disopyramide, that is, EAD and DAD (**Figure 3**). The risk of EAD is directly associated with AP prolongation (49). The shortening of AP by disopyramide is therefore the main mechanism behind the reduction of EAD (15). DAD result from the activation of the electrogenic (depolarizing) NCX secondary to spontaneous diastolic Ca^{2+} release from the SR (50). The likelihood of DAD is therefore increased in all conditions leading to increased open probability of RyR during diastole, that is increased SR Ca^{2+} load, increased diastolic cytosolic [Ca^{2+}] or altered intrinsic properties of the RyR (e.g., phosphorylation by Ca^{2+}/calmodulin-dependent protein kinase II). All these features are present in HCM cardiomyocytes, explaining the observed increase of DAD with respect to control cells (15). Interestingly, we observed that disopyramide reduced diastolic cytosolic [Ca^{2+}] (**Figure 2**) and SR Ca^{2+} content and stabilized the closed state of RyR (**Figure 5**), thus lowering the likelihood of diastolic Ca^{2+} waves.

SAFETY OF DISOPYRAMIDE IN CLINICAL PRACTICE. The multichannel inhibitory effects and the membrane stabilizing actions of disopyramide in vitro provide an explanation to the clinical observation that, even though the drug prolongs QT intervals, it does not increase arrhythmic propensity in HCM. In a multicenter study of disopyramide, with a relatively low dosage, there was a clear trend toward lower sudden cardiac death mortality in disopyramide-treated patients with HCM (5). Subsequent studies have shown that the incidence of sudden cardiac death, appropriate ICD discharges or resuscitated cardiac arrest in a cohort of over 200 patients treated with disopyramide is only 0.3% per year, as evaluated after an average follow-up of 5 years (4,6). This rate of lethal or potentially lethal events compares favorably with the natural history of HCM and even with the long-term outcome of patients with obstructive HCM treated with surgical myectomy (51). Disopyramide appears to have an intrinsic safety mechanism in HCM cells, whereby the QT prolonging effects are most evident in cells with short baseline AP duration and are overcome by QT shortening effects in those with longer AP. Combined with its potential protective action from ventricular arrhythmias, this provides disopyramide with a very favorable profile for clinical use in HCM. Following the results of this work, an investigation with prolonged arrhythmia event monitoring before and after disopyramide would be of great interest. In addition to its beneficial electrophysiological effects described herein, the hemodynamic effect of gradient reduction is likely to be antiarrhythmic by decreasing myocardial work and supply-demand ischemia, and by improving myocardial energy efficiency. Despite the demonstrated electrophysiologic and clinical safety, we continue to believe it is prudent to avoid concomitant administration of other QT-prolonging medications along with disopyramide (**Figure 7**).

STUDY LIMITATIONS. First, in this work, we only studied cardiomyocytes isolated from the hypertrophied upper septum; therefore, we could not verify whether the effects of disopyramide are different in cells from other less affected regions. Second, disopyramide hastens the decay of Ca^{2+} transients and accelerates myocardial relaxation in HCM myocardium (**Figures 1 and 2**), as a consequence of the increased Ca^{2+}-extrusion activity of NCX (15,18) (**Figure 5**). Such effect is expected to improve diastolic function in vivo. However, echocardiographic data from our patients did not show any amelioration of active mechanical diastolic parameters (Table 4). This is in line with previous results obtained in patients with HCM using ranolazine, which failed to improve diastolic parameters, despite reducing circulating pro-B-type natriuretic peptide (52). Third, we did not directly evaluate the effects of disopyramide on atrial or ventricular arrhythmia burden in the patients included in the clinical study, as no ambulatory ECG monitoring was performed. Fourth, our results do not provide clear mechanistic insights into why up to 30% of patients with obstructive HCM started on disopyramide are nonresponders. Given the relatively small number of patient samples, we could not observe a subset of them showing minimal or no response to the drug. However, as the response to disopyramide appears to be higher in cells with more pronounced electrophysiological changes (e.g., increase of I_{NaL} and decrease of I_K [see **Figures 6C and 6D**]) and the severity of electrical remodeling varies substantially among different patients (as we previously reported in [15]), interpatient variability in the severity of cellular abnormalities may underlie the differences in the clinical response to disopyramide. Moreover, prior clinical investigations have shown that a subset of patients with a combination of both high resting gradients >85 mm Hg and long anterior mitral leaflets ≥33 mm Hg have a suboptimal response to oral disopyramide due to a combination of adverse anatomy and excessive leaflet slack (6). Fifth, due to the limited number of patient samples and

FIGURE 7 Effects of Disopyramide in HCM Cardiomyocytes

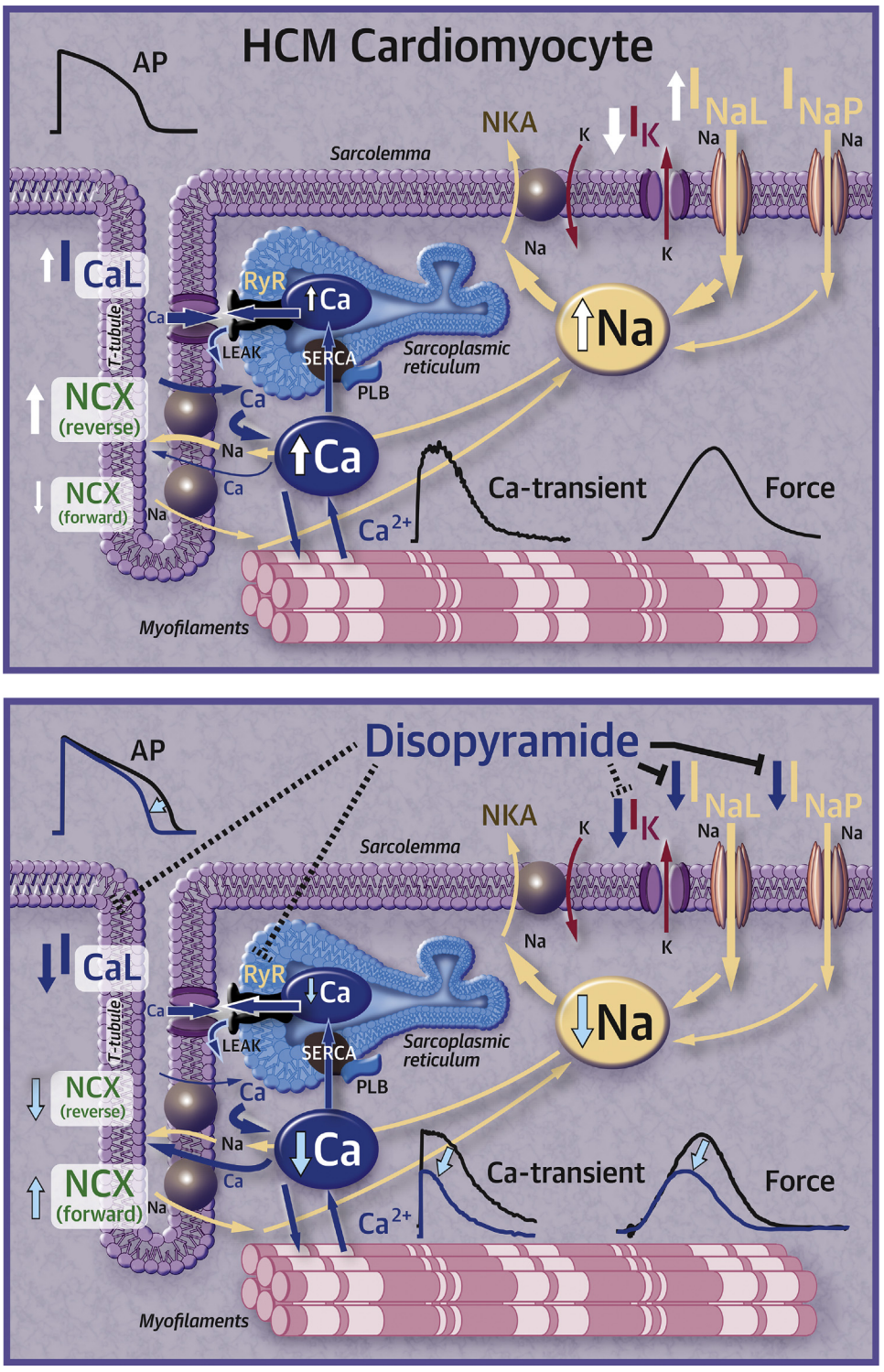

(Top) In HCM cardiomyocytes, $I_{Ca\text{-}L}$ and I_{NaL} are increased, while I_K is markedly decreased, leading to prolonged APs; Na overload impairs NCX, contributing to cytosolic Ca-overload. **(Bottom)** Disopyramide inhibits $I_{Na\text{-}peak}$ (I_{NaP}), I_{NaL}, $I_{Ca\text{-}L}$ and I_K, while also stabilizing ryanodine receptors. These effects lead to shortening of APs. Moreover, normalization of NCX function and $I_{Ca\text{-}L}$ inhibition and RyR stabilization contribute to reduce diastolic Ca and systolic Ca-release, determining negative inotropic effects. APs = action potentials; HCM = hypertrophic cardiomyopathy; $I_{Ca\text{-}L}$ = L-type Ca current; I_K = delayed-rectifier K current; I_{NaL} = Late Na current; NCX = Na^+/Ca^{2+} exchanger; RyR = ryanodine receptor.

incomplete genetic data (Supplemental Table 1), we were unable to correlate specific parameters of drug effectiveness with the different disease-causing mutated genes. As disopyramide does not directly interacts with sarcomeres (**Figure 1**), we believe it is unlikely that mutations in different sarcomeric genes affect the efficacy of the drug. Moreover, we previously observed that the degree of electrical abnormalities at cardiomyocyte level is similar in samples from patients carrying mutations in *MYH7* and in *MYBPC3* and patients with no sarcomeric gene mutations. As disopyramide targets ion channels, these results support the idea that the effects of the drug do not vary depending on the different causing mutations. Sixth, one-half of the patients with HCM included in this study were under disopyramide therapy prior to surgery (Supplemental Table 1); as it is unknown whether long-term disopyramide treatment alters the expression or function of ion channels and other functional cardiomyocyte proteins, we cannot exclude that this may have influenced the results of this study.

CONCLUSIONS

Disopyramide emerges as a safe drug due to its multichannel blocking effects. Disopyramide is an effective negative inotrope that avoids interference with sarcomere protein function. This promises to enrich the pharmacological armamentarium to control obstruction as well as arrhythmias. Indeed, our data suggest a potential protective effect of disopyramide from ventricular arrhythmias mediated by suppression of afterdepolarizations and transmural re-entry; future studies aimed at evaluating the antiarrhythmic potential of disopyramide in patients with HCM are warranted. The results of this study provide a measure of reassurance to clinicians still concerned with the use of disopyramide in a complex structural disease such as HCM.

ADDRESS FOR CORRESPONDENCE: Dr. Raffaele Coppini, Department NeuroFarBa, University of Florence, Viale G. Pieraccini 6, 50139 Firenze, Italy. E-mail: raffaele.coppini@unifi.it.

PERSPECTIVES

COMPETENCY IN MEDICAL KNOWLEDGE 1: The effects of disopyramide in the hearts of patients with HCM are mediated by the combined inhibition of peak Na^+ current, I_{NaL}, Ca^{2+} channels, K^+ channels, and RyR. Such multichannel inhibition explains the marked negative inotropic effect of the drug, which is responsible for the reduction of LV outflow gradients in patients with obstructive HCM. Moreover, these combined actions also result in shortening of the HCM cardiomyocyte AP, improvement of intracellular Ca overload, reduction of afterdepolarizations, and smaller dispersion of repolarization, conferring additional antiarrhythmic potential.

COMPETENCY IN MEDICAL KNOWLEDGE 2: Our translational study provides the mechanistic explanation for the safety and efficacy of disopyramide in patients with obstructive HCM, which has been confirmed by over 40 years of clinical use. These results support the idea that disopyramide treatment can be safely initiated in the outpatient setting and requires only an initial evaluation of the changes in QTc interval, which are usually rather small and are not associated with an increased risk of arrhythmias.

TRANSLATIONAL OUTLOOK 1: The negative inotropic effect of disopyramide does not depend on direct inhibition of myofilament contraction. As such, it does not appear incompatible with the new class of allosteric myosin modulators currently under investigation (mavacamten). As disopyramide and mavacamten act on different targets, they could potentially be combined with synergic effects, if the efficacy and safety of mavacamten on long-term administration is confirmed in the ongoing phase III studies.

TRANSLATIONAL OUTLOOK 2: The use of drugs that inhibit hERG channels and cause drug-related QT prolongation are commonly considered to be more dangerous in patients with pre-existing structural heart disease, such as HCM. This assumption does not take into consideration the disease-related changes in cardiomyocyte ion channel expression. In HCM, the baseline expression of hERG channels is reduced, so the QT prolonging effect of disopyramide (and probably that of other hERG blocking drugs) is reduced. Paradoxically, the proarrhythmic consequences of hERG-blocking QT-prolonging drugs might be less severe in hearts with structural disease and profound electrical remodeling, as compared with healthy hearts.

TRANSLATIONAL OUTLOOK 3: The promising antiarrhythmic properties of disopyramide in vitro suggest a role for clinical use also in patients without obstructive HCM, such as, as a less toxic alternative to amiodarone for control of atrial fibrillation.

REFERENCES

1. Pollick C, Giacomini KM, Blaschke TF, et al. The cardiac effects of d- and l-disopyramide in normal subjects: a noninvasive study. Circulation 1982;66:447–53.

2. Pollick C. Muscular subaortic stenosis: hemodynamic and clinical improvement after disopyramide. N Engl J Med 1982;307:997–9.

3. Sherrid M, Delia E, Dwyer E. Oral disopyramide therapy for obstructive hypertrophic cardiomyopathy. Am J Cardiol 1988;62:1085–8.

4. Ball W, Ivanov J, Rakowski H, et al. Long-term survival in patients with resting obstructive hypertrophic cardiomyopathy comparison of conservative versus invasive treatment. J Am Coll Cardiol 2011;58:2313–21.

5. Sherrid MV, Barac I, McKenna WJ, et al. Multicenter study of the efficacy and safety of disopyramide in obstructive hypertrophic cardiomyopathy. J Am Coll Cardiol 2005;45:1251–8.

6. Sherrid MV, Shetty A, Winson G, et al. Treatment of obstructive hypertrophic cardiomyopathy symptoms and gradient resistant to first-line therapy with beta-blockade or verapamil. Circ Heart Fail 2013;6:694–702.

7. Gersh BJ, Maron BJ, Bonow RO, et al. 2011 ACCF/AHA guideline for the diagnosis and treatment of hypertrophic cardiomyopathy: executive summary: a report of the American College of Cardiology Foundation/American Heart Association Task Force on Practice Guidelines. J Am Coll Cardiol 2011;58:2703–38.

8. Authors/Task Force Members, Elliott PM, Anastasakis A, et al. 2014 ESC guidelines on diagnosis and management of hypertrophic cardiomyopathy: the Task Force for the Diagnosis and Management of Hypertrophic Cardiomyopathy of the European Society of Cardiology (ESC). Eur Heart J 2014;35:2733–79.

9. Adler A, Fourey D, Weissler-Snir A, et al. Safety of outpatient initiation of disopyramide for obstructive hypertrophic cardiomyopathy patients. J Am Heart Assoc 2017;6:e005152.

10. Sherrid MV, Arabadjian M. A primer of disopyramide treatment of obstructive hypertrophic cardiomyopathy. Prog Cardiovasc Dis 2012;54:483–92.

11. Maron BJ. Clinical course and management of hypertrophic cardiomyopathy. N Engl J Med 2018;379:655–68.

12. Kus T, Sasyniuk BI. Electrophysiological actions of disopyramide phosphate on canine ventricular muscle and purkinje fibers. Circ Res 1975;37:844–54.

13. Kojima M. Effects of disopyramide on transmembrane action potentials in guinea-pig papillary muscles. Eur J Pharmacol 1981;69:11–24.

14. Sakai Y, Sekiya S, Inazu M, Homma I, Honda H, Irino O. Evidence that the Na+-Ca2+ exchange system is related to the antiarrhythmic action of disopyramide. Gen Pharmacol 1989;20:105–9.

15. Coppini R, Ferrantini C, Yao L, et al. Late sodium current inhibition reverses electromechanical dysfunction in human hypertrophic cardiomyopathy. Circulation 2013;127:575–84.

16. Ferrantini C, Pioner JM, Mazzoni L, et al. Late sodium current inhibitors to treat exercise-induced obstruction in hypertrophic cardiomyopathy: an in vitro study in human myocardium. Br J Pharmacol 2018;175:2635–52.

17. Coppini R, Ferrantini C, Aiazzi A, et al. Isolation and functional characterization of human ventricular cardiomyocytes from fresh surgical samples. J Vis Exp 2014:86. https://doi.org/10.379/51116.

18. Coppini R, Mazzoni L, Ferrantini C, et al. Ranolazine prevents phenotype development in a mouse model of hypertrophic cardiomyopathy. Circ Heart Fail 2017;10:e003565.

19. Ferrantini C, Coppini R, Pioner JM, et al. Pathogenesis of hypertrophic cardiomyopathy is mutation rather than disease specific: a comparison of the cardiac troponin T E163R and R92Q mouse models. J Am Heart Assoc 2017;6:e005407.

20. Fernandez-Velasco M, Rueda A, Rizzi N, et al. Increased Ca2+ sensitivity of the ryanodine receptor mutant RyR2R4496C underlies catecholaminergic polymorphic ventricular tachycardia. Circ Res 2009;104:201–9.

21. Picht E, Zima AV, Blatter LA, Bers DM. SparkMaster: automated calcium spark analysis with ImageJ. Am J Physiol Cell Physiol 2007;293:C1073–81.

22. Sikkel MB, Francis DP, Howard J, et al. Hierarchical statistical techniques are necessary to draw reliable conclusions from analysis of isolated cardiomyocyte studies. Cardiovasc Res 2017;113:1743–52.

23. Passini E, Minchole A, Coppini R, et al. Mechanisms of pro-arrhythmic abnormalities in ventricular repolarisation and anti-arrhythmic therapies in human hypertrophic cardiomyopathy. J Mol Cell Cardiol 2016;96:72–81.

24. Lyon A, Bueno-Orovio A, Zacur E, et al. Electrocardiogram phenotypes in hypertrophic cardiomyopathy caused by distinct mechanisms: apico-basal repolarization gradients vs. Purkinje-myocardial coupling abnormalities. Europace 2018;20 Suppl 3:iii102–12.

25. Arnman K, Graffner C, Rikner L, Ryden L, Voog L. Plasma concentration of disopyramide given as capsules and controlled release tablets. Eur J Clin Pharmacol 1983;24:199–203.

26. Paul AA, Witchel HJ, Hancox JC. Inhibition of HERG potassium channel current by the class 1a antiarrhythmic agent disopyramide. Biochem Biophys Res Commun 2001;280:1243–50.

27. Endresen K, Amlie JP, Forfang K. Effects of disopyramide on repolarisation and intraventricular conduction in man. Eur J Clin Pharmacol 1988;35:467–74.

28. Savio-Galimberti E, Knollmann BC. Channel activity of cardiac ryanodine receptors (RyR2) determines potency and efficacy of flecainide and R-propafenone against arrhythmogenic calcium waves in ventricular cardiomyocytes. PLoS One 2015;10:e0131179.

29. Sherrid MV, Pearle G, Gunsburg DZ. Mechanism of benefit of negative inotropes in obstructive hypertrophic cardiomyopathy. Circulation 1998;97:41–7.

30. Joshi S, Patel UK, Yao SS, et al. Standing and exercise Doppler echocardiography in obstructive hypertrophic cardiomyopathy: the range of gradients with upright activity. J Am Soc Echocardiogr 2011;24:75–82.

31. Barac I, Upadya S, Pilchik R, et al. Effect of obstruction on longitudinal left ventricular shortening in hypertrophic cardiomyopathy. J Am Coll Cardiol 2007;49:1203–11.

32. Kajimoto K, Imai T, Minami Y, Kasanuki H. Comparison of acute reduction in left ventricular outflow tract pressure gradient in obstructive hypertrophic cardiomyopathy by disopyramide versus pilsicainide versus cibenzoline. Am J Cardiol 2010;106:1307–12.

33. Kimball BP, Bui S, Wigle ED. Acute dose-response effects of intravenous disopyramide in hypertrophic obstructive cardiomyopathy. Am Heart J 1993;125:1691–7.

34. Green EM, Wakimoto H, Anderson RL, et al. A small-molecule inhibitor of sarcomere contractility suppresses hypertrophic cardiomyopathy in mice. Science 2016;351:617–21.

35. Honerjager P. The contribution of Na channel block to the negative inotropic effect of antiarrhythmic drugs. Basic Res Cardiol 1986;81 Suppl 1:33–7.

36. Honerjager P, Loibl E, Steidl I, Schonsteiner G, Ulm K. Negative inotropic effects of tetrodotoxin and seven class 1 antiarrhythmic drugs in relation to sodium channel blockade. Naunyn Schmiedebergs Arch Pharmacol 1986;332:184–95.

37. Ito K, Nagafuchi K, Taga A, Yorikane R, Koike H. Possible involvement of altered Na+ -Ca2+ exchange in negative inotropic effects of class I antiarrhythmic drugs on rabbit and rat ventricles. J Cardiovasc Pharmacol 1996;27:355–61.

38. Despa S, Bers DM. Na(+) transport in the normal and failing heart—remember the balance. J Mol Cell Cardiol 2013;61:2–10.

39. Coppini R, Ferrantini C, Mazzoni L, et al. Regulation of intracellular Na(+) in health and disease: pathophysiological mechanisms and implications for treatment. Glob Cardiol Sci Pract 2013;2013:222–42.

40. Applegate RJ, Walsh RA, O'Rourke RA. Frequency-dependent myocardial depression induced by verapamil in conscious dogs. Am J Physiol 1987;253:H487–92.

41. Gloor HO, Urthaler F. Differential effect of verapamil isomers on sinus node and AV junctional region. Am J Physiol 1983;244:H80–8.

42. Hilliard FA, Steele DS, Laver D, et al. Flecainide inhibits arrhythmogenic Ca2+ waves by open state block of ryanodine receptor Ca2+ release channels and reduction of Ca2+ spark mass. J Mol Cell Cardiol 2010;48:293–301.

43. Sacherer M, Sedej S, Wakula P, et al. JTV519 (K201) reduces sarcoplasmic reticulum Ca(2)(+) leak and improves diastolic function in vitro in murine and human non-failing myocardium. Br J Pharmacol 2012;167:493–504.

44. El Harchi A, Zhang YH, Hussein L, Dempsey CE, Hancox JC. Molecular determinants of hERG potassium channel inhibition by disopyramide. J Mol Cell Cardiol 2012;52:185–95.

45. Wyse KR, Ye V, Campbell TJ. Action potential prolongation exhibits simple dose-dependence for sotalol, but reverse dose-dependence for quinidine and disopyramide: implications for proarrhythmia due to triggered activity. J Cardiovasc Pharmacol 1993;21:316–22.

46. Sakai R, Inoue D, Ishibashi K, et al. Kinetics of frequency-dependent conduction delay by class I antiarrhythmic drugs in human atrium. J Cardiovasc Pharmacol 1995;25:953–60.

47. Magri D, Piccirillo G, Ricotta A, et al. Spatial QT dispersion predicts nonsustained ventricular tachycardia and correlates with confined systo-diastolic dysfunction in hypertrophic cardiomyopathy. Cardiology 2015;131:122–9.

48. Chiang WT, von Bahr C, Calissendorff B, et al. Kinetics and dynamics of disopyramide and its dealkylated metabolite in healthy subjects. Clin Pharmacol Ther 1985;38:37–44.

49. Antzelevitch C, Belardinelli L. The role of sodium channel current in modulating transmural dispersion of repolarization and arrhythmogenesis. J Cardiovasc Electrophysiol 2006;17 Suppl 1:S79–85.

50. Bers DM. Calcium cycling and signaling in cardiac myocytes. Ann Rev Physiol 2008;70:23–49.

51. Ommen SR, Maron BJ, Olivotto I, et al. Long-term effects of surgical septal myectomy on survival in patients with obstructive hypertrophic cardiomyopathy. J Am Coll Cardiol 2005;46:470–6.

52. Olivotto I, Camici PG, Merlini PA, et al. Efficacy of ranolazine in patients with symptomatic hypertrophic cardiomyopathy: the RESTYLE-HCM randomized, double-blind, placebo-controlled study. Circ Heart Fail 2018;11:e004124.

KEY WORDS action potentials, arrhythmias, diastolic dysfunction, hypertrophic cardiomyopathy, QT interval, safety

APPENDIX For supplemental tables, please see the online version of this paper.

JACC: BASIC TO TRANSLATIONAL SCIENCE VOL. 4, NO. 7, 2019

EDITORIAL COMMENT

Out With the Old and in With the New

Not So Fast in Hypertrophic Cardiomyopathy*

Martin S. Maron, MD

Over 50 years ago, Dr. Eugene Braunwald commenced the therapeutic era in hypertrophic cardiomyopathy (HCM) with the introduction of the beta-blocker propranolol. Over the last several decades, pharmacological intervention with beta-blockers or calcium-channel blockers continues to be the initial treatment for limiting heart failure symptoms due to left ventricular outflow tract obstruction (1). In 1985, the class IA antiarrhythmic drug disopyramide was also demonstrated to be effective and safe at lowering outflow gradients and improving heart failure symptoms, largely as a result of its negative inotropic properties. Although its use can be limited by parasympathetic side effects and limited long-term efficacy (2–5), North American and European expert consensus HCM guidelines have promoted disopyramide as an additional treatment option for symptomatic obstructive patients with HCM before considering highly effective invasive septal reduction therapy (6,7). However, despite the availability of disopyramide for over 35 years, the mechanism by which this drug provides the observed clinical benefit has not been well characterized in this complex heart disease, contributing to some apprehension and concern within the practicing cardiology community in recommending disopyramide therapy to patients with HCM (4,5).

In this issue of *JACC: Basic to Translational Science*, Coppini et al. (8) perform a number of elegant basic science experiments on isolated HCM cardiomyocytes derived from ventricular septal muscle obtained from obstructive patients with HCM at the time of surgical myectomy. A variety of effects of disopyramide were studied at the cellular level, including changes to ion fluxes, afterdepolarizations, and twitch tension. To relate these experimental findings to the clinical effect of disopyramide, electrocardiograms and echocardiograms were performed before and after 3 months of disopyramide therapy in a separate study cohort of 39 symptomatic obstructive patients with HCM.

SEE PAGE 795

At first glance, this investigation characterizing the mechanism of a drug that has been used clinically in HCM for some time could be inadvertently dismissed as old news. However, this is far from the reality because the basic and clinical observations derived from Coppini et al. (8) establish a number of principles that advance our understanding of an important therapy for controlling symptoms in patients with HCM and also provide an example for similar future initiatives in this disease.

One of the major observations derived from the extensive in vitro experiments performed in this study was the lack of a direct effect by disopyramide on the contractile apparatus of the heart. Instead, the substantial reduction (60%) in resting outflow tract gradient achieved with disopyramide was accomplished by altering myocardial contractile force by mitigating intracellular Ca^{2+} levels through direct action on multiple ion channels, including the peak and late Na channel current, the L-type Ca^{2+} current, and the ryanodine receptor (8). The negative

*Editorials published in *JACC: Basic to Translational Science* reflect the views of the authors and do not necessarily represent the views of *JACC: Basic to Translational Science* or the American College of Cardiology.

From the Hypertrophic Cardiomyopathy Center, Division of Cardiology, Tufts Medical Center, Boston, Massachusetts. Dr. Maron is on a steering committee for Cytokinetics; and is a consultant for Celltrion. Dr. Maron has reported that he has no relationships relevant to the contents of this paper to disclose.

The author attests they are in compliance with human studies committees and animal welfare regulations of the authors' institutions and Food and Drug Administration guidelines, including patient consent where appropriate. For more information, visit the *JACC: Basic to Translational Science* author instructions page.

ISSN 2452-302X https://doi.org/10.1016/j.jacbts.2019.10.002

inotropic effect resulting from this alteration in cellular Ca^{2+} levels decreased early systolic flow acceleration enough to mitigate the abnormal hemodynamic drag forces that contribute to the mechanism of mitral valve-ventricular septal contact.

Of note, the impact of disopyramide on contractile force was associated with only a minimal decrease in ejection fraction (8). This is not a trivial issue because any intervention associated with a more significant decrease in systolic function would likely raise safety concerns, including potentially new heart failure symptoms resulting from diminished cardiac output. Therefore, these data by Coppini et al. (8), as well as prior prospective clinical studies with disopyramide (3,4,9), suggest that the minimal negative inotropic effect of disopyramide is not associated with increased risk. The excellent safety profile also results from the fact that disopyramide use resulted in only a very minimal increase in the corrected QT interval, an observation that further supports the growing practice of initiating disopyramide on an outpatient basis unless certain high-risk electrocardiographic features are present in a patient (4,8).

As the authors correctly point out, the mechanism of action of disopyramide in reducing outflow tract gradients contrasts sharply to the proposed mechanism of action of myosin inhibitors, an emerging novel class of drug therapy that is currently under evaluation in a number of clinical trials for the treatment of symptomatic obstructive HCM (10). The myosin inhibitors have been noted in early clinical investigations to lower gradients by producing a potent negative inotropic effect achieved by direct inhibition of cardiac myosin, with little off-target effect and an early acceptable safety profile (10). Although speculative at this point, the data by Coppini et al. (8) do raise the future prospect that outflow obstruction may be more effectively mitigated by using a therapeutic strategy utilizing the benefits of 2 drugs that lower gradient through different but potentially complementary (and hopefully synergistic) mechanisms. This is particularly relevant because treatment with disopyramide alone is associated with limited long-term efficacy in improving heart failure symptoms in an important subset of obstructive patients with HCM.

Coppini et al. (8) also establish rational for the observed safety and potentially beneficial antiarrhythmic effects of disopyramide in obstructive HCM. Early and delayed afterdepolarizations, a cellular trigger for arrhythmias, were noted to be decreased in HCM endocardial cardiomyocyte due to the effect of disopyramide on shortening the actional potential as well as decreasing the content of Ca^{2+} within the sarcoplasmic reticulum (8). Determining if the effects of disopyramide on early and delayed afterdepolarizations in human tissue culture translates into an actual decrease in clinical burden of atrial or ventricular arrhythmias in patients with HCM was not assessed in this study. Nevertheless, these rigorous basic science observations provide strong rational for future clinical investigations to determine the efficacy of disopyramide in reducing arrhythmic burden across the entire spectrum of patients with HCM, including patients without outflow tract obstruction.

An important issue not addressed by this investigation was clarifying the mechanism responsible for why close to one-third of obstructive patients with HCM do not achieve a significant decrease in outflow gradients (i.e., nonresponders) or why efficacy of the drug often diminishes over extend periods of time in other patients (3,4). Further work directed at identifying the cellular mechanisms responsible for these limitations of disopyramide would represent another critical next step forward for this translative science initiative, with the opportunity to potentially develop novel drug therapy specifically tailored to target all the basic mechanisms responsible generating outflow tract obstruction and in the process potentially further increase the number of drug therapy options available for patients with obstructive HCM.

Despite over 60 years since the first contemporary clinical descriptions of HCM (5), this genetic heart disease has been subjected to limited translational scientific investigation, a reason there has been no additional novel drug therapy for HCM since disopyramide. Coppini et al. (8) should be commended for a unique “bench to bedside” initiative in this complex, heterogenous genetic heart disease. By providing the basic mechanisms responsible for the observed clinical response of disopyramide in HCM, a large measure of reassurance has now been provided on the safety and efficacy of this drug to the practicing cardiology community and patients with HCM. Also, this translational study represents an important “call to arms” to the scientific community to continue to pursue investigation aimed at clarifying the basic mechanisms responsible for limiting symptoms in HCM and to identify novel therapeutic targets to further our treatment options for patients with this complex genetic heart disease, providing all HCM patients an even greater opportunity for improved quality of life.

ADDRESS FOR CORRESPONDENCE: Dr. Martin S. Maron, Hypertrophic Cardiomyopathy Center, Division of Cardiology, Tufts Medical Center, 800 Washington Street, #70, Boston, Massachusetts 02111. E-mail: mmaron@tuftsmedicalcenter.org.

JACC: BASIC TO TRANSLATIONAL SCIENCE VOL. 4, NO. 7, 2019
NOVEMBER 2019:814–6

REFERENCES

1. Cohen LS, Braunwald E. Amelioration of angina pectoris in idiopathic hypertrophic subaortic stenosis with beta-adrenergic blockade. Circulation 1967;35:847–51.

2. Sherrid M, Delia E, Dwyer E. Oral disopyramide therapy for obstructive hypertrophic cardiomyopathy. Am J Cardiol 1988;62:1085–8.

3. Sherrid MV, Barac I, McKenna WJ, et al. Multicenter study of the efficacy and safety of disopyramide in obstructive hypertrophic cardiomyopathy. J Am Coll Cardiol 2005;45:1251–8.

4. Adler A, Fourey D, Weissler-Snir A, et al. Safety of outpatient initiation of disopyramide for obstructive hypertrophic cardiomyopathy patients. J Am Heart Assoc 2017;6:e005152.

5. Maron BJ. Clinical course and management of hypertrophic cardiomyopathy. N Engl J Med 2018;379:655–68.

6. Gersh BJ, Maron BJ, Bonow RO, et al. 2011 ACCF/AHA guideline for the diagnosis and treatment of hypertrophic cardiomyopathy: executive summary: a report of the American College of Cardiology Foundation/American Heart Association Task Force on Practice Guidelines. J Am Coll Cardiol 2011;58:2703–38.

7. Elliott PM, Anastasakis A, Borger MA, et al. 2014 ESC guidelines on diagnosis and management of hypertrophic cardiomyopathy: the Task Force for the Diagnosis and Management of Hypertrophic Cardiomyopathy of the European Society of Cardiology (ESC). Eur Heart J 2014;35:2733–79.

8. Coppini C, Ferrantini C, Pioner JM, et al. Electrophysiological and contractile effects of disopyramide in patients with obstructive hypertrophic cardiomyopathy: a translational study. J Am Coll Cardiol Basic Trans Science 2019;4:795–813.

9. Sherrid MV, Shetty A, Winson G, et al. Treatment of obstructive hypertrophic cardiomyopathy symptoms and gradient resistant to first-line therapy with beta-blockade or verapamil. Circ Heart Fail 2013;6:694–702.

10. Heitner SB, Jacoby D, Lester SJ, et al. Mavacamten treatment of obstructive hypertrophic cardiomyopathy: a clinical trial. Ann Intern Med 2019;117:741–8.

KEY WORDS action potential, arrhythmias, hypertrophic cardiomyopathy, QT interval, safety

JACC: BASIC TO TRANSLATIONAL SCIENCE VOL. 4, NO. 7, 2019

PRECLINICAL RESEARCH

Cardiac Myosin Binding Protein-C Phosphorylation Mitigates Age-Related Cardiac Dysfunction

Hope for Better Aging?

Paola C. Rosas, MD, PhD, BSPharm,[a] Chad M. Warren, MS,[a] Heidi A. Creed, BS,[b] Jerome P. Trzeciakowski, PhD,[b] R. John Solaro, PhD,[a] Carl W. Tong, MD, PhD[b,c]

VISUAL ABSTRACT

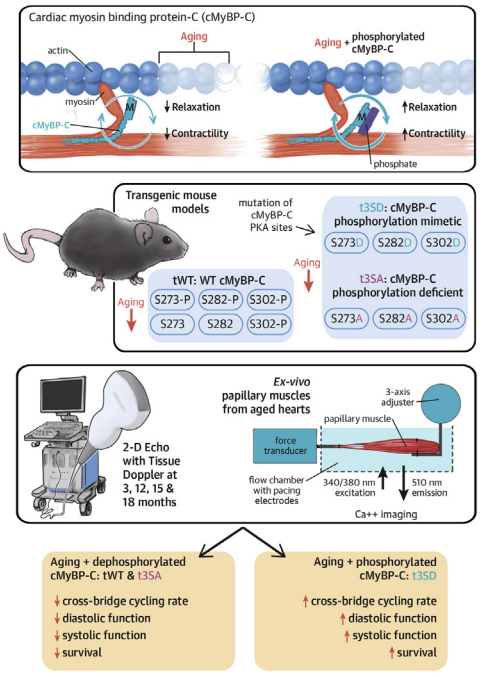

Rosas, P.C. et al. J Am Coll Cardiol Basic Trans Science. 2019;4(7):817–30.

HIGHLIGHTS

- **With aging, phosphorylated-mimetic cMyBP-C mice exhibited better survival, better preservation of systolic and diastolic functions, and unchanging wall thickness compared with control mice.**
- **Aged wild-type equivalent mice exhibited decreasing cMyBP-C phosphorylation (S273 and S282) along with worsening cardiac function and hypertrophy similarly to what was observed in hypophosphorylated cMyBP-C mice.**
- **Intact papillary muscle experiments suggest that cMyBP-C phosphorylation increased cross-bridge detachment rates as the underlying mechanism.**
- **Phosphorylating cMyBP-C is therefore a novel mechanism that can prevent aging-related development of cardiac dysfunction.**

ISSN 2452-302X https://doi.org/10.1016/j.jacbts.2019.06.003

ABBREVIATIONS AND ACRONYMS

3SA = mutated 3 serines to 3 alanines to mimic hypophosphorylated cardiac myosin binding protein-C (S273A, S282A, and S302A)

3SD = mutated 3 serines to 3 aspartic acids to mimic phosphorylated cMyBP-C (S273D, S282D, and S302D)

ANOVA = analysis of variance

cMyBP-C = cardiac myosin binding protein-C

cTnI = cardiac troponin I

EF = ejection fraction

HF = heart failure

HFpEF = heart failure with preserved ejection fraction

HOP = hydroxyproline

LV = left ventricular

SUMMARY

Cardiac myosin binding protein-C (cMyBP-C) phosphorylation prevents aging-related cardiac dysfunction. We tested this hypothesis by aging genetic mouse models of hypophosphorylated cMyBP-C, wild-type equivalent, and phosphorylated-mimetic cMyBP-C for 18 to 20 months. Phosphorylated-mimetic cMyBP-C mice exhibited better survival, better preservation of systolic and diastolic functions, and unchanging wall thickness. Wild-type equivalent mice showed decreasing cMyBP-C phosphorylation along with worsening cardiac function and hypertrophy approaching those found in hypophosphorylated cMyBP-C mice. Intact papillary muscle experiments suggested that cMyBP-C phosphorylation increased cross-bridge detachment rates as the underlying mechanism. Thus, phosphorylating cMyBP-C is a novel mechanism with potential to treat aging-related cardiac dysfunction. (J Am Coll Cardiol Basic Trans Science 2019;4:817–30) © 2019 The Authors. Published by Elsevier on behalf of the American College of Cardiology Foundation. This is an open access article under the CC BY-NC-ND license (http://creativecommons.org/licenses/by-nc-nd/4.0/).

Heart failure (HF) afflicts 6.2 million Americans as of 2019 (1). The prevalence of HF is expected to increase to >8 million by 2030 (2). HF prevalence also increases with age, from 0.3% (male) and 0.2% (female) of the population at ages 20 to 39 years to 6.9% (male) and 4.8% (female) at ages 60 to 79 years according to the National Health and Nutrition Examination Survey (2013 to 2016). Aging alone can lead to deterioration of diastolic function, despite improvement in blood pressure control (3). Moreover, HF is the leading cause of hospitalization in elderly patients (4). Despite new treatments, ~50% of patients diagnosed with HF will die within 5 years (1). Therefore, we need to search for novel strategies to treat this deadly disease in our aging population.

Cardiac myosin binding protein-C (cMyBP-C), a heart muscle thick filament protein, can regulate cross-bridge attachment/detachment processes by its phosphorylation status. Once phosphorylated, cMyBP-C accelerates cross-bridge cycling to enhance the ability of the heart to contract and relax (5,6). Hearts from patients with hypertension (7), atrial fibrillation (8), hypertrophic cardiomyopathy (9–11), and HF (9,11,12) all exhibit decreased cMyBP-C phosphorylation levels. Moreover, cMyBP-C mutations are a predominant cause of hypertrophic cardiomyopathy that progresses to HF (13). Thus, there is sufficient evidence to suggest that cMyBP-C phosphorylation mediates normal heart physiology.

We hypothesized that cMyBP-C phosphorylation mitigates aging-related cardiac dysfunction. To test this idea, we used existing mouse models of cMyBP-C phosphorylation mimetic cMyBP-C(t3SD) mutant, cMyBP-C dephosphorylated mimetic cMyBP-C(t3SA) mutant, and cMyBP-C wild-type cMyBP-C(tWT). These mice were aged to >18 months to mimic a 60- to 70-year-old human. Our studies found that cMyBP-C phosphorylation preserves heart function during aging.

METHODS

MOUSE LINES. All protocols for animal care and use were approved by the Institutional Animal Care and Use Committee at the Texas A and M University Health Science Center College of Medicine Temple and College Station campuses. Three mice models were used that were previously generated by transgenic expression of cMyBP-C phosphorylation mimetics on a cMyBP-C$^{(-/-)}$ null background that was

From the [a]Department of Physiology and Biophysics, Center for Cardiovascular Research, College of Medicine, University of Illinois at Chicago, Chicago, Illinois; [b]Department of Medical Physiology, Texas A and M University Health Science Center, College of Medicine, College Station, Texas; and the [c]Catholic Health Initiatives-St. Joseph Health, Bryan, Texas. This work was supported by the American Heart Association (16POST29990013 to Dr. Rosas) and the National Heart, Lung, and Blood Institute of the National Institutes of Health (K08HL114877, R03HL140266, and R01HL145534 to Dr. Tong, and R01HL128468 and P01HL624026 to Dr. Solaro). Dr. Solaro is a consultant for Cytokinetics, Inc. and Pfizer. All other authors have reported that they have no relationships relevant to the contents of this paper to disclose.

The authors attest they are in compliance with human studies committees and animal welfare regulations of the authors' institutions and Food and Drug Administration guidelines, including patient consent where appropriate. For more information, visit the *JACC: Basic to Translational Science* author instructions page.

Manuscript received March 30, 2019; revised manuscript received June 14, 2019, accepted June 19, 2019.

generated on an E129X1 (SVE-129) strain (14). Three cMyBP-C protein kinase-A sites (S273, S282, and S302) were mutated to nonphosphorylatable alanine to mimic phosphorylation deficiency, cMyBP-C(t3SA) (15), or else substituted to nonphosphorylatable aspartic acid to mimic the negative charge of the phosphorylated residue, cMyBP-C(t3SD) (6). The cMyBP-C(tWT) control was generated by re-introducing wild-type cMyBP-C into the cMyBP-$C^{(-/-)}$ null background (15). Because the phosphorylation status of cMyBP-C can change with various conditions, we used cMyBP-C(t3SD), which mimics constitutively phosphorylated cMyBP-C, to test our hypothesis. The 3 models exhibited similar cMyBP-C expression levels: cMyBP-C(tWT): 72%; cMyBP-C(t3SA): 74%; and cMyBP-C(t3SD): 84% (6,15).

SURVIVAL. The mice models were aged to >18 months to mimic 60- to 70-year-old human subjects. Both male and female mice were used. Mice euthanized for experiments or for noncardiac reasons (e.g., dermatitis, teeth problems, penile prolapse) were censored at the date of event. Survival analyses were done on day 600. Mice living beyond 600 days were censored at day 600. Censored mice were not counted as death.

MEASUREMENT OF PHYSIOLOGICAL PARAMETERS. Blood glucose and systolic blood pressure levels (tail cuff measurements on restrained conscious mice) were measured in all 3 mice models at 15 to 18 months of age. Mice were euthanized and organs were harvested to measure lung weight/body weight, heart weight/body weight, and heart weight/tibia length ratios as indicators of pulmonary edema and cardiac hypertrophy.

ECHOCARDIOGRAPHY. The Vevo 2100 system (FUJIFILM VisualSonics, Toronto, Ontario, Canada) was used to perform echocardiography on mice 3 to 18 months old by using a previously developed protocol (6). Mice were anesthetized with 0.5% to 2.5% of isoflurane and placed in a warmed echocardiogram table at 39°C. Electrocardiogram, heart rate, and respiration rates were continuously monitored. The isoflurane concentration was adjusted to keep the heart rate at 380 to 450 beats/min. We performed transthoracic 2-dimensional, M-mode, color-flow Doppler, and tissue Doppler imaging. All mice completely recovered after the echocardiography studies.

FORCE AND CALCIUM MEASUREMENTS ON INTACT PAPILLARY MUSCLES. Intact papillary muscles were isolated from 12- to 15-month-old mice models. We performed simultaneous intracellular calcium $[Ca^{2+}]_i$ and force measurements using a previously developed protocol (6,16). Briefly, right ventricular papillary muscles were isolated, mounted in a chamber, and superfused with Krebs-Henseleit solution (NaCl 119 mmol/l, glucose 12 mmol/l, KCl 4.6 mmol/l, $NaHCO_3$ 25 mmol/l, KH_2PO_4 1.2 mmol/l, $MgCl_2$ 1.2 mmol/l, and $CaCl_2$ 1.8 mmol/l) at room temperature. Muscles were stretched to achieve maximum twitch force while maintaining steady diastolic force and paced at 1, 1.5, and 2 Hz to mimic increasing heart rate. Force was measured by using a force transducer (Aurora Scientific, Aurora, Ontario, Canada), and intracellular calcium $[Ca^{2+}]_i$ was estimated by using Fura-2 as an indicator along with a hyperswitch system (IonOptix LLC, Westwood, Massachusetts). Fluorescence was recorded at 510 nm from calcium-bound Fura-2 (340 nm excitation) and calcium-free Fura-2 (380 nm of excitation). We calculated $[Ca^{2+}]_i$ using calcium-bound Fura-2/calcium-free Fura-2 ratios after background correction (6).

MYOFIBRILLAR PREPARATIONS. Snap-frozen left ventricular (LV) tissue was homogenized twice by using glass Dounce homogenizers in standard relax buffer (imidazole 10 mM, pH 7.2, KCl 75 mM, $MgCl_2$ 2 mM, ethylenediaminetetraacetic acid 2 mM , and NaN_3 1 mM) with 1% (v/v) Triton X-100, as previously described (17). Myofibrils were centrifuged, and the supernatant fraction was removed. The pellets were then washed once in standard relax buffer to remove the Triton X-100. The standard relax buffers contained both the protease (MilliporeSigma, St. Louis, Missouri) and phosphatase (Calbiochem, Darmstadt, Germany) inhibitors at a 1:100 dilution and Calyculin A (Cell Signaling Technology, Danvers, Massachusetts) to 100 nM final concentration. The pellet was solubilized in the sample buffer containing urea 8 M, thiourea 2 M, Tris 0.05 M, dithiothreitol 75 mM , and sodium dodecyl sulfate 3% . Protein concentration of the samples was determined with a Pierce 660 nm protein assay reagent with the addition of an ionic detergent compatibility reagent (Thermo Fisher Scientific, Waltham, Massachusetts). Samples were stored at -80°C until used.

PROTEIN PHOSPHORYLATION. Myofibrillar preparations were analyzed with a 12% sodium dodecyl sulfate-polyacrylamide gel electrophoresis method. Pro-Q Diamond phosphoprotein staining (Thermo Fisher Scientific) was used to estimate the amount of phosphorylated proteins, and Coomassie staining was used to estimate the amount of loaded proteins as previously described (6). The gel was imaged on a ChemiDoc MP (Bio-Rad, Hercules, California), and band densities were determined by using Image Lab 6.0.1 software.

FIGURE 1 Survival

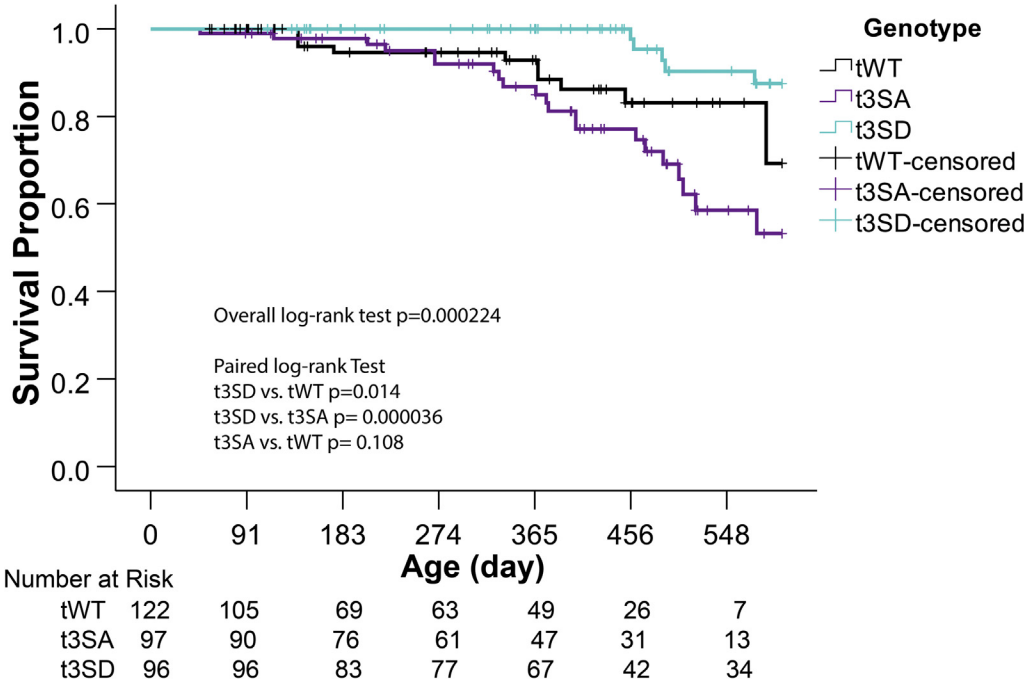

All 3 mouse models were aged to 18 to 20 months. Mice that were used for experiments or euthanized for noncardiac causes were censored. Kaplan-Meier analysis with log-rank testing was then performed to identify differences in survival. Proportional hazard remaining constant was verified by using the Grambsch and Therneau test. cMyBP-C(t3SD) showed the best overall survival.

WESTERN BLOTTING WITH FLUORESCENT DETECTION. After gel electrophoresis, proteins were transferred to a 0.22 μm WesternBright PVDF-FL membrane (Advansta, San Jose, California). Blots were blocked for 1 h with AdvanBlock Fluor (Advansta) and then probed in primary antibodies diluted in AdvanBlock Fluor overnight at 4°C. The phospho-specific (S273P, S282P, and S302P) cMyBP-C antibodies were generous gifts from Sakthivel Sadayappan, PhD (University of Cincinnati College of Medicine, Cincinnati, Ohio), and the total mouse monoclonal cMyBP-C antibody was from Santa Cruz Biotechnology (Dallas, Texas) (#SC-137181) and was diluted to 1:2,500. The membranes were washed and then incubated with secondary antibodies diluted in AdvanBlock Fluor. We used secondary goat anti-rabbit DyLight 800 4X PEG (#SA5-35571, Thermo Fisher Scientific) 1:10,000 and secondary goat anti mouse StarBright Blue 700 (#12004158, Bio-Rad) 1:5,000. Membranes were imaged on a ChemiDoc MP (Bio-Rad), and band densities were determined by using Image Lab 6.0.1 software.

HYDROXYPROLINE ASSAY. Hydroxyproline (HOP) content was determined as previously described (18). A portion of the LV posterior wall (i.e., LV free wall) was removed in a similar region for all hearts. This region corresponded to echocardiographic measurements of posterior wall thickness. To determine the exact weight of the tissue, 15 to 25 mg of snap-frozen cardiac tissue was minced into a screw cap vial. Tissue was covered with 6 M of hydrochloric acid and incubated in an oven at 105°C to 110°C overnight. We used a standard curve of *trans*-4-Hydroxy-L-proline (H-55409, MilliporeSigma) (0 to 500 μM) to determine the content of HOP per milligram of tissue.

STATISTICAL ANALYSES. SPSS version 25 (IBM SPSS Statistics, IBM Corporation, Armonk, New York) and Stata version 14 (StataCorp, College Station, Texas) software were used to complete statistical analyses. Kaplan-Meier curves and log-rank tests were used to identify significant differences in survival. Analysis of variance (ANOVA) was used to identify significant differences among 3 groups with a post hoc Tukey

FIGURE 2 De-Phosphorylated Mimetic cMyBP-C(t3SA) Exhibits Signs of Heart Failure

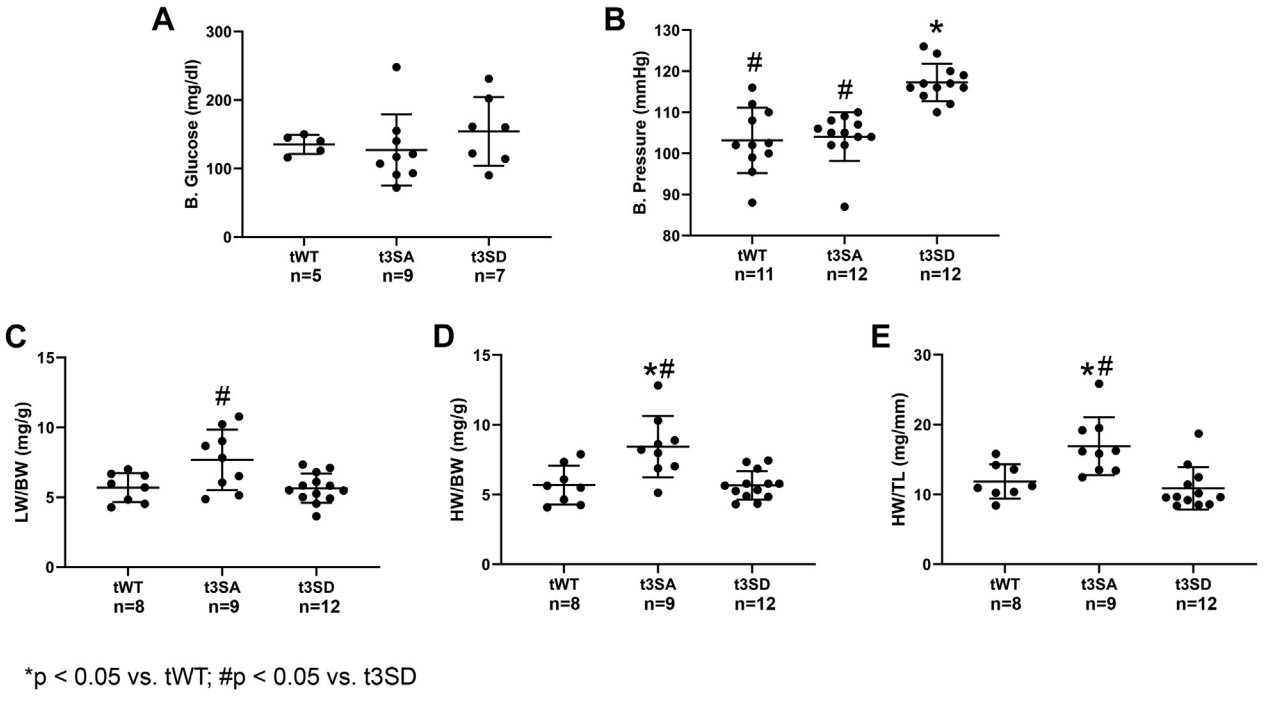

(A) Nonfasting blood glucose levels were similar in all 3 mice models at 15 to 18 months of age. **(B)** All 3 mice models exhibited mean blood pressures within 95 to 120 mm Hg; however, cMyBP-C(t3SD) mice showed significantly higher blood pressure. **(C)** cMyBP-C(t3SA) showed an increased lung weight to body weight ratio (LW/BW), suggesting pulmonary edema. **(D and E)** cMyBP-C(t3SA) showed increased heart weight to body weight (HW/BW) and increased heart weight to tibia length (HW/TL) ratios, suggesting hypertrophy. Comparisons between 3 strains were analyzed with an analysis of variance post hoc Tukey method. Data are presented as dot plots with mean ± SD.

alpha-correction method to adjust for multiple pairwise comparisons. Student's *t*-test was used to compare 2 independent groups. Repeated measure ANOVA with intergroup comparison was used to identify significant differences in responses to increasing pacing frequency on intact papillary muscles among the 3 mouse models. Pearson correlation was used to test for a linear correlation between 2 continuous variables. When possible, dot plots with mean ± SD were used to present data. Statistical significance was determined by using a 2-sided p value <0.05.

RESULTS

cMyBP-C PHOSPHORYLATION MIMETIC cMyBP-C(t3SD) MICE EXHIBITED BETTER SURVIVAL. Kaplan-Meier analysis showed significantly different survival at 600 days in all 3 mice models (overall log-rank test, $p < 0.001$). Results are as follows: cMyBP-C(tWT) at 69.3 ± 0.1% survival, starting n = 122 (112 censored; 5 censored for age >600 days); cMyBP-C(t3SA) at 53.2 ± 0.1% survival, starting n = 97 (76 censored; 10 censored for age >600 days); and cMyBP-C(t3SD) at 87.5 ± 0.1% survival, starting n = 96 (91 censored; 22 censored for age >600 days). Pairwise comparison log-rank testing revealed that cMyBP-C(t3SD) exhibited significantly better survival than the other 2 mouse models, and cMyBP-C(tWT) trended toward better survival than cMyBP-C(t3SA) (Figure 1).

cMyBP-C(t3SA) HYPOPHOSPHORYLATED MIMETIC AGED MICE SHOWED SIGNS OF HEART FAILURE NOT ATTRIBUTABLE TO DIABETES OR HYPERTENSION. Nonfasting blood glucose measurements were similar between mice models age 15 to 18 months (Figure 2A). Tail cuffs were used to measure systolic blood pressure at 15 to 18 months of age. All 3 models exhibited blood pressure levels within normal ranges (mean systolic blood pressure <120 mm Hg) (19); however, cMyBP-C(t3SD) showed significantly higher blood pressures than the other 2 groups (Figure 2B). cMyBP-C(t3SA) mice exhibited an increased lung/body weight ratio, indicating pulmonary edema (Figure 2C). cMyBP-C(t3SA) mice showed increased heart weight/

FIGURE 3 cMyBP-C Phosphorylated Mimetic (t3SD) Demonstrated Better Preservation of Diastolic and Systolic Functions With Aging

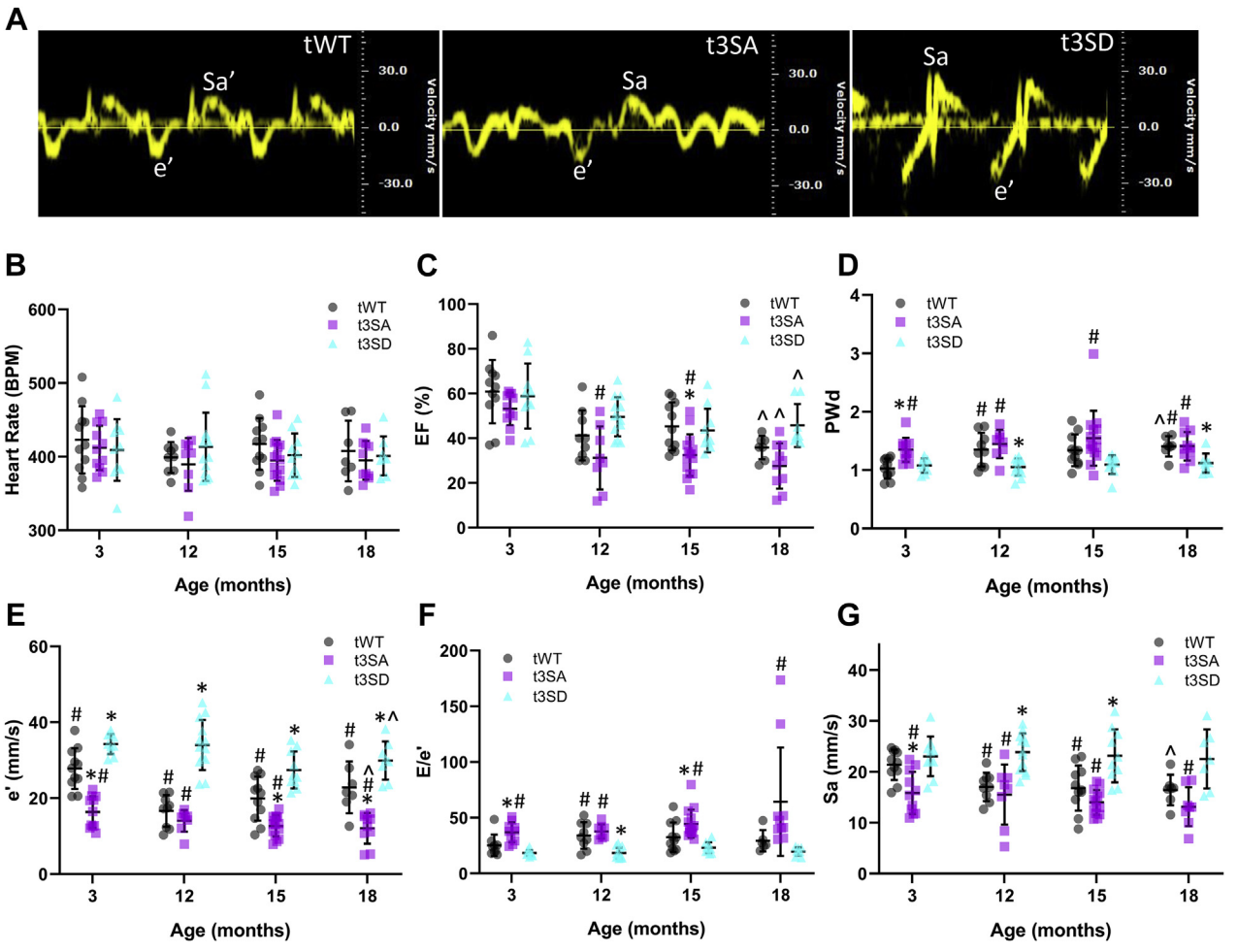

(A) Sample tissue Doppler traces showed that cMyBP-C(t3SD) myocardium relaxes at a much faster velocity (e′) during early diastole at 15 months of age. **(B)** All mice models showed similar heart rates. **(C)** cMyBP-C(t3SD) showed better preservation of ejection fraction (EF). **(D)** Only cMyBP-C(t3SD) showed preserved posterior wall thickness during diastole (PWd) with aging. **(E)** cMyBP-C(t3SD) exhibited faster peak myocardial relaxation velocity (e′) that was preserved with aging. **(F)** cMyBP-C(t3SD) showed preservation of E/e′ with aging. **(G)** Peak myocardial contraction velocity (Sa) was preserved in cMyBP-C(t3SD) hearts. cMyBP-C(tWT), 3 months: n = 11; 12 months: n = 9; 15 months: n = 11; and 18 months: n = 7. cMyBP-C(t3SA), 3 months: n = 11; 12 months: n = 8; 15 months: n = 15; and 18 months: n = 10. cMyBP-C(t3SD), 3 months: n = 10; 12 months: n = 13; 15 months: n = 10; and 18 months: n = 8. Data are presented as dot plots with mean ± SD. *p < 0.05 versus tWT. #p < 0.05 versus t3SD. ^p < 0.05 for 3 months versus 18 months within the same strain according to an independent Student's *t*-test. All comparisons between 3 strains were analyzed with an analysis of variance post hoc Tukey method. Multiple comparisons between all time points within the same strain were not performed.

body weight and heart weight/tibia length ratios, suggesting hypertrophy (Figures 2D and 2E). Meanwhile, cMyBP-C(t3SD) and cMyBP-C(tWT) mice exhibited similar lung/body, heart/body, and heart/tibia length ratios. Combination of increased lung/body weight ratio, heart/body weight ratio, worst cardiac dysfunction according to echocardiography (described in the following section), and lowest survival represented signs of HF in the hypophosphorylated cMyBP-C(t3SA) mice.

cMyBP-C(t3SD) PHOSPHORYLATED-MIMETIC AGED MICE SHOWED BETTER PRESERVATION OF DIASTOLIC AND SYSTOLIC FUNCTIONS BY ECHOCARDIOGRAPHY. Echocardiography was used to study in vivo cardiac structure and function starting at 3 months until 18 months of age (Figures 3A to 3G, Supplemental Figure 1, Supplemental Table 1). All mice had similar heart rates (Figure 3B). cMyBP-C(t3SA) hearts showed hypertrophy as seen by increased LV posterior wall thickness at diastole starting at 3 months of age.

FIGURE 4 cMyBP-C Phosphorylated Mimetic (t3SD) Preserves Myocardial Relaxation With Aging Independently of $[Ca^{2+}]_i$ Kinetics

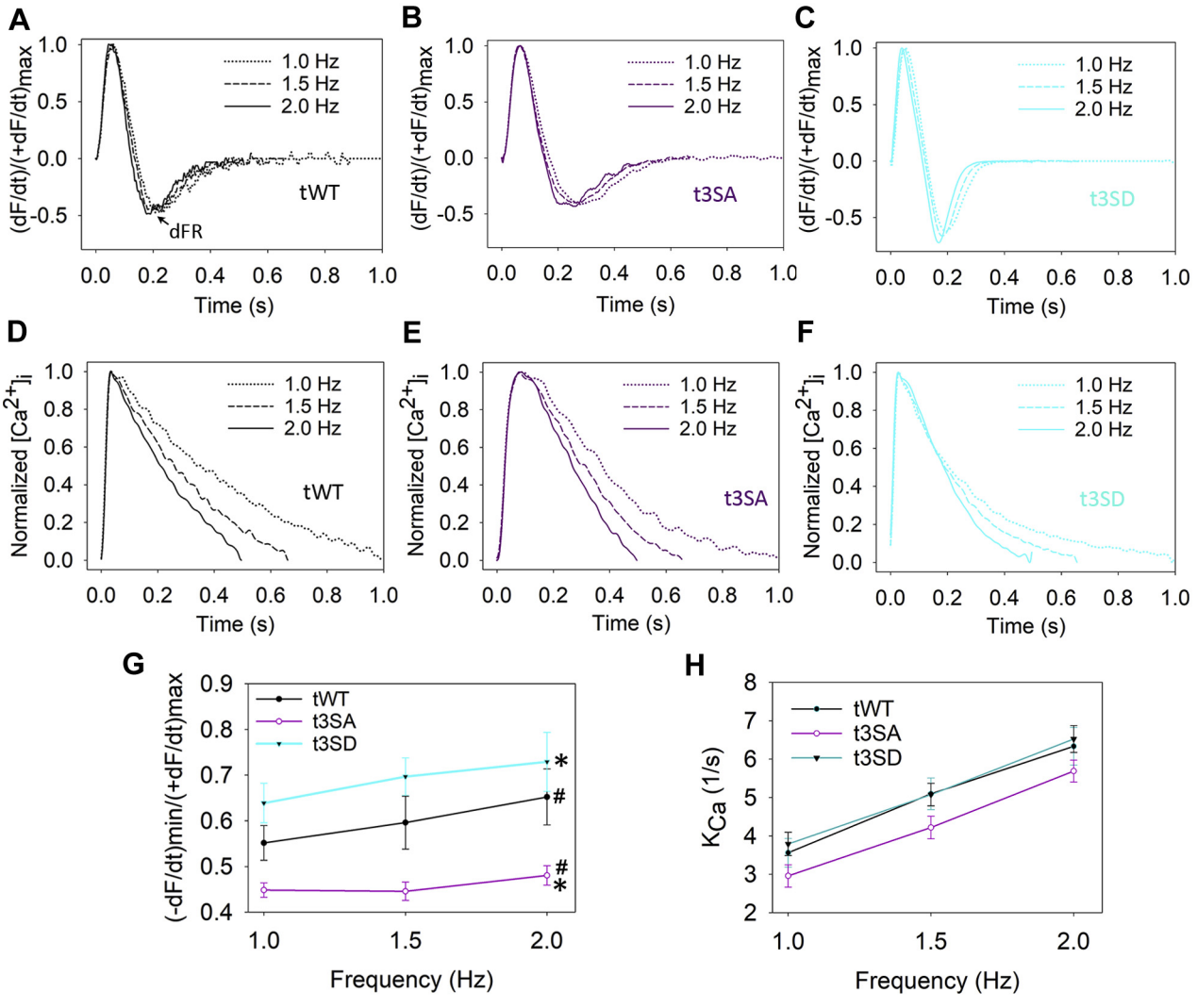

Force and intracellular calcium $[Ca^{2+}]_i$ were simultaneously measured on intact papillary muscles from mouse models 12 to 15 months old with increasing pacing frequency (1.0 to 2.0 Hz). **(A to C)** cMyBP-C(t3SD) showed greater acceleration of relaxation in response to increased pacing frequency with increasing magnitude of dFR, dFR = $[(-dF/dt)_{min}/(+dF/dt)_{max}]$. **(D to F)** Normalized $[Ca^{2+}]_i$ traces show that increasing pacing frequency shortens $[Ca^{2+}]_i$ decay times in a similar manner for all models. **(G)** Increased pacing frequency causes faster relaxation in the cMyBP-C(t3SD) aged model. **(H)** Increasing pacing frequency causes similar increases in the $[Ca^{2+}]_i$ decay rate constant (k_{Ca}) in all mouse models. Repeated measure analysis of variance with intergroup comparison was used to identify significant differences in responses to increasing pacing frequency on intact papillary muscles among the 3 strains.

cMyBP-C(tWT) increased LV wall thickness at diastole with aging (**Figure 3D**, Supplemental Table 1). Meanwhile, cMyBP-C(t3SD) hearts maintained the same LV wall thickness throughout life. cMyBP-C(t3SD) hearts maintained an ejection fraction (EF) >45% (**Figure 3C**) and exhibited enhanced contractility with faster tissue Doppler of myocardial contraction velocity during systole (Sa) throughout aging (**Figures 3A and 3G**) compared with other strains. cMyBP-C(tWT) showed deterioration of EF from 61% at 3 months to 36% at 18 months. In addition, cMyBP-C(t3SD) hearts showed enhanced myocardial relaxation velocity during early diastole (e′) at 3, 12, 15, and 18 months and smallest blood flow Doppler (E) to e′ ratio (E/e′) at 12 months

(Figures 3A, 3E, and 3F). Meanwhile, cMyBP-C(t3SA) hearts exhibited impaired relaxation throughout aging as shown by the slowest e′ and the biggest E/e′ ratio.

Using a separate independent Student's *t*-test comparing only 2 mouse models at 18 months, cMyBP-C(t3SD) hearts exhibited lower E/e′ than cMyBP-C(tWT) hearts: the E/e′ values consisted of cMyBP-C(t3SD) 19.8 ± 1.3 (n = 8) and cMyBP-C(tWT) 29.4 ± 3.9 (n = 6); p = 0.021 (Supplemental Figure 1). The large differences between the models, resulting in a large ensemble variance with relatively small numbers at 18 months, likely made the ANOVA-Tukey method unable to detect differences among the 3 models despite dot plots indicating differences of E/e′ and significant differences according to the Student's *t*-test (Figure 3F). Thus, phosphorylation mimetic cMyBP-C(t3SD) hearts exhibited better preservation of systolic function (greater EF and Sa) and diastolic function (faster e′ and smaller E/e′) with aging. In contrast, hypophosphorylated mimetic cMyBP-C(t3SA) hearts, as previously shown (6), first present as HF with preserved EF (with predominant diastolic dysfunction, EF >50%, and evidence of pulmonary edema) and then deteriorate into HF with reduced EF (EF <30%) and diastolic dysfunction. Similar to cMyBP-C(t3SA), cMyBP-C(tWT) hearts exhibit hypertrophy, deterioration of systolic function, and deterioration of diastolic function with aging.

INTACT PAPILLARY MUSCLES FROM PHOSPHORYLATED MIMETIC AGED MICE MODEL SHOWED FASTEST RATES OF RELAXATION. We simultaneously measured force and intracellular calcium concentration $[Ca^{2+}]_i$ on intact papillary muscles from aged mice hearts to differentiate contributions of $[Ca^{2+}]_i$ handling versus cross-bridge detachment rates. For this purpose, intact papillary muscles from mice 12 to 15 months old were isolated. Increasing pacing frequency was used to mimic increasing heart rate during exercise stress. We used the peak relaxation rate $(-dF/dt)_{min}$ to peak force generation rate $(+dF/dt)_{max}$ ratio, dFR = $[(-dF/dt)_{min}/(+dF/dt)_{max}]$, to compare lusitropy of intact papillary muscles and to assess the effect of increasing pacing frequency in all 3 models. Normalization of $(-dF/dt)_{min}$ to $(+dF/dt)_{max}$ adjusted for an increasing peak rate of relaxation as a result of increasing rate of peak contraction; therefore, enhancement of relaxation beyond what is expected due to increased contractility will manifest as increasing dFR because $(-dF/dt)_{min}$ increase > $(+dF/dt)_{max}$ increase. Increased pacing frequency accelerated relaxation, which is manifested as increasing dFR in cMyBP-C(tWT) and cMyBP-C(t3SD) but not in cMyBP-C(t3SA) (Figures 4A to 4C). cMyBP-C(t3SD) and cMyBP-C(tWT) consistently exhibited greater dFR, meaning enhanced relaxation (Figure 4G). Furthermore, cMyBP-C(t3SD) showed the highest dFR, suggesting that persistent cMyBP-C phosphorylation provided the best rates of relaxation. A single negative exponential was used to calculate the $[Ca^{2+}]_i$ decay rate constant; all models showed similar rate constant values (Figures 4D to 4F and 4H). Therefore, enhanced relaxation in cMyBP-C(t3SD) is attributed to cross-bridge cycling but not differences in $[Ca^{2+}]_i$ handling.

cMyBP-C PHOSPHORYLATION DECREASES WITH AGING IN THE cMyBP-C(tWT) STRAIN. Phosphorylated-protein staining showed that middle-aged (9 months) and old-age (18 to 24 months) cMyBP-C(tWT) mice exhibited reduced total cMyBP-C phosphorylation compared with the younger counterpart cMyBP-C(tWT) (2 to 6 months) (Figures 5A to 5C). Moreover, Western blot analyses revealed that aging significantly decreased cMyBP-C phosphorylation at S273 and S282 (Figures 5D and 5E) but not at S302 (Figure 5F). Pearson correlation analyses consisting of mice at their age according to month (2, 4 ,6, 9, 18, and 24) and site-specific phosphorylation level revealed that cMyBP-C phosphorylation at S273-P and S282-P decreased in a linear fashion with age (Figure 6). Thus, decreased levels of cMyBP-C phosphorylation in the aging hearts should be considered as an important contributor to aging-related cardiac dysfunction.

cMyBP-C PHOSPHORYLATION MUTATIONS ALTERED PHOSPHORYLATION OF OTHER MYOFILAMENT PROTEINS WITH AGING. At a young age, all 3 strains showed similar tropomyosin, cardiac troponin I (cTnI), regulated myosin light chain, and titin phosphorylation levels (Supplemental Figure 2). These findings are similar to those from our previous study (6). Moreover, we detected no differences in cTnI, regulated myosin light chain, or titin phosphorylation among the 3 strains at old age. However, both cMyBP-C(t3SA) and cMyBP-C(t3SD) strains exhibited different cardiac troponin T and tropomyosin phosphorylation levels than cMyBP-C(tWT) with aging. Unlike the other 2 strains, aging changed tropomyosin and regulated myosin light chain phosphorylation in the cMyBP-C(t3SA) model. The cMyBP-C(t3SA) model exhibited both reduced contractility (15) and impaired relaxation (6,15) at 3 months of age; therefore, these myofilament phosphorylation differences are likely caused by long-term response to inherent myofilament dysfunction.

AGED MICE SHOWED SIMILAR LEVELS OF FIBROSIS. HOP levels were determined to assess

FIGURE 5 cMyBP-C Phosphorylation Decreases With Aging in cMyBP-C(tWT) Strain

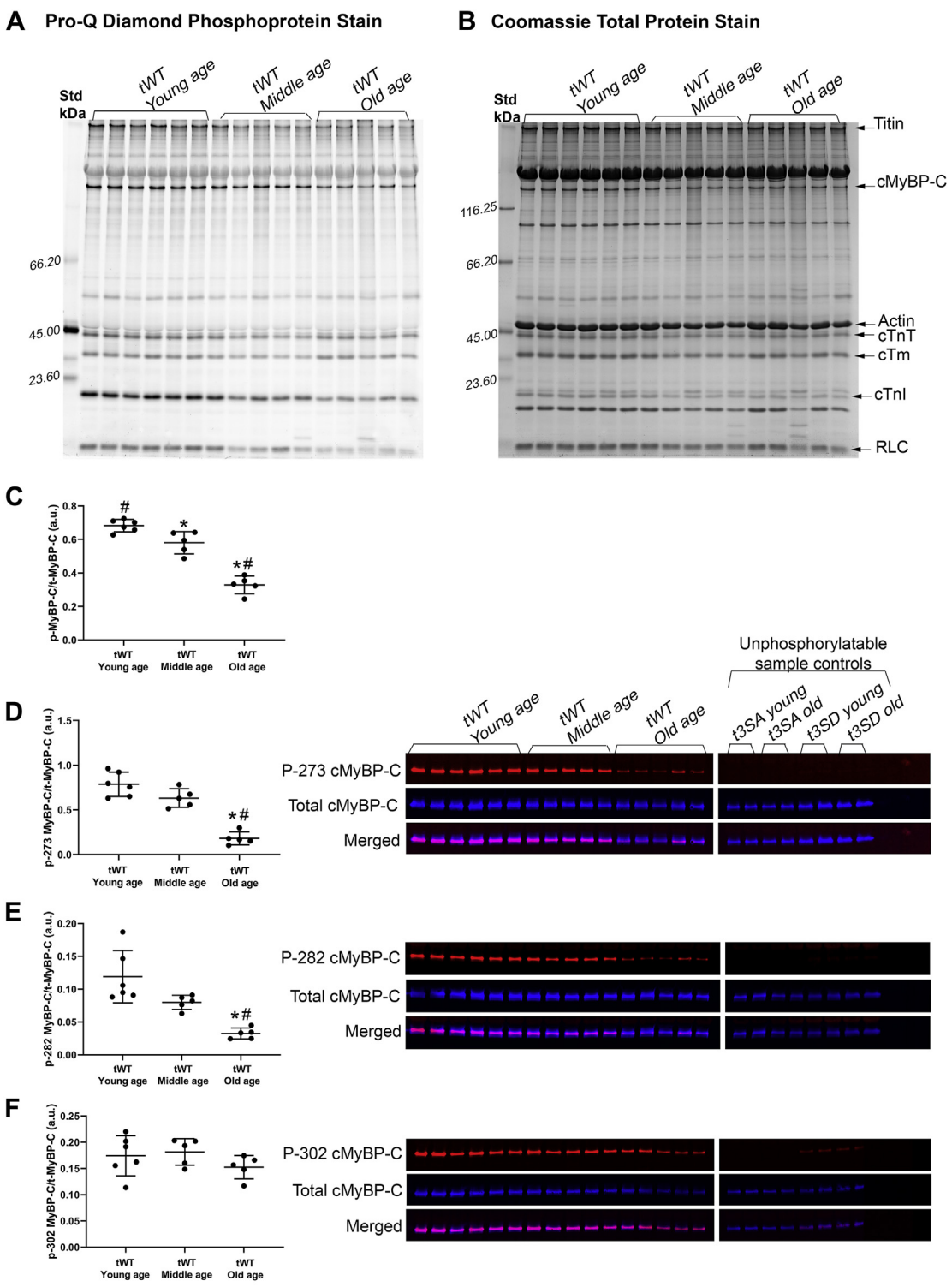

*p < 0.05 vs. tWT-Young age, #p<0.05 vs. tWT-Middle age. tWT-Young age n=6, tWT-Middle age n=5, tWT-Old age n=5. Unphosphorylatable sample controls: n=2

Continued on the next page

whether differences in tissue fibrosis in the aged mice contributed to the observed differences in diastolic function, systolic function, and hypertrophy. The HOP assay is a method that directly quantifies tissue collagen. We found no differences in the amount of HOP content between the 3 mouse models in the aged hearts or young hearts (Figure 7). Because there were no significant differences in the amount of HOP between mouse models, we could not attribute heart function and structure differences among the 3 models to differences in fibrosis. However, the cMyBP-C(t3SA) aged hearts exhibited significantly higher HOP content than their younger counterparts. This finding could explain the more severe decline in systolic and diastolic functions observed in the cMyBP-C(t3SA) model with aging.

WT MICE EXHIBITED SIMILAR DECLINE IN CARDIAC FUNCTION WITH AGING. We aged the same strain of WT (SVE-129) mice as our mouse models to serve as a control to check if the cMyBP-C$^{(-/-)}$ background unduly influenced the observed aging outcomes. The WT mice age categories were young (3.0 ± 0.01 months; $n = 6$) and aged (23.9 ± 0.04 months, $n = 6$). Aging decreased EF from $82.04 \pm 2.03\%$ to $52.62 \pm 5.08\%$ ($p < 0.001$); increased E/e′ from 16.54 ± 1.56 to 40.62 ± 5.33 ($p = 0.001$); and induced hypertrophy in which LV posterior wall thickness at diastole increased from 0.84 ± 0.08 mm to 1.22 ± 0.06 mm ($p = 0.004$). Thus, aging caused systolic dysfunction, diastolic dysfunction, and hypertrophy in WT mice in a fashion similar to our cMyBP-C models (Supplemental Table 2).

DISCUSSION

MAINTAINING cMyBP-C PHOSPHORYLATION MITIGATED AGE-RELATED DEVELOPMENT OF CARDIAC DYSFUNCTION. We aged mouse models of cMyBP-C phosphorylation mimetic cMyBP-C(t3SD), cMyBP-C phosphorylation-deficient cMyBP-C(t3SA), and wild-type cMyBP-C(tWT) to test the hypothesis that cMyBP-C phosphorylation can resist age-related development of cardiac dysfunction. Echocardiographic studies revealed that the phosphorylation mimetic cMyBP-C(t3SD) exhibited better preservation of systolic function, diastolic function, and structure with aging. Importantly, phosphorylation mimetic cMyBP-C(t3SD) mice also exhibited superior survival with aging. Conversely, control cMyBP-C(tWT) mice showed decreasing cMyBP-C phosphorylation along with deterioration of cardiac structure and function with aging. As expected with slowed contractility and impaired relaxation starting at a young age (6,15), the negative control cMyBP-C(t3SA) fared the worst. With aging and de-phosphorylation of cMyBP-C, the cMyBP-C(tWT) cardiac structure, cardiac function, and mortality drifted toward the cMyBP-C(t3SA) phenotype. This drift provided further evidence that cMyBP-C de-phosphorylation contributed to age-related development of cardiac dysfunction. Thus, better preservation of cardiac function and improved survival of cMyBP-C(t3SD) showed that maintaining cMyBP-C phosphorylation mitigated age-related development of cardiac dysfunction.

PRESERVATION OF CARDIAC FUNCTION DURING AGING WITH cMyBP-C PHOSPHORYLATION IS SUPPORTED BY EXISTING STUDIES. Previously, a protein phosphatase-1 overexpression mouse model exhibited decreased cMyBP-C phosphorylation along with development of cardiac dysfunction with aging (20). Also, decreased norepinephrine-induced cMyBP-C phosphorylation was found in aged rat hearts (21). Older hypertensive dogs with heart failure with preserved ejection fraction (HFpEF) exhibited hypophosphorylation of cMyBP-C (22). These studies showed that aging

FIGURE 5 Continued

The cMyBP-C(tWT) age groups consist of: young, 2 to 6 months; middle age, 9 months; and old, 18 to 24 months. cMyBP-C(t3SA) and cMyBP-C(t3SD) strains, which have the known protein kinase-A sites mutated to nonphosphorylatable residues, served as negative controls. cMyBP-C(t3SA) age groups consist of: young, 6 months; and old, 23 months. cMyBP-C(t3SD) age groups consist of: young, 3 to 4 months; old, 20 and 24 months. **(A)** Pro-Q diamond staining of phosphorylated proteins on sodium dodecyl sulfate-polyacrylamide **gel** electrophoresis that were extracted from cMyBP-C(tWT) hearts. **(B)** Subsequent Coomassie staining of total protein on the same gel from **A**. **(C)** Quantification of cMyBP-C phosphorylation from Pro-Q-stained and Coomassie-stained gels showed that cMyBP-C phosphorylation decreased with age. **(D) (Left)** quantification of cMyBP-C S273 phosphorylation over total cMyBP-C from cMyBP-C(tWT) strain showed that aging decreased cMyBP-C phosphorylation at S273. **(Middle)** Western blotting detected cMyBP-C phosphorylation at S273 in the cMyBP-C(tWT) strain. **(Right)** Western blotting showed that mutations from serine to alanine (t3SA) or aspartic acid (t3SD) residues removed the proper epitope for S273 phospho-specific antibody recognition. **(E) (Left)** quantification of cMyBP-C S282 phosphorylation over the total cMyBP-C from cMyBP-C(tWT) strain showed that S282 phosphorylation decreased with aging. **(Middle)** Western blotting detected cMyBP-C phosphorylation at S282 in the cMyBP-C(tWT) strain. **(Right)** Western blotting showed that S to A or S to D mutations removed the proper epitope for S282 phospho-specific antibody recognition. **(F) (Left)** quantification of cMyBP-C S302 phosphorylation over total cMyBP-C from cMyBP-C(tWT) strain showed no significant changes at S302 with aging. **(Middle)** Western blotting detected cMyBP-C phosphorylation at S302 in the cMyBP-C(tWT) strain. **(Right) Western blotting** showed that S to A and S to D mutations removed the proper epitope for S302 phospho-specific antibody recognition. Comparisons between the 3 age-groups were analyzed with an analysis of variance post hoc Tukey method. Data are presented as dot plots with mean ± SD.

FIGURE 6 **cMyBP-C Phosphorylation at S273 and S282 Decrease Linearly With Age**

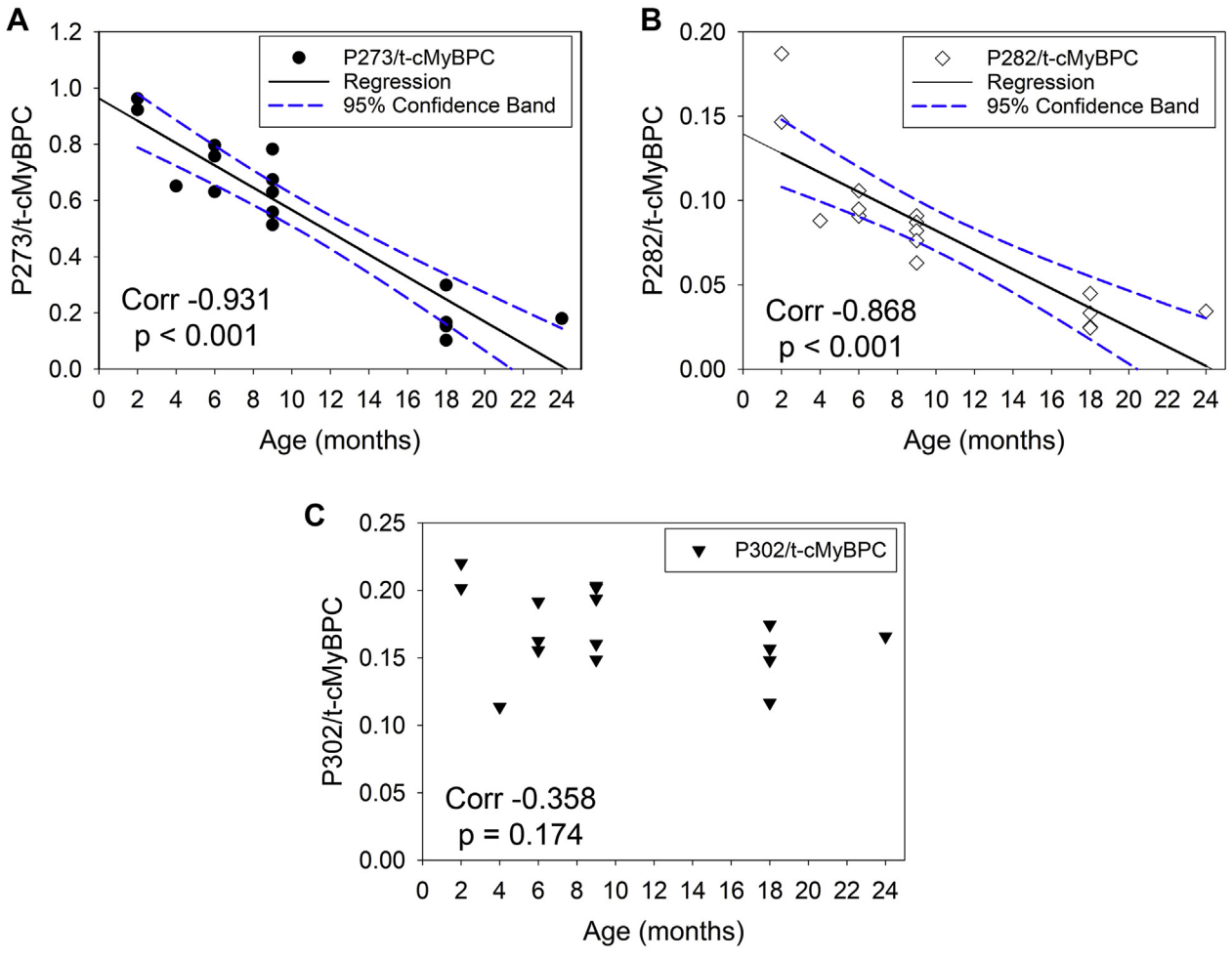

Pearson correlation analyses and linear regressions were performed on cMyBP-C site-specific phosphorylation Western blots for cMyBP-C(tWT) with n = 16 at ages 2 to 24 months. Correlation coefficient (-1 to 1) quantifies strength of correlation, in which strong is: |coefficient| >0.5; moderate is: 0.3 ≤ |coefficient| <0.5; and weak is: 0.1 ≤ |coefficient| <0.3. **(A)** Analyses showed that cMyBP-C S273 phosphorylation decreased in a strongly correlated linear fashion with increasing age. **(B)** Analyses showed that cMyBP-C S282 phosphorylation decreased in a strongly correlated linear fashion with increasing age. **(C)** cMyBP-C S302 phosphorylation did not correlate with increasing age.

correlated with decreasing cMyBP-C phosphorylation and worsening cardiac dysfunction. Exercise improved diastolic function in elderly patients with HF and reduced EF (23). Exercise also increased the phosphorylation of cMyBP-C and other contractile proteins in mice (24). Thus, it is plausible that exercise increased cMyBP-C phosphorylation to improve diastolic function. Previously, we found that phosphorylated cMyBP-C increased the force of contraction by accelerating cross-bridge cycling and, by inference, increasing the number of cross-bridges that generate force in response to dobutamine and increased pacing frequency (5). We also showed that acceleration of cross-bridge cycling by phosphorylated cMyBP-C also resulted in enhanced relaxation (6).

In the present study, cTnI phosphorylation did not differ among the 3 mouse models; therefore, differences in function cannot be attributed to differences in cTnI phosphorylation (Supplemental Figure 2). Furthermore, similar levels of cTnI phosphorylation suggest that protein kinase-A and protein kinase-C overall activity remained similar among the 3 mouse models. We acknowledge that cardiac troponin T and tropomyosin phosphorylation levels changed in the cMyBP-C(t3SA) and cMyBP-C(t3SD) models with aging; however, we believe that these changes are compensatory mechanisms

FIGURE 7 Quantification of Fibrosis

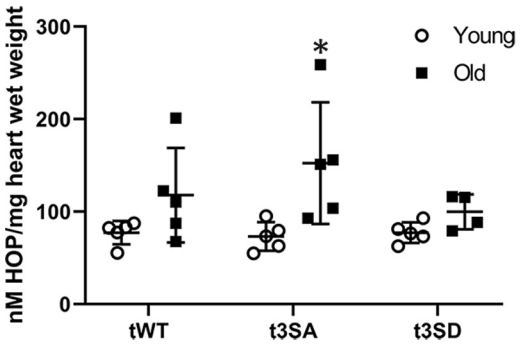

t3SD-old n=4, all others n=5. *p < 0.05 vs. young.

Hydroxyproline (HOP) assay was used to quantify collagen content as a measure of fibrosis. Age groups were as follows: cMyBP-C(tWT)—young, 5 to 6 months; old, 19 to 20 months; cMyBP-C(t3SA)—young, 6 months; old, 19 to 20 months; and cMyBP-C(t3SD)—young, 4 months; old, 22 months. HOP levels were similar among all 3 mouse models in both the young and old age groups. However, aging increased HOP levels significantly only in the cMyBP-C(t3SA) hearts. Two-way analysis of variance was used to detect differences between groups. Data are presented as dot plots with mean ± SD.

driven by our mutations. Taken together, these results support the idea that cMyBP-C phosphorylation is a key player in the regulation and maintenance of normal systolic and diastolic functions in the elderly. Our study made a novel translation step of this concept by showing that maintaining cMyBP-C phosphorylation preserved cardiac function and improved survival with aging.

PRESERVATION OF MYOCARDIAL CONTRACTION AND RELAXATION IN AGED cMyBP-C PHOSPHORYLATION MIMETIC MICE IS LIKELY DUE TO FASTER CROSS-BRIDGE CYCLING. With echocardiography, the aged WT equivalent cMyBP-C(tWT) and the hypophosphorylated cMyBP-C(t3SA) model showed slower peak myocardial contraction velocities (Sa) than the phosphorylation mimetic cMyBP-C(t3SD) model (Figure 3G). Peak myocardial relaxation velocities (e′) were slower in the cMyBP-C(t3SA) and cMyBP-C(tWT) hearts, reflecting impaired relaxation (Figure 3E) (25). E/e′ ratios were higher in the cMyBP-C(t3SA) and cMyBP-C(tWT) models, suggesting compromised diastolic function (Figure 3F) (25). Also, cMyBP-C(t3SA) and cMyBP-C(tWT) exhibited increased posterior ventricular wall thickness with aging (Figure 3D), reminiscent of human LV hypertrophy with HFpEF (26,27). Similar to our findings, echocardiographic data from humans showed that age is associated with increased LV mass (increasing wall thickness) and EF abnormalities (28,29). Meanwhile, cMyBP-C(t3SD) maintains a constant wall thickness with aging (Figure 3D), suggesting that cMyBP-C phosphorylation prevented remodeling. Better preservation of systolic and diastolic functions may have decreased the drive for hypertrophic response. cMyBP-C(t3SD) showed higher systolic blood pressure within the normal range, providing additional evidence of better cardiac function. Similar collagen content of aged hearts as estimated by using HOP among the 3 mouse models found that functional differences could not be attributed to fibrosis (Figure 7). We then performed simultaneous force and $[Ca^{2+}]_i$ on intact papillary muscles from aged mice to elucidate the underlying mechanism for better preservation of cardiac function in cMyBP-C(t3SD). Papillary muscles isolated from cMyBP-C(t3SD) aged mice showed enhanced lusitropy in response to increased pacing frequencies in the absence of differences in $[Ca^{2+}]_i$ decay rates (Figure 4). These results suggest that phosphorylation of cMyBP-C accelerated the rates of cross-bridge cycling, independently of $[Ca^{2+}]_i$ variations, as the underlying mechanism of an enhanced diastolic function in cMyBP-C(t3SD) aged mice.

MOUSE STRAIN BACKGROUND AND UNINTENDED GENETIC CHANGES MOST LIKELY DID NOT CAUSE THE OBSERVED DIFFERENCE. The cMyBP-C$^{(-/-)}$ background has cardiac function that is very different from WT (15). Furthermore, multiple genetic manipulation used to produce our models (6,15) could have introduced unintended gene changes. Background differences and potential unintended genetic changes could have strongly influenced the outcomes. We aged a group of WT mice in the same SVE-129 strain as our models. We found that aging WT mice developed cardiac dysfunctions (i.e., decreased EF, increased E/e′, developed hypertrophy) in a similar fashion as cMyBP-C(tWT) mouse. Thus, aging-related development of cardiac dysfunction within our models could not be attributed to cMyBP-C$^{(-/-)}$ background or unintended genetic changes.

POTENTIAL STUDY LIMITATIONS. The 3 mouse models have incomplete expression of cMyBP-C of 72% to 84% in the myofilaments (6). However, because cMyBP-C expression levels among the models are similar, the functional differences are most likely caused by the phosphorylation status. Our study did not address murine cMyBP-C phosphorylation sites outside of S273, S282, and S302

(12,30); therefore, the phosphorylation of more recently identified sites can either enhance or oppose the effects seen in this study. To address these limitations, we will develop a new knock-in mouse model with 100% expression level and better coverage of additional important phosphorylation sites.

We fully understand that many changes occur with the aging heart (31,32). In this context, cMyBP-C phosphorylation is only 1 of the contributors. Aging will decrease phosphorylation of other myofilament proteins. Furthermore, our cMyBP-C phosphorylation mimetic mutations altered phosphorylation of other myofilament proteins differently with aging. These alterations are likely to be compensatory responses to functional differences caused by our mutations. Thus, a follow-on study of mimicing isolated cMyBP-C phosphorylation with cardiac trophic adeno-associated virus expression of cMyBP-C phosphorylation mimetics after aging is needed to better define specificity of the cMyBP-C phosphorylation effect. We also understand that our results need to be confirmed in a large animal model that better resembles humans.

CONCLUSIONS

We aged mouse models to test the hypothesis that cMyBP-C phosphorylation can mitigate age-related development of cardiac dysfunction. Superior survival, better preservation of cardiac function, and preservation of structure in the cMyBP-C(t3SD) model combined to show that maintaining cMyBP-C phosphorylation mitigated age-related development of cardiac dysfunction. Intact papillary muscle experiments showed that faster cross-bridge detachment rates independent of calcium re-uptake are a contributing mechanism.

ACKNOWLEDGMENTS The authors thank Piyali Chartejee, PhD (Baylor Scott and White Health), for the blood pressure measurements on mice, and Ashley Batra, BS, (University of Illinois at Chicago) for sample preparation.

ADDRESS FOR CORRESPONDENCE: Dr. Paola C. Rosas, Department of Physiology and Biophysics, Center for Cardiovascular Research, University of Illinois, 835 South Wolcott Avenue, Chicago, Illinois 60612. E-mail: prosas@uic.edu. OR Dr. Carl W. Tong, Department of Medical Physiology, Texas A&M University, 8447 Riverside Parkway, RM 2346 MREB-2, Bryan, Texas 77807. E-mail: CTong@tamu.edu.

PERSPECTIVES

COMPETENCY IN MEDICAL KNOWLEDGE: This paper helps readers to improve or maintain medical knowledge core competency by describing the novel mechanism by which cMyBP-C phosphorylation increases cross-bridge cycling rates to improve cardiac function; consequently, this mechanism holds potential to treat age-related heart failure.

TRANSLATIONAL OUTLOOK: Our study showed that maintaining cMyBP-C phosphorylation can preserve systolic and diastolic functions, resulting in improved survival with aging. This is a novel finding. The underlying mechanism of increasing cross-bridge detachment rates can be a central method that compensates for multiple upstream causes (e.g., aging, hypertension, diabetes). Furthermore, cMyBP-C phosphorylation also holds potential to treat HFpEF by improving diastolic function. Our results place phosphorylation of cMyBP-C at the beginning of translation toward treatment. Thus, the logical next steps include developing methods to increase cMyBP-C phosphorylation in vivo and verifying our mouse model findings in a large animal model. These methods include inhibiting phosphatase that dephosphorylates cMyBP-C and by using adeno-associated virus to perform gene therapy of expressing phosphorylated cMyBP-C mimetic. The use of 3-dimensional human pluripotent stem cell–derived engineered heart tissue could be used to verify cMyBP-C phosphorylation effects on representative human cardiac tissue. Completion of these next steps will ready the cMyBP-C phosphorylation mechanism for human clinical trial. With an aging population and lack of treatment for HFpEF, this mechanism needs to be translated to a new treatment.

REFERENCES

1. Benjamin EJ, Muntner P, Alonso A, et al. Heart disease and stroke statistics—2019 update: a report from the American Heart Association. Circulation 2019;139:e56–66.

2. Heidenreich PA, Albert NM, Allen LA, et al. Forecasting the impact of heart failure in the United States: a policy statement from the American Heart Association. Circ Heart Fail 2013;6:606–19.

3. Borlaug BA, Redfield MM, Melenovsky V, et al. Longitudinal changes in left ventricular stiffness: a community-based study. Circ Heart Fail 2013;6:944–52.

4. Blecker S, Paul M, Taksler G, Ogedegbe G, Katz S. Heart failure-associated hospitalizations in the United States. J Am Coll Cardiol 2013;61:1259–67.

5. Tong CW, Wu X, Liu Y, et al. Phosphoregulation of cardiac inotropy via myosin binding protein-C during increased pacing frequency or beta1-adrenergic stimulation. Circ Heart Fail 2015;8:595–604.

6. Rosas PC, Liu Y, Abdalla MI, et al. Phosphorylation of cardiac myosin-binding protein-C is a critical mediator of diastolic function. Circ Heart Fail 2015;8:582–94.

7. Donaldson C, Palmer BM, Zile M, et al. Myosin cross-bridge dynamics in patients with

hypertension and concentric left ventricular remodeling. Circ Heart Fail 2012;5:803–11.

8. El-Armouche A, Boknik P, Eschenhagen T, et al. Molecular determinants of altered Ca2+ handling in human chronic atrial fibrillation. Circulation 2006;114:670–80.

9. Copeland O, Sadayappan S, Messer AE, Steinen GJ, van der Velden J, Marston SB. Analysis of cardiac myosin binding protein-C phosphorylation in human heart muscle. J Mol Cell Cardiol 2010;49:1003–11.

10. van Dijk SJ, Paalberends ER, Najafi A, et al. Contractile dysfunction irrespective of the mutant protein in human hypertrophic cardiomyopathy with normal systolic function. Circ Heart Fail 2012;5:36–46.

11. Jacques AM, Copeland O, Messer AE, et al. Myosin binding protein C phosphorylation in normal, hypertrophic and failing human heart muscle. J Mol Cell Cardiol 2008;45:209–16.

12. Kooij V, Holewinski RJ, Murphy AM, Van Eyk JE. Characterization of the cardiac myosin binding protein-C phosphoproteome in healthy and failing human hearts. J Mol Cell Cardiol 2013;60:116–20.

13. Harris SP, Lyons RG, Bezold KL. In the thick of it: HCM-causing mutations in myosin binding proteins of the thick filament. Circ Res 2011;108:751–64.

14. Harris SP, Bartley CR, Hacker TA, et al. Hypertrophic cardiomyopathy in cardiac myosin binding protein-C knockout mice. Circ Res 2002;90:594–601.

15. Tong CW, Stelzer JE, Greaser ML, Powers PA, Moss RL. Acceleration of cross-bridge kinetics by protein kinase A phosphorylation of cardiac myosin binding protein C modulates cardiac function. Circ Res 2008;103:974–82.

16. Tong CW, Gaffin RD, Zawieja DC, Muthuchamy M. Roles of phosphorylation of myosin binding protein-C and troponin I in mouse cardiac muscle twitch dynamics. J Physiol 2004;558:927–41.

17. Solaro RJ, Pang DC, Briggs FN. The purification of cardiac myofibrils with Triton X-100. Biochim Biophys Acta 1971;245:259–62.

18. Pena JR, Szkudlarek AC, Warren CM, et al. Neonatal gene transfer of Serca2a delays onset of hypertrophic remodeling and improves function in familial hypertrophic cardiomyopathy. J Mol Cell Cardiol 2010;49:993–1002.

19. Whelton PK, Carey RM, Aronow WS, et al. 2017 ACC/AHA/AAPA/ABC/ACPM/AGS/APhA/ASH/ASPC/NMA/PCNA guideline for the prevention, detection, evaluation, and management of high blood pressure in adults: a report of the American College of Cardiology/American Heart Association Task Force on Clinical Practice Guidelines. J Am Coll Cardiol 2018;71:e127–248.

20. Florea S, Anjak A, Cai WF, et al. Constitutive phosphorylation of inhibitor-1 at Ser67 and Thr75 depresses calcium cycling in cardiomyocytes and leads to remodeling upon aging. Basic Res Cardiol 2012;107:279.

21. Sakai M, Danziger RS, Staddon JM, Lakatta EG, Hansford RG. Decrease with senescence in the norepinephrine-induced phosphorylation of myofilament proteins in isolated rat cardiac myocytes. J Mol Cell Cardiol 1989;21:1327–36.

22. Hamdani N, Bishu KG, von Frieling-Salewsky M, Redfield MM, Linke WA. Deranged myofilament phosphorylation and function in experimental heart failure with preserved ejection fraction. Cardiovasc Res 2013;97:464–71.

23. Sandri M, Kozarez I, Adams V, et al. Age-related effects of exercise training on diastolic function in heart failure with reduced ejection fraction: the Leipzig Exercise Intervention in Chronic Heart Failure and Aging (LEICA) Diastolic Dysfunction Study. Eur Heart J 2012;33:1758–68.

24. Davis RT 3rd, Simon JN, Utter M, et al. Knockout of p21-activated kinase-1 attenuates exercise-induced cardiac remodelling through altered calcineurin signalling. Cardiovasc Res 2015;108:335–47.

25. Nagueh SF, Smiseth OA, Appleton CP, et al. Recommendations for the evaluation of left ventricular diastolic function by echocardiography: an update from the American Society of Echocardiography and the European Association of Cardiovascular Imaging. J Am Soc Echocardiogr 2016;29:277–314.

26. Zile MR, Gottdiener JS, Hetzel SJ, et al. Prevalence and significance of alterations in cardiac structure and function in patients with heart failure and a preserved ejection fraction. Circulation 2011;124:2491–501.

27. Mohammed SF, Hussain S, Mirzoyev SA, Edwards WD, Maleszewski JJ, Redfield MM. Coronary microvascular rarefaction and myocardial fibrosis in heart failure with preserved ejection fraction. Circulation 2015;131:550–9.

28. Gardin JM, Siscovick D, Anton-Culver H, et al. Sex, age, and disease affect echocardiographic left ventricular mass and systolic function in the free-living elderly. The Cardiovascular Health Study. Circulation 1995;91:1739–48.

29. Lakatta EG, Levy D. Arterial and cardiac aging: major shareholders in cardiovascular disease enterprises: part II: the aging heart in health: links to heart disease. Circulation 2003;107:346–54.

30. Jia W, Shaffer JF, Harris SP, Leary JA. Identification of novel protein kinase A phosphorylation sites in the M-domain of human and murine cardiac myosin binding protein-C using mass spectrometry analysis. J Proteome Res 2010;9:1843–53.

31. Lakatta EG. Arterial and cardiac aging: major shareholders in cardiovascular disease enterprises: part III: cellular and molecular clues to heart and arterial aging. Circulation 2003;107:490–7.

32. Paneni F, Diaz Canestro C, Libby P, Luscher TF, Camici GG. The aging cardiovascular system: understanding it at the cellular and clinical levels. J Am Coll Cardiol 2017;69:1952–67.

KEY WORDS aging, cardiac myosin binding protein-C, dyastolic dysfunction, heart failure, phosphorylation

APPENDIX For supplemental tables and figures, please see the online version of this paper.

JACC: BASIC TO TRANSLATIONAL SCIENCE VOL. 4, NO. 7, 2019

PRECLINICAL RESEARCH

Unraveling the Molecular Mechanism of Action of Empagliflozin in Heart Failure With Reduced Ejection Fraction With or Without Diabetes

Oriol Iborra-Egea, MSc,[a,b,c] Evelyn Santiago-Vacas, MD,[a,b,c] Salva R. Yurista, MD,[d] Josep Lupón, MD, PhD,[a,b,c] Milton Packer, MD,[e] Stephane Heymans, MD,[f] Faiez Zannad, MD,[g] Javed Butler, MD,[h] Domingo Pascual-Figal, MD,[i] Antonio Lax, PhD,[i] Julio Núñez, MD, PhD,[j] Rudolf A. de Boer, MD, PhD,[d] Antoni Bayés-Genís, MD, PhD[a,b,c]

VISUAL ABSTRACT

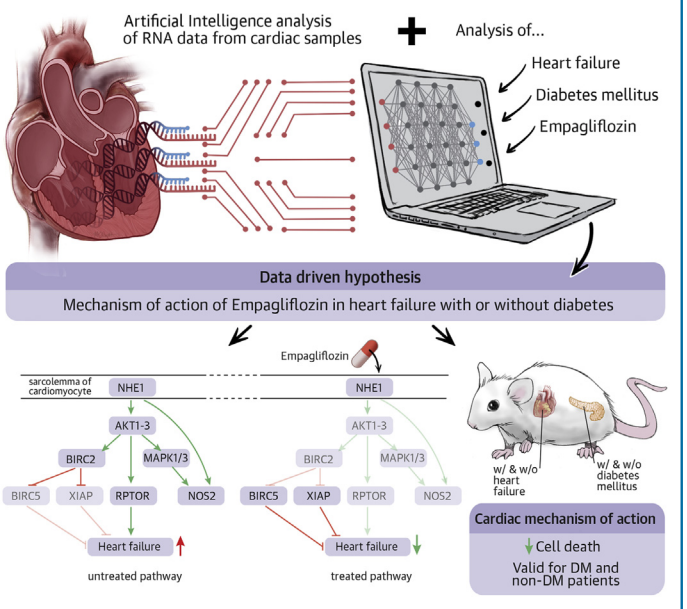

Iborra-Egea, O. et al. J Am Coll Cardiol Basic Trans Science. 2019;4(7):831–40.

HIGHLIGHTS

- **Using artificial intelligence, followed by in vivo validation, this study identified the key cardiac mechanism of action of empagliflozin in heart failure in patients with or without diabetes mellitus.**
- **The most robust mechanism of action involved the NHE-1 co-transporter with 94.7% accuracy.**
- **NHE-1 blockade by empagliflozin administration in rats restored the antiapoptotic activity of XIAP and BIRC5.**
- **The beneficial reduction in cardiomyocyte cell death after empagliflozin treatment is independent of the presence of diabetes mellitus.**
- **Empagliflozin could emerge as a new treatment for heart failure patients regardless of their glycemic status.**

ISSN 2452-302X https://doi.org/10.1016/j.jacbts.2019.07.010

JACC: BASIC TO TRANSLATIONAL SCIENCE VOL. 4, NO. 7, 2019
NOVEMBER 2019:831–40

ABBREVIATIONS AND ACRONYMS

ANN = artificial neural network

DM = diabetes mellitus

HF = heart failure

HFrEF = HF with reduced ejection fraction

MI-HF = post-infarct heart failure

NHE = sodium-hydrogen exchanger

RNAseq = RNA sequencing

SGLT2i = sodium-glucose co-transporter 2 inhibitor

SUMMARY

The mechanism of action of empagliflozin in heart failure with reduced ejection fraction (HFrEF) was deciphered using deep learning in silico analyses together with in vivo validation. The most robust mechanism of action involved the sodium-hydrogen exchanger (NHE)-1 co-transporter with 94.7% accuracy, which was similar for diabetics and nondiabetics. Notably, direct NHE1 blockade by empagliflozin ameliorated cardiomyocyte cell death by restoring expression of X-linked inhibitor of apoptosis (XIAP) and baculoviral IAP repeat-containing protein 5 (BIRC5). These results were independent of diabetes mellitus comorbidity, suggesting that empagliflozin may emerge as a new treatment in HFrEF. (J Am Coll Cardiol Basic Trans Science 2019;4:831–40)

Both type 1 and 2 diabetes mellitus (DM) are major risk factors for the development of cardiovascular diseases, increasing morbidity and mortality (1). For decades, long-term clinical studies of DM have shown value in reducing glycemic levels without a substantial effect on cardiovascular outcomes and certainly no benefit in heart failure (HF) (2). The advent of a new class of agents, sodium-glucose co-transporter 2 inhibitors (SGLT2i), heralds a new era and may represent a turning point. Indeed, in the EMPA-REG OUTCOME (Empagliflozin Cardiovascular Outcome Event Trial in Type 2 Diabetes Mellitus Patients) study, patients with type 2 DM who were at high risk for cardiovascular events and who received empagliflozin in addition to standard care showed lower rates of the following compared to those who received placebo: a) primary composite cardiovascular outcome (death from cardiovascular causes, nonfatal myocardial infarction (MI) or nonfatal stroke); and b) HF-related hospitalizations; death from cardiovascular causes; and death from any cause (3). Similar results with other SGLT2is have been reported subsequently by both randomized clinical trials and observational studies (4,5).

SEE PAGE 841

SGLT2 receptors are located in the proximal renal tubule and are responsible for 90% of glucose reabsorption into the bloodstream. Inhibition of SGLT2 receptors causes glucosuria and reduces glycemic levels (6). However, control of glycemic levels in response to SGLTis alone seems insufficient to explain the reported cardiovascular benefits. In fact, the EMPA-TROPISM (Are the "Cardiac Benefits" of Empagliflozin Independent of Its Hypoglycemic Activity? [ATRU-4]) trial (NCT03485222) is an ongoing trial that aims to elucidate whether the benefits obtained in the EMPA-REG OUTCOME trial were mediated, at least in part, by a glucose-

From the [a]Heart Institute, Hospital Universitari Germans Trias i Pujol, Badalona, Spain; [b]Department of Medicine, Universitat Autònoma de Barcelona, Barcelona, Spain; [c]Centro de Investigación Biomédica en Red Enfermedades Cardiovascualres (CIBERCV), Madrid, Spain; [d]Department of Cardiology, University Medical Center Groningen, University of Groningen, Groningen, the Netherlands; [e]Baylor Heart and Vascular Institute, Baylor University Medical Center, Dallas, Texas; [f]Maastricht University Medical Centre, Cardiovascular Research Institute Maastricht, Maastricht, the Netherlands; [g]Centre d'Investigation Clinique Plurithématique 1433, INSERM U1116, Université de Lorraine, Centre Hospitalier Régional et Universitaire de Nancy, French Clinical Research Infrastructure Network (F-CRIN), Investigation Network Initiative-Cardiovascular and Renal Clinical Trialists (INI-CRCT), Nancy, France; [h]Department of Medicine, University of Mississippi, Jackson, Mississippi; [i]Domingo Hospital Universitario Virgen de la Arrixaca, University of Murcia, Centro Nacional de Investigaciones Cardiovasculares, CIBERCV, Murcia, Spain; and the [j]Cardiology Department, Hospital Clínico Universitario, CIBERCV, INCLIVA, Universitat de València, València, Spain. Dr. Yurista is supported by Indonesia Endowment Fund for Education grant LPDP 20150722083422. Dr. Packer is a consultant with Abbvie, Amgen, Akcea, AstraZeneca, Bayer, Boehringer Ingelheim, Cardiorentis, Gilead, Johnson and Johnson, NovoNordisk, Pfizer, Sanofi, Synthetic Biologics, Relypsa, and Theravance. Dr. Zannad is a member of the Boehringer Ingelheim steering committee; and is a consultant for AstraZeneca, Mundipharma, NovoNordisk, and Merck. Dr. Butler is a consultant with Abbott, Adrenomed, Amgen, Array, AstraZeneca, Bayer, BerlinCures, Boehringer Ingelheim, Bristol-Myers Squibb, Cardiocell, Corvidia, CVRx, G3 Pharmaceutical, Innolife, Janssen, Lantheus, LinaNova, Luitpold, Medscape, Medtronic, Merck, Novartis, NovoNordisk, Relypsa, Roche, Sanofi, StealthPeptide, SC Pharma, V-Wave Limited, Vifor, and ZS Pharma. Dr. Núñez has received speaker fees from Boehringer Ingelheim. Dr. De Boer holds equity in scPharmaceuticals; has received honoraria from Mandalmed, Novartis, and Servier; and has received research support through his institution from AstraZeneca, Abbott, Bristol-Myers Squibb, Novartis, Roche, Trevena, and ThermoFisher GmbH. All other authors have reported that they have no relationships relevant to the contents of this paper to disclose. The authors attest they are in compliance with human studies committees and animal welfare regulations of the authors' institutions and Food and Drug Administration guidelines, including patient consent where appropriate. For more information, visit the *JACC: Basic to Translational Science* author instructions page.

Manuscript received May 20, 2019; revised manuscript received July 9, 2019, accepted July 9, 2019.

FIGURE 1 Flow Chart Depicting the Machine Learning Approach Used in This Study

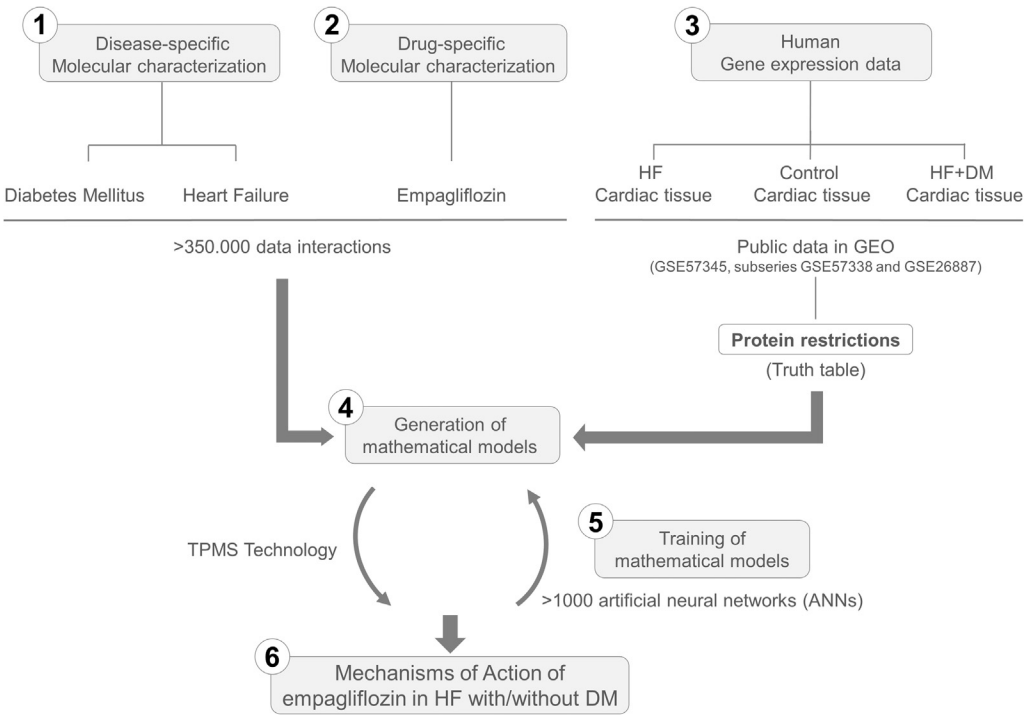

See Supplemental Video 1. DM = diabetes mellitus; GEO = Gene Expression Omnibus database; HF = heart failure; TPMS = therapeutic performance mapping system.

independent mechanism (7). A recent viewpoint postulated the hypothesis that the benefit of SGLTis in HF may be mediated by the sodium-hydrogen exchanger (NHE) rather than by the effect on glucose reabsorption (8); however, a comprehensive mechanistic explanation of the extra-renal cardioprotective SGLTi effects remains elusive.

Machine learning is an interdisciplinary field based on computational and mathematical models that aims to unravel key interactions within complex biological networks (9). It is particularly well suited for investigating the mechanisms underlying the effects of drugs, including SGLTis. Accordingly, this study used deep learning analysis to investigate what the key cardiac mechanisms may be by which empagliflozin exerts its effects in HF and reduced ejection fraction (HFrEF) in patients with or without DM (Figure 1). Machine learning-driven pathways were validated in an in vivo empagliflozin-treated post-infarct HF (MI-HF) rat model.

METHODS

MACHINE LEARNING IN SILICO ANALYSES. Molecular characterization of HF and DM pathology and drug treatments. First, extensive and careful review of full-length articles in PubMed was conducted to obtain information about HF and DM. When specific molecular information describing the condition was found, the articles were thoroughly reviewed to identify protein/gene candidates to feed the mathematical models. When the evidence of the implication of a candidate in the condition was judged inconsistent enough to be assigned as an effector, an additional search was performed specifically for the candidate, including all the protein names according to UniProtKB (UniProt Knowledge Base, Geneva, Switzerland). No text-mining tools were used to avoid intrinsic technical biases, and only English-language articles were included, which accounted for more than 6,509 items reviewed.

Moreover, empagliflozin pharmacological data and molecular relationships described for HF and DM were extracted by integrating massive, publicly available databases such as Drugbank, Reactome, MINT, and BioGrid. All this information accounted for more than 350,000 interactions (Figure 1). Briefly, by integrating published data, a set of molecular profiles characterizing HF and DM were defined, which were used to build the protein network and the mathematical model.

Compilation of transcriptomic data. Next, an RNA sequencing (RNAseq) dataset (public data available in Gene Expression Omnibus [GEO], accession GSE57345 and subseries GSE57338 and GSE26887) of myocardial tissue data derived from HFrEF patients with (10) or without DM (11) was thoroughly analyzed to model the molecular effects of empagliflozin in each scenario. Gene information was mapped one-to-one to proteins for introduction into the protein network, which included 280 proteins of interest (Supplemental Table 1). This collection of experimental pathophysiological signals was used as a list of principles, termed a "truth table," which apply to a specific condition (i.e., some proteins are overexpressed only in HF patients with DM) (**Figure 1**) and allow delineation of the molecular behavior of each situation (12).

Generation of mathematical models. Finally, artificial neural network (ANN)-based analyses were used to identify the most relevant pathophysiological processes implicated in HF and DM. To train the mathematical models, this large collection of well-established pathophysiological signals and clinical information relevant to the pathologies under study was reviewed. The molecular description of these input-output signals was investigated as follows:

1. Model inputs, for example, information about drugs, pathologies, and protein/gene relationships provided by public databases to assess inhibition or activation of 1 or more nodes of the protein network (their targets) triggering a perturbation through the system.
2. Model outputs, for example, experimental RNAseq data (upregulated or downregulated genes/proteins) and clinical information.
3. Hidden mechanisms of action (MoAs). Using the model's input and output data, mathematical algorithms were generated to trace a change or perturbation from 1 to another, elucidating the MoAs that would explain this connection.

The models are then able to weight the relative value of each protein (node) relationship.

Therapeutic performance mapping system technology. Details about how therapeutic performance mapping system (TPMS) (Anaxomics, Barcelona, Spain) machine learning analyses work have been reported previously (13). Briefly, TPMS incorporated massive amounts of biological information relevant to both the disease(s) and the drug under study, drawn from curated reports and from public and private databases (**Figure 1**). Next, TPMS adopted the gene expression dynamics stored in the truth table as a reference framework to shape all the biological information. Finally, TPMS generated mathematical models to form complex relationships between datasets or to find patterns in the data (14,15). The system built an ANN, which was trained with 1,000 iterations. During this process, the models generated different MoAs, which progressively increased in accuracy by correcting itself with already-known clinical and biomedical information, and cross-validation with independent sets of data (**Figure 1**, Supplemental Video 1). Eventually, the algorithms reached a plateau which yielded the final accuracy performance (maximum = 100%) to explain the MoA of empagliflozin in HFrEF (**Figure 1**).

POST-INFARCT HEART FAILURE IN VIVO RAT MODEL. A total of 74 rats were used for the experimental validations. The nondiabetic, post-infarct heart failure (MI-HF) study was performed in male Sprague Dawley rats weighing 250 to 280 g, obtained from Envigo (Huntingdon, United Kingdom). The diabetic MI-HF study (MI-HF-DM) was performed in male Wistar rats weighing 160 to 200 g obtained from Envigo (Barcelona, Spain).

Animals were housed in groups under standard laboratory condition of 12L:12D cycle. All animals received food and water ad libitum during the study (n = 7 to 12 per group). All experiments were conducted in accordance with U.S. National Institutes of Health Guide for the Care and Use of Laboratory Animals and were approved by the Committee for Animal Experiments.

Induction of diabetes mellitus in Wistar rats. DM was induced by a single intraperitoneal injection of streptozotocin (STZ) (50 mg/kg of body weight) (catalog number S0130, Sigma-Aldrich, St. Louis, Missouri) dissolved in freshly prepared 0.1 M citrate buffer (pH 4.5, catalog number 71402, Sigma-Aldrich). In order to prevent hypoglycemia in the first 24 h after STZ injection, rats were allowed to have free access to water with 5% glucose. Three days after STZ injection, rats with blood glucose levels >300 mg/dl were considered diabetic.

Induction of myocardial infarction. Initially, animals were anesthetized using intraperitoneal ketamine (75 mg/kg) and medetomidine (0.5 mg/kg) before being intubated and ventilated under 2% isoflurane anesthesia. Rats were randomly allocated to MI or sham surgery, as described elsewhere (16). Left-sided thoracotomy was performed by a small incision between the third and fourth intercostal spaces. The pericardial sac surrounding the heart was cut open, but the heart was not exteriorized. The infarction was performed by ligation of the left anterior descending coronary artery. Visible blanching and cyanosis of the anterior wall of the left ventricle and swelling of the left atrium were taken as

indicative of successful ligation. Sham surgery was identical to the MI surgery but without any ligation.

Experimental design and study protocol. Two weeks after surgery, nondiabetic rats (n = 40) were fed either with standard rat chow (product R/M-H V1534-70, Ssniff-Spezialdiäten, Soest, Germany) or chow containing empagliflozin (product BI 10773, in concentration of 200 mg/kg per day to reach a dose of 30 mg/kg per day), and this was continued for a period of 12 weeks. After 12 weeks, hearts were rapidly excised, weighed, and processed for further analysis. Animals were divided into 4 groups: group 1 (n = 7) were sham rats receiving vehicle treatment; group 2 (n = 10) were sham rats receiving empagliflozin; group 3 (n = 12) were infarcted rats receiving vehicle treatment; group 4 were infarcted rats receiving empagliflozin.

Immediately after diabetes was induced, the Wistar rats were treated with empagliflozin (10 mg/kg per day) (n = 34). This treatment was maintained for 4 weeks before MI was induced and was continued for a period of 4 weeks after MI. After 4 weeks, hearts were rapidly excised, weighed, and processed for further analysis. Animals were divided into 4 groups: group 1 (n = 8) were diabetic sham rats receiving phosphate buffered saline (PBS) for 56 days; group 2 (n = 9) were diabetic sham rats receiving empagliflozin for 56 days; group 3 (n = 7) were diabetic infarcted rats receiving PBS for 56 days; group 4 (n = 10) were diabetic infarcted rats receiving empagliflozin for 56 days.

Real time PCR. Total RNA from tissues were isolated by the TRIzol RNA isolation protocol. cDNA was further isolated from RNA by using the QuantiTecht RT kit (Qiagen, Venlo, the Netherlands), following the manufacturer's instructions. Quantitative real-time polymerase chain reaction (qRT-PCR) was performed in a model CFX384 real-time system (Bio-Rad, Philadelphia, Pennsylvania) using SYBR Green mix (Thermo Fisher Scientific, Waltham, Massachusetts) was used to determine the relative gene expression. Gene expression was determined by correcting the reference gene (*36B4*), and the calculated values are expressed relative to the control group per experiment. The primers for BIRC5 and XIAP qRT-PCR used in this study can be found in Supplemental Table 2.

DATA INTEGRATION AND STATISTICAL ANALYSIS. The RNAseq data were compiled and processed using the GEO2R tool, using the neqc method for normalization, allowing identification of differential expression levels and calculation of fold changes. The p values obtained for each RNA probe were adjusted using the Benjamini-Hochberg false discovery rate at a significance level of 0.01. Only genes with an adjusted p value of <0.01 and log fold changes of >0.25 were considered. In the in vivo analysis, gene expression was determined by correcting the reference gene (*36B4*), and the calculated values were expressed relative to the control group per experiment. The $2\text{-}\Delta\Delta_{CT}$ method for comparing relative expression results between treatments in real-time PCR was applied. To compare normally distributed parameters, one-way analysis of variance (ANOVA) followed by Tukey post hoc test was used. When data were not normally distributed, a nonparametric Kruskal-Wallis test followed by a Mann-Whitney *U* test with correction for multiple comparisons was used. To compare empagliflozin with vehicle treatment, an independent *t*-test or a Mann-Whitney *U* test was used where appropriate. Two-sided test results yielding a p value of <0.05 were considered statistically significant. SPSS statistics (version 23.0, IBM, Armonk, New York) for Windows (Microsoft, Redmond, Washington) was used to perform all statistical analysis.

TABLE 1 Mechanisms Involved in Heart Failure and Associated Conditions Considered in the Mechanistic Study

Pathology	Pathological Mechanisms	Proteins Implicated*
Heart failure		**106**
	Heart hypertrophy	33
	Cardiomyocyte cell death	47
	Inefficient myocardial fuel metabolism	7
	Oxidative stress	8
	Inflammation	11
Obesity		**140**
	Hyperphagia and dysregulated appetite	135
	White adipose tissue formation	5
Hypertension		**42**
	Retention of sodium	42
Hyperuricemia		**16**
	Decreased renal excretion of uric acid	16

Values are n. **Bold** numbers indicate the total number of proteins implicated in the general condition, later dissected by more specific motives. *Number of proteins implicated in each mechanism.

RESULTS

EMPAGLIFLOZIN ACTS UPON A SPECIFIC HF-RELATED PATHOLOGICAL SIGNATURE. First, the protein signatures of HFrEF and empagliflozin were defined and an ANN analysis identified the processes most likely associated with the beneficial effects of empagliflozin observed in HFrEF (Supplemental Table 1). Obesity, hypertension, and hyperuricemia contributed the most to the HF pathological signature and encompassed the possible effects of empagliflozin, with 140, 42, and 16 proteins of interest, respectively. For each of these 3 disorders, a series of mechanisms and the involved proteins were

TABLE 2 Proteins Known to Be Modulated by Empagliflozin

Gene Name	Protein Name	Reference (PMID)
STAT3	Signal transducer and activator of transcription 3	29311992
NOS2	Nitric oxide synthase, inducible	29311992
IL6	Interleukin-6	29311992
BDH1	D-beta-hydroxybutyrate dehydrogenase, mitochondrial	27289126
IFNG	Interferon gamma	29311992
ALDH2	Aldehyde dehydrogenase, mitochondrial	29311992
GCG	Glucagon	26590679
INS	Insulin	27289126
ACE2	Angiotensin-converting enzyme 2	26880444
BDNF	Brain-derived neurotrophic factor	25344694
HDAC1	Histone deacetylase 1	27829948
HDAC2	Histone deacetylase 2	27829948
HDAC3	Histone deacetylase 3	27829948
HDAC8	Histone deacetylase 8	27829948

PMID = unique identifier number used in PubMed for each article.

established (Table 1). The efficacy analysis identified the 3 following complementary strategies: 1) Consider sodium/glucose cotransporter 2, Na(+)/glucose cotransporter 2 (SGLT2); 2) consider sodium/hydrogen exchangers 1 and 3 (NHE1 and NHE3); and 3) considering empagliflozin bioflags; those proteins known to be modulated by the drug (Table 2).

ANN EVALUATES THE RELATIONSHIPS AMONG PROTEIN SETS INSIDE THE NETWORK, PROVIDING A PREDICTIVE SCORE. Once the pathological signatures were identified, the possible relationships between empagliflozin and heart failure, including associated processes, were evaluated by ANN analyses. Thus, the study of the MoA of empagliflozin was focused on the following specific pathways (motives) of the diseases affected by the treatment:

1) None of the evaluated diseases and motives are strongly related to SGLT2 according to the established criterion ($p > 0.3$).
2) Considering NHE1 and NHE3 as effectors, 2 conditions appear to be highly related (>75%) to empagliflozin's complete target profile:
   Hypertension: retention of sodium is the main motive identified, with a predictive score of 80%.
   HF: heart hypertrophy and cardiomyocyte cell death are the main motives identified, with a predictive score of 75.6%.
3) Three conditions appear to be highly related (>75%) to empagliflozin's bioflags:
   Hyperuricemia: decreased renal excretion of uric acid is the motive most related to empagliflozin, with 77% of predictive score.
   Obesity: the most related motives are hyperphagia and dysregulated appetite and white adipose tissue formation.
   HF: the most related motives are energy-inefficient myocardial fuel metabolism, oxidative stress, and inflammation.

NHE1 IS RESPONSIBLE FOR THE CARDIAC EFFECTS OF EMPAGLIFLOZIN IN HFrEF WITH OR WITHOUT DM. By using the differentially expressed proteins found to be related to HF and the specific motives affected during the pharmacological treatment, the mathematical models determined the molecular mechanisms involved in the heart-focused beneficial effects of empagliflozin relative to heart failure in DM and non-DM patients.

The most robust MoA identified in this study involved the cardiac sodium/hydrogen exchanger 1 (NHE1) with 94.7% accuracy (Figure 2, Supplemental Table 3), which was similar for DM and non-DM patients, indicating a DM-independent mechanism (Table 3). This approach describes mainly the mitigation of cell death but also the prevention of heart hypertrophy and the improvement upon an inefficient myocardial fuel metabolism as the potential heart-mediated mechanisms by which empagliflozin may counteract heart failure.

Direct empagliflozin-driven NHE1 blockade ameliorates cardiomyocyte cell death. In this scenario, the amelioration of cardiomyocyte cell death was established as the main driver of empagliflozin beneficial effects in HFrEF. In the absence of empagliflozin, protein kinases B (AKTs; referred to as AKT1 to -3 in Figure 2) were identified as downstream effectors of NHE1 activation responsible for the induction of baculoviral IAP repeat-containing protein 2 (BIRC2), which in turn induced degradation of proteasome-mediated X-linked inhibitor of apoptosis (XIAP) and BIRC5 and prompted the progression of HFrEF. In empagliflozin-enriched models, by inhibiting NHE1, repressed AKT1-3 and BIRC2 allowed the expression of the antiapoptotic mediators XIAP and BIRC5, ultimately halting HFrEF progression.

To validate these data obtained in silico, mRNA levels of XIAP and BIRC5, as last effectors of the pathway, were examined in vivo in an empagliflozin-treated MI-HF rat model. Confirming in silico findings, gene expression of *XIAP* and *BIRC5* fell 45% and 36%, respectively, in vehicle-treated MI-HF animals compared to sham controls ($p < 0.01$ for both, respectively). Remarkably, empagliflozin-treated MI-HF animals without diabetes showed upregulation of *XIAP* and *BIRC5* mRNA expression similar to that in sham controls and significantly higher than vehicle-treated MI-HF counterparts ($p = 0.003$ and $p = 0.05$, respectively) (Figure 3). More importantly, these changes in gene expression occurred ubiquitously regardless of DM presence, further strengthening the

FIGURE 2 **NHE1-Identified Signaling Pathways in Cardiomyocytes in Heart Failure**

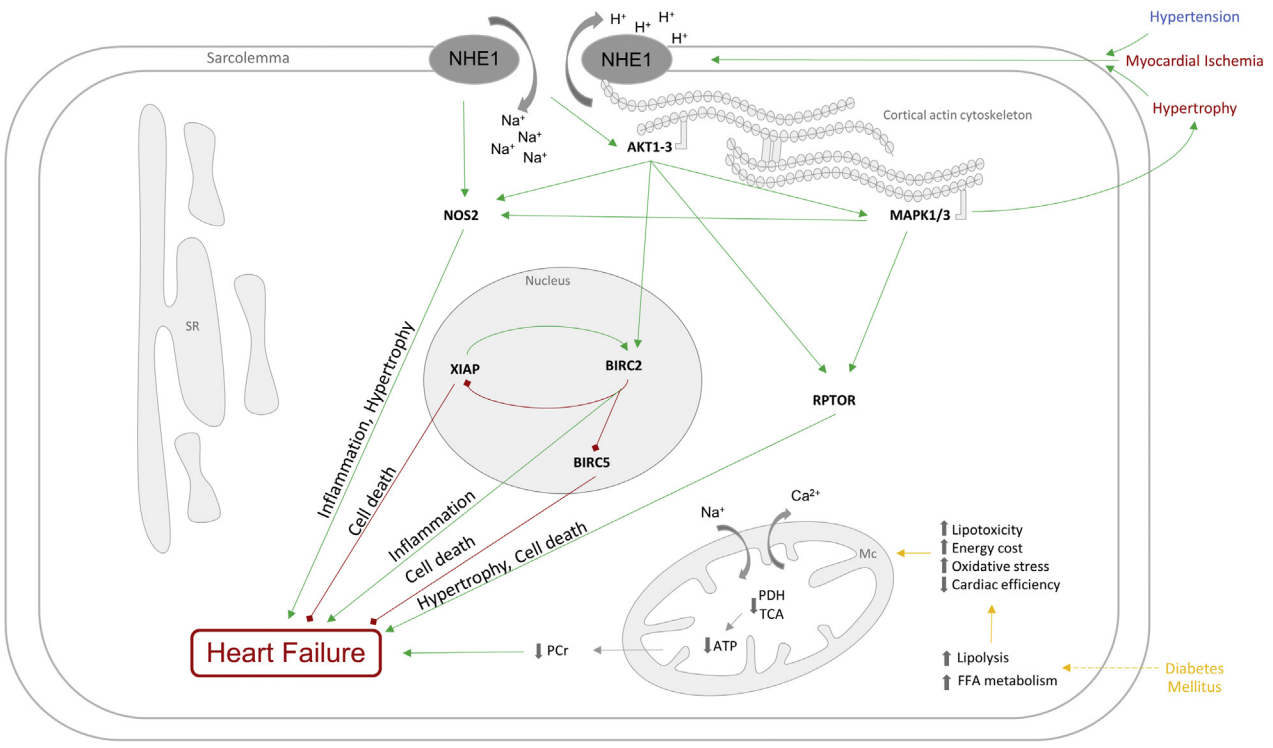

Each relationship represents a mechanism that may directly or indirectly (via downstream effectors) impact on HF, either through the activation (green arrows) or inhibition (red arrows) of downstream proteins. AKT1 = RAC-alpha serine/threonine-protein kinase 1; AKT2 = RAC-beta serine/threonine-protein kinase 2; AKT3 = RAC-gamma serine/threonine-protein kinase 3; ATP = adenosine triphosphate; BIRC2 = baculoviral IAP repeat-containing protein 2; BIRC5 = baculoviral IAP repeat-containing protein 5; LEP = leptin; MAPK1 = mitogen-activated protein kinase 1; MAPK3 = mitogen-activated protein kinase 3; MC = mitochondria.;NHE1 = sodium/hydrogen exchanger 1; NOS2 = nitric oxide synthase = inducible; PCr = phosphocreatine. ; PDH = pyruvate dehydrogenase; RPTOR = regulatory-associated protein of mTOR; SR = sarcoplasmic reticulum; TCA = tricarboxylic acid; XIAP = E3 ubiquitin-protein ligase XIAP.

in silico predictions. Indeed, empagliflozin-treated MI-HF-DM animals showed upregulation of *XIAP* and *BIRC5* mRNA expression similar to sham controls and significantly higher than vehicle-treated MI-HF-DM counterparts ($p = 0.01$ and $p = 0.005$, respectively) (**Figure 3**). Thus, empagliflozin-driven NHE1 inhibition ultimately counteracted reduced function of *XIAP* and *BIRC5*.

Additionally, the analyses also suggested that empagliflozin could further ameliorate cardiomyocyte cell death by inhibiting the AKT-dependent regulation- associated mTOR protein (RPTOR) and by down-regulation of nitric oxide synthase (NOS2)-inducible actions (**Figure 2**).

DISCUSSION

The EMPA-REG OUTCOME trial reported that empagliflozin exerted cardiovascular benefits which did not depend on its effects on blood glucose. This observation led to the hypothesis that empagliflozin exerted an effect on the myocardium independent of its inhibition of SGLT2 in the kidneys, thereby benefiting HF patients (6). The exact mechanism remains unknown, but it was postulated to have a direct action on the heart. The present study used artificial intelligence and machine learning, further validated in an in vivo animal model, to investigate whether empagliflozin could exert direct effects on the heart and whether these effects were the same for patients with and without DM.

This study has 2 main findings. First, these results validate the fact that empagliflozin interacts with the cardiac Na^+/H^+ exchanger NHE1 directly and identifies a mechanistic pathway acting primarily by reducing cardiomyocyte cell death, the main effector of its cardioprotective effects. Indeed, the activity of cardiac NHE1 seems to be increased in HFrEF patients, and previous data in experimental models (17–21) showed that NHE1 inhibition attenuated cardiomyocyte injury, remodeling, systolic dysfunction, and ultimately HF. Second, these data suggest that

TABLE 3 Mathematical Models Generated in This Study*

Mathematical Models	Stimulus	Response	Restrictions
HF with DM	Cardiac NHE1	Cardiomyocyte cell death Hypertrophy Inflammation	Truth Table + GSE57345 subseries GSE57338 dataset
HF without DM	Cardiac NHE1	Cardiomyocyte cell death Hypertrophy Inflammation	Truth Table + GSE26887 dataset

*The stimulus, response, and restrictions included in each model are shown.

DM = diabetes mellitus; GSE designations = Gene Expression Omnibus accession and subseries; HF = heart failure; NHE1 = sodium-hydrogen exchanger-1.

the cardiac effects of empagliflozin are independent of the presence of DM.

Uthman et al. (22) reported that SGLT2i reduced cardiac cytosolic Na^+ and cytosolic Ca^{2+} concentrations by inhibiting NHE1 in mouse cardiomyocytes. Cardiac NHE1 activity and cytosolic Na^+ were measured in the presence of clinically relevant concentrations of empagliflozin (1 μmol/l), dapagliflozin (1 μmol/l), and canagliflozin (3 μmol/l). All 3 SGLT2is bound with high affinity to the extracellular Na+-binding site of NHE1 (23). Recently, Baartscheer et al. (23) proposed a possible relationship between empagliflozin and NHE1 inhibition in rats and rabbits. In their study, an increase in extracellular glucose produced an increase in cytosolic levels of Na^+ and Ca^{2+}, an effect that was inhibited by empagliflozin. The effects of empagliflozin were strongly reduced after cells were pre-treated with the NHE1 inhibitor cariporide. In addition, empagliflozin affected cytosolic Na^+ and NHE1 flux in the absence of extracellular glucose, which demonstrated its putative effects in normoglycemic conditions.

These mechanistic studies have the power to address specific mechanisms in detail, but the unravelling of the global molecular effects of empagliflozin in HFrEF with or without DM requires the integration of complex big data, best handled by artificial intelligence and deep learning analyses. Considering all possible empagliflozin-derived cardiac mechanisms, the present analysis pinpointed NHE1 modulation as the most likely effector of the beneficial effects. Moreover, amelioration of cardiomyocyte cell death was found to be the most important effect of empagliflozin in HF.

Most importantly, the algorithm predicted a modulation of AKTs resulting in an inability of BIRC2 to degrade the antiapoptotic factors XIAP and BIRC5. XIAP expression was found to be decreased in failing human hearts, suggesting that this potent inhibitor of apoptosis may play a key role in protecting the heart from cell damage (24,25). Using an adenoviral-associated vector, Piacentino et al. (24) increased XIAP expression in neonatal rat cardiomyocytes, which inhibited caspase-3/7 activity, showing a reduction of myocardial injury. Relative to BIRC5, Lee et al. (26) found that overexpression of this pathway may attenuate the progression of LV systolic dysfunction in doxorubicin-induced cardiomyopathy. Furthermore, Levkau et al. (27) showed that cardiac-specific deletion of BIRC5 pathway resulted in premature cardiac death caused by a dramatic reduction in total cardiomyocyte numbers. Again, using adenoviral vectors to restore this pathway (through restoration of survivin) expression in cardiomyocytes inhibited doxorubicin-induced apoptosis, induced DNA synthesis, and promoted cell cycle progression (27). Following this rationale and, to further confirm the present study's in silico data, mRNA levels of both *XIAP* and *BIRC5* were measured in an in vivo MI-HF rat model. In agreement with existing studies, both expression levels of XIAP and BIRC5 were substantially lower in vehicle-treated animals with dysfunctional myocardium. Remarkably, in the empagliflozin-treated groups, expression levels of both XIAP and BIRC5 returned to normal, thus they were able to exert their antiapoptotic effects.

The present study was designed to investigate whether the MoA of empagliflozin in HF in patients with DM was different from that in patients without DM. Surprisingly, the most robust MoA identified here was identical in both groups, suggesting that empagliflozin may have value in treating HFrEF patients regardless of their glycemic status, acting to ameliorate adverse cardiac remodeling. In other words, empagliflozin, currently indicated only for the treatment of DM, may eventually be repurposed to treat patients with HFrEF. Several ongoing randomized clinical trials are testing the value of SGLTi in HF patients (both with reduced and preserved ejection fraction) with and without DM.

The mathematical models reported here were robust, and each link described is validated in the existing research publications. However, there is an ongoing discussion about the mathematical algorithms used in artificial intelligence, often termed "black boxes," because sometimes it may not be easy to follow the determination of the output, no matter how good or reliable this may be. This study's analysis took a massive amount of collected information and analyzed it for hidden patterns in the data that would be otherwise inaccessible to human stand-alone analysis, to understand how the drug could lead to a specific clinical outcome. These algorithms are widely used in other fields, and the techniques are among the best understood and developed, with time-tested characteristics which ensure an accurate

FIGURE 3 mRNA Levels of Antiapoptotic Proteins XIAP and BIRC5 In Vivo

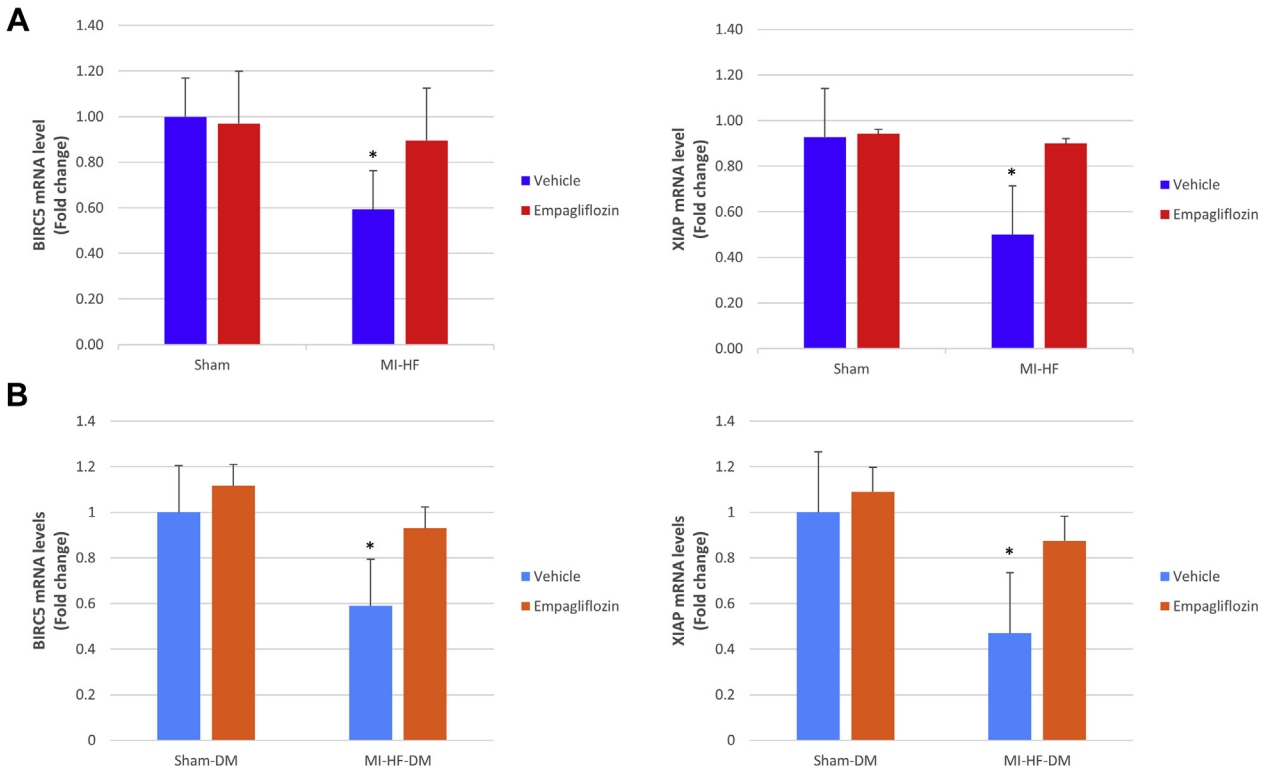

(A) Upper panels show nondiabetic rats. **(B) Lower panels** show diabetic rats. Data are mean ± SEM. *p < 0.05 vs. empagliflozin-MI and Vehicle-Sham. One-way ANOVA followed by Tukey post hoc test was used for normally distributed data, whereas Kruskal-Wallis followed by Mann-Whitney *U* test was used for non-normally distributed data. Abbreviations as in Figure 2.

application. A key differentiating feature of deep learning compared with other subtypes of artificial intelligence is the ability to operate without external guidance to draw conclusions. The neural network is not designed by humans, rather, the number of layers is determined by the data itself. Deep ANNs have used primarily supervised learning, with training from known patterns and labeled input data (truth table) to prospect reliable insights in large datasets. At the same time, all the outputs from the algorithm are restricted by the current scientific and medical standards. Taken together, all this limits human bias, and the algorithm can act as a hypothesis-free, independent data-driven analysis (28).

STUDY LIMITATIONS. However, this study has some limitations. The same premise that makes the models robust also serves as a potential downside. Specifically, the information considered here has already been described or uploaded in public repositories, which in turn limits the capacity of the analyses to incorporate data that have not been yet collected. The data reported here are valid for HFrEF and cannot be extrapolated to HF with preserved ejection fraction (HFpEF). Further research is required to better understand the MoA of empagliflozin in HFpEF.

CONCLUSIONS

Deep learning in silico analyses, together with in vivo validation, allowed deciphering the MoA of empagliflozin in HFrEF. Our data suggest that empagliflozin interacts and blocks the NHE1 co-transporter at the cardiomyocyte level, triggering a signaling cascade that halts detrimental cell death. These results were independent of DM comorbidity, suggesting that empagliflozin may emerge as a new treatment in HFrEF.

ACKNOWLEDGMENTS The authors thank Boehringer Ingelheim for providing animal control subjects and chow containing empagliflozin.

ADDRESS FOR CORRESPONDENCE: Dr. Antoni Bayes-Genis, Heart Institute, Hospital Universitari Germans Trias i Pujol, Carretera de Canyet s/n, 08916 Barcelona, Spain. E-mail: abayesgenis@gmail.com.

PERSPECTIVES

COMPETENCY IN MEDICAL KNOWLEDGE: The MoA of empagliflozin in HFrEF was deciphered by using deep learning in silico analyses together with in vivo validation. The most robust MoA involved the sodium-hydrogen exchanger-1 (NHE1), which was similar for diabetics and nondiabetics. Notably, direct NHE1 blockade by empagliflozin ameliorated cardiomyocyte cell death.

TRANSLATIONAL OUTLOOK: Empagliflozin, in addition to its renal effects, has direct cardioprotective effects at the cardiomyocyte level. These effects were independent of DM comorbidity, suggesting that empagliflozin may emerge as a new treatment in HFrEF.

REFERENCES

1. Emerging Risk Factors Collaboration, et al. Association of cardiometabolic multimorbidity with mortality. JAMA 2015;314:52–60.

2. Gerstein HC, Bosch J, Dagenais GR, et al., for the ORIGIN Trial Investigators. Basal insulin and cardiovascular and other outcomes in dysglycemia. N Engl J Med 2012;367:319–28.

3. Zinman B, Wanner C, Lachin JM, et al., for the EMPA-REG OUTCOME Investigators. empagliflozin, cardiovascular outcomes, and mortality in type 2 diabetes. N Engl J Med 2015;373:2117–28.

4. Wiviott SD, Raz I, Bonaca MP, et al., for the Sabatine MS; DECLARE-TIMI 58 Investigators. Dapagliflozin and cardiovascular outcomes in type 2 diabetes. N Engl J Med 2019;380:1881–2.

5. Cavender MA, Norhammar A, Birkeland KI, et al., for the CVD-REAL Investigators and Study Group. SGLT-2 inhibitors and cardiovascular risk: an analysis of CVD-REAL. J Am Coll Cardiol 2018;71:2497–506.

6. Zelniker TA, Braunwald E. Cardiac and renal effects of sodium-glucose co-transporter 2 inhibitors in diabetes: JACC State-of-the-Art Review. J Am Coll Cardiol 2018;72:1845–55.

7. Flores E, Santos-Gallego CG, Diaz-Mejia N, Badimon JJ. Do the SGLT-2 inhibitors offer more than hypoglycemic activity? Cardiovasc Drugs Ther 2018;32:213–22.

8. Packer M, Anker SD, Butler J, Filippatos G, Zannad F. Effects of sodium-glucose cotransporter 2 inhibitors for the treatment of patients with heart failure proposal of a novel mechanism of action. JAMA Cardiol 2017;2:1025–9.

9. Waltemath D, Wolkenhauer O. How modeling standards, software, and initiatives support reproducibility in systems biology and systems medicine. IEEE Trans Biomed Eng 2016;63:1999–2006.

10. Greco S, Fasanaro P, Castelvecchio S, et al. MicroRNA dysregulation in diabetic ischemic heart failure patients. Diabetes 2012;61:1633–41.

11. Liu Y, Morley M, Brandimarto J, et al., for the MAGNet consortium. RNA-Seq identifies novel myocardial gene expression signatures of heart failure. Genomics 2015;105:83–9.

12. Irving H. Peirce's truth-functional analysis and the origin of the truth table. History and Philosophy of Logic 2012;33:87–97.

13. Iborra-Egea O, Gálvez-Montón C, Roura S, et al. Mechanisms of action of sacubitril/valsartan on cardiac remodeling: a systems biology approach. NPJ Syst Biol Appl 2017;3:12.

14. Romeo-Guitart D, Forés J, Herrando-Grabulosa M, et al. Neuroprotective drug for nerve trauma revealed using artificial intelligence. Sci Rep 2018;8:1879.

15. Enderton H. A Mathematical Introduction to Logic. 2nd edition. New York: Harcourt Academic, 2001.

16. Yurista SR, Silljé HHW, Oberdorf-Maass SU, et al. Sodium-glucose co-transporter 2 inhibition with empagliflozin improves cardiac function in nondiabetic rats with left ventricular dysfunction after myocardial infarction. Eur J Heart Fail 2019;21:862–73.

17. Kilić A, Huang CX, Rajapurohitam V, Madwed JB, Karmazyn M. Early and transient sodium-hydrogen exchanger isoform 1 inhibition attenuates subsequent cardiac hypertrophy and heart failure following coronary artery ligation. J Pharmacol Exp Ther 2014;351:492–9.

18. Aker S, Snabaitis AK, Konietzka I, et al. Inhibition of the Na+/H+ exchanger attenuates the deterioration of ventricular function during pacing-induced heart failure in rabbits. Cardiovasc Res 2004;63:273–82.

19. Baartscheer A, Schumacher CA, van Borren MM, Belterman CN, Coronel R, Fiolet JW. Increased Na+/H+-exchange activity is the cause of increased [Na+]; and underlies disturbed calcium handling in the rabbit pressure and volume overload heart failure model. Cardiovasc Res 2003;57:1015–24.

20. Engelhardt S, Hein L, Keller U, Klämbt K, Lohse MJ. Inhibition of Na+/H+ exchange prevents hypertrophy, fibrosis, and heart failure in beta 1-adrenergic receptor transgenic mice. Circ Res 2002;90:814–9.

21. Kusumoto K, Haist JV, Karmazyn M. Na+/H+ exchange inhibition reduces hypertrophy and heart failure after myocardial infarction in rats. Am J Physiol Heart Circ Physiol 2001;280:H738–74.

22. Uthman L, Baartscheer A, Bleijlevens B, et al. Class effects of SGLT2 inhibitors in mouse cardiomyocytes and hearts: inhibition of Na+/H+ exchanger, lowering of cytosolic Na+ and vasodilation. Diabetologia 2018;61:722–6.

23. Baartscheer A, Schumacher CA, Wüst RC, et al. empagliflozin decreases myocardial cytoplasmic Na+ through inhibition of the cardiac Na+/H+ exchanger in rats and rabbits. Diabetologia 2017;60:568–73.

24. Piacentino V III, Milano CA, Bolanos M, et al. X-linked inhibitor of apoptosis protein-mediated attenuation of apoptosis, using a novel cardiac-enhanced adeno-associated viral vector. Hum Gene Ther 2012;23:635–46.

25. Haider N, Arbustini E, Gupta S, et al. Concurrent upregulation of endogenous proapoptotic and antiapoptotic factors in failing human hearts. Nat Clin Pract Cardiovasc Med 2009;6:250–61.

26. Lee PJ, Rudenko D, Kuliszewski MA, et al. Survivin gene therapy attenuates left ventricular systolic dysfunction in doxorubicin cardiomyopathy by reducing apoptosis and fibrosis. Cardiovasc Res 2014;101:423–33.

27. Levkau B, Schäfers M, Wohlschlaeger J, et al. Survivin determines cardiac function by controlling total cardiomyocyte number. Circulation 2008;117:1583–93.

28. Topol EJ. High-performance medicine: the convergence of human and artificial intelligence. Nat Med 2019;25:44–56.

KEY WORDS empagliflozin, heart failure, machine learning

APPENDIX For supplemental tables and a video, please see the online version of this paper.

JACC: BASIC TO TRANSLATIONAL SCIENCE VOL. 4, NO. 7, 2019

EDITORIAL COMMENT

Empagliflozin and HFrEF

Known and Possible Benefits of NHE1 Inhibition*

Seungho Jun, MD,[a] Miguel A. Aon, PhD,[b,c] Nazareno Paolocci, MD, PhD[a,d]

"Where is the wisdom we have lost in knowledge?
Where is the knowledge
we have lost in information?"
—T.S. Eliot (1)

Heart failure (HF) contributes to cardiovascular morbidity and mortality in patients with diabetes (DM). Mortality and hospitalization rate, the most meaningful endpoints for prognosis in patients with HF, have a higher incidence in subjects with concomitant DM compared with DM-free patients with HF. HF and DM are highly interweaved pathological conditions. In fact, hyperglycemia predicts the risk of developing HF, whereas the latter frequently occurs in patients with DM, worsening their prognosis. Moreover, a large cohort of patients with HF has manifest or latent DM. Finally, the presence of glucose intolerance in subjects with HF increases the risk of disease progression and death from a cardiovascular accident. Thus, similar mechanisms may underlie the onset or progression of HF and DM. By extension, targeting a biochemical/molecular alteration in one condition should also benefit the other. However, although long-term measures apt to reduce glycemic levels show benefit in patients with DM, these agents do not improve cardiovascular outcomes in those with HF. Thus, one could argue that correcting hyperglycemia per se would unlikely arrest the myriad of other triggers/cofactors and subsequent unrolling of countless signaling pathways/cascades of events ultimately conducive of chronic cardiac decompensation.

At the same time, however, this failure could be the impetus for a "we don't know what we don't know" type of approach. This strategy, consisting of searching for molecular/genome signatures that distinguish, for example, one disease from another, will allow us to gain information that can be used in turn to enhance protein networks and mathematical models; these networks and models will enable us to unravel functionally meaningful interactions within complex biological systems. This in silico analysis may help to investigate, for example, the inner workings of a given drug in a specific pathological context. In essence, this approach may aid us in solving a "we do know what we don't know" type of question, such as "Why correcting high glucose levels is so beneficial in DM but not so much so in HF?" or "Is a given drug effective by modifying the same or different targets in different pathological contexts"?

In humans, sodium-glucose cotransporter-2 (SGLT2) is a protein located in the proximal part of the tubule in the kidneys, where it facilitates the reabsorption of 90% glucose, inhibiting SGLT2 results in decreased blood glucose due to glucosuria. Members of this new class of anti-type 2 DM drugs, such as empagliflozin (EMPA), increase insulin sensitivity and uptake in the muscle cells, while decreasing gluconeogenesis and improving the first phase of insulin release from pancreatic β cells. Data from EMPA-REG OUTCOME (Empagliflozin Cardiovascular Outcome Event Trial in Type 2 Diabetes Mellitus Patients) showed that, in patients with type 2 DM, the

*Editorials published in *JACC: Basic to Translational Science* reflect the views of the authors and do not necessarily represent the views of *JACC: Basic to Translational Science* or the American College of Cardiology.

From the [a]Division of Cardiology, Department of Medicine, Johns Hopkins School of Medicine, Baltimore, Maryland; [b]Laboratory of Cardiovascular Science, National Institute on Aging, National Institutes of Health, Baltimore, Maryland; [c]Translational Gerontology Branch, National Institute on Aging, National Institutes of Health, Baltimore, Maryland; and the [d]Department of Biomedical Sciences, University of Padova, Padova, Italy. This work was supported by the National Institutes of Health (R01 HL136918 to Dr. Paolocci as Principal Investigator and R01 HL063030 to Dr. Paolocci as co-Principal Investigator) and by the JHU Magic-That-Matters Fund (to Dr. Paolocci). The other authors have reported that they have no relationships relevant to the contents of this paper to disclose.

The authors attest they are in compliance with human studies committees and animal welfare regulations of the authors' institutions and Food and Drug Administration guidelines, including patient consent where appropriate. For more information, visit the *JACC: Basic to Translational Science* author instructions page.

ISSN 2452-302X https://doi.org/10.1016/j.jacbts.2019.10.005

administration of empagliflozin led to lower rates of death from cardiovascular causes, nonfatal myocardial infarction (MI), or stroke, as well as HF-related hospitalizations, compared with those patients receiving a placebo. It is particularly relevant that beneficial effects of empagliflozin on cardiovascular outcomes emerged early and remained sustained throughout the observation period. However, we still need to fully uncover the potential, as well as the underlying mechanisms, of empagliflozin as an anti-HF measure. EMPA-REG OUTCOME has shown that it is unlikely that these benefits stem from the reduction or prevention of atherothrombotic events such as MI or stroke. Moreover, HF and mortality diverged early during treatment, suggesting that EMPA can benefit cardiovascular function via glucose-independent mechanisms, a hypothesis currently tested in the EMPA-TROPISM (Safety and Efficacy of Empagliflozin versus Placebo on Top of Guideline-directed Medical Therapy in Heart Failure Patients with Reduced Ejection Fraction without Diabetes) trial.

SEE PAGE 831

In this issue of *JACC: Basic to Translational Science*, Iborra-Egea et al. (2) posed precisely this question: through what mechanisms does empagliflozin benefit the failing heart, with or without DM? To answer this question, the investigators designed a complex experimental matrix, including the emerging tool of machine learning, with a family of algorithms that correspond to artificial neural networks. In brief, they used in-depth learning analysis (integrating massive, publicly available databases) to investigate how empagliflozin eventually improves outcomes in patients with HF and reduced ejection fraction (HFrEF) with or without DM. The information gathered from this in silico approach (i.e., the empagliflozin-predicted mechanism of action that explains the connection between a model's input and output data) was then validated in rats in which HFrEF was induced by MI, either in the absence or presence of empagliflozin. The machine learning approach allowed them to identify the activation of the sodium-hydrogen exchanger-1 (NHE1) cotransporter as the most robust mechanism of action that was similar for diabetic and nondiabetic patients, thus suggesting a DM-independent mechanism. With the same in silico (mathematical model) design, they determined that, in the absence of empagliflozin, NHE1 is activated, prompting the induction of baculoviral 1AP repeat-containing protein 2. This event, in turn, induces the degradation of the proteasome-mediated X-linked inhibitors of apoptosis (XIAP) and baculoviral 1AP repeat-containing protein 5 (BIRC5), thus fueling HFrEF progression. These changes were absent in empagliflozin-treated rats with MI, thus accounting for the halted HF progression. In the hearts of rats with MI, the investigators then validated these in silico findings by assessing the messenger ribonucleic acid levels of XIAP and BIRC5 as the end-effectors of the proposed pathway, in the absence and presence of empagliflozin. They found that the drug counteracted the reduction in gene expression of both XIAP and BIRC5, thus preserving their antiapoptotic effects. In essence, empagliflozin can benefit the failing heart even in the absence of overt diabetic conditions and very likely countering NHE1-triggered myocyte apoptosis.

Empagliflozin has cardiac and extracardiac protective actions, including enhanced diuretic efficiency, renal protection, augmented cardiac substrate metabolism (i.e., enhanced ketone formation and utilization), and decreased vascular stiffness. Moreover, empagliflozin can inhibit transforming growth factor-beta-induced fibroblast activation, collagen deposition, and fibrosis, as well as reduce production of the proinflammatory adipokine leptin and increase production of the anti-inflammatory adipokine adiponectin. In terms of empagliflozin's primary cardiac effects, an essential study by Byrne et al. (3), conducted in mice with pressure overload-induced HF, revealed that empagliflozin-treated hearts exhibited significantly improved cardiac output and cardiac work ex vivo, with no differences in heart rate; these findings suggest improved cardiac contractility independent of and in addition to changes in vascular resistance. However, mechanisms accounting for these primary cardiac effects remained unclear. Among its other merits, the current research by Iborra-Egea et al. (2) contributes to filling this gap by confirming and expanding previous evidence attesting that NHE1 is a primary target of empagliflozin in the heart. Baartscheer et al. (4) had already reported that empagliflozin reduces $[Na^+]$ and $[Ca^{2+}]$ in isolated ventricular myocytes, independently from the presence of glucose but in a manner sensitive to the NHE1 inhibitor cariporide, thus suggesting that empagliflozin inhibits this antiporter. More recently, Bertero et al. (5) advanced the "sodium hypothesis" according to which "…empagliflozin may reduce intracellular sodium (Na^+) load observed in failing cardiac myocytes by inhibiting the sarcolemmal Na^+/H^+ exchanger. Because elevated intracellular Na^+ hampers mitochondrial Ca^{2+} handling and thereby, deteriorates energy supply and demand matching and the mitochondrial antioxidative defense systems, empagliflozin may positively affect cardiac function by restoring mitochondrial function, and redox state

FIGURE 1 Empagliflozin and Heart Failure

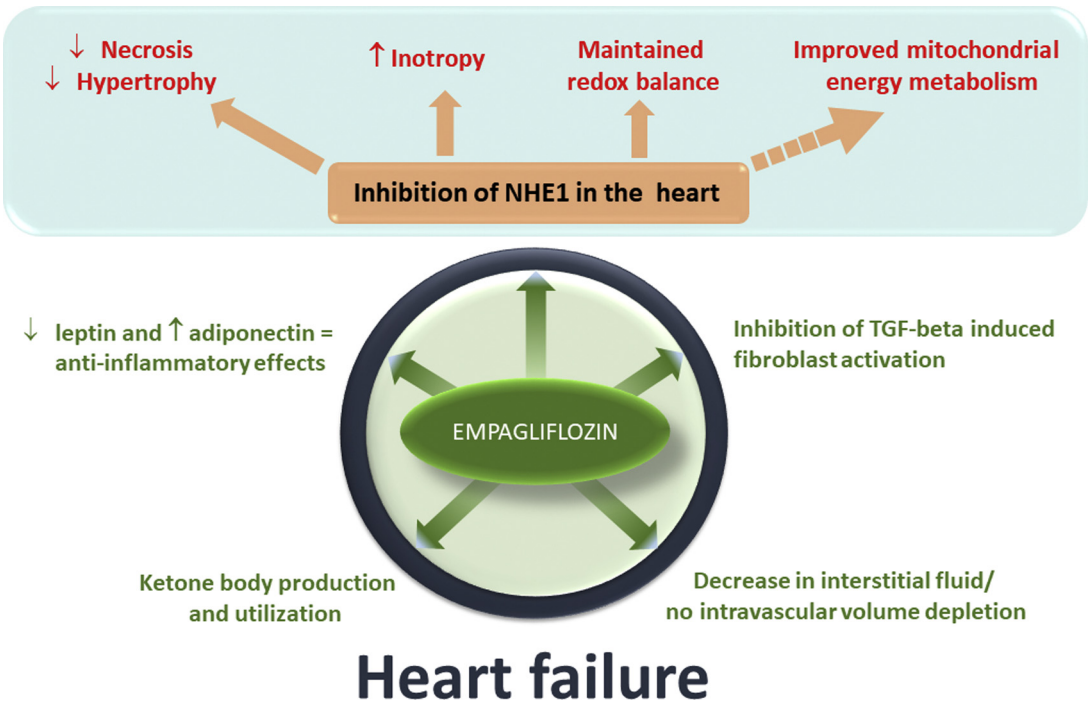

Some mechanisms that explain the benefits afforded by empagliflozin to patients with heart failure and reduced ejection fraction, and cardiac effects already attributed to the inhibition of NHE1 activity. The **dotted line** represents additional yet to be verified salutary actions.
TGF = transforming growth factor.

in the failing heart." Accordingly, the long-term ablation of NHE1 activity enhances the myocyte redox potential and mitigates high-fat diet-induced myocardial stress and fatty liver disease, leading to better-preserved insulin sensitivity, while potentially altering both cardiac and systemic metabolic substrate handling in mice (6).

In aggregate, the study by Iborra-Egea et al. (2), as well as earlier reports, imply that by reducing intercellular Na^+ and Ca^{2+}, SGLT-2 inhibitors such as empagliflozin can not only modulate myocyte mechanical function by affecting Ca^{2+} handling/cycling but also afford myocardial protection by maintaining proper myocardial redox balance, and possibly mitochondrial energy metabolism (**Figure 1**). In-depth future studies shall evaluate whether empagliflozin helps in maintaining mitochondrial energetic and redox assets in HFrEF and other cardiac disorders.

Sarcolemmal NHE activity of human ventricular myocytes stems from the NHE1 isoform, and its expression is significantly higher in recipient hearts with chronic end-stage HF than it is in unused donor hearts. Moreover, inhibiting NHE1 can attenuate cardiomyocyte injury, remodeling, and systolic dysfunction. Along with the fact that empagliflozin is a well-tolerated drug that can be administered once daily with a lower risk of inducing hypoglycemia, these facts provide a solid mechanistic ground for repurposing empagliflozin as an anti-HF drug, at least for HFrEF treatment, which is the major translational message emanating from the studies performed by Iborra-Egea et al. (2). Among the additional questions raised by their contribution is whether NHE1 expression/activity is altered also in patients with heart failure with preserved ejection fraction. Is NHE1 upregulated under this condition too? Would features of HF with preserved ejection fraction such as diastolic dysfunction and left ventricular hypertrophy be effectively corrected by empagliflozin? Another important pending issue comes from the evidence that aldosterone stimulates NHE1 in the heart and vasculature; therefore, would empagliflozin be able to obviate or attenuate cardiac and vascular stigmata brought by any conditions linked to hyperaldosteronism? This has self-evident implications when we are in the need of attenuating the neurohormonal overdrive typical of many cardiovascular disorders.

JACC: BASIC TO TRANSLATIONAL SCIENCE VOL. 4, NO. 7, 2019
NOVEMBER 2019:841–4

Thanks to the present study (2) and other contributions, we are no longer outside, looking in, regarding the role of NHE1 in HF pathogenesis. Moreover, the multifaceted and complex approach adopted herein by Iborra-Egea et al. reiterates that gathering more information/predictions (integrating big data with computer modeling) increases our wisdom, namely our acuity in orienting ourselves when facing a "we don't know what we don't know" type of issue. One may argue, however, that despite the excellent help offered by machine learning, sometimes human ingenuity/intuition gets it first.

ADDRESS FOR CORRESPONDENCE: Dr. Nazareno Paolocci, Division of Cardiology, Department of Medicine, Johns Hopkins School of Medicine, Traylor 911, 720 Rutland Avenue, Baltimore, Maryland 21205. E-mail: npaoloc1@jhmi.edu.

REFERENCES

1. T.S. Eliot quotes. Available at Brainyquotes. Available at: https://www.brainyquote.com/quotes/t_s_eliot_121647. Accessed October 15, 2019.

2. Iborra-Egea O, Santiago-Vacas E, Yurista SR, et al. Unraveling the molecular mechanism of action of empagliflozin in heart failure with reduced ejection fraction with or without diabetes. J Am Coll Cardiol Basic Trans Science 2019;4:831–40.

3. Byrne NJ, Parajuli N, Levasseur JL, et al. Empagliflozin prevents worsening of cardiac function in an experimental model of pressure overload-induced heart failure. J Am Coll Cardiol Basic Trans Science 2017;2:347–54.

4. Baartscheer A, Schumacher CA, Wust RC, et al. Empagliflozin decreases myocardial cytoplasmic Na(+) through inhibition of the cardiac Na(+)/H(+) exchanger in rats and rabbits. Diabetologia 2017;60:568–73.

5. Bertero E, Prates Roma L, Ameri P, Maack C. Cardiac effects of SGLT2 inhibitors: the sodium hypothesis. Cardiovasc Res 2018;114:12–8.

6. Prasad V, Lorenz JN, Miller ML, et al. Loss of NHE1 activity leads to reduced oxidative stress in heart and mitigates high-fat diet-induced myocardial stress. J Mol Cell Cardiol 2013;65:33–42.

KEY WORDS cardiac redox balance, diabetes, empagliflozin, heart failure with reduced ejection fraction, mitochondrial energy metabolism, NHE1, SGLT2

JACC: BASIC TO TRANSLATIONAL SCIENCE VOL. 4, NO. 7, 2019

TRANSLATIONAL PERSPECTIVE

Limitations of Animal Studies for Predicting Toxicity in Clinical Trials

Is it Time to Rethink Our Current Approach?

Gail A. Van Norman, MD

SUMMARY

Animal testing is used in pharmaceutical and industrial research to predict human toxicity, and yet analysis suggests that animal models are poor predictors of drug safety in humans. The cost of animal research is high—in dollars, delays in drug approval, and in the loss of potentially beneficial drugs for human use. Human subjects have been harmed in the clinical testing of drugs that were deemed safe by animal studies. Increasingly, investigators are questioning the scientific merit of animal research. This review discusses issues in using animals to predict human toxicity in pharmaceutical development. Part 1 focuses on scientific concerns over the validity of animal research. Part 2 will discuss alternatives to animal research and their validation and use in production of human pharmaceuticals. (J Am Coll Cardiol Basic Trans Science 2019;4:845–54) © 2019 The Author. Published by Elsevier on behalf of the American College of Cardiology Foundation. This is an open access article under the CC BY-NC-ND license (http://creativecommons.org/licenses/by-nc-nd/4.0/).

There is no doubt that the use of animals in science and medicine has significantly benefitted human beings (**Table 1**). However, many investigators are increasingly concerned that animal experimentation may be based on a scientifically flawed premise and that it retains its acceptability only because clear alternatives have not been identified. Dramatically rising costs and extremely high failure rates in drug development have led many to re-evaluate the value of animal studies. This review focuses on questions regarding the scientific validity of nonhuman animal models (hereafter referred to simply as "animal research") in predicting human toxicity in preclinical pharmaceutical testing.

HISTORICAL PERSPECTIVE

In the United States, the use of animals to test human pharmaceuticals dates to 1937, when a liquid formulation of a sulfa antibiotic dissolved in ethylene glycol resulted in the deaths of 107 adults and children. The incident resulted in passage of the 1938 U.S. Federal Food, Drug, and Cosmetic Act, mandating animal toxicity testing (1,2). In 1946, language was incorporated into the Nuremberg code (3) and later the Helsinki Declaration (4) requiring human experiments to be "*designed and based on the results of animal experimentation* [author's italics] and a knowledge of the natural history of the disease." The statement was written by Andrew Ivy, a strong proponent of animal research, but was not based on scientific evidence that such a requirement would improve safety or efficacy of human drug development (3).

Today, the U.S. Food and Drug Administration (FDA) generally requires preclinical testing of any new drug or biological therapeutic "for pharmacologic activity and acute toxicity in animals" prior to

From the Department of Anesthesiology and Pain Medicine, University of Washington, Seattle, Washington. Dr. Van Norman has received financial support from the *Journal of the American College of Cardiology*.
The author attests they are in compliance with human studies committees and animal welfare regulations of the authors' institutions and Food and Drug Administration guidelines, including patient consent where appropriate. For more information, visit the *JACC: Basic to Translational Science* author instructions page.

Manuscript received October 14, 2019; accepted October 14, 2019.

ISSN 2452-302X https://doi.org/10.1016/j.jacbts.2019.10.008

ABBREVIATIONS AND ACRONYMS

FDA = U.S. Food and Drug Administration

LR = likelihood ratio

NLR = negative likelihood ratio

NPV = negative predictive value

PLR = positive likelihood ratio

PPV = positive predictive value

entering human clinical trials (5). In certain cases, such as emergency treatment for hazardous exposure, the FDA may even approve in-human use based solely on animal testing under "The Animal Efficacy Rule" (6).

Despite the deeply rooted assumption that animal models accurately predict human toxicity (7–9), even cursory examination of the concordance of animal and human trials raises concerns. A 2006 review of 76 animal studies, for example, found that approximately 20% were contradicted in humans and only 37% were ever replicated in humans (10). A review of 221 animal experiments found agreement in human studies just 50% of the time—essentially randomly (11). Review of 37 chemicals studied in the U.S. National Toxicology Program concluded that toxicities other than carcinogenesis were not reproducible between rats and mice, between sexes, or compared with historic control animals. Average positive predictive value (PPV) from mouse to rat was 55.3% and 44.8% for long-term and short-term studies, respectively. Combining organ, length of exposure, and sex, PPV between mice and rats hovered around 50%, which is no greater than random chance (12). An analysis of 2,366 drugs concluded that "results from tests on animals (specifically rat, mouse and rabbit models) are highly inconsistent predictors of toxic responses in humans, and are little better than what would result merely by chance—or tossing a coin—in providing a basis to decide whether a compound should proceed to testing in humans" (13). Similar results were found for nonhuman primates and dogs (14). Indeed, we need go no farther than the failure rates in drug development to have serious questions about whether animal testing accurately predicts toxicity in human trials.

About 12% of pharmaceuticals pass preclinical testing to enter clinical trials (15). Of those, only 60% successfully complete phase I trials (16). Overall, approximately 89% of novel drugs fail human clinical trials, with approximately one-half of those failures due to unanticipated human toxicity (**Figure 1**) (17). If animal tests accurately predict human toxicity, then why are toxicity-related failure rates in human clinical trials so high?

THE PRICE OF WRONG DECISIONS

Two critical "wrong" decisions regarding animal tests of human pharmaceuticals are 1) falsely identifying a toxic drug as "safe" and 2) falsely labeling a potentially useful therapeutic agent as toxic.

When a human-toxic drug is identified as "safe" by animal testing, the most likely outcome by far is that the drug will fail in clinical testing, often due to unacceptable adverse human effects, and sometimes significantly harming volunteer research subjects in the process. Drugs that survive clinical trials and attain market approval may still be recalled later due to toxicity identified only after months or years of in-human use. Vioxx (Merck, Kenilworth, New Jersey) was found after release to significantly increase the risk of cardiovascular morbidity and mortality, costing Merck more than $8.5 billion in legal settlements alone (18). An estimated 88,000 people suffered heart attacks after taking Vioxx and 38,000 died (19).

Of 578 discontinued and withdrawn drugs in Europe and the United States, almost one-half were withdrawn or discontinued in post-approval actions due toxicity (20). Van Meer et al. (21) found that of 93 post-marketing serious adverse outcomes, only 19% were identified in preclinical animal studies. In the first decade of the 21st century, approximately one-third of FDA-approved drugs were subsequently cited for safety or toxicity issues. or a combination of both, including human cardiovascular toxicity and brain damage, after remaining on the market for a median of 4.2 years (22,23). The most common toxicity types associated with drug withdrawals in the United States and Europe are hepatic (21%), cardiovascular (16%), hematological (11%), neurological (9%), and carcinogenicity (8%) (**Figure 2**) (20).

Protein-based biologics (e.g., monoclonal antibodies), fusion proteins, and recombinant proteins now account for most development stage and marketed biopharmaceuticals (15). These present a particular challenge in predicting human toxicity, due to their propensity to provoke production of antidrug antibodies. Safety concerns include cross reactivity, potentially exaggerated pharmacology, and slow recovery from toxicity, among others (15,24)—and immunogenic responses in animals do not predict immunogenicity in humans (15,25–27).

There are many notable examples of cases in which animal trials did not predict severe human toxicity. Isuprel for treatment of asthma caused over 3,500 deaths in Great Britain alone, despite safety in rats, guinea pigs, dog, and monkeys, all of which had received doses far exceeding those administered in humans (2,28). Thalidomide caused devastating phocomelia in an estimated 20,000 to 30,000 infants before it was withdrawn. However, animal tests failed to reveal significant teratogenicity in 10 strains of rats; 11 breeds of rabbit; 2 breeds of dog; 3 strains of

TABLE 1 Animal Uses in Science, Medicine, and Research

Predictive models for human diseases and their processes
Predictive models for testing drugs and other chemicals for human toxicity and efficacy
"Spare parts"— e.g., pig-derived aortic valve prostheses
Bioreactors or factories— e.g., production of monoclonal antibodies
Sources of tissue to study physiological principles
Educational "material" to educate and train biology and medical students and others
Subjects in research to benefit other animals
Subjects of research to gain basic knowledge for its own sake

FIGURE 1 Failures in Translational Research: Preclinical and Clinical Trials

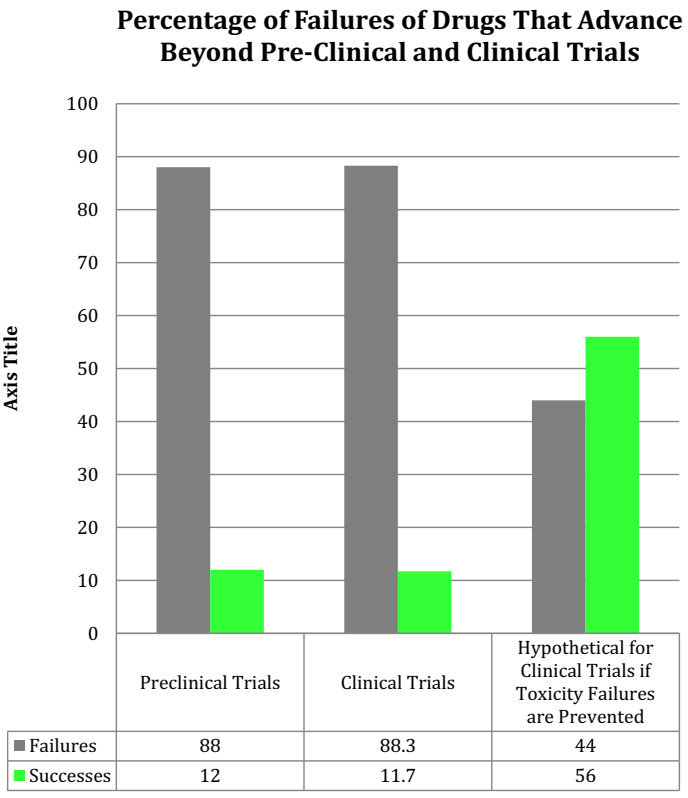

Percentages of drugs that fail in preclinical trials (due to drug toxicity or failure of efficacy in animal testing) and in clinical trials (due drug toxicity or failure of efficacy in human testing) are shown in columns 1 and 2. The third column demonstrates what would happen if animal and human toxicity were closely correlated and therefore drugs with human toxicity were eliminated at the preclinical testing stage by animal toxicity testing (one-half of all drug failures in clinical trials are due to toxicity issues despite safety in animals). Success rates of clinical trials increase from 11.7% overall to approximately 56%.

hamsters; 8 species of primates; and various cats, armadillos, guinea pigs, swine, and ferrets (29). An antibody to treat human autoimmune disease, TGN1412, was given at 1/500th the dose found safe in animal testing to 6 human volunteers in a phase I trial (30,31), rendering them all critically ill within minutes and leaving them all with long-term complications (32–34). BIA-102474-101, a drug developed for a range of disorders from anxiety to Parkinsonism, caused deep brain hemorrhage and necrosis in all 5 human volunteers during a phase I clinical trial after it was administered in doses that were 1/500th of the safe dose for dogs. One volunteer died (35). Fialuridine, for treatment of hepatitis B, caused the deaths of 5 volunteers during phase II clinical trials despite being safe in mice, rats, dogs, monkeys, and woodchucks in doses that were hundreds of times higher. Two other volunteers only survived after receiving liver transplants (32).

When animal tests falsely identify a safe chemical as "toxic," the almost certain outcome is abandonment of further development. Undoubtedly many potentially beneficial drugs have failed animal testing and been lost to patients, even though they would have been both safe and effective (36,37). Because a drug that shows toxicity in animal models is unlikely to ever undergo human testing, the magnitude of this type of "error" is unknown. However, many highly beneficial drugs would have failed animal testing and would never have been brought to market, except that they were developed before animal testing was required (38). Examples include penicillin (fatal to guinea pigs) (39), paracetamol (toxic in dogs and cats) (40), and aspirin (embryo toxicity in rats and rhesus monkeys) (41).

Lack of animal tests has also caused deleterious delays in critical drug approvals. Compassionate human use of ganciclovir demonstrated efficacy and safety in treating acquired immunodeficiency syndrome-related cytomegalovirus retinitis in more human patients than would generally be required for a phase I clinical trial, but the FDA refused to license it due to lack of animal studies. Ganciclovir had also been used safely in over 300 patients under compassionate use to treat cytomegalovirus colitis—more than would generally be required in a phase II clinical trial—but the FDA delayed clinical trials for more than a year due to lack of animal studies. The drug was finally approved after a 4-year delay (42).

TIME AND DOLLARS. Rodent testing in cancer therapeutics adds an estimated 4 to 5 years to drug development and costs $2 to $4 million. For industrial toxicity testing, it takes about 10 years and $3 million

FIGURE 2 Toxicity Failures in Pharmaceutical Development

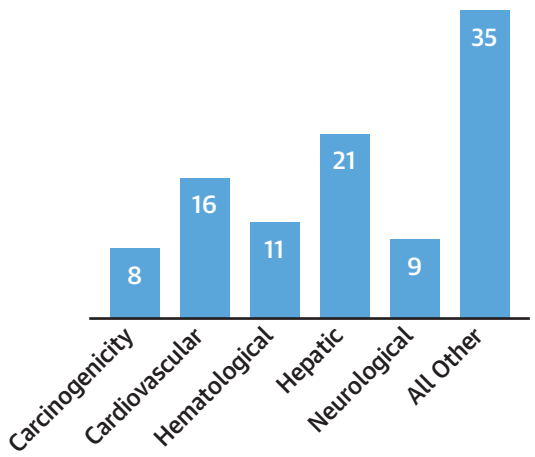

to complete all required animal studies to register a single pesticide (43). Compared with the costs of in vitro testing, animal tests range from 1.5× to >30× as expensive (44,45).

No comprehensive reviews of the total overall cost of animal testing in pharmaceutical development appear to exist. In part, this may be because even the total number of animals or of such studies is unknown. The 2002 amendments to the Animal Welfare Act exempted mice, rats, fish, and birds used in animal research from required reporting to the U.S. Department of Agriculture (46). These are the 4 most common types of animals used, and they account for >90% of all U.S. animal subjects and 81% of European animal subjects (45,47).

Costs of animal toxicity tests can be estimated from other industries, however, and are eye-opening. According to the Organization for Economic Development, which determines animal testing guidelines and methodology for government, industry, and independent laboratories in its several dozen member countries, the average cost of a single, 2-generation reproductive animal toxicity study worldwide is €318,295 and for Europe alone is €285,842 (45), or roughly $349,890 and $314,215, respectively.

Contract research organizations account for most of the animal testing done in the United States and Europe. Statista, a global data portal for market and economic sector statistics, estimates the global markets for animal testing in 2018 at $7.4 billion for drug discovery, $11.2 billion for preclinical development and safety, $58.5 billion for clinical development, and $2.3 billion for central laboratory testing (48). Keen (49) estimates that annual U.S. biomedical and agricultural research and development investments involving animal research exceed $26 billion.

REPRODUCIBILITY AND INTERSPECIES RELIABILITY OF ANIMAL TESTS

Reproducibility of animal studies within species, even when carried out under rigorous protocols, is questionable. Using a database of more than 800,000 animal toxicity studies performed for 350 chemicals under rigorous guidelines, a reviewer found toxicity was repeatable just 70% of the time in the same species (45). Another reviewer found that results for a single chemical often differed with animal model, strain, dose, and delivery route. About 26% of chemicals demonstrated contradictory results on repeat testing in the same species. Furthermore, discordant results sometimes ranged over 3 orders of magnitude within the same species (50).

PPV, NPV, AND LR. Sensitivity reflects how likely a positive test is to detect all subjects with a condition, and specificity reflects how likely a negative test is to exclude all subjects without the condition (**Figure 3**). PPV reflects how often a positive test actually identifies a subject with the condition, and the power of the negative predictive value (NPV) of a test reflects the proportion of subjects with negative tests that actually do not have the condition. Whereas sensitivity, specificity, PPV, and NPV are often used to describe the accuracy of tests, they are not sufficient to inform us how much "value" to attribute to any given test. For example, suppose a positive toxicity test in mice for a group of drugs always predicts human toxicity (sensitivity = 100%), but it also indicates human toxicity when it is not present—in fact the test results always indicate that the drug is toxic. Such a test would have virtually no use in determining human toxicity despite being 100% sensitive. A useful toxicity test is 1 that also indicates accurately when toxicity in animals is not present in humans or has high specificity. Furthermore, we want to know how often the test accurately indicates human toxicity, compared with how accurately it indicates human nontoxicity.

Sensitivity, specificity, PPV, and NPV are all strongly affected by the prevalence of the condition they test for and are therefore of limited value in assessing the reliability of a test when the prevalence of the condition is unknown. Lower prevalence increases the likelihood of false positive results, and higher prevalence increases the

likelihood of false negative results. Once a drug tests positive for toxicity in animals, it is rarely tested against humans, and the prevalence of the real condition the test is being used to "detect"—human toxicity—remains unknown.

However, the "value" of using a given test to improve the post-test probability of ruling in or ruling out a condition can be calculated using likelihood ratios even if the prevalence of the condition is unknown, so long as the sensitivity and specificity of the test are known. LR are indicators of whether the results of a given test will "add weight" over the pre-test probabilities (i.e., prevalence rate) of the condition in deciding what the probability is that a condition is actually present or absent.

There are 2 types of LR: the positive likelihood ratio (PLR) indicates how much more likely it is that a condition exists after a positive test result, when compared with its pre-test probability. The negative likelihood ratio (NLR) indicates how much the probability that a condition exists decreases compared with its pre-test probability, given a negative test result. The change in post-test probability from pre-test probability is calculated by multiplying the pre-test probability (prevalence) by the PLR or NLR. If the change in post-test probability from the pre-test probability is small (i.e., LR, the multiplier, is small), then the test is unlikely to help determine the presence or absence of a condition over simply knowing its prevalence. LR of <1.0 actually indicate a negative shift in post-test probabilities. In other words, if a PLR is <1.0, then for any subject that has a positive test result, the probability that they have the condition decreases compared with the pre-test probability. For an NLR of <1.0, for any subject with a negative test, the probability that they do not have the condition also decreases compared with the pre-test probability. For an LR of 1.0, there is no change from pre-test probabilities (pre-test probabilities are simply multiplied by 1), and the test also was not useful. For LR >1.0, the probability of the condition being present increases in the face of a positive test, and the probability of the condition being absent increases in the presence of a negative test. For LR from 1.0 to 10, these changes are relatively small (meaning the test will not add much), but for LR >10, the changes increase exponentially and are considered significant (51-54).

Using LR to calculate the probability that a test will improve detection of a condition or ruling it out is complex; it requires knowing the sensitivity and specificity of a test and pre-test probabilities, conversion of probabilities to odds and back again, and then using a log table (i.e., a Fagan's nomogram) or log calculator to determine how much a test is likely to improve (or decrease) the chances of detecting the condition (53).

LR are increasingly being used to express translatability of animal toxicity testing (52-55). Bailey et al. (14) found that the presence of toxicity in a species sometimes added evidentiary weight to the risk of toxicity in another, but the reverse was not true: negative toxicity tests in animals did not significantly increase the probability that a toxic test would also be negative in humans, and a lack of toxicity in any species would not reliably indicate a

FIGURE 3 Calculating LR

	Mouse toxicity +	Mouse toxicity –
Rat toxicity +	M^+R^+	M^-R^+
Rat toxicity –	M^+R^-	M^-R^-

Sensitivity =

$$\frac{M^+R^+}{M^+R^+ + M^+R^-}$$

Specificity =

$$\frac{M^-R^-}{M^-R^+ + M^-R^-}$$

Positive Likelihood ratio (PLR) =

$$\frac{\text{Sensitivity}}{(1 - \text{Specificity})} = \frac{\left(\frac{M^+R^+}{M^+R^+ + M^+R^-}\right)}{\left(1 - \frac{M^-R^-}{M^-R^+ + M^-R^-}\right)}$$

Negative LR (iNLR) =

$$\frac{\text{Specificity}}{(1 - \text{Sensitivity})} = \frac{\left(\frac{M^-R^-}{M^-R^+ + M^-R}\right)}{\left(1 - \frac{-M^+R^+}{M^+R^+ + M^+R^-}\right)}$$

The likelihood that a test showing toxicity in a mouse predicts toxicity in the rat (positive likelihood ratio [PLR]) or that a test showing no toxicity in a mouse predicts nontoxicity in a rat (negative likelihood ratio [NLR]). M^+R^+ = toxicity present in both mouse and rat; M^+R^- = toxicity present in mouse but not in rat; M^-R^+ = toxicity not present in mouse, but present in rat; and M^-R^- = toxicity not present in mouse and also not present in rat.

probable lack of toxicity in any other species, including comparisons of primate to human toxicity tests (14). Furthermore, even in the presence of animal toxicity, LRs were extremely inconsistent and varied considerably for different classes of drugs (13,52). Similar findings have been reported in multiple analyses and reviews in other studies (52,54–56).

A number of studies have reviewed LR of specific drug toxicity tests for which both animal and human data are available. In a review of 2,366 drugs, including data from 3 of the most common animal research species—rat, mouse, and rabbit—PLRs were generally high (i.e., there is a likelihood that positive toxicity tests in animals would show toxicity in humans). But median NLRs were very low—1.12 (rabbit), 1.39 (mouse), and 1.82 (rat); in other words, they were of little or no value in excluding human toxicity (13). The investigators also examined canine models and found that PPV and PLR for human toxicity were not correlated with 1 another: NLR were low, indicating that the dog provided little evidentiary weight to ruling out toxicity in humans (52). Later analysis of 3,000 drugs found that tests inferring no toxicity in any 1 species, including nonhuman primates, have no evidentiary weight with regard to toxicity in any other species (14). In a comparison study reported by pharmaceutical companies of 150 drugs associated with adverse events or toxicity in humans (55), LR could not be determined due to a lack of specificity reporting on the tests. Paglialunga et al. (56) examined translatability of respiratory safety pharmacology studies from animal models to humans and found that PPV and PLR were so low that animal tests provided little value in predicting human toxicity.

GROWING SCIENTIFIC CRITICISM

As early as 1962, scientists questioned the assumption that animal models reliably predicted human responses. Lichtfield (57) examined 6 drugs studied in animal models and found that rats and dogs demonstrated PPVs (for human response) of 0.49 and 0.55, respectively, essentially random chance. He opined that the differences between species in specific drug responses were so striking that one could actually use the results of drug toxicity tests alone to identify whether an entity was a rat, rather than a dog or a man, and concluded there was no basis for predicting adverse human effects for the 6 drugs from animal studies. A 1990 analysis of the toxicities of 24 drugs abandoned during human clinical trials demonstrated that 16 had no animal model toxicity correlation (58).

In 1981, the Council on Scientific Affairs of the American Medical Association stated, "The Council's consultants agree that to identify carcinogenicity in animal tests does not *per se* predict either risk or outcome in human experience. . . . the Council is concerned about the hundred[s] of millions of dollars that are spent each year (both in the public and private sectors) for the carcinogenicity testing of chemical substances. The concern is particularly grave in view of the questionable scientific value of the tests when used to predict the human experience" (59).

The 2019 West Coast Regional Safety Pharmacology Society Meeting discussed concerns about the lack of concordance between animal and human safety studies, including lack of canine and human concordance for proarrhythmia risks of new cardiovascular drugs and the failure of animal research to predict drug-related risks in the human central nervous and respiratory systems (60,61).

Regulatory and research leaders are increasingly taking notice of the issue. In 2006, Michael Levitt, then U.S. Secretary of Health and Human Services, stated, "nine out of ten experimental drugs fail in clinical studies because we cannot accurately predict how they will behave in people based on laboratory and animal studies" (62,63). A landmark review and report by the Institute of Medicine in 2011 concluded that the use of chimpanzees in biomedical research is unnecessary (64). Although the reasons for it are complex, in 2015, the National Institutes of Health announced they would be ending all chimpanzee research (65). Andrew Wheeler, administrator of the U.S. Environmental Protection Agency, pledged in September 2019 to phase out all toxicity testing in mammals over the next 16 years (66).

IS THE SCIENTIFIC PREMISE BEHIND ANIMAL MODELS VALID?

Many concerns regarding reliability of animal models in predicting human toxicity are not based on the scientific underpinnings of interspecies translation, but rather call out collateral, potentially correctable issues, such as technical competence in executing animal research, the soundness of animal research study design, and publication bias (**Table 2**) (67–71). Indeed, Knight (72) could find no review of animal research studies that rated a majority of the experiments as having "good" methodological quality. An obvious solution would be correction of these problems to improve translation rates of animal research. Despite widespread efforts to improve the quality of methodology in animal studies, however, studies examining whether such measures consistently improve the reliability of animal models in predicting human toxicity have yet to be published, although a

TABLE 2 Commonly Used Arguments Against Animal Research

Argument	Critique
Methodological: Animal models should be abandoned because the scientific methodology of the experiment was poor.	The quality of methodology in an individual experiment cannot be extrapolated to the question of whether animal experimentation as a whole is invalid, merely to whether the individual experiment is yielding true results.
Historical: Historically, medical dependence on animal modeling is much less robust than we are led to believe.	Historical use of animal modeling is a poor measure of the validity of current experimentation and methods. To determine whether animal modeling is reliable in current science, we need to use modern scientific knowledge and examine modern methodology to determine whether animal modeling is predictive of human outcomes today. This takes into account information and methods that may or may not have been historically available.
Reviews: Review articles have determined that certain animal species have not been critical in various medical developments, and therefore animal experimentation should be abolished.	The invalidity of using certain specific animals does not necessarily rule out animal models as a whole.
Alternatives: The existence of alternative models requires us to abandon animal research.	Whereas alternatives to animal research exist or are developing in many areas of medical research, in many instances such alternatives do not exist. This argument does not address whether continued use of animal models is scientifically valid, regardless of alternative methods, and it does not attempt to define whether certain animal models are predictably successful and others are predictably unsuccessful.

number of studies do demonstrate continued problems with predicting human efficacy (73).

Instead of methodologies and publication bias, an increasing number of investigators propose that the problem may lie with the basic premise of animal testing itself (69,74). The biological sciences have increasingly embraced theories regarding complex systems (e.g., chaos theory and complexity theory) to explain mechanisms in evolution, the biology of cancer, the divergent properties of animal species, as well as the failures of translation of drug therapeutics from animal species to humans (75,76). Because animals and humans are classic examples of incompletely understood complex systems, some investigators propose that it may simply be scientifically invalid to assume that toxicity of a substance in any one species can reliably predict toxicity in any other, no matter how stringent animal testing standards are made (69).

ALTERNATIVES TO ANIMAL TESTING

Alternatives to animal testing will be discussed in more detail in part 2 of this review; they include in vitro tests using cell lines, tissue samples, use of alternative organisms such as bacteria, 3-dimensional modeling and bioprinting, in silico tests, organ-on-chip technologies such as 3-dimensional organoids, computer modeling, and phase 0 in-human microdosing trials (77–82). A comprehensive study of the accuracy, LR, and costs of alternative testing methods compared with animal toxicity testing has not been published; however, there is data suggesting that in vitro testing and other methods are significantly faster and less expensive than animal models (42,44). Using human cells, tissue, or organ models to form the basis of an in vitro test may improve accuracy in weeding out drugs with significant adverse human effects; however, this assumption, too, will require rigorous study.

Researchers will undoubtedly be challenged sooner rather than later to reduce animal research as the result of public advocacy efforts. A 2019 spending bill passed by the U.S. House of Representatives includes a directive to the National Institutes of Health to accelerate the replacement of nonhuman primates in research with alternative research models (83).

The FDA states that for the purposes of cosmetic testing, they believe "that prior to use of animals, consideration should be given to the use of scientifically valid alternative methods to whole-animal testing" (84). The Interagency Coordinating Committee on Validation of Alternative Methods and the National Toxicology Program Interagency Center for the Evaluation of Alternative Toxicological Methods were established in 1997 to coordinate the development, validation, acceptance, and harmonization of alternative toxicological test methods throughout the U.S. government (85) and have as a part of their mission the explicit mandate to reduce or eliminate whole animal testing. The Biennial Progress Report of the Interagency Coordinating Committee on Validation of Alternative Methods for 2016 to 2017 details actions they have taken, including, among others: 1) publication of guidance documents waiving all acute dermal lethality studies for pesticides and describing a process for evaluating; 2) publication of notices reducing the number of hamsters for potency testing of certain vaccines; and 3) publication of a roadmap for

integrating predictive toxicology methods into safety and risk assessments by the FDA (86). At this time, the FDA generally still requires submission of preclinical animal data in investigational new drug applications (5).

CONCLUSIONS

Although animal toxicity testing has been the stalwart basis of "ensuring" safety of in-human clinical testing and use, examination of the published data raises significant questions about whether it is reliable and should be abandoned or at least significantly curtailed in favor of other potentially more reliable methods. Savings in time and cost for new therapeutics could be substantial, if the safety of nonanimal preclinical testing is proven. Increasingly, scientific organizations and government regulatory agencies are recognizing that alternative methods may replace animal testing and improve the flow and safety of new therapeutics to human use.

ADDRESS FOR CORRESPONDENCE: Dr. Gail A. Van Norman, Department of Anesthesiology and Pain Medicine, University of Washington, 2141 8th Avenue West, Seattle, Washington 98119. E-mail: gvn@uw.edu.

REFERENCES

1. Wax PM. Elixirs, diluents and the passage of the 1938 Federal Food, Drug and Cosmetics Act. Ann Intern Med 1995;122:456–61.

2. Greek R, Pippus A, Hansen LA. The Nuremberg Code subverts human health and safety by requiring animal modeling. BMC Med Ethics 2012;13:16.

3. National Institutes of Health. Regulations and Ethical Guidelines. Reprint from: Trials of War Criminals before the Nuremberg Military Tribunals under Control Council Law no. 10, Vol. 2. 1949 1949. Washington, DC: U.S. Government Printing Office, 1949:181–2. Available at: https://history.nih.gov/research/downloads/nuremberg.pdf. Accessed October 5, 2019.

4. World Medical Assembly. Declaration of Helsinki 1964: Recommendations Guiding Doctors in Clinical Research. World Medical Association. June 1964. Available at: https://www.wma.net/what-we-do/medical-ethics/declaration-of-helsinki/doh-jun1964/. Accessed October 5, 2019.

5. U.S. Food and Drug Administration. Investigational New Drug (IND) Application. U.S. Food and Drug Administration. October 5, 2017. Available at: https://www.fda.gov/drugs/types-applications/investigational-new-drug-ind-application. Accessed August 20, 2019.

6. U.S. Food and Drug Administration. Product Development Under the Animal Rule: Guidance for Industry. U.S. Food and Drug Administration. October 2015. Available at: https://www.fda.gov/regulatory-information/search-fda-guidance-documents/product-development-under-animal-rule. Accessed September 23, 2019.

7. Fomchenko EK, Holland EC. Mouse models of brain tumors and their applications in preclinical trials. Clin Cancer Res 2006;12:5288–97.

8. Huff J, Jacobson MF, Davis DL. The limits of two-year bioassay exposure regimens for identifying chemical carcinogens. Environ Health Perspect 2008;116:1439–42.

9. Gad S. Preface. In: Gad S, editor. Animal Models in Toxicology. Boca Raton, FL: CRC Press, 2007:1–18.

10. Hackam DG, Redelmeier DA. Translation of research evidence from animals to humans. JAMA 2006;296:1731–2.

11. Perel P, Roberts I, Sena E, et al. Comparison of treatment effects between animal experiments and clinical trials: systematic review. BMJ 2007;334:197–203.

12. Wang B, Gray G. Concordance of noncarcinogenic endpoints in rodent chemical bioassays. Risk Anal 2015;35:1154–66.

13. Bailey J, Thew M, Balls M. An analysis of the use of animal models in predicting human toxicology and drug safety. Altern Lab Anim 2014;42:189–99.

14. Bailey J, Thew M, Balls M. Predicting human drug toxicity and safety via animal tests: can any one species predict drug toxicity in any other, and do monkeys help? Altern Lab Anim 2015;43:393–403.

15. American Pharmaceutical Review. Preclinical Development: The Safety Hurdle Prior to Human Trials. American Pharmaceutical Review. April 30, 2016. Available at: https://www.americanpharmaceuticalreview.com/Featured-Articles/187349-Preclinical-Development-The-Safety-Hurdle-Prior-to-Human-Trials/. Accessed September 24, 2019.

16. Van Norman GA. Drugs, devices and the FDA: part 1: an overview of approval processes for drugs. J Am Coll Cardiol Basic Trans Science 2016;1:170–9.

17. Van Norman GA. Phase II trials in drug development and adaptive trial design. J Am Coll Cardiol Basic Trans Science 2019;4:428–37.

18. Compton K. Vioxx Lawsuits. Drugwatch. Available at: https://www.drugwatch.com/vioxx/lawsuits/. Accessed September 16, 2019.

19. Juni P, Dip LN, Reichenback S, Sterchi R, Dieppe PA, Egger M. Risk of cardiovascular events and rofecoxib: cumulative meta-analysis. Lancet 2004;364:2021–9.

20. Siramshetty BV, Nickel J, Omieczynski C, et al. WITHDRAWN—a resource for withdrawn and discontinued drugs. Nucl Acids Res 2016;44:D1080–6.

21. van Meer PJ, Kooijman M, Gispen-de Wied CC, Moors EH, Schellekens H. The ability of animal studies to detect serious post marketing adverse events is limited. Reg Tox Pharm 2012;64:345–9.

22. Lupkin S. One-Third of New Drugs Had Safety Problems After FDA Approval. NPR: Shots: Health News From NPR. May 9, 2017. Available at: https://www.npr.org/sections/health-shots/2017/05/09/527575055/one-third-of-new-drugs-had-safety-problems-after-fda-approval. Accessed October 5, 2019.

23. Downing NS, Shah ND, Aminawung JA, et al. Postmarket safety events among novel therapeutics approved by the US Food and Drug Administration between 2001 and 2010. JAMA 2017;317:1854–63.

24. Brinks V, Jiskoot W, Schellekns H. Immunogenicity of therapeutic proteins: the use of animal models. Pharm Res 2011;28:2379–85.

25. McDougal AJ. Preclinical development [CDER]: biological therapeutics for cancer treatment. Paper presented to iSBTc Oncology Biologics Development Primer; February 28, 2008; Gaithersburg, MD. Available at: https://sitc.sitcancer.org/meetings/am08/primer08_oncology/presentations/3_mcdougal.pdf. Accessed September 24, 2019.

26. De Groot AS, Moise L. Prediction of immunogenicity for therapeutic proteins: state of the art. Curr Opin Drug Discov Devel 2007;10:332–40.

27. Pedras-Vasconcelos JA. The Immunogenicity of therapeutic Proteins—What You Don't Know Can Hurt YOU and the Patient. U.S. Food and Drug Administration. Fall 2014. Available at: https://www.fda.gov/media/91668/download. Accessed September 24, 2019.

28. Stolley PD. Asthma mortality: why the United States was spared an epidemic of deaths due to asthma. Am Rev Respir Dis 1972;105:883–90.

29. Schardein J. Drugs as Teratogens. Cleveland, OH: CRC Press, 1976:49.

30. Suntharalingam G, Perry MR, Ward S, et al. Cytokine storm in phase 1 trial of the anti-CD28

monoclonal antibody TGN1312. N Engl J Med 2006;355:1018–28.

31. Dayan CM, Wraith DC. Preparing for first-in-man studies: the challenges for translational immunology post TGN1412. Clin Exp Immunol 2008;151:231–4.

32. Attarwala H. TGN1412: from discovery to disaster. J Young Pharm 2010;2:332–6.

33. Allen F. "Like a horror film": what was the "Elephant Man" drug testing trial, what is TGN1412 and what happened to the men involved? The Sun (UK). February 21, 2017. Available at: https://www.thesun.co.uk/news/2917810/elephant-man-drug-testing-trial-tgn1412/. Accessed October 5, 2019.

34. Vial T, Descotes J, Braun F, Behrend M. Chapter 37. Drugs that act on the immune system: 37—cytokines and monoclonal antibodies. Side Effects Drugs Annu 2007;29:383–423.

35. Eddleston M, Cohen AF, Webb DJ. Implications of the BIA-102474-101 study for review of first-into-human clinical trials. Brit J Clin Pharm 2016;81:582–6.

36. Sankar U. The delicate toxicity balance in drug discovery. Scientist 2005;19:32.

37. Gura T. Systems for identifying new drugs are often faulty. Science 1997;273:1041–2.

38. Koppanyi T, Avery MA. Species differences and the clinical trial of new drugs: a review. Clin Pharmacol Ther 1966;7:250–70.

39. Cormia FE, Lewis GM, Hopper ME. Toxicity of penicillin for the guinea pig. J Invest Dermatol 1947;9:261–7.

40. Villar D, Buck WB, Gonzalez JM. Ibuprofen, aspirin and acetaminophen toxicosis and treatment in dogs and cats. Vet Human Toxicol 1998;40:156–62.

41. Wilson JG, Ritter EJ, Scott WJ, Fradkin R. Comparative distribution and embryotoxicity of acetylsalicylic acid in pregnant rats and rhesus monkeys. Toxicol Appl Pharmacol 1977;41:67–78.

42. Buhles WC. Compassionate use: a story of ethics and science in the development of a new drug. In: Monticello M, editor. Perspectives and Biology in Medicine, Vol. 54. Baltimore, MD: Johns Hopkins University Press, 2011:304–15.

43. Humane Society International. Limitations of Animal Tests. Humane Society International. February 24, 2019. Available at: https://www.hsi.org/news-media/limitations-of-animal-tests/. Accessed September 14, 2019.

44. Humane Society International. Costs of Animal and Non-animal Testing. Humane Society International. October 23, 2012. Available at: https://www.hsi.org/news-media/time_and_cost/. Accessed September 14, 2019.

45. Meigs L, Smirova L, Rovida C, Leist M, Hartung T. Animal testing and its alternatives—the most important omics is economics. ALTEX 2018;35:275–305.

46. USDA National Agricultural Library, U.S. Department of Agriculture. Animal Welfare Act. USDA National Agricultural Library, U.S. Department of Agriculture. Available at: https://www.nal.usda.gov/awic/animal-welfare-act. Accessed October 5, 2019.

47. Taylor K, Gordon N, Langley G, Higgins W. Estimates for worldwide laboratory animal use in 2005. Altern Lab Anim 2008;36:327–42.

48. Statista Research Department. Total Addressable Contract Research Organization (CRO) Market Worldwide in 2018, by Function (in Million U.S. Dollars). Statista. July 22, 2019. Available at: https://www.statista.com/statistics/814232/total-addressable-cro-market-estimates-worldwide-by-function/. Accessed September 16, 2019.

49. Keen J. Wasted money in United States biomedical and agricultural animal research. In: Hermann K, Jayne K, editors. Animal Experimentation: Working Towards a Paradigm Change, Vol 22. Boston, MA: Brill, 2019:244–72.

50. Browne P, Judson RS, Casey WM, Kleinstreuer NC, Thomas RS. Screening chemicals for estrogen receptor bioactivity using a computations model. Environ Sci Technol 2015;49:8804–14.

51. Deeks JJ, Altman DG. Diagnostic tests 4: likelihood ratios. BMJ 2004;329:168.

52. Bailey J, Thew M, Balls M. An analysis of the use of dogs in predicting human toxicology and drug safety. Altern Lab Anim 2013:335–50.

53. McGee S. Simplifying likelihood ratios. J Gen Intern Med 2002;17:646–9.

54. Grimes DA, Schultz KF. Refining clinical diagnosis with likelihood ratios. Lancet 2005;365:1500–5.

55. Matthews RA. Medical progress depends on animal models—doesn't it? J R Soc Med 2008;101:95–8.

56. Paglialunga S, Morimoto BH, Clark M, Friedrichs GS. Translatability of the S7A core battery respiratory safety pharmacology studies: preclinical respiratory and related clinical adverse events. J Pharmacol Toxicol Methods 2019 Jun 5 [E-pub ahead of print].

57. Lichtfield JT Jr. Symposium on clinical drug evaluation and human pharmacology. XVI. Evaluation of the safety of new drugs by means of tests in animals. Clin Pharmacol Ther 1962;3:665–72.

58. Lumley C. Clinical toxicity: could it have been predicted? Premarketing experience. In: Lumley C, Walker S, editors. Animal Toxicity Studies: Their Relevance for Man. London, UK: Quay Publishing, 1990:49–56.

59. Council on Scientific Affairs. Carcinogen regulation. JAMA 1981;246:253–6.

60. Abi-Gerges N, McMahon C, Vargas H, et al. The west coast regional safety pharmacology society meeting update: filling in the translational gaps in safety assessment. J Pharmacol Toxicol Methods 2019;98:106582.

61. Ewert L, Aylott M, Deurinck M, et al. The concordance between nonclinical and phase I clinical cardiovascular assessment from a cross-company data sharing initiative. Toxicol Sci 2014;142:427–35.

62. Shanks N, Greek R, Greek J. Are animal models predictive for humans? Philos Ethics Humanit Med 2009;4:2.

63. U.S. Food and Drug Administration. Press release: FDA issues advice to make earliest stages of clinical drug development more efficient. January 12. Washington DC: U.S. Food and Drug Administration, 2006.

64. Institute of Medicine Committee on the Use of Chimpanzees in Biomedical and Behavioral Research. Chimpanzees in Biomedical and Behavioral Research: Assessing the Necessity. Washington, DC: National Academic Press, 2011.

65. Milman O. National Institutes of Health announces end to chimpanzee research. The Guardian. November 19, 2015. Available at: https://www.theguardian.com/us-news/2015/nov/19/national-institutes-health-end-chimpanzee-research. Accessed September 26, 2019.

66. Greenfieldboye N. EPA Chief Pledges to Severely Cut Back on Animal Testing of Chemicals. NPR Health News. September 10, 2019. Available at: https://www.npr.org/sections/health-shots/2019/09/10/759435118/epa-chief-pledges-to-severely-cut-back-on-animal-testing-of-chemicals. Accessed September 26, 2019.

67. Bracken MB. Why animal studies are often poor predictors of human reactions to exposure. J R Soc Med 2009;102:120–2.

68. van der Worp HB, Howells DW, Sena ES, et al. Can animal models of disease reliably inform human studies? PLoS Med 2010;7:e10000245.

69. Greek R, Kramer LA. How to evaluate the science of non-human animal use in biomedical research and testing: a proposed format for debate. In: Herrmann K, Jayne K, editors. Animal Experimentation: Working Towards a Paradigm of Change, Vol. 22. Boston, MA: Brill Open, 2019:65–87.

70. Ioannidis JPA. Extrapolating from animals to humans. Sci Transl Med 2012;4:151.

71. Greek R, Menache A. Systematic reviews of animal models: methodology versus epistemology. Int J Med Sci 2013;10:206–21.

72. Knight A. Systematic reviews of animal experiments demonstrate poor human clinical and toxicological utility. Altern Lab Anim 2007;35:641–59.

73. Akhtar A. The flaws and human harms of animal experimentation. Camb Q Healthc Ethics 2015;24:407–19.

74. Pound P, Ritskes-Hoiting M. Is it possible to overcome issues of external validity in preclinical animal research? Why most animal models are bound to fail. J Transl Med 2018;16:304.

75. Miquel PA. Extended physics as a theoretical framework for systems biology? Prog Biophys Mol Biol 2011;106:348–52.

76. Soto AM, Sonnenschein C, Maini PK, Novle D. Systems biology and cancer. Prog Biophys Mol Biol 2011;106:337–46.

77. Groell F, Jordan O, Borchard G. In vitro models for immunogenicity prediction of therapeutic proteins. Eur J Pharm Biopharm 2018;130:128–42.

78. Mittal R, Woo FW, Castro CS, et al. Organ-on-chip models: implications in drug discovery and clinical applications. J Cell Physiol 2019;234:8352–80.

79. Benam KH, Gilchrist S, Kleensang A, Satz AB, Willet C, Zhang Q. Exploring new technologies in

biomedical research. Drug Discov Today 2019;24:1242–7.

80. Doke SK, Dhawale SC. Alternatives to animal testing: a review. Saudi Pharm J 2015;23:223–9.

81. Burt T, Vuong LT, Baker E, et al. Phase 0, including microdosing approaches: applying the three Rs and increasing the efficiency of human drug development. Altern Lab Anim 2018;46. 335–4.

82. Herrmann K, Pistollato F, Stephens ML. Beyond the 3 Rs: expanding the use of human-relevant replacement methods in biomedical research. ALTEX 2019;36:343–52.

83. Reardon S. U.S. Lawmakers Propose Plan to Reduce Primate Research at the National Institutes of Health. Nature. May 9, 2019. Available at: https://www.nature.com/articles/d41586-019-01511-0?utm_source=twt_nnc and utm_medium=social and utm_campaign=naturenews and sf212424116=1. Accessed September 26, 2019.

84. U.S. Food and Drug Administration. Animal Testing and Cosmetics. U.S. Food and Drug Administration. May 31, 1999, updated 2006. Available at: https://www.fda.gov/cosmetics/product-testing-cosmetics/animal-testing-cosmetics. Accessed October 1, 2019.

85. U.S. ICCVAM. Interagency Coordinating Committee on Validation of Alternative Methods. Research Triangle Park, NC: U.S. ICCVAM, 2019. Available at: https://www.niehs.nih.gov/health/materials/interagency_coordinating_committee_on_the_validation_of_alternative_methods_508.pdf. Accessed October 12, 2019.

86. U.S. ICCVAM. Biennial Progress Report 2016–2017: Interagency Coordinating Committee on Validation of Alternative Methods. July 2018. Available at: https://ntp.niehs.nih.gov/iccvamreport/2017/bienrpt-txt.pdf. Accessed October 10, 2019.

KEY WORDS **animal research, drug development, toxicity, translational research**

JACC: BASIC TO TRANSLATIONAL SCIENCE VOL. 4, NO. 7, 2019

STATE-OF-THE-ART REVIEW

Telomeres as Therapeutic Targets in Heart Disease

Jih-Kai Yeh, MD,[a] Mei-Hsiu Lin, MS,[a] Chao-Yung Wang, MD[a,b]

HIGHLIGHTS

- **Age-associated CVDs impose a great burden on current health systems. Despite the fact that current strong evidence supports the links among aging, telomere attrition, and CVDs, there is no clear direction for the development of telomere therapeutics against CVDs.**
- **This review focuses on immune modulation, CHIP, pharmaceutical interventions, and gene therapy for their therapeutic roles in age-associated CVDs.**
- **The future goal of telomere cardiovascular therapy in young subjects is to prevent senescence and diseases, whereas in older adult subjects, the goal is restoration of cardiovascular functions. Further studies on the telomere-CHIP-atherosclerosis axis may shed insights on how to achieve these 2 different therapeutic targets.**

SUMMARY

Telomeres are double-stranded repeats of G-rich tandem DNA sequences that gradually shorten with each cell division. Aging, inflammation, and oxidative stress accelerate the process of telomere shortening. Telomerase counteracts this process by maintaining and elongating the telomere length. Patients with atherosclerotic diseases and cardiovascular risk factors (e.g., smoking, obesity, sedentary lifestyle, and hypertension) have shorter leukocyte telomere length. Following myocardial infarction, telomerase expression and activity in cardiomyocytes and endothelial cells increase significantly, implying that telomerase plays a role in regulating tissue repairs in heart diseases. Although previous studies have focused on the changes of telomeres in heart diseases and the telomere length as a marker for aging cardiovascular systems, recent studies have explored the potential of telomeres and telomerase in the treatment of cardiovascular diseases. This review discusses the significant advancements of telomere therapeutics in gene therapy, atherosclerosis, anti-inflammation, and immune modulation in patients with cardiovascular diseases.
(J Am Coll Cardiol Basic Trans Science 2019;4:855-65) © 2019 The Authors. Published by Elsevier on behalf of the American College of Cardiology Foundation. This is an open access article under the CC BY-NC-ND license (http://creativecommons.org/licenses/by-nc-nd/4.0/).

Telomeres are repetitive hexanucleotides (TTAGGG)n found at the end of linear chromosomes; they prevent chromosome ends from being recognized as DNA strand breaks and becoming inappropriately degraded by DNA damage responses (1,2). In humans, telomeres are 10 to 15 kb of tandem DNA repeats. There are significant variations of telomere length among individuals, but

From the [a]Department of Cardiology, Chang Gung Memorial Hospital, and Chang Gung University College of Medicine, Taoyuan City, Taiwan; and the [b]Institute of Cellular and System Medicine, National Health Research Institutes, Zhunan, Taiwan. Dr. Wang was supported by the National Health Research Institute (NHRI-EX106-10617SI), National Science Council (105-2628-B-182-009-MY4), and Chang Gung Memorial Hospital (CMRPG3H0132, CMRPG3I0321, and CMRPG3H0842). All other authors have reported that they have no relationships relevant to the contents of this paper to disclose.
The authors attest they are in compliance with human studies committees and animal welfare regulations of the authors' institutions and Food and Drug Administration guidelines, including patient consent where appropriate. For more information, visit the *JACC: Basic to Translational Science* author instructions page.

Manuscript received March 7, 2019; revised manuscript received May 27, 2019, accepted May 28, 2019.

ISSN 2452-302X https://doi.org/10.1016/j.jacbts.2019.05.009

ABBREVIATIONS AND ACRONYMS

AAV = adeno-associated virus

CVD = cardiovascular diseases

CHIP = clonal hematopoiesis of indeterminate potential

LTL = leukocyte telomere length

TCA = telomere-CHIP-atherosclerosis

TERC = telomerase RNA component

TERT = telomerase reverse transcriptase

TRF2 = telomere repeat-binding factor 2

telomeres invariably shorten with age and cell division (3).

Although there could be asynchrony of telomere length among different tissues (4), peripheral leukocyte DNA has been most commonly used in clinical studies to measure leukocyte telomere length (LTL) (5). Several methods have been used to measure LTL, including terminal restriction fragment analysis by hybridization with telomere sequence probes, single telomere amplification and blotting, flow cytometry of cells following hybridization with fluorescent peptide nucleic acid probes, quantitative fluorescence in situ hybridization with fluorescent telomere peptide nucleic acid probes, and quantitative polymerase chain reaction assays (6). Due to the different methods used in clinical trials and large interbatch coefficients of variations, there is no current gold standard of telomere length measurement, and therefore, comparison of telomere lengths between different clinical trials could be misleading (7).

Traditional risk factors for cardiovascular diseases (CVD), such as smoking, diabetes mellitus, dyslipidemia, hypertension, obesity, and shift work, have been associated with short LTL (8). In the prospective WOSCOPS (West of Scotland Primary Prevention Study) trial, subjects in the lowest tertile of LTL had a 44% increased risk of 5-year major cardiovascular events compared with subjects in the highest tertile of LTL (9). Another meta-analysis study with 43,725 participants and 8,400 patients revealed that short LTL had a pooled relative risk for coronary heart disease of 1.54 (95% confidence interval: 1.30 to 1.83). In addition, short LTL was associated with coronary artery disease risk independent of traditional vascular risk factors. The association of short LTL with cerebrovascular disease is less significant than that with coronary artery disease (10). Short LTL also affects the prognosis of coronary artery disease. In a prospective WHI (Women's Health Initiative) study with 1,525 post-menopausal women, shorter LTL was associated with higher risks of mortality (11). Further analysis showed that patients with myocardial infarction had shorter LTL, which was equivalent to that observed in individuals without myocardial infarction but who were 8 to 12 years older in biological age (12). Shorter LTL was also associated with increased proinflammatory activity in high-risk unstable plaque on virtual histology intravascular ultrasound (13) and delayed re-endothelialization after drug-eluting stent implantation (14) in acute coronary syndrome. When patients developed chronic heart failure, they were also observed to have shorter LTL (15). Moreover, short LTL was also associated with congestive heart failure severity and clinical outcomes (16).

Despite the fact that current robust epidemiological and animal study evidence supports the telomere attrition links between age and CVDs, there is no clear route that leads to the development of telomere therapeutics against CVDs in the future due to the following limitations. First, in adult somatic cells, manipulation of the telomere system bears an oncogenic risk (17,18). Thus, therapeutic techniques based on the overexpression of telomerase and other telomere-related signals should be applied after considering cell-type and tissue interactions. Second, there is still no clear mechanistic insight into the link between telomere and/or telomerase and atherosclerosis development (19). Third, the telomere system is complex and regulated by various feedback mechanisms, including circadian rhythm oscillations (20), and a direct interruption of 1 target in the telomere pathway can lead to various side effects.

TELOMERES AND TELOMERASE

Because DNA polymerase is unable to replicate the 3′ ends of chromosomes fully, the so-called "end-replication problem," telomeres shorten during each cell replicated cycle (21). When telomeres reach a critically short length, genomic instability activates the DNA repair system and induces replicative arrest, senescence, and cell death (22).

In primary human cells, each time a cell divides, 50 to 100 bases are lost from the telomeres on each chromosome. This loss is much larger than the estimation from end-replication mechanisms, indicating that there are other contributing factors for telomere attrition in human cells (23). Oxidative stress and tissue inflammation have been observed to accelerate telomere shortening and reduced replicative lifespans (24). Telomere shortening is considered a biological molecular clock and is the underlying mechanism proposed to explain the limited lifespan of cells in culture, known as the Hayflick limit (25). During the progressive accumulation of senescent cells in aging, there is a marked increase in the secretion of proinflammatory cytokines, adhesion molecules, growth factors, and proteases from senescent cells (26,27). This inflammatory signaling initiates a vicious cycle that enhances telomere dysfunction, triggers replicative senescence, and promotes aging and development of age-associated diseases (28).

Telomerase is a crucial component in telomere maintenance and regulation. It consists of an RNA

template known as telomerase RNA component (TERC) and a DNA reverse transcriptase polymerase known as telomerase reverse transcriptase (TERT) (**Figure 1**). Telomerase synthesizes new telomeric DNAs to compensate for the loss during cell divisions (29). The overexpression of telomerase extends the lifespan of cells in culture and transforms them into cancerous cells (30). Adult somatic cells typically have a low or undetectable level of telomerase activity with limited longevity; high telomerase activity is restricted to germ cells, pluripotent embryonic stem cells, and hematopoietic progenitor cells (31).

Telomere length is determined by genetic and nongenetic factors. Based on genome-wide association studies, several genomic variants were identified to be associated with the average LTL (32). A large-scale meta-analysis also reported a consistent and high heritability for telomere length (10). Several nongenetic factors that contribute to inflammation and oxidative stress were reported to have significant impacts on LTL, such as psychosocial stress, alcohol consumption, physical inactivity, unhealthy diet, smoking, and obesity (33,34). Thus, shortened LTL reflects inheritable genomic features, previous mitotic history, cumulative exposure to inflammation and oxidation stress, and the availability of telomerase activity for cells.

Although its causal relationships are still unclear, based on epidemiology studies, telomere attrition is considered to be associated with aging and aging-related diseases, such as CVDs, chronic lung disease, metabolic disorders, neurodegenerative diseases, cognitive disorders, and dysregulated immune function (35). The lifespan of older adults was reported to positively correlate with telomere length (36).

It was observed that the specific telomere syndromes or telomeropathies that affect humans, such as Hoyeraal-Hreidarsson syndrome, dyskeratosis congenita, and aplastic anemia, are caused by germline mutations in telomere maintenance genes. These telomere syndromes present a diverse manifestation but share the features of premature aging, loss of tissue regenerative capacity, increases in inflammation, and prominent organ failure (37).

GENE THERAPY WITH TELOMERE AND TELOMERASE FOR CVDs

Robust epidemiological and genetic evidence linking telomere length and CVD risk support the therapeutic hypothesis that genetic manipulations of the telomere system can be a potential treatment target for CVDs. Mice with genetic knockout of *TERC* or *TERT* had progressively shorter telomeres over generations and showed features such as severe developmental defects, aging pathologies, and premature death (38). Reconstitution of *TERC* or *TERT* expression in the *TERC*- or *TERT*-deficient mice with critically short telomeres resulted in elongation of telomeres, less DNA damage, decreases in aging biomarkers, and delay in age-related pathologies (39). In these mice models, short telomeres and associated pathologies were treated and halted by telomerase re-expression. These findings provided the concept for therapeutic strategies to delay age-associated pathologies by transiently increasing telomerase expression.

Telomerase gene therapy was first achieved by delivering mouse *TERT* with an adeno-associated virus (AAV) into young and old mice. This non-integrative gene therapy resulted in elongated telomeres, extended lifespans, and delayed age-associated pathologies, such as insulin sensitivity, osteoporosis, and neuromuscular coordination, in both age groups (40). Importantly, telomerase-treated mice did not develop cancer at a higher rate than the corresponding control group (41). With the nonintegrative and replication incompetent properties of AAVs, this strategy restricted *TERT* expression to a few cell divisions and provided a relatively genome-safe TERT activation. Thus, these studies in mice supported the feasibility of telomerase activation treatment to overcome the adverse consequences of critically short telomeres. Applications of AAV-*TERT* gene therapy in specific telomere syndromes also showed expected therapeutic effects in preclinical mice models, such as aplastic anemia and pulmonary fibrosis (42,43). A report for age-associated diseases, such as CVDs, demonstrated improved ventricular function and limited infarct scars after acute myocardial infarction with *TERT* gene therapy in a preclinical mouse model (44). *TERT* gene therapy is a promising candidate that deserves further research efforts for clinical implementation for the treatment of age-associated diseases.

Apart from direct *TERT* delivery by nonintegrative AAV vectors, new gene therapy methods using modified mRNA for in vitro encoding of TERT in human fibroblasts can transiently increase telomerase activity, rapidly extend telomeres, and increase proliferative capacity without the risks of insertional mutagenesis and off-target effects (45). In addition to proof-of-concept experimental data in mice, the development of safe strategies for transient and controllable telomerase activation in humans can be a subject of future studies.

FIGURE 1 The Human Telomerase Complex

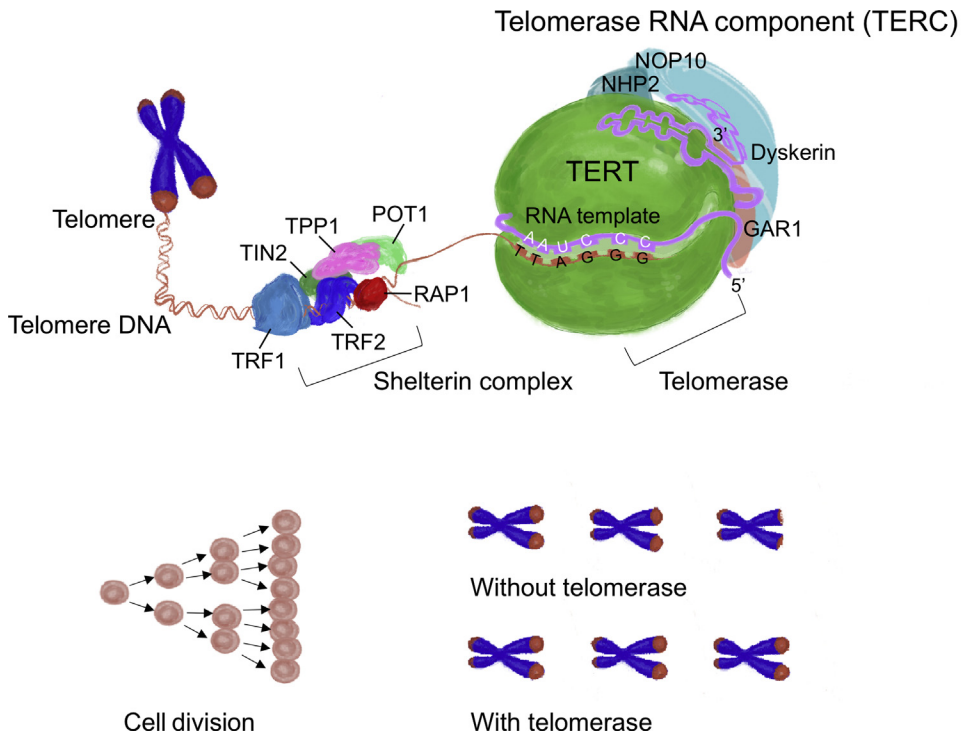

The human telomerase complex consists of human telomerase reverse transcriptase (TERT), telomerase RNA component (TERC), dyskerin, and ribonucleoproteins (GAR1, NHP2, and NOP10). The telomerase complex protects chromosome ends by lengthening telomeres in DNA strands. TERT is responsible for catalyzing the addition of DNA nucleotides to the ends of telomeres. TERC serves as an RNA template for telomere replications by TERT. Shelterin complex protects telomeres and regulates telomerase activity. Shelterin has 6 subunits, including telomere repeat binding factor 1 (TRF1), telomere repeat binding factor 2 (TRF2), repressor/activator protein 1 (RAP1), protection of telomere 1 (POT1), TRF1- and TRF2-interacting nuclear protein 2 (TIN2), and ACD shelterin complex subunit and telomerase recruitment factor (TPP1). Without telomerase, telomeres lose approximately 120 bp of DNA in human cells. Shortened and dysfunctional telomeric ends will result in genomic instability, tumorigenesis, and cardiovascular aging.

PHARMACEUTICAL INTERVENTIONS FOR TELOMERES AND TELOMERASE ACTIVITY

Because of the pertinence of telomerase in antiaging gene therapy in mice models, several studies focused on the therapeutic interventions for telomerase modulations in humans. Several cardiovascular medications, which have been used for decades and have been shown to have significant survival benefits in patients, possess the effects of telomere length maintenance and senescence prevention.

Statins (3-hydroxy-3-methylglutaryl coenzyme A reductase inhibitors) exert various pleiotropic effects to prevent the development of atherosclerotic plaque (46). A cross-sectional analysis of 3,496 subjects from the U.S. National Health and Nutrition Examination Survey showed that telomere length appeared to be longer with a longer duration of statin usage (47). Statin therapy was associated with higher telomerase activity independently of multiple covariates, such as age, sex, smoking, lipid profile, and inflammation (48). Statins can enhance telomerase activity and protect telomeres through upregulation of the telomere repeat-binding factor (TRF)-2 in endothelial cells and endothelial progenitor cells (49). A more specific analysis of human T-lymphocytes showed that atorvastatin in pharmacologically relevant doses led to a transient increase in telomerase activity in T-cells. This effect, which could be blocked by inhibitors of Akt and phosphatidylinositol-4,5-bisphosphate 3 (PI3)-kinase, was more pronounced in the CD4+ than in the CD8+ T-cell subsets (50). In addition, it also prevented telomere shortening by accelerating DNA repair through Nijmegen breakage syndrome-1 protein stabilization and telomere maintenance in vascular smooth muscle cells (51).

The crosstalk between angiotensin II and telomere systems are noteworthy. Overexpression of TERT in vivo modified the angiotensin II–induced microvascular endothelial dysfunction (52). Angiotensin II induces oxidative stress and senescence in vascular smooth muscle cells with telomerase-independent oxidative stress-induced senescence and telomerase-dependent replicative senescence (53). Acute exposure of vascular smooth muscle cells to angiotensin II results in vascular smooth muscle senescence, which is not associated with telomerase activity changes and cannot be reversed by TERT overexpression. However, long-term exposure of vascular smooth muscle cells to angiotensin II induced reduction in proliferation and replicative senescence with telomere shortening (54). Angiotensin II receptor blockers (e.g., losartan) and angiotensin-converting enzyme inhibitors (e.g., captopril) were both shown to protect endothelial progenitor cells from senescence and dysfunction through telomerase cross-talk (55,56). However, some studies showed that captopril and losartan had no effect on telomere attrition caused by cardiac hypertrophy after abdominal aortic constriction in rats (57). Therefore, the clinical use of angiotensin-converting enzyme inhibitors or angiotensin II inhibitors for the modification of telomere systems requires further clinical studies.

Peroxisome proliferator-activated receptor agonists (e.g., pioglitazone) can increase the activity of telomerase and expression of TRF-2 in mice aorta and in mononuclear cells. Pioglitazone-treated mice were shown to possess the reduced senescence markers, p16, cell-cycle checkpoint kinase 2, and p53 (58). Angiotensin II–induced endothelial progenitor cells senescence was significantly reversed by pioglitazone through telomerase activity enhancement (59). Moreover, pioglitazone was able to increase the *TERT* and *TRF-2* expression in the hearts of diabetic rats (60).

The low potency telomerase activator TA-65, a bioactive molecule extracted from *Astragalus membranaceus,* has been historically used in Chinese traditional medicine as an antiaging drug and has been shown to have effects on telomere lengthening in mice. TA-65 treatment induces telomerase-dependent elongation of short telomeres and reverses DNA damages in fibroblasts (61) and human T cells (62). Randomized, double-blind, and placebo-controlled clinical trials showed that TA-65 treatment increased high-density lipoprotein cholesterol and reduced C-reactive protein in patients with metabolic syndrome (63) and was also found to elongate telomeres (64).

In addition, sex hormones were also reported to activate *TERT* transcription. For decades, androgen therapy was considered as the first treatment choice for aplastic anemia, without a clear understanding of the underlying mechanism. A recent study showed that the upregulated telomerase activity is responsible for the effectiveness of the androgen treatment effect in aplastic anemia. In mice with aplastic anemia induced by short telomeres, testosterone therapy halted telomere attrition and prevented subsequent death, by enhancing telomerase expression and lengthening telomeres (65). Moreover, a synthetic androgen, danazol, which was used in the treatment of human telomeropathies, was shown to elongate telomeres in circulating leukocytes and improve hematological parameters (66).

Although specific telomere-lengthening effects of telomerase activation affect cardiovascular health and aging, noncanonical, extracellular, and non–telomere-lengthening functions of telomerase were recently described (67). The off-target effects of these telomerase activating or telomere-lengthening compounds, including those in mitogen signaling and oncogenesis, should be considered before clinical usage.

INFLAMMATION, ATHEROSCLEROSIS, AND CLONAL HEMATOPOIESIS OF INDETERMINATE POTENTIAL

Atherosclerosis is the dominant pathology of CVD, including myocardial infarction, heart failure, stroke, and peripheral artery diseases (68). The prevalence of these diseases progressively increases with age. In addition, the risk factors of atherosclerotic diseases, such as aging, smoking, obesity, sedentary lifestyle, and unhealthy diet, have been reported to be associated with telomere shortening based on observational epidemiological studies (69). As observed in 1 of these studies, each kilobase pair shortening of telomeres in peripheral blood cells was estimated to result in 2.8- to 3.2-fold higher risk of myocardial infarction and stroke (70).

Telomeres in coronary endothelial cells are shorter in patients with atherosclerosis than in healthy individuals (71). Telomere shortening of endothelial cells might play a role in atherogenesis by increasing proinflammatory reactions and promoting high-risk unstable atherosclerotic plaques (72). In human abdominal aorta analysis, shorter telomere and higher attrition were observed in aged vessels with increased shear wall stress (73). Significant telomere attrition, shorter telomeres, and DNA damages were demonstrated in biopsied tissue from a failing heart;

these effects were only specific to cardiomyocytes, regardless of the age of the patients (74). Moreover, asynchronous shortening of the telomere length between cardiac atrial tissue and leukocytes served as a better biomarker than leukocyte length alone for post-cardiovascular surgery events (75).

Atherosclerosis is an inflammatory disease that involves vascular endothelium, smooth muscle, and blood cells (76). With aging, telomeres shorten, and blood cells start to accumulate somatic genetic mutations. As these blood cells gain a competitive expansion advantage, they give rise to some expanded clones of leukocytes that circulate in the peripheral blood, which is termed clonal hematopoiesis of indeterminate potential (CHIP) (77). More than 10% of septuagenarians exhibit CHIP, and its prevalence increases with age (78). Individuals with CHIP have increased cardiovascular mortalities independent of traditional risk factors (e.g., diabetes, hypertension, and dyslipidemia) (79). Current evidence shows that de novo mutations in *DNMT3A*, *TET2*, and *ASXL1* facilitate the clonal expansion of leukocytes (80,81). Macrophages from *TET2*-knockout mice resulted in the abnormal activation of the NLRP3 (Nucleotide-Binding Domain, Leucine-Rich-Containing Family, Pyrin Domain-Containing-3)-mediated inflammasome and contribute to enhanced atherosclerosis (82). Mice with CHIP mutations in hematopoietic cells also exhibited aggravated the development of heart failure (83).

Both telomere attrition and CHIP increase with age. Accordingly, progressive leukocyte telomere attrition can lead to genomic instability, which later results in CHIP (84). Therefore, it is assumed that the manipulation of the telomere system would be a possible treatment target of CHIP-related CVDs. Although current clinical evidence supports this concept, further research needs to be conducted. In a whole-genome sequencing study, the strongest association of CHIP was found to be an 8-bp deletion in intron 3 of the *TERT* gene (85). In the same study, telomere lengths were observed to be significantly shortened in individuals with CHIP. Dyskeratosis congenita is a rare progressive congenital disease with skin pigmentation, nail dystrophy, and leukoplakia of the oral mucosa. Dyskeratosis congenita is characterized by short telomeres with poor telomere maintenance, mainly caused by some abnormal mutations in ribosome and telomerase RNA components (86). Clonal expansion of hematopoietic cells bearing non-synonymous coding somatic mutations is a common feature that occurs in one-half of patients with dyskeratosis congenita (87). The telomerase complex controls hematopoietic cell differentiation and senescence in the induced pluripotent stem cell model (88). The telomere-CHIP-atherosclerosis (TCA) axis may provide several possible therapeutic targets, including modulating telomerase activity, rescuing senescent or mutated clonal cells, and inhibiting the inflammation from CHIP (**Central Illustration**). However, future investigations are required to understand the TCA axis before comprehensive clinical trials can be undertaken in the future.

Furthermore, several aspects of the TCA axis remain to be understood. First, telomere attrition and CHIP are a progressive, long-term processes, like atherosclerosis, and thus require better cellular or animal models to simulate these 2 chronic processes (e.g., low-density lipoprotein receptor knockout mice for atherosclerosis). Second, the evidence for the connection between telomere attrition and CHIP is based on a clinical association study. Therefore, a future study is required to understand their underlying mechanisms. Third, the telomere length variations between individuals and different attrition rates between tissues are not directly linked to CHIP occurrence and atherosclerosis. The connections could be affected by other factors, such as different responses to critical short telomeres or inflammation. Even among patients with dyskeratosis congenita, >10% of them do not develop CHIP (87). Lastly, there is still no evidence showing that CHIP can be prevented or reversed via telomere modulation.

IMMUNE MODULATION

Inflammation is a protective response to injury of a process that delivers leukocytes to sites of infection or tissue damage. Acute inflammation usually lasts for hours and has many positive (e.g., interleukin-6/tumor necrosis factor-α) and negative (e.g., interleukin-10) regulators. If infection and tissue damage persists, if the healing process is somehow disturbed, or if 1 of the negative control mechanisms fails, inflammation may progress to a chronic state that can last for weeks, months, or maybe years (89). In many common chronic diseases, such as atherosclerosis, the chronic inflammatory process does not follow a manifestation of an acute reaction but begins as a low grade and smoldering response (90).

Aging, DNA damage, and stem cell failure are closely associated with low levels of chronic inflammation (91). Chronic low-grade inflammation increases oxidative stress and enhances telomere dysfunction (92). The links between telomere dysfunction and chronic inflammation are bidirectional and can result in complex vicious cycles. Telomerase is active in the human coronary artery

CENTRAL ILLUSTRATION **Telomere, CHIP, and Atherosclerosis (TCA) Pathway in the Treatment of Cardiovascular Diseases**

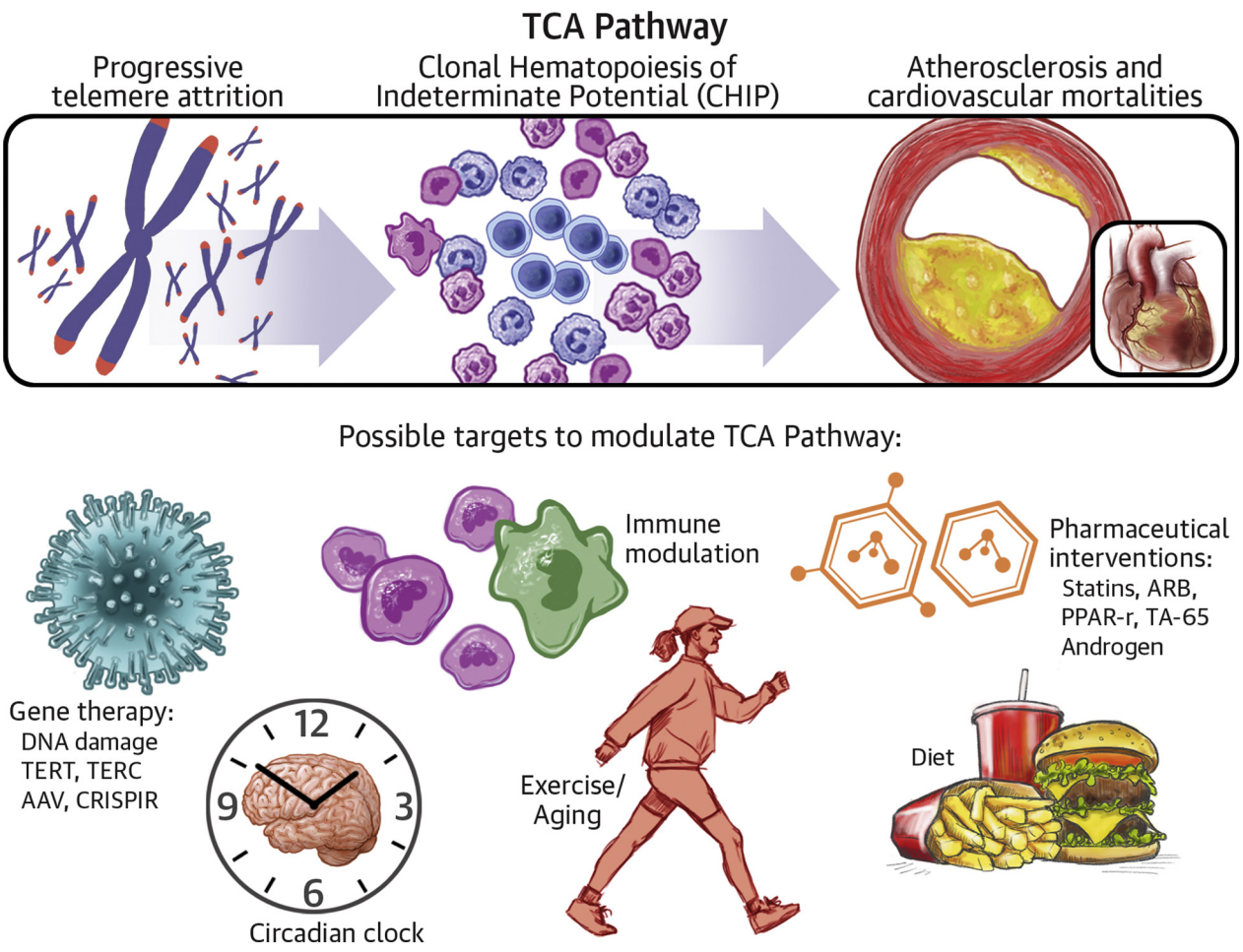

Yeh, J.-K. et al. J Am Coll Cardiol Basic Trans Science. 2019;4(7):855-65.

Progressive telomere attrition can lead to genomic instability, which later results in clonal hematopoiesis of indeterminate potential (CHIP). Individuals with CHIP have increased atherosclerosis and cardiovascular mortalities independent of traditional risk factors, such as diabetes, hypertension, and dyslipidemia. Gene therapy, pharmaceutical interventions, immune modulation, circadian clock, exercise, and diet are possible targets to modulate the telomere/telomerase system, CHIP, and atherosclerosis pathway. AAV = adeno-associated virus; ARB = angiotensin II receptor blocker; CRISPR = clustered regularly interspaced short palindromic repeats; IL = interleukin; NF-κB = nuclear factor-kappa B; PPAR = peroxisome proliferator-activated receptor; TCA = telomere-CHIP-atherosclerosis; TERC = telomerase RNA component; TERT = telomerase reverse transcriptase; TNF = tumor necrosis factor.

and its activity is increased during atherosclerosis formation (93). Different proinflammatory mediators increased *TERT* mRNA and telomerase activity in macrophages in atherosclerosis through nuclear factor-κB signaling (93). Premature telomere erosion in peripheral blood mononuclear cells is a common phenomenon in obesity, myocardial infarction, and atherosclerosis (8). In telomerase-deficient mice, marked increases in proinflammatory cytokines interleukin-6, CXCL16 (Chemokine (C-X-C motif) ligand 16), and tumor necrosis factor-α were observed in pulmonary tissues (94). Chronic inflammation aggravates telomere dysfunction and cellular senescence through oxidative stress activation and cyclooxygenase-2–dependent reactive oxygen species production (95). From this evidence, the telomere system and chronic inflammation are suspected to be linked closely.

The aging process in humans is associated with changes in circadian rhythm patterns (96). Circadian rhythm controls telomeres and telomerase activity through circadian locomotor output cycles kaput

gene–aryl hydrocarbon receptor nuclear translocator-like protein 1 heterodimers (97). Mice and humans with circadian rhythm abnormalities not only have increased vascular senescence (98), impaired endothelial progenitor cell function, enhanced atherosclerosis (99), and obesity (100) but are also prone to chronic inflammation and sepsis (101). The intersection of circadian mechanics into the linkage between telomere and chronic inflammation provides more opportunities in combating atherosclerosis. For example, experimental evidence in mice indicate that melatonin regulates the transactivation of telomerase and the expression of core clock and clock-related genes (102). Melatonin inhibits smooth muscle cell inflammation and atherosclerosis in mice (103,104). For example, physicians in emergency departments are known to lose their telomerase oscillation, and have low telomerase activities and circadian misalignments that increases CVD risk factors (105). Further research on the connections between telomerase and circadian rhythm will shed more light upon this area.

However, the connections between telomere and atherosclerosis are not definitive. Although mice with double deficiency in *ApoE* and *TERC* have extensive telomere attritions, a substantial reduction of atherosclerosis was observed in them compared to mice with normal telomerases (106). Short telomeres result in immunosenescence and lead to protection from atherosclerosis (107). Moreover, not all clinical studies have found significant associations between telomere lengths in white blood cells and morbidity or mortalities (108).

AGING CARDIOVASCULAR PATIENTS AND TELOMERE THERPAY

According to World Health Organization data, by 2020, all countries across the world will face significant challenges to their health and social systems due to the aging demographic shift (109). The number of people aged 60 years and older will outnumber children younger than 5 years. The pace of the aging population will be faster in future decades. There are 3 significant differences in telomere therapy between the young and older adult population. First, in older adult individuals, the evidence supporting the telomere length and remaining lifespan is controversial (110). The contradictory results of these studies suggest that in septuagenarians and octogenarians, the role of telomere in survival becomes less important (111). A recent study indicated that healthy lifestyle habits such as not smoking and not being obese at the age of 71 were the most significant associated factors with survival at the age of 85 years or older in men (112). The efficacy of manipulation of the telomere system with younger subjects versus older subjects will need exploratory studies in the future. Second, the goals of telomere cardiovascular therapy in young subjects and older adults subjects are different. In young subjects, the goal of telomere therapy is to prevent cardiovascular senescence and diseases, whereas in older adult subjects, the goal of telomere therapy is to restoration of cardiovascular functions. Third, the prevention of CHIP and atherosclerosis with telomere targets in young subjects requires long-term treatments. Moreover, the efficacy and effectiveness of the treatment involving CHIP detection, prevention, and correction in octogenarians are questionable. Further clinical studies are required to overcome these limitations.

TELOMERE THERAPY FROM THE BENCH TO THE BEDSIDE

Telomere biology could be potentially involved in the development of age-associated CVDs including atherosclerosis, hypertension, myocardial infarction, and heart failure. Critically shortened telomeres activate a series of downstream changes that induce cardiomyocyte cell cycle arrest and cellular senescence (38). The reduced proliferative potential of cardiovascular systems limits the regenerative capacity of aged and injured myocardium and vasculature (113). Thus, therapeutic strategies to restore the proliferative potential of adult cardiovascular systems are considered as a promising alternative treatment for CVDs. In mouse models, telomerase gene transfer therapy provides an attractive way for cardiovascular restoration and deserves future investigations. Although we are still far from applying the current knowledge in daily therapeutic protocols, many studies seem to agree with the fact that a combination of exercise, healthy diet, low everyday stress, and anti-inflammatory agents intake may prove to be beneficial in promoting human longevity by modulating the telomere system and in slowing down the effects of many chronic disorders. The present knowledge in this regard still requires input from different studies, and further investigations are needed to uncover the true molecular relationships involved in the previously described phenomena.

ADDRESS FOR CORRESPONDENCE: Dr. Chao-Yung Wang, Department of Cardiology, Chang Gung Memorial Hospital, and Chang Gung University College of Medicine, 5 Fu-Hsing Street, Taoyuan 333, Taiwan. E-mail: cwang@ocean.ag.

REFERENCES

1. Blackburn EH. Telomere states and cell fates. Nature 2000;408:53–6.

2. d'Adda di Fagagna F. Living on a break: cellular senescence as a DNA-damage response. Nat Rev Cancer 2008;8:512–22.

3. Rehkopf DH, Needham BL, Lin J, et al. Leukocyte telomere length in relation to 17 biomarkers of cardiovascular disease risk: a cross-sectional study of US adults. PLoS Med 2016;13:e1002188.

4. Wang C-Y. Asynchronous shortening of telomere length and cardiovascular outcomes. J Am Coll Cardiol Basic Trans Sci 2018;3:601–3.

5. Fitzpatrick AL, Kronmal RA, Gardner JP, et al. Leukocyte telomere length and cardiovascular disease in the cardiovascular health study. Am J Epidemiol 2007;165:14–21.

6. Fasching CL. Telomere length measurement as a clinical biomarker of aging and disease. Crit Rev Clin Lab Sci 2018;55:443–65.

7. Martin-Ruiz CM, Baird D, Roger L, et al. Reproducibility of telomere length assessment: an international collaborative study. Int J Epidemiol 2015;44:1673–83.

8. Valdes AM, Andrew T, Gardner JP, Kimura M. Obesity, cigarette smoking, and telomere length in women. Lancet 2005.

9. Brouilette SW, Moore JS, McMahon AD, et al. Telomere length, risk of coronary heart disease, and statin treatment in the West of Scotland Primary Prevention Study: a nested case-control study. Lancet 2007;369:107–14.

10. Haycock PC, Heydon EE, Kaptoge S, Butterworth AS, Thompson A, Willeit P. Leukocyte telomere length and risk of cardiovascular disease: systematic review and meta-analysis. BMJ 2014;349:g4227.

11. Carty CL, Kooperberg C, Liu J, et al. Leukocyte telomere length and risks of incident coronary heart disease and mortality in a racially diverse population of postmenopausal women. Arterioscler Thromb Vasc Biol 2015;35:2225–31.

12. Samani NJ, Boultby R, Butler R, Thompson JR, Goodall AH. Telomere shortening in atherosclerosis. Lancet 2001;358:472–3.

13. Calvert PA, Liew T-V, Gorenne I, et al. Leukocyte telomere length is associated with high-risk plaques on virtual histology intravascular ultrasound and increased proinflammatory activity. Arterioscler Thromb Vasc Biol 2011;31:2157–64.

14. Armstrong EJ, Xing L, Zhang J, et al. Association between leukocyte telomere length and drug-eluting stent strut coverage by optical coherence tomography. J Am Coll Cardiol 2012;59:2218–9.

15. van der Harst P, van der Steege G, de Boer RA, et al. Telomere length of circulating leukocytes is decreased in patients with chronic heart failure. J Am Coll Cardiol 2007;49:1459–64.

16. Haver VG, Mateo Leach I, Kjekshus J, et al. Telomere length and outcomes in ischaemic heart failure: data from the COntrolled ROsuvastatin multiNAtional Trial in Heart Failure (CORONA). Eur J Heart Fail 2015;17:313–9.

17. Smith L, Luchini C, Demurtas J, et al. Telomere length and health outcomes: an umbrella review of systematic reviews and meta-analyses of observational studies. Ageing Res Rev 2019;51:1–10.

18. Hannen R, Bartsch JW. Essential roles of telomerase reverse transcriptase hTERT in cancer stemness and metastasis. FEBS Lett 2018;592:2023–31.

19. De Meyer T, Nawrot T, Bekaert S, De Buyzere ML, Rietzschel ER, Andrés V. Telomere length as cardiovascular aging biomarker: JACC review topic of the week. J Am Coll Cardiol 2018;72:805–13.

20. Qu Y, Mao M, Li X, et al. Telomerase reconstitution contributes to resetting of circadian rhythm in fibroblasts. Mol Cell Biochem 2008;313:11–8.

21. Levy MZ, Allsopp RC, Futcher AB, Greider CW, Harley CB. Telomere end-replication problem and cell aging. J Mol Biol 1992;225:951–60.

22. Hackett JA, Feldser DM, Greider CW. Telomere dysfunction increases mutation rate and genomic instability. Cell 2001;106:275–86.

23. O'Sullivan RJ, Karlseder J. Telomeres: protecting chromosomes against genome instability. Nat Rev Mol Cell Biol 2010;11:171–81.

24. Kawanishi S, Oikawa S. Mechanism of telomere shortening by oxidative stress. Ann N Y Acad Sci 2004;1019:278–84.

25. Shay JW, Wright WE. Hayflick, his limit, and cellular ageing. Nat Rev Mol Cell Biol 2000;1:72–6.

26. Jiang H, Schiffer E, Song Z, et al. Proteins induced by telomere dysfunction and DNA damage represent biomarkers of human aging and disease. Proc Natl Acad Sci U S A 2008;105:11299–304.

27. López-Otín C, Blasco MA, Partridge L, Serrano M, Kroemer G. The hallmarks of aging. Cell 2013;153:1194–217.

28. Gilley D, Tanaka H, Herbert B-S. Telomere dysfunction in aging and cancer. Int J Biochem Cell Biol 2005;37:1000–13.

29. Shay JW, Wright WE. Telomeres and telomerase: three decades of progress. Nat Rev Genet 2019;20:299–309.

30. Mitchell JR, Collins K. Human telomerase activation requires two independent interactions between telomerase RNA and telomerase reverse transcriptase. Mol Cell 2000;6:361–71.

31. Wright WE, Piatyszek MA, Rainey WE, Byrd W, Shay JW. Telomerase activity in human germline and embryonic tissues and cells. Dev Genet 1996;18:173–9.

32. Codd V, Nelson CP, Albrecht E, et al. Identification of seven loci affecting mean telomere length and their association with disease. Nat Genet 2013;45:422–7. 427e1–2.

33. Bekaert S, De Meyer T, Rietzschel ER. Telomere length and cardiovascular risk factors in a middle-aged population free of overt cardiovascular disease. Aging Cell 2007;6:639–47.

34. Yeh J-K, Wang C-Y. Telomeres and telomerase in cardiovascular diseases. Genes 2016;7(9). pii: E58.

35. Mangaonkar AA, Patnaik MM. Short telomere syndromes in clinical practice: bridging bench and bedside. Mayo Clin Proc 2018;93:904–16.

36. Heidinger BJ, Blount JD, Boner W, Griffiths K, Metcalfe NB, Monaghan P. Telomere length in early life predicts lifespan. Proc Natl Acad Sci U S A 2012;109:1743–8.

37. Calado RT, Young NS. Telomere diseases. N Engl J Med 2009;361:2353–65.

38. Leri A, Franco S, Zacheo A, et al. Ablation of telomerase and telomere loss leads to cardiac dilatation and heart failure associated with p53 upregulation. EMBO J 2003;22:131–9.

39. Samper E, Flores JM, Blasco MA. Restoration of telomerase activity rescues chromosomal instability and premature aging in Terc-/- mice with short telomeres. EMBO Rep 2001;2:800–7.

40. de Jesus BB, Vera E, Schneeberger K, et al. Telomerase gene therapy in adult and old mice delays aging and increases longevity without increasing cancer. EMBO Mol Med 2012;4:691–704.

41. Bernardes de Jesus B, Blasco MA. Telomerase at the intersection of cancer and aging. Trends Genet 2013;29:513–20.

42. Bär C, Povedano JM, Serrano R, et al. Telomerase gene therapy rescues telomere length, bone marrow aplasia, and survival in mice with aplastic anemia. Blood 2016;127:1770–9.

43. Povedano JM, Martinez P, Serrano R, et al. Therapeutic effects of telomerase in mice with pulmonary fibrosis induced by damage to the lungs and short telomeres. Elife 2018;7.

44. Bär C, Bernardes de Jesus B, Serrano R, et al. Telomerase expression confers cardioprotection in the adult mouse heart after acute myocardial infarction. Nat Commun 2014;5:5863.

45. Ramunas J, Yakubov E, Brady JJ, et al. Transient delivery of modified mRNA encoding TERT rapidly extends telomeres in human cells. FASEB J 2015;29:1930–9.

46. Wang C-Y, Liu P-Y, Liao JK. Pleiotropic effects of statin therapy: molecular mechanisms and clinical results. Trends Mol Med 2008;14:37–44.

47. Tran PT, Meeker AK, Platz EA. Association between statin drug use and peripheral blood leukocyte telomere length in the National Health and Nutrition Examination Survey 1999–2002: a cross-sectional study. Ann Epidemiol 2018;28:529–34.

48. Boccardi V, Barbieri M, Rizzo MR, et al. A new pleiotropic effect of statins in elderly: modulation of telomerase activity. FASEB J 2013;27:3879–85.

49. Spyridopoulos I, Haendeler J, Urbich C, et al. Statins enhance migratory capacity by upregulation of the telomere repeat-binding factor TRF2 in endothelial progenitor cells. Circulation 2004;110:3136–42.

50. Bennaceur K, Atwill M, Al Zhrany N, et al. Atorvastatin induces T cell proliferation by a telomerase reverse transcriptase (TERT) mediated mechanism. Atherosclerosis 2014;236:312–20.

51. Mahmoudi M, Gorenne I, Mercer J, Figg N, Littlewood T, Bennett M. Statins use a novel Nijmegen breakage syndrome-1–dependent pathway to accelerate DNA repair in vascular smooth muscle cells. Circ Res 2008;103:717–25.

52. Ait-Aissa K, Kadlec AO, Hockenberry J, Gutterman DD, Beyer AM. Telomerase reverse transcriptase protects against angiotensin II-induced microvascular endothelial dysfunction. Am J Physiol Heart Circ Physiol 2018;314:H1053–60.

53. Matthews C, Gorenne I, Scott S, et al. Vascular smooth muscle cells undergo telomere-based senescence in human atherosclerosis: effects of telomerase and oxidative stress. Circ Res 2006;99:156–64.

54. Herbert KE, Mistry Y, Hastings R, Poolman T, Niklason L, Williams B. Angiotensin II-mediated oxidative DNA damage accelerates cellular senescence in cultured human vascular smooth muscle cells via telomere-dependent and independent pathways. Circ Res 2008;102:201–8.

55. Imanishi T, Tsujioka H, Akasaka T. Endothelial progenitor cells dysfunction and senescence: contribution to oxidative stress. Curr Cardiol Rev 2008;4:275–86.

56. Donnini S, Terzuoli E, Ziche M, Morbidelli L. Sulfhydryl angiotensin-converting enzyme inhibitor promotes endothelial cell survival through nitric-oxide synthase, fibroblast growth factor-2, and telomerase cross. J Pharmacol Exp Ther 2010;332:776–84.

57. Sheng R, Gu Z-L, Xie M-L. Epigallocatechin gallate, the major component of polyphenols in green tea, inhibits telomere attrition mediated cardiomyocyte apoptosis in cardiac hypertrophy. Int J Cardiol 2013;162:199–209.

58. Werner C, Gensch C, Pöss J, Haendeler J, Böhm M, Laufs U. Pioglitazone activates aortic telomerase and prevents stress-induced endothelial apoptosis. Atherosclerosis 2011;216:23–34.

59. Imanishi T, Kobayashi K, Kuroi A, Ikejima H, Akasaka T. Pioglitazone inhibits angiotensin II-induced senescence of endothelial progenitor cell. Hypertens Res 2008;31:757–65.

60. Makino N, Maeda T, Oyama J-I, Higuchi Y, Mimori K. Improving insulin sensitivity via activation of PPAR-gamma increases telomerase activity in the heart of OLETF rats. Am J Physiol Heart Circ Physiol 2009;297:H2188–95.

61. Bernardes de Jesus B, Schneeberger K, Vera E, Tejera A, Harley CB, Blasco MA. The telomerase activator TA-65 elongates short telomeres and increases health span of adult/old mice without increasing cancer incidence. Aging Cell 2011;10:604–21.

62. Molgora B, Bateman R, Sweeney G, et al. Functional assessment of pharmacological telomerase activators in human T cells. Cells 2013;2:57–66.

63. Fernandez ML, Thomas MS, Lemos BS, et al. TA-65, a telomerase activator improves cardiovascular markers in patients with metabolic syndrome. Curr Pharm Des 2018;24:1905–11.

64. Salvador L, Singaravelu G, Harley CB, Flom P, Suram A, Raffaele JM. A natural product telomerase activator lengthens telomeres in humans: a randomized, double blind, and placebo controlled study. Rejuvenation Res 2016;19:478–84.

65. Ziegler P, Schrezenmeier H, Akkad J, et al. Telomere elongation and clinical response to androgen treatment in a patient with aplastic anemia and a heterozygous hTERT gene mutation. Ann Hematol 2012;91:1115–20.

66. Townsley DM, Dumitriu B, Young NS. Danazol treatment for telomere diseases. N Engl J Med 2016;375:1095–6.

67. Ait-Aissa K, Ebben JD, Kadlec AO, Beyer AM. Friend or foe? Telomerase as a pharmacological target in cancer and cardiovascular disease. Pharmacol Res 2016;111:422–33.

68. Libby P, Ridker PM, Hansson GK. Progress and challenges in translating the biology of atherosclerosis. Nature 2011;473:317–25.

69. Fernández-Alvira JM, Fuster V, Dorado B, et al. Short telomere load, telomere length, and subclinical atherosclerosis: the PESA study. J Am Coll Cardiol 2016;67:2467–76.

70. Zee RYL, Michaud SE, Germer S, Ridker PM. Association of shorter mean telomere length with risk of incident myocardial infarction: a prospective, nested case-control approach. Clin Chim Acta 2009;403:139–41.

71. Minamino T, Miyauchi H, Yoshida T, Ishida Y, Yoshida H, Komuro I. Endothelial cell senescence in human atherosclerosis: role of telomere in endothelial dysfunction. Circulation 2002;105:1541–4.

72. Kurz DJ, Decary S, Hong Y, Trivier E, Akhmedov A, Erusalimsky JD. Chronic oxidative stress compromises telomere integrity and accelerates the onset of senescence in human endothelial cells. J Cell Sci 2004;117:2417–26.

73. Okuda K, Khan MY, Skurnick J, Kimura M, Aviv H, Aviv A. Telomere attrition of the human abdominal aorta: relationships with age and atherosclerosis. Atherosclerosis 2000;152:391–8.

74. Sharifi-Sanjani M, Oyster NM, Tichy ED, et al. Cardiomyocyte-specific telomere shortening is a distinct signature of heart failure in humans. J Am Heart Assoc 2017;6(9).

75. Yin H, Akawi O, Fox SA, et al. Cardiac-referenced leukocyte telomere length and outcomes after cardiovascular surgery. J Am Coll Cardiol Basic Trans Sci 2018;3:591–600.

76. Hansson GK, Libby P. The immune response in atherosclerosis: a double-edged sword. Nat Rev Immunol 2006;6:508–19.

77. Libby P, Ebert BL. CHIP (clonal hematopoiesis of indeterminate potential). Circulation 2018;138:666–8.

78. Ebert BL, Libby P. Clonal hematopoiesis confers predisposition to both cardiovascular disease and cancer: a newly recognized link between two major killers. Ann Intern Med 2018;169:116–7.

79. Jaiswal S, Natarajan P, Silver AJ, et al. Clonal hematopoiesis and risk of atherosclerotic cardiovascular disease. N Engl J Med 2017;377:111–21.

80. Jaiswal S, Fontanillas P, Flannick J, et al. Age-related clonal hematopoiesis associated with adverse outcomes. N Engl J Med 2014;371:2488–98.

81. Fuster JJ, MacLauchlan S, Zuriaga MA, et al. Clonal hematopoiesis associated with TET2 deficiency accelerates atherosclerosis development in mice. Science 2017;355:842–7.

82. Basiorka AA, McGraw KL, Eksioglu EA, et al. The NLRP3 inflammasome functions as a driver of the myelodysplastic syndrome phenotype. Blood 2016;128:2960–75.

83. Sano S, Oshima K, Wang Y, et al. Tet2-mediated clonal hematopoiesis accelerates heart failure through a mechanism involving the IL-1β/NLRP3 inflammasome. J Am Coll Cardiol 2018;71:875–86.

84. Aviv A, Levy D. Hemothelium, clonal hematopoiesis of indeterminate potential, and atherosclerosis. Circulation 2019;139:7–9.

85. Zink F, Stacey SN, Norddahl GL, et al. Clonal hematopoiesis, with and without candidate driver mutations, is common in the elderly. Blood 2017;130:742–52.

86. Mitchell JR, Wood E, Collins K. A telomerase component is defective in the human disease dyskeratosis congenita. Nature 1999;402:551–5.

87. Perdigones N, Perin JC, Schiano I, et al. Clonal hematopoiesis in patients with dyskeratosis congenita. Am J Hematol 2016;91:1227–33.

88. Jose SS, Tidu F, Burilova P, Kepak T, Bendickova K, Fric J. The telomerase complex directly controls hematopoietic stem cell differentiation and senescence in an induced pluripotent stem cell model of telomeropathy. Front Genet 2018;9:345.

89. Rymer JA, Newby LK. Failure to launch: targeting inflammation in acute coronary syndromes. J Am Coll Cardiol Basic Trans Sci 2017;2:484–97.

90. Felisbino MB, McKinsey TA. Epigenetics in cardiac fibrosis: emphasis on inflammation and fibroblast activation. J Am Coll Cardiol Basic Trans Sci 2018;3:704–15.

91. Khatami M. Theories of aging and chronic diseases: chronic inflammation an interdependent "roadmap" to age-associated illnesses. In: Khatami M, editor. Inflammation, Aging and Cancer: Biological Injustices to Molecular Village of Immunity that Guard Health. Cham, Switzerland: Springer International Publishing, 2017:91–174.

92. Demissie S, Levy D, Benjamin EJ, et al. Insulin resistance, oxidative stress, hypertension, and leukocyte telomere length in men from the Framingham Heart Study. Aging Cell 2006;5:325–30.

93. Gizard F, Heywood EB, Findeisen HM, et al. Telomerase activation in atherosclerosis and induction of telomerase reverse transcriptase expression by inflammatory stimuli in macrophages. Arterioscler Thromb Vasc Biol 2011;31:245–52.

94. Liu T, Yu H, Ding L, et al. Conditional knockout of telomerase reverse transcriptase in

mesenchymal cells impairs mouse pulmonary fibrosis. PLoS One 2015;10:e0142547.

95. Jurk D, Wilson C, Passos JF, et al. Chronic inflammation induces telomere dysfunction and accelerates ageing in mice. Nat Commun 2014;2:4172.

96. Brown SA, Schmitt K, Eckert A. Aging and circadian disruption: causes and effects. Aging 2011;3:813–7.

97. Chen W-D, Wen M-S, Shie S-S, et al. The circadian rhythm controls telomeres and telomerase activity. Biochem Biophys Res Commun 2014;451:408–14.

98. Wang C-Y, Wen M-S, Wang H-W, et al. Increased vascular senescence and impaired endothelial progenitor cell function mediated by mutation of circadian gene Per2. Circulation 2008;118:2166–73.

99. McAlpine CS, Swirski FK. Circadian influence on metabolism and inflammation in atherosclerosis. Circ Res 2016;119:131–41.

100. Bass J, Takahashi JS. Circadian integration of metabolism and energetics. Science 2010;330:1349–54.

101. Wang C-Y, Hsieh M-J, Hsieh I-C, et al. CLOCK modulates survival and acute lung injury in mice with polymicrobial sepsis. Biochem Biophys Res Commun 2016;478:935–41.

102. Blask DE, Hill SM, Dauchy RT, et al. Circadian regulation of molecular, dietary, and metabolic signaling mechanisms of human breast cancer growth by the nocturnal melatonin signal and the consequences of its disruption by light at night. J Pineal Res 2011;51:259–69.

103. Li H-Y, Leu Y-L, Wu Y-C, Wang S-H. Melatonin inhibits in vitro smooth muscle cell inflammation and proliferation and atherosclerosis in apolipoprotein E-deficient mice. J Agric Food Chem 2019;67:1889–901.

104. Li H, Li J, Jiang X, et al. Melatonin enhances atherosclerotic plaque stability by inducing prolyl-4-hydroxylase α1 expression. J Hypertens 2019;37:964–71.

105. Morris CJ, Purvis TE, Hu K, Scheer FAJL. Circadian misalignment increases cardiovascular disease risk factors in humans. Proc Natl Acad Sci U S A 2016;113:E1402–11.

106. Rasmiena AA, Stefanovic N, Huynh K, et al. Attenuation of atherosclerosis in ApoE- and ApoE/GPX1-deficient mice by plasmalogen enrichment. Atherosclerosis 2015;241:e10.

107. Armanios M, Alder JK, Parry EM, Karim B, Strong MA, Greider CW. Short telomeres are sufficient to cause the degenerative defects associated with aging. Am J Hum Genet 2009;85:823–32.

108. Bischoff C, Petersen HC, Graakjaer J, et al. No association between telomere length and survival among the elderly and oldest old. Epidemiology 2006;17:190–4.

109. World Health Organization. World Report on Ageing and Health. Geneva, Switzerland: World Health Organization, 2015.

110. Zhan Y, Hägg S. Telomere length and cardiovascular disease risk. Curr Opin Cardiol 2019;34:270–4.

111. Martin-Ruiz CM, Gussekloo J, van Heemst D, von Zglinicki T, Westendorp RGJ. Telomere length in white blood cells is not associated with morbidity or mortality in the oldest old: a population-based study. Aging Cell 2005;4:287–90.

112. Franzon K, Byberg L, Sjögren P, Zethelius B, Cederholm T, Kilander L. Predictors of independent aging and survival: a 16-year follow-up report in octogenarian men. J Am Geriatr Soc 2017;65:1953–60.

113. Booth SA, Charchar FJ. Cardiac telomere length in heart development, function, and disease. Physiol Genomics 2017;49:368–84.

KEY WORDS aging, atherosclerosis, cardiomyocytes, immune modulation, telomeres

Letters

TO THE EDITOR

Breastfeeding in Patients With Heart Failure

Lack of Evidence and Consensus

We read with interest the paper by Koczo et al. (1). Breastfeeding in patients with peripartum cardiomyopathy (PPCM) remains highly controversial. Because positive effects for the health of both mothers and infants have been reported, exclusive breastfeeding is recommended in healthy women up to 6 months. In contrast, convincing data are scarce regarding infant safety and breastfeeding women who take medications, and evidence to support breastfeeding by critically ill women is lacking (2). Potential long-term sequelae induced by drugs may be underestimated for the mother and the infant.

In this context, some aspects of the paper by Koczo et al. (1) must be scrutinized.

First, only 15% of all women enrolled in the Investigations of Pregnancy-Associated Cardiomyopathy (IPAC) registry were breastfeeding at the time of entry. This number is substantially lower than the U.S. national rate (83.2%) reported by the Centers for Disease Control and Prevention (3). In addition, the total duration of breastfeeding in the IPAC registry is unknown, thus precluding any firm conclusions.

Second, patients with severe heart failure were substantially underrepresented in the breastfeeding group (1). Mean left ventricular ejection fraction (LVEF) was 39% at entry, and the vast majority of patients were in New York Heart Association functional class I and II (80%). Compared with other PPCM cohorts, the breastfeeding group displayed only mild cardiac dysfunction.

Third, in their original IPAC report (4), the authors described significant numbers of heart transplantations, ventricular assist device implantations, and deaths. Moreover, there was a substantial difference in outcome depending on the LVEF at initial diagnosis (<30% vs. >30%). Event rates (ventricular assist device implantation or death) in the first year postpartum were significantly higher in patients with LVEF <30% at baseline. These important outcome data are not included in the current analysis (1).

In summary, it is not possible to make conclusions regarding outcome and prognosis of PPCM patients with moderate to severe heart failure based on this analysis (1). Given the concerns, we advocate against broadly recommending breastfeeding in patients with PPCM, particularly in women with severe heart failure. In line with this advice, the European Society of Cardiology advises against breastfeeding in women with severe heart failure (Class IIb recommendation) (5). If a shared decision is made to continue breastfeeding (e.g., in patients with mild to moderate heart failure), cautious use of heart failure drugs is recommended (6).

Tobias Koenig, MD
Denise Hilfiker-Kleiner, PhD
***Johann Bauersachs, MD**

*Department of Cardiology and Angiology
Hannover Medical School
Carl-Neuberg-Strasse 1
30625 Hannover, Germany
E-mail: bauersachs.johann@mh-hannover.de

https://doi.org/10.1016/j.jacbts.2019.09.006

Please note: The authors have reported that they have no relationships relevant to the contents of this paper to disclose.

The authors attest they are in compliance with human studies committees and animal welfare regulations of the authors' institutions and Food and Drug Administration guidelines, including patient consent where appropriate. For more information, visit the *JACC: Basic to Translational Science* author instructions page.

REFERENCES

1. Koczo A, Marino A, Jeyabalan A, et al. Breastfeeding, cellular immune activation, and myocardial recovery in peripartum cardiomyopathy. J Am Coll Cardiol Basic Trans Science 2019;4:291-300.

2. Byrne JJ, Spong CY. "Is it safe?"—the many unanswered questions about medications and breast-feeding. N Engl J Med 2019;380:1296-7.

3. Centers for Disease Control and Prevention. Breastfeeding Report Card. Available at: https://www.cdc.gov/breastfeeding/data/reportcard.htm. Accessed September 25, 2019.

4. McNamara DM, Elkayam U, Alharethi R, et al. Clinical outcomes for peripartum cardiomyopathy in North America: results of the IPAC study (Investigations of Pregnancy-Associated Cardiomyopathy). J Am Coll Cardiol 2015;66:905-14.

5. Regitz-Zagrosek V, Roos-Hesselink JW, Bauersachs J, et al. 2018 ESC guidelines for the management of cardiovascular diseases during pregnancy. Eur Heart J 2018;39:3165–241.

6. Bauersachs J, König T, van der Meer P, et al. Pathophysiology, diagnosis and management of peripartum cardiomyopathy: a position statement from the Heart Failure Association of the European Society of Cardiology Study Group on peripartum cardiomyopathy. Eur J Heart Fail 2019;21:827–43.

REPLY: Breastfeeding in Patients With Heart Failure

Lack of Evidence and Consensus

We appreciate the response of Dr. Koenig and colleagues to our publication on breastfeeding in patients with peripartum cardiomyopathy (PPCM) in the Investigations of Pregnancy-Associated Cardiomyopathy (IPAC) study (1). They have highlighted important considerations in this patient population.

In response to concerns that "many mothers are inappropriately advised to discontinue breastfeeding or avoid taking essential medications because of fears of adverse effects on their infants," the American Academy of Pediatrics published a comprehensive database, LactMed, and reported on medications within each heart failure drug class regarding significant adverse effects based on clinical studies and on drug concentrations found in breast milk (2). Specifically, there is evidence that supports the safety of several beta-blockers and angiotensin-converting enzyme inhibitors, including metoprolol and enalapril (3).

Regarding the difference in the proportion of patients who were breastfeeding in IPAC compared with the U.S. national average, women who were breastfeeding in IPAC represented a more compensated subset because 80% were New York Heart Association functional class I and II, and metabolic demands clearly limit the ability of women with more severe heart failure to breastfeed. A retrospective study of PPCM patients with a mean baseline left ventricular ejection fraction of 28% included 67% that reported breastfeeding and found no evidence that breastfeeding limited subsequent myocardial recovery (4).

Although our study did not investigate physician recommendations, in a recent study of patients with PPCM, 69% reported their physician had instructed them not to breastfeed (5). This may provide an alternative explanation behind the decreased proportion of patients in IPAC who reported breastfeeding.

Regarding heart transplant, ventricular assist device implantations, and death, the breastfeeding cohort from IPAC experienced no events. As Dr. Koenig and colleagues pointed out, most of the complications occurred in patient with a baseline ejection fraction $< 30\%$, and women who breastfed in IPAC tended to have a higher baseline ejection fraction.

Our study supports that in women with compensated heart failure, breastfeeding does not limit myocardial recovery. Physicians should not deter women who feel well enough to breastfeed based on any theoretical concerns about the safety of heart failure medications or subsequent impact on myocardial recovery. We agree that more studies are needed to elicit the potential impacts of breastfeeding on outcomes in PPCM patients with more symptomatic heart failure and worse baseline cardiac function.

Agnes Koczo, MD
Amy Marino, MD
***Dennis M. McNamara, MD, MS**

*Heart and Vascular Institute
University of Pittsburgh Medical Center
Scaife Hall, Room S-566
200 Lothrop Street
Pittsburgh, Pennsylvania 15213
E-mail: mcnamaradm@upmc.edu

https://doi.org/10.1016/j.jacbts.2019.10.001

Please note: The authors have reported that they have no relationships relevant to the contents of this paper to disclose.

The authors attest they are in compliance with human studies committees and animal welfare regulations of the authors' institutions and Food and Drug Administration guidelines, including patient consent where appropriate. For more information, visit the *JACC: Basic to Translational Science* author instructions page.

REFERENCES

1. Koczo A, Marino A, Jeyabalan A, et al. Breastfeeding, cellular immune activation, and myocardial recovery in peripartum cardiomyopathy. J Am Coll Cardiol Basic Trans Science 2019;4:291–300.

2. Sachs HC, Committee on Drugs. The transfer of drugs and therapeutics into human breast milk: an update on selected topics. Pediatrics 2013;132:e796–809.

3. Kearney L, Wright P, Fhadil S, et al. Postpartum cardiomyopathy and considerations for breastfeeding. Card Fail Rev 2018;4:112–8.

4. Safirstein JG, Ro AS, Grandhi S, et al. Predictors of left ventricular recovery in a cohort of peripartum cardiomyopathy patients recruited via the internet. Int J Cardiol 2012;154:27–31.

5. Davis M, Kawamoto K, Langen E, Jackson E, et al. Breastfeeding is not associated with worse outcomes in peripartum cardiomyopathy (abstr.). J Am Coll Cardiol 2017;69:842.

JACC: BASIC TO TRANSLATIONAL SCIENCE VOL. 4, NO. 7, 2019

EDITOR'S PAGE

Can One Person Make a Difference?

Remembering the Remarkable Life and Career of Alfred Bove

Douglas L. Mann, MD, *Editor-in-Chief: JACC: Basic to Translational Science*

"One person can make a difference, and everyone should try."
—John F. Kennedy (1)

Dr. Alfred Bove

I performed my first research project with Alfred "Fred" Bove, MD, PhD, in 1981, while I was a medical resident at Temple University Hospital (2). In keeping with my complete naiveté about how to perform research, Fred suggested a clinical project that was simple by today's standards but allowed me to learn first-hand about the difficulties inherent in performing rigorous and reproducible quantitative measurements. The project also afforded me the opportunity to learn something about statistics. Sadly, Fred passed away on October 17, 2019, after a long battle with cancer. During the years that Fred was battling his illness, he also taught me a lot about life: dignity in the face of hardship, respect for everyone, passion and positivity for everything, and the importance of maintaining a sense of humor (albeit quirky).

Alfred Bove, MD, PhD, earned both his medical and doctoral degrees at Temple University and was Professor Emeritus, having served as Section Chief of Cardiology (twice) and as Associate Dean. He was also an expert in underwater physiology and medicine, which he learned as an undersea Medical Officer in the U.S. Navy. After leaving the Navy, he became an officer in the Naval Reserve and was active duty during Operation Desert Storm; he retired from the Navy after serving his country for 33 years. Fred devoted his career to seeing patients, doing research, and teaching medical students, residents, and fellows at Temple. The breadth of his research interests was extremely broad and included studies on basic cardiac physiology, coronary disease, exercise physiology, environmental medicine, and management of heart failure and cardiovascular risk factors. He was an early adopter of what has now become telemedicine. As an educator, Fred was almost without peer in terms of the breadth of his educational impact. He served as Editor-in-Chief of ACC's member magazine *Cardiology*, ACC's former educational website *Cardiosource.com*, the news magazine *CardioSource WorldNews*, and until very recently, was also the editor-in-chief of *ACCEL*, the ACC's audio journal, which has had enormous impact for physicians who were interested in keeping abreast of the latest developments in cardiovascular medicine. Along the way, he also became Master of the American College of Cardiology, President and Trustee of the American College of Cardiology, a team physician for the Philadelphia 76ers, and was a leader in the Undersea and Hyperbaric Medical Society. All of this brings me to another 1 of Fred's remarkable qualities: he had boundless energy.

Can 1 person make a difference? If 1 is extraordinarily lucky, 1 gets the chance to meet and learn from a person like Dr. Alfred Bove once in a lifetime. Fred made a huge difference through his service to his country, to the lives of his patients, and to the lives of the countless trainees whom he influenced over the 50-year arc of his career. However, I think that Fred's

ISSN 2452-302X https://doi.org/10.1016/j.jacbts.2019.10.009

unique gift was not that he made a difference in the lives of people but rather that he had the ability to inspire so many of us to make a conscious decision to try to make a difference with our own lives. For me personally, he introduced me to the joys of research, the imperative of teaching and mentoring others, and the importance of facing personal challenges with strength and courage. Since Fred's death was announced, there has been a constant stream of warm comments about him on multiple e-mail chains and texts. I wanted to close this remembrance with the comments of Dr. Ralph Brindis (with permission), who became the ACC president the year after Fred: "A huge loss of an incredible man. Focused, brilliant, kind and disciplined with a moral compass surpassed by none. A mentor to so many at both Temple and at the ACC. I learned so much at the feet of this giant. His legacy will be long lasting." I could not agree more.

ADDRESS FOR CORRESPONDENCE: Dr. Douglas L. Mann, Editor-in-Chief, *JACC: Basic to Translational Science,* American College of Cardiology, Heart House, 2400 N. Street NW, Washington, DC 20037. E-mail: jaccbts@acc.org.

REFERENCES

1. Goodreads. John F. Kennedy. Quotes. Available at: https://www.goodreads.com/quotes/129734-one-person-can-make-a-difference-and-everyone-should-try. Accessed October 22, 2019.

2. Mann DL, Denenberg BS, Gash AK, Makler PT, Bove AA. Effects of age on ventricular performance during graded supine exercise. Am Heart J 1986;111:108–15.